Title
Modeling Periodicity or Almost Periodicity in an Inhomogeneous Gamma Point Process

Author
Gaitan, Rodrigo Saul

Publication Date
2017

Peer reviewed|Thesis/dissertation

UNIVERSITY OF CALIFORNIA
RIVERSIDE

Modeling Periodicity or Almost Periodicity in an Inhomogeneous Gamma Point Process

A Dissertation submitted in partial satisfaction
of the requirements for the degree of

Doctor of Philosophy

in

Applied Statistics

by

Rodrigo Saul Gaitan

September 2017

Dissertation Committee:
Dr. Keh-Shin Lii, Chairperson
Dr. Barry Charles Arnold
Dr. Subir Ghosh

The Dissertation of Rodrigo Saul Gaitan is approved:

Committee Chairperson

University of California, Riverside

Acknowledgements

I would like to express my greatest appreciation to my advisor, Dr. Keh-Shin Lii, for his patience, guidance, and support. Thank you for sharing your knowledge with me and for showing me how to reason mathematically. I am grateful to Dr. Dimitris N. Politis, who inspired me to study time series and who made it possible for me to achieve a Master of Science degree from the UCSD mathematics department. I am thankful to my committee members, Dr. Barry C. Arnold, who gave me a one-on-one course in asymptotics, and Dr. Subir Ghosh for his inspiring words and guidance. For the late Dr. D.V. Gokhale, thank you for always challenging me and for all your personal advice. I would also like to thank Dr. Linda M. Penas, Dr. Analisa Flores, and Jill E. Smith for inspiring me to become a mathematics and statistics instructor. Lastly, my special thanks go to my family for making my college journey possible. I am most grateful to my mother and father who have always worked hard to support our family.

To my mother, father, and two sisters, for all their support.

ABSTRACT OF THE DISSERTATION

Modeling Periodicity or Almost Periodicity in an Inhomogeneous Gamma Point Process

by

Rodrigo Saul Gaitan

Doctor of Philosophy, Graduate Program in Applied Statistics
University of California, Riverside, September 2017
Dr. Keh-Shin Lii, Chairperson

We propose a model for the analysis of an inhomogeneous Gamma processes (IGP) with a periodic or almost periodic baseline intensity function and shape parameter greater than zero. The IGP is a generalization of both the nonhomogeneous Poisson process and the renewal process with independent and identically distributed $\Gamma(\kappa,\ \lambda)$ interarrival times, where $\kappa > 0$ is the shape parameter and $\lambda > 0$ is the scale parameter. The model deals with point events which are randomly spaced and show a pattern of periodicity or almost periodicity, such as the arrival times of customers to a store or the occurrence times of financial transactions. The concept of almost periodicity is described, and the purely periodic baseline intensity function is a particular case of the almost periodic baseline intensity function. We model the baseline intensity function as a sum of cosinusoidal functions plus a baseline constant. Given the number of periodic components K and shape parameter $\kappa > 0$, we propose a mostly Bartlett periodogram based approach of constructing consistent frequency, amplitude, phase, and baseline constant estimators. Two methods of prediction of the next occurrence are also discussed. In practice, the values of K and κ are unknown, and we suggest the AIC and the BIC model selection criteria for determining $K \in \{0\} \cup \mathbb{N}$ and $\kappa \in \mathbb{N}$. A simulation study is conducted to support theoretical results. A real data example is used to illustrate the theoretical results of our model.

Contents

List of Figures

List of Tables

List of Algorithms

Chapter 1

Introduction

This thesis presents a general model for inhomogeneous Gamma processes which show a pattern of periodicity or almost periodicity. In Chapter 1, we provide an introduction to point processes on the nonnegative real line. For a more in-depth introduction to point processes on different topological spaces, which are not restricted to be on the nonnegative real line, the author suggests the book by Daley and Vere-Jones (2003). For an elementary introduction to stationary point processes, the author suggests the books by Cox and Isham (1980) and Sigman (1995). Chapter 1 is organized as follows. In Section 1.1, the basic concepts, terminology, and restrictions imposed on a point process are set down. In Section 1.2, the renewal point process (RP), homogeneous Poisson point process (HPP), nonhomogeneous Poisson point process (NHPP), and inhomogeneous Gamma point process (IGP) are introduced. In Section 1.3, some more point process concepts and terminology, in the framework of an IGP, are presented. In Section 1.4, a goodness of fit model checking procedure is introduced. In Section 1.5, a method of simulating a point process is provided.

In Section 1.6, the Finite Fourier-Stieltjes transform and Bartlett Periodogram of a point process are defined. In Section 1.7, a literature review of the IGP is provided. The aim of this literature review is to show that the research presented in this thesis is original. No researcher has attempted a Bartlett Periodogram based approach of estimating unknown parameters of an IGP. In Section 1.8, some of the distributional properties of the IGP and its corresponding infinitesimal forward increment process are provided. This thesis is on modeling almost periodic IGP, and the motivation for studying such processes and the concept of almost periodicity are introduced in Chapter 2. The proposed model is presented and analyzed in Chapter 2 and Chapter 3. The procedure of implementing the proposed methodology is given in Chapter 3. A discussion of potential future research is provided in Chapter 4.

1.1 Some Basic Concepts, Terminology, and Assumptions Imposed on Point Processes

In many scientific investigations, the main aspect of interest is the repeated recurrence times of some particular event and not on the physical attributes of the event itself. For instance, an event of interest may be the repeated malfunctioning times of an automobile that is put back in service once the component causing the malfunction is replaced or repaired (Bandyopadhyay and Sen (2005)). Other such recurrent events may be the admission times of an alpha particle from a radioactive source, the arrival times of customers to a store, or the times of an electrical discharge from a nerve cell (Brown (1998)). In this research, the emphasis is not on the event itself, or the particular location of occurrence, but rather only on the random times at which the events occur. Throughout this research, the assumption that the events of interest can only occur on the nonnegative real line is imposed. Since the time of occurrence of an event of interest can be viewed as a point on $\mathbb{R}^+$, the time instant of a given event is referred to as a **point event** (point events are often called **epochs**). The random stream of successive point events is referred to as a **point process,** and we denote the random occurrence times of the point events with $\{T_n,\ n = 1,\ 2,\ \ldots\}$, where $0 \leq T_1 \leq T_2 \leq \cdots \leq T_n < \infty$. We assume that the **ensemble of a point process** is the collection of discrete sets of point events on the set $\mathbb{R}^+$ such that:

(i) All epochs are distinct.

(ii) Any finite time interval contains only a finite number of epochs[1].

(iii) Any infinite time interval contains an infinite number of epochs[2].

(iv) There exists no fixed time instant for which a point event may occur with positive probability.

Under assumption (i), the point process has the natural ordering $0 < T_1 < T_2 < \cdots < T_n < \infty$ of the random stream of point events. Under assumption (ii) there exists no

[1]A point process such that $P\left\{\sum_{n=1}^{\infty} \mathbf{1}_{\{0<T_n\leq t\}} < \infty\right\} = 1$ for all $t > 0$ is said to be stable (Jacobsen (1982), page 5), where $\mathbf{1_A}$ is the indicator function of an event $\mathbf{A}$. So we assume that the point process is stable.

[2]A point process such that $P\left\{\sup_{t>0} \sum_{n=1}^{\infty} \mathbf{1}_{\{0<T_n\leq t\}} < \infty\right\} > 0$ is said to allow absorption (Jacobsen (1982), page 5), where $\mathbf{1_A}$ is the indicator function of an event $\mathbf{A}$. So we assume that the point process does not allow absorption.

interval which contains an explosion of events. Under assumption (iii) there is no time $t > 0$ for which no more point events can occur after time $t > 0$. Assumption (iv) eliminates point processes where point events can occur at known deterministic times points and restricts the distribution of each random point event to be a continuous distribution. A **regular** point process is a point process for which the probability that an event will occur at any specified time $t \geq 0$ is 0. An **orderly** point process is a point process for which the probability of two or more events occurring at any time $t \geq 0$ is 0. Therefore, by assumptions (i) and (iv) we only consider regular and orderly point processes. Under assumptions (i)-(iii), the n-th **interarrival time** between events, say $\{X_n,\ n = 1,\ 2,\ \ldots\}$, can then be defined as $X_n = T_n - T_{n-1}$, where $T_0 = 0$. Associated with the point process, $\{T_n,\ n = 1,\ 2,\ \ldots\}$, is the stochastic process $\{N(0,\ t),\ t > 0\}$, which counts the number of point events which occurred in the time interval $(0,\ t] \subseteq \mathbb{R}^+$. That is, for each $t > 0$, $N(0,\ t) \coloneqq \sum_{n=1}^{\infty} \mathbf{1}_{\{0<T_n \leq t\}}$, where $\mathbf{1_A}$ is the indicator function of an event $\mathbf{A}$. The restriction of a count of 0 at time $t = 0$ is imposed. The stochastic process, $\{N(0,\ t),\ t > 0\}$, is called a **counting process**. Under the assumption of a count of 0 at time $t = 0$ and assumptions (i)-(iv), the ensemble of the sample paths of the counting process, $\{N(0,\ t),\ t > 0\}$, will consist of right continuous step functions which are anchored at the origin having unit jumps at the epochs of a point process. Under the imposed assumptions, there is a one-to-one correspondence between the point process, its associated counting process, and the interarrival time sequence. Therefore, under the set assumptions imposed on the point process, the random epochs, the interarrival time sequence, or the counting process can be used to specify the probability law of the point process completely.

Since with probability one, for any time points $0 < t_1 < t_2 < \infty$, $N(0,\ t_2) - N(0,\ t_1)$ counts the number of point events which occurred in the time interval $(t_1,\ t_2]$, it is natural to define an **increment counting process** as $N(t_1,\ t_2) := \sum_{n=1}^{\infty} \mathbf{1}_{\{t_1 < T_n \leq t_2\}}$. For simplicity, if $t_1 = 0$ and $t_2 = t$, the notation $N(t)$ will be used in place of $N(0,\ t)$. Also, to emphasize a count of 0 at time $t = 0$, we use the notation $N(0) = 0$. In the next section, we introduce the point processes which are considered throughout this research. After that, in Section 1.3, we continue to introduce more point process concepts and terminology in the framework of the point processes presented in Section 1.2.

1.2 The Renewal Point Process, the Nonhomogeneous Poisson Point Process, and the Inhomogeneous Gamma Point Process

In this section, the renewal point process, homogeneous Poisson point process, nonhomogeneous Poisson point process, and inhomogeneous Gamma point process will be introduced. First, a formal introduction of the above point processes will be given. Next, the relationships between the above point processes is explained. Lastly, applications of the above point processes, borrowed from maintenance and reliability theory, are provided.

Consider a counting process for which the interarrival times are independent and identically distributed with arbitrary nonnegative distribution, say $\{X_n,\ n = 1,\ 2,\ \ldots\}$. Such a counting process is called a **renewal point process** (RPP, Ross (2013)). Throughout this research, a renewal process for which the interarrival sequences, $\{X_n,\ n = 1,\ 2,\ \ldots\}$, are independent and identically $\Gamma(\alpha,\ \beta)$ distributed random variables, will be defined to be a **gamma renewal process** (GRP). Here, $\alpha > 0$ is the shape parameter and $\beta > 0$ is the scale parameter of the gamma random variable. More explicitly, a GRP is a renewal process for which the interarrival times X_n are independent and identically distributed $\Gamma(\alpha,\ \beta)$, the random epoch times are defined as $T_0 = 0$ and $T_n = \sum_{i=1}^{n} X_i$, and $N(t) = \sup\{n :\ T_n \leq t\}$, where $n = 0,\ 1,\ 2,\ \ldots$ and $t > 0$. If one restricts $\alpha = 1$ and $\beta = \frac{1}{\lambda} > 0$, then the GRP is called a **homogeneous Poisson point process** (or a homogeneous Poisson process (HPP)) with intensity function $\lambda > 0$ (Ross (2013)). It can be shown that $\{N(t),\ t > 0\}$ is a HPP with intensity function $\lambda > 0$ if $\{N(t),\ t > 0\}$ is a renewal process which satisfies

(i) $P\{N(0) = 0\} = 1$,

(ii) $\{N(t),\ t > 0\}$ has stationary (1.14) and independent increments,

(iii) $P\{N(h) \geq 2\} = o(h)$,

(iv) $P\{N(h) = 1\} = \lambda h + o(h)$,

where $h \to 0$, $h > 0$, and a function $f(\cdot)$ is said to be $o(h)$ if $\lim_{h\to 0^+} \frac{f(h)}{h} = 0$. It can be shown that for a HPP with intensity function λ,

$$P\{N(t,\ t+s)=n\} = \exp\{-\lambda s\}\frac{[\lambda s]^n}{n!}, \tag{1.1}$$

for all $t > 0$, $s > 0$, and $n = 0,\ 1,\ 2,\ \ldots$ (Ross (2013)). Such a process is referred to as homogeneous because it has stationary increments.

A natural generalization of a HPP is to relax the stationary increment assumption and let the constant intensity function $\lambda > 0$ be a positive bounded function of time $t > 0$. More explicitly, let $\{N(t),\ t > 0\}$ be a counting process such that

(i) $P\{N(0) = 0\} = 1$,

(ii) $\{N(t),\ t > 0\}$ has independent increments,

(iii) $P\{N(t,\ t+h) \geq 2\} = o(h)$,

(iv) $P\{N(t,\ t+h) = 1\} = \lambda(t)h + o(h)$,

where $0 < \lambda(t) \leq M < \infty$, $h \to 0$, and $h > 0$. The resulting counting process $\{N(t),\ t > 0\}$ is called a **nonhomogeneous Poisson point process** (or nonhomogeneous Poisson process (NHPP)). It can be shown that for a NHPP,

$$P\{N(t,\ t+s)=n\} = \exp\left\{-\int_t^{t+s}\lambda(u)du\right\}\frac{\left[\int_t^{t+s}\lambda(u)du\right]^n}{n!}, \tag{1.2}$$

for all $t > 0$, $s > 0$, and $n = 0,\ 1,\ 2,\ \ldots$ (Ross (2014)). As one can see, the HPP is a particular case of the NHPP with $\lambda(t) = \lambda > 0$ for all $t > 0$.

Consider a NHPP with intensity function $\lambda_1(t) > 0$, where $t > 0$. Suppose that an event has just occurred, call this occurrence time the origin, and that thereafter only every κ-th event of the NHPP is observed. Then, if $0 < T_1 < T_2 < \cdots < T_n < \infty$ are the occurrence times of the first n events observed after the origin, the joint density function of the occurrence times is given by

$$f_n(t_1, \ldots, t_n) = \frac{1}{\Gamma(\kappa)^n} \left\{ \prod_{i=1}^{n} \lambda_1(t_i) \left[\Lambda_1(t_i) - \Lambda_1(t_{i-1})\right]^{\kappa-1} \right\} \exp\left\{-\Lambda_1(t_n)\right\} I_{\{0<t_1<\cdots<t_n<\infty\}}, \tag{1.3}$$

where

$$\Lambda_1(t) := \int_0^t \lambda_1(u)du,$$

and $t_0 = 0$. If κ is any positive number, not necessarily an integer, then (1.3) still defines a joint density function of a point process. As defined in Berman (1981), a point process with joint density (1.3) for all positive integers n is defined to be an **inhomogeneous Gamma point process** (or inhomogeneous Gamma process (IGP)) **with intensity function** $\lambda_1(\cdot)$ **and shape parameter** $\kappa > 0$. In this research, we refer to the function $\lambda_1(\cdot)$ as the **baseline intensity function of the IGP** and not as the intensity function of the IGP (The intensity function of the IGP, say $\lambda_2(\cdot)$, is defined as in equation (1.12).). Also, for all $t > 0$, we assume that the baseline intensity function is such that $0 < \lambda_1(t) \leq M < \infty$, $\Lambda_1(t) = \int_0^t \lambda_1(u)du < \infty$, and $\Lambda_1(\infty) = \infty$. Lastly, the counting process of the IGP which satisfies the above assumptions will be denoted by $\{N_G(t),\ t > 0\}$.

The beauty of the IGP is the following:

1. If $\kappa = 1$, then (1.3) defines the joint density function of a NHPP.

2. If $\kappa = 1$ and $\lambda_1(t) = \lambda > 0$ $(0 < t < \infty)$, then (1.3) defines the joint density function of a HPP.

3. If $\kappa > 0$ and $\lambda_1(t) = \lambda > 0$ $(0 < t < \infty)$, then (1.3) defines the joint density function of a GRP, with interarrival distribution $\Gamma(\kappa,\ \lambda)$.

An alternate method of defining the IGP is the following. For all $t > 0$, let $0 < \lambda_1(t) \leq M < \infty$, $\Lambda_1(t) = \int_0^t \lambda_1(u)du < \infty$, and $\Lambda_1(\infty) = \infty$. Suppose that for $i = 1,\ 2,\ \ldots,\ n$ and $T_0 = 0$, the random variables $\Lambda_1(T_i) - \Lambda_1(T_{i-1})$ are independent and identically $\mathit{\Gamma}(\kappa,\ 1)$ distributed. It then follows that (1.3) is the joint density function of the random epochs $T_1,\ \ldots,\ T_n$ [3]. From this representation of the IGP, it follows that for each $n = 1,\ 2,\ \ldots$, $\Lambda_1(T_n) = \sum_{i=1}^n \{\Lambda_1(T_i) - \Lambda_1(T_{i-1})\}$ is $\mathit{\Gamma}(n\kappa,\ 1)$ distributed.

Next, we provide an illustration of how researchers have used the RPP, NHPP, and IGP to model real-life phenomenon. In maintenance and reliability theory, the failure times of a piece of equipment is often of primary interest. As many complex and expensive systems encountered in practice are meant to be repaired rather than replaced upon failure, predicting the recurrent failure times of a system becomes an interesting problem. For instance, an event of primary interest may be the repeated

[3] The proof of the claim that the alternate method of defining the IGP is equivalent to the original method of defining the IGP is provided in the Appendix A.1.1.

malfunctioning times of an automobile that is put back in service once the component causing the malfunction is replaced or repaired (Bandyopadhyay and Sen (2005)). Many times after a piece of equipment has been repaired, the piece of equipment is brought to a like new condition. In other words, after each repair time the equipment is perfectly maintained, it is as though we are starting over with a new piece of equipment. This implies that the times between successive failures are independent and identically distributed. The failure times of such a piece of equipment can then be modeled as a renewal process (Pulcini (2003)). Furthermore, many times after a piece of equipment has been repaired, the corrective maintenance brings the piece of equipment to the condition it was in just before the failure occurrence. In such a case, the equipment reliability is unchanged by the failure and the repaired equipment failure times can then be modeled by a NHPP (Pulcini (2003)). Lastly, many times a piece of equipment receives shocks according to a Poisson process; failure does not necessarily occur at every shock but every $\kappa = 1,\ 2,\ \ldots$ shock. The failure time of such a piece of equipment can then be modeled by an IGP (Pulcini (2003)).

1.3 Some More Point Processes Concepts

In this section, we introduce some more concepts of point processes which satisfy assumptions (i)-(iv) of Section 1.1 and which are defined to have a count of 0 at time $t = 0$. Also, in the framework of the inhomogeneous Gamma process (IGP) introduced in Section 1.2, we provide some examples of the mathematical concepts introduced. Throughout this section, let $\{N_G(t),\ t > 0\}$ be an IGP with baseline intensity function $\lambda_1(t)$ and shape parameter $\kappa > 0$ which satisfies the assumptions set down in Section 1.2. Let $\{N(t),\ t > 0\}$ be a counting process which satisfies assumptions (i)-(iv) of Section 1.1 and which is defined to have a count of 0 at time $t = 0$. Since the counting process, $\{N(t),\ t > 0\}$, is a random variable for all $t > 0$ and is restricted to be 0 at time $t = 0$, it is meaningful to define its mean value as a function of $t > 0$, provided that the expectation is finite. The definition of the mean value function of the point process is formally presented next.

Definition 1. The **mean value function** of a point process.

Let $\{N(t),\ t > 0\}$ be the counting process associated with the point process $\{T_n,\ n = 1,\ 2,\ \ldots\}$, then for $t > 0$ the mean value function of the point process is defined as

$$M(t) \coloneqq E\left[N(t)\right], \tag{1.4}$$

provided the expectation exist.

For the IGP considered in this research, $\{N_G(t),\ t > 0\}$, the mean value function of a point process (1.4) can be expressed in the form[4]

$$\begin{aligned} M(t) &= \int_0^t \sum_{n=1}^{\infty} \frac{\lambda_1(u)}{\Gamma(n\kappa)} \left\{\Lambda_1(u)\right\}^{n\kappa-1} \exp\left\{-\Lambda_1(u)\right\} du & (1.5) \\ &\coloneqq \int_0^t \lambda_2(u) du, & (1.6) \end{aligned}$$

[4]The proof of equation (1.5) is provided in the Appendix A.2.3.

where we define $\lambda_2(t) \coloneqq \sum_{n=1}^{\infty} \frac{\lambda_1(t)}{\Gamma(n\kappa)} \{\Lambda_1(t)\}^{n\kappa-1} \exp\{-\Lambda_1(t)\}$, which is a bounded positive function of $t > 0$. Since such a function $\lambda_2(t)$ exists, it follows that for some infinitely small time increment, say $h > 0$, as $h \to 0$, the mean value function of the IGP, $\{N_G(t),\ t > 0\}$, has the following property

$$\begin{aligned} E\left[N_G(t,\ t+h)\right] &= E\left[N_G(t+h)\right] - E\left[N_G(t)\right] \\ &= \int_t^{t+h} \lambda_2(u)du \\ &= \lambda_2(t)h + o(h), \end{aligned} \tag{1.7}$$

for all $t > 0$.

Let $h > 0$ be an infinitely small time increment, then $N(t,\ t+h)$ counts the number of events that occur in an infinitely small time interval of length h. Define the stochastic process $\{dN(t),\ t > 0\}$ as $dN(t) \coloneqq N(t,\ t+h)$, where $t > 0$, $h > 0$, and $h \to 0$. The stochastic process, $\{dN(t),\ t > 0\}$, is called the **infinitesimal forward increment process.** For the IGP considered in this research, $\{N_G(t),\ t > 0\}$, the function $\lambda_2(t)$ of equations (1.6) and (1.7) and the first order probability structure of the infinitesimal forward increment point process are related as follows[5]:

[5]The proof of equations (1.8)-(1.10) is provided in the Appendix A.2.2.

$$P\{dN_G(t) = 0\} = 1 - \lambda_2(t)h + o(h), \tag{1.8}$$

$$P\{dN_G(t) = 1\} = \lambda_2(t)h + o(h), \tag{1.9}$$

$$P\{dN_G(t) \geq 2\} = o(h), \tag{1.10}$$

for all $t > 0$. It must be stressed that conditions (1.8)-(1.10) do not uniquely specify the probability law of a point process. For the point process model considered in this research, we therefore have from equation (1.7) and the first order probability structure of the infinitesimal forward increment point process that[6]

$$\lim_{h \to 0^+} \frac{P\{N_G(t,\ t+h) \geq 1\}}{h} = \lim_{h \to 0^+} \frac{E\{N_G(t,\ t+h)\}}{h}, \tag{1.11}$$

for all $t > 0$. By the definition of an expected value, it follows from equation (1.11) that $\lambda_2(t)$ can be interpreted as the expected rate of occurrence at time $t > 0$. The function $\lambda_2(t)$ of equation (1.7) is called the **intensity function** of a point process. The formal definition of the intensity function of a point process is provided next.

Definition 2. The **intensity function** of a point process.

Let $\{N(t),\ t > 0\}$ be the counting process associated with the point process $\{T_n,$

[6]The proof of equation (1.11) is provided in the Appendix A.2.3.

$n = 1,\ 2,\ \ldots\}$, then for $t > 0$, the intensity function of a point process is defined as

$$\lambda_2(t) \coloneqq \lim_{h \to 0^+} \frac{P\{N(t,\ t+h) \geq 1\}}{h}, \tag{1.12}$$

provided the limit exists.

For future reference, we provide the functional form the intensity function of the IGP. For $t > 0$, the **intensity function of the IGP,** $\{N_G(t),\ t > 0\}$**,** has the functional form[7]

$$\lambda_2(t) = \sum_{n=1}^{\infty} \frac{\lambda_1(t)}{\Gamma(n\kappa)} \{\Lambda_1(t)\}^{n\kappa-1} \exp\{-\Lambda_1(t)\}. \tag{1.13}$$

Since $\lambda_1(t)$ is a bounded positive function of $t > 0$, we notice that $\lambda_2(t) = \lambda_1(t)$ for all $t > 0$, if and only if $\kappa = 1$.

In point processes, the only observations are the events times and the counts of the number of events which have occurred up to and including time $t > 0$. So, the intensity function of the point process is not directly observed. However, the intensity function can be used to describe the occurrence patterns of events. If a point process has a large intensity function over a given time interval, then one should expect to observe a lot of events over this time interval, and vice versa. Because the intensity function can be used to predict occurrence patterns, much of the research in this thesis is focused on estimating the intensity function of the point process.

[7]The proof of equation (1.13) is provided in the Appendix A.2.1.

Next, we introduce the concept of a stationary point process. A stochastic process is said to be **stationary** if its probability law is invariant with respect to time shift. In the point process literature, there are many non-equivalent definitions of stationarity which do not render the probability law of the point process invariant with respect to time shift. In this research, we express the definition of stationarity in terms of the increments of the counting process. A point process is said to be stationary if the joint distribution of the respective numbers of events (counts) in a set of fixed time intervals is invariant with respect to a time shift. The formal definition of a stationary point process is provided next.

Definition 3. A **stationary point process**.

A point process $\{T_n,\ n = 1,\ 2,\ \ldots\}$ with associated counting process $\{N(t),\ t > 0\}$ is said to be stationary when for every $r = 1,\ 2,\ \ldots$ and all bounded Borel subsets $A_1, \ldots,\ A_r$ of $(0,\ \infty)$, the joint distribution of

$$\{N(A_1 + t),\ \ldots,\ N(A_r + t)\} \tag{1.14}$$

does not depend on t $(0 < t < \infty)$, (Daley and Vere-Jones (2003), Chapter 3.2).

Throughout this research, we only use definition (1.14) when referring to the stationarity of a point process.

We now introduce the concept of a conditional intensity function of a point process on $\mathbb{R}^+$. For most point processes, the time of the first event after some fixed time

$t > 0$ depends on the evolution of the point events up to and including time $t > 0$. For the IGP considered in this research, $\{N_G(t),\ t > 0\}$, the probability structure of the time of the first event after some fixed time $t > 0$ depends on a stochastic process called the **conditional intensity function** of the point process (Pulcini (2003)). As mentioned in Jacobsen (1982), under regularity conditions placed on a point process, $\{N(t),\ t > 0\}$, the conditional intensity function completely specifies the probability structure of the point process[8]. As we will see, the conditional intensity function of a point process is the key to likelihood analysis and to solving problems of prediction, filtering, and simulating point processes on the half-line (Daley and Vere-Jones (2003, Chapter 7.2)). The formal definition of the conditional intensity function is provided next.

Definition 4. The **condition intensity function** of a point process.

Let $\{N(t),\ t > 0\}$ be the counting process associated with the point process $\{T_n,$ $n = 1,\ 2,\ \ldots\}$. For $t > 0$, the conditional intensity function of a point process is defined as

$$\lambda_2(t \mid H_t) \quad := \quad \lim_{h \to 0^+} \frac{P\left\{N(t,\ t+h) \geq 1 \mid H_t\right\}}{h}, \tag{1.15}$$

where H_t specifies the history of the point process up to and including time t, that is, the history of the point process consist of the $\sigma-$algebras $H_t := \sigma\left\{N(s)\ ,\ 0 < s \leq t\right\}$.

[8]The regularity conditions which insure the existence of the limit (1.15) and the one-to-one correspondence between the point process and a conditional intensity function are provided in Theorem 3.1 and Proposition 4.2 of Jacobsen (1982).

Conditional on the realization $H_t = \{T_1 = t_1,\ \ldots\ ,\ T_{n-1} = t_{n-1},\ N_G(t) = n-1\}$, for $t_{n-1} < t \leq t_n$ the **conditional intensity function (1.15) of the IGP,** $\{N_G(t),\ t > 0\}$**,** is

$$\lambda_2(t \mid H_t) = \lambda_1(t)\frac{\frac{1}{\Gamma(\kappa)}\left\{\int_{t_{n-1}}^{t}\lambda_1(u)du\right\}^{\kappa-1}\exp\left\{-\int_{t_{n-1}}^{t}\lambda_1(u)du\right\}}{\int_t^\infty \frac{\lambda_1(z)}{\Gamma(\kappa)}\left\{\int_{t_{n-1}}^{z}\lambda_1(u)du\right\}^{\kappa-1}\exp\left\{-\int_{t_{n-1}}^{z}\lambda_1(u)du\right\}dz}, \tag{1.16}$$

where $t_0 = 0$ and $n = 1,\ 2,\ \ldots$ (Pulcini (2003)).

We close by presenting how the conditional intensity function is related to the time truncated joint density function of the counting process $\{N(t),\ t > 0\}$, which satisfies assumptions (i)-(iv) of Section 1.1 and which is defined to have a count of 0 at time $t = 0$. For a non-random observational time period $(0,\ T]$ of the counting process $\{N(t),\ t > 0\}$, the likelihood of the realization $0 < T_1 = t_1 < \cdots < T_{N(T)} = t_{n(T)}$, is given by

$$\begin{aligned}
&f_{T_1,\ldots,T_{N(T)}}(t_1,\ldots,t_{n(T)}) \\
&\quad = \exp\left\{-\int_{t_{n(T)}}^{T}\lambda_2(u \mid H_u)du\right\}\prod_{j=1}^{n(T)}\lambda_2(t_j \mid H_{t_j})\exp\left\{-\int_{t_{j-1}}^{t_j}\lambda_2(u \mid H_u)du\right\} \\
&\quad = \exp\left\{-\int_0^T\lambda_2(u \mid H_u)du + \int_0^T\log\left(\lambda_2(u \mid H_u)\right)dN(u)\right\},
\end{aligned} \tag{1.17}$$

where $t_0 = 0$, $H_t := \{N(s)\ ,\ 0 < s \leq t\}$, and the $dN(u)$ term refers to a counting measure jumping by 1 at each point event and by 0 otherwise (Brillinger (1998), (Pulcini (2003))).

1.4 The Residual Analysis of a Point Process

After fitting a model to point process data, it is crucial to have a method of evaluating the goodness of fit. Berman (1983) and Ogata (1988), have used the results of Papangelou (1972) to develop graphical and analytic techniques for amplifying the features of the data that deviate from the assumed model if any (Daley and Vere-Jones (2003, Chapter 7.4)). The residual analysis based approach of the goodness of fit, which can be found in Section 3.3 of Ogata (1988), is presented below.

Let $0 < T_1 < T_2 < \cdots < T_n < \infty$ be a point process with associated counting process $\{N(t),\ t > 0\}$ and conditional intensity function $\lambda(t \mid H_t)$ (defined as in equation (1.15)), where $H_t = \{N(s),\ 0 < s \leq t\}$, $0 < \lambda(t \mid H_t) \leq M < \infty$ for all $t > 0$, $\int_0^t \lambda(u \mid H_u)du < \infty$ for all $t > 0$, and $\int_0^\infty \lambda(u \mid H_u)du = \infty$. Consider the random time change $\tau = \int_0^t \lambda(u \mid H_u)du$ from t to τ, then $\{T_n,\ n \in \mathbb{N}\}$ is transformed one to one into $\{\tau_n,\ n \in \mathbb{N}\}$. It is known that $\{\tau_n,\ n \in \mathbb{N}\}$ has the distribution of a Poisson process (Daley Vere-Jones 2003). Since $\lambda(t \mid H_t)$ uniquely specifies the joint distribution of the point process, it then follows that if the estimated conditional intensity function $\widehat{\lambda}(t \mid H_t)$ is a good approximation to the true conditional intensity function $\lambda(t \mid H_t)$, then the transformed data $\{\tau_n,\ n \in \mathbb{N}\}$ should behave like the random epoch times of a Poisson process. In other words, portions of the sequence $\{\tau_n,\ n \in \mathbb{N}\}$ which deviate from what is expected from a Poisson process imply the existence of a corresponding feature of the data $\{T_n,\ n \in \mathbb{N}\}$ that is not captured by the model $\widehat{\lambda}(t \mid H_t)$. The sequence $\{\tau_n,\ n \in \mathbb{N}\}$ is called the **residual process,** and any elementary method can be used to check if the residual process is that of a Poisson process. For instance, if $\lambda(t \mid H_t)$ is a correct model, the transformed residual process $\{e_n = \tau_n - \tau_{n-1},\ \tau_0 = 0,\ n \in \mathbb{N}\}$ is a sequence of independent and identically distributed exponential random variables with unit rate parameter (Berman (1983)). Therefore, to check goodness of fit one can then use a Kolmogorov-Smirnov test to evaluate whether or not the transformed residual process is a sequence of independent and identically distributed exponential random variables with unit rate parameter. For a residual process based goodness of fit procedure, see Algorithm 7.4.V. from Daley and Vere-Jones (2003). A formal definition of the transformed residual process is provided next.

Definition 5. Let $0 < T_1 < T_2 < \cdots < T_n < \infty$ be the random epoch sequence of a point process with associated counting process $\{N(t),\ t > 0\}$ and conditional intensity function $\lambda(t \mid H_t)$, such that for all $t > 0$, $0 < \lambda(t \mid H_t) \leq M < \infty$, $\int_0^t \lambda(u \mid H_u)du < \infty$, and $\int_0^\infty \lambda(u \mid H_u)du = \infty$, where $H_t = \{N(s),\ 0 < s \leq t\}$. The **transformed residual process** is defined as

$$e_n \quad := \quad \int_{T_{n-1}}^{T_n} \lambda(u \mid H_u)du, \tag{1.18}$$

where $n = 1,\ 2,\ \ldots$ and $T_0 = 0$.

1.5 Simulation of a Point Process

Lewis and Shedler (1979) developed a method of simulating a nonhomogeneous Poisson process which was termed thinning. Ogata (1981) generalized this thinning method to simulate point processes which have a random locally bounded conditional intensity function. For an overview of Ogata's extension of Lewis and Shedler (1979) thinning algorithm, the author suggests Section 7.5 of Daley and Vere-Jones (2003). The particular models of the point processes that are simulated in this thesis evolve as a sub-sampling of a nonhomogeneous Poisson process (NHPP). Therefore, we present Lewis and Shedler (1979) thinning algorithm of simulating a NHPP with intensity function $\lambda_1(t)$, where $0 < \lambda_1(t) \leq \lambda < \infty$ for all $t > 0$. For all $t > 0$, let $0 < \lambda < \infty$ be the intensity function of a homogeneous Poisson process (HPP), and denote the random epoch times of the HPP with $0 < X_1 < X_2 < \cdots < X_n < \infty$.

Algorithm 1.1 Thinning Algorithm (Lewis and Shedler (1979)).

1. Fix an observational length $T > 0$.
2. Simulate the epochs $X_1, \ \ldots, \ X_i$ according to a HPP with intensity function $\lambda > 0$, stopping as soon as $X_i > T$.
3. Simulate $Y_1, \ \ldots, \ Y_i$ as a set of independent and identically distributed uniform $(0, \ 1)$ random variables.
4. Initialize $i = 1$ and $j = 1$.
5. If $X_i > T$, terminate. Otherwise, evaluate $\lambda_1(X_i)$.
6. If $Y_i \leq \frac{\lambda_1(X_i)}{\lambda}$, set $T_j = X_i$, advance j to $j + 1$.
7. Advance i to $i + 1$.
8. The output consists of the random epochs times $0 < T_1 < T_2 < \cdots < T_j < \infty$ of a NHPP with intensity function $\lambda_1(\cdot)$.

1.6 The Finite Fourier-Stieltjes Transform of a Point Process and the Bartlett Periodogram

When observing point processes, the only observations are the events times, the time between successive events, and the number of events (counts) which have occurred up to and including time $t > 0$. Therefore, the intensity function of the point process (1.12) is not directly observed. However, it is still possible to develop methods for estimating the intensity function of a point process. This section defines the finite Fourier-Stieltjes transform and the Bartlett periodogram of a point process, which will be used throughout this research to estimate unknown parameters of an intensity function.

Assume that the counting process $\{N(t),\ t > 0\}$ is observed for a fixed non-random time interval $(0,\ T]$. Then at time T, $N(T)$ is a random variable. The **finite Fourier-Stieltjes transform** of a point process is defined as

$$d_T(\omega) := \frac{1}{\sqrt{2\pi T}} \int_0^T \exp\{-i\omega t\}\, dN(t). \tag{1.19}$$

The **Bartlett periodogram** of a point process is defined as the squared norm of the finite Fourier-Stieltjes transform as

$$I_T(\omega) := \frac{1}{2\pi T} \left| \int_0^T \exp\{-i\omega t\}\, dN(t) \right|^2, \tag{1.20}$$

where $i = \sqrt{-1}$ and the $dN(t)$ term refers to a counting measure jumping by 1 at each point event and 0 otherwise (Bartlett (1963)). For a one-dimensional stationary point process, the distributional properties of the Bartlett periodogram are developed in Bartlett (1963). For the particular case of an r dimensional interval stationary point process, the asymptotic properties of (1.19) and (1.20) are given in Theorem 4.2 and its corollary 4.1 of Brillinger (1972).

Much of this thesis is devoted to establishing the distributional properties of the Bartlett periodogram in the context of an inhomogeneous Gamma point process with a baseline intensity function that is a periodic or almost periodic function of time $t > 0$ (For the definition of an inhomogeneous Gamma point process, see equation (1.3)).

1.7 A Literature Review on the Estimation of Periodicity in the Framework of an Inhomogeneous Gamma Process

In this section, we provide a brief literature review of the estimation of periodicity in an inhomogeneous Gamma process (IGP). Due to the awkward form of the conditional intensity function of the IGP, the IGP has rarely been fitted to point process data (Hurley (1992)). When fitting the IGP to data, a parametric form of the baseline intensity function of the IGP is assumed. In the literature, the baseline intensity function is chosen in such a way that the conditional intensity function will take a parametric form which will render the maximum likelihood based approach of estimating unknown parameters tractable. The actual sequence of steps of fitting a parametric point process model to point process data is outlined in Section 3.2 of Ogata (1988). After a point process model had been fitted, the goodness of fit is determined by using some form of Residual analysis of the point process data (Ogata (1998)). Also, when deciding between competing fitted models, researchers have used the Akaike information criterion (AIC) as a model selection criterion (Ogata (1998)). Although not every researcher has taken this exact sequence of steps to fitting an IGP to point process data, the novelty of this research is that a Bartlett Periodogram (1.20) based approach has not been attempted to estimate the unknown parameters of a baseline intensity function which is a periodic or almost periodic function of time.

Neuroscience researchers have fit an IGP model to neural spike train data. First, neuroscientists define a desired conditional intensity function; then they use the one-to-one correspondence between the conditional intensity function and the joint density function of the point process to employ a maximum likelihood based approach to estimating the unknown IGP model parameters. In the bibliography, we provide a series of neuroscience papers, written mostly by Emery N. Brown (1998, 2003, 2005) and Riccardo Barbieri et al (2001), that take the above approach to fitting an IGP model to spatial-temporal point process data. Furthermore, many reliability theorists have attempted to fit the IGP to failure time data. The reliability theory papers usually assume a parametric form of the baseline intensity function which will then render the maximum likelihood, of the event truncated joint density function of the IGP, based approach of estimation tractable. For instance, reliability theorists commonly assume a baseline intensity function of the Weibull form (1.21) with $\rho = \beta_1/\theta^{\beta_1} > 0$, $\beta_1 > 0$, $\beta = \beta_1 - 1$, and $z_1(t) = \log(t)$ (Bandyopadhyay and Sen (2005)). However, the details of this literature review are restricted to research papers which have attempted to model periodicity in an IGP.

The IGP was introduced in paper by Berman (1981). In his article, Berman defines a **modulated gamma process** as an IGP with baseline intensity function of the form

$$\lambda_1(t) = \rho \exp\left\{\beta z(t)\right\}, \tag{1.21}$$

where $\beta = (\beta_1, \ldots, \beta_p)$, $z(t)^T = \{z_1(t), \ \ldots, \ z_p(t)\}$, and with shape parameter $\kappa > 0$. The relationship (1.21) expresses a possible dependence of the occurrence of events on a vector $z(\cdot)$ of explanatory variables. For instance, cyclic variation of known wavelength ω can be tested by taking $z_1(t) = \cos(\omega t)$ and $z_2(t) = \sin(\omega t)$. In such a case,

$$\begin{aligned} \lambda_1(t) &= \rho \exp\left\{\beta_1 \cos(\omega t) + \beta_2 \sin(\omega t)\right\} \\ &= \rho \exp\left\{\alpha \sin(\omega t + \phi)\right\}, \end{aligned} \tag{1.22}$$

where $\rho > 0$, $\alpha = \sqrt{\beta_1^2 + \beta_2^2}$, and $\theta = \tan^{-1}(\beta_1/\beta_2)$. This model was considered for the case when $\kappa = 1$ by Lewis (1970, 1972). When $\beta = 0$, there is no dependence of the point process on $z(\cdot)$, and then the interarrival times are independent and identically distributed gamma random variables with scale parameter ρ and shape parameter $\kappa > 0$. Berman's paper focuses on testing the null hypotheses that $\beta = 0$ against the alternative that $\beta \neq 0$. As one can see, when $\beta = 0$ in (1.21), the modulated gamma process becomes a gamma renewal process (GRP). The method of estimation in Berman's paper was to assume that ω is known, and to use a maximum likelihood based approach of estimation for β, κ, and ρ.

In Hurley (1992), a maximum likelihood iterative least squares based approach of estimating the unknown parameters in (1.22) was introduced. Hurley's method allows for more seasonal parameters to be fitted in (1.22), and his method only applies when κ is a known natural number and ω is known a priori. Hurley then estimates κ by fitting candidate models with different values of κ; then he selects κ as the value which gives rise to the candidate model with the largest maximum likelihood.

In both Berman (1981) and Hurley (1992), the frequencies of the baseline intensity function (1.22) are assumed known a priori. However, Vere-Jones (1982) considered estimating periodicity in a nonhomogeneous Poisson process (NHPP, an IGP with shape parameter $\kappa = 1$) with intensity function of the form

$$\lambda(t) = A \exp\left\{\rho \cos\left(\omega t + \phi\right)\right\}, \tag{1.23}$$

where $A > 0$, $\rho > 0$, $\omega > 0$, and ϕ $(0 < \phi < 2\pi)$ are all unknown. Vere-Jones (1982) established the asymptotic properties of a consistent estimate of the unknown frequency ω in (1.23), which is based on the maximum of the Bartlett periodogram

(1.20) over a specified frequency range. Shao and Lii (2010), generalized Vere-Jones (1982) results to estimating frequency in a NHPP (an IGP with shape parameter $\kappa = 1$) with intensity function of the form

$$\lambda(t) := \sum_{k=1}^{K} A_k \cos(\omega_k t + \phi_k) + B, \tag{1.24}$$

where $A_1 > A_2 > \cdots > A_K > 0$, $-\frac{\pi}{2} \leq \phi_k < \frac{3\pi}{2}$, $\omega_k > 0$, $B > \sum_{k=1}^{K} A_k$, and K are unknown parameters. In this thesis, we generalize the results of Shao and Lii (2010) to an IGP (a point process with joint density function of the form (1.3)) with baseline intensity function (1.24) and shape parameter $\kappa > 0$.

1.8 Some Distributional Properties of an Inhomogeneous Gamma Process with Baseline Intensity Function $\lambda_1(t)$ and Shape Parameter $\kappa > 0$

In this section, we present some distributional properties of an inhomogeneous Gamma process (IGP), $\{N_G(t),\ t > 0\}$, with a baseline intensity function $\lambda_1(t)$ and shape parameter $\kappa > 0$, which satisfy the assumptions set down in Section 1.2. We define $\Lambda_1(t) := \int_0^t \lambda_1(u)du$, let $\{dN_G(t),\ t > 0\}$ be the corresponding infinitesimal forward increment process of the IGP, and let $\{T_n,\ n \in \mathbb{N}\}$ be the corresponding random epoch sequence of the IGP. For the functional form of the variance-covariance function of the IGP, introduced below, we define

$$\begin{aligned} M_1(t) &= \int_0^t \sum_{n=1}^{\infty} \frac{u^{n\kappa-1}}{\Gamma(n\kappa)} \exp\{-u\}\, du, \\ m_1(t) &= \exp\{-t\} \sum_{n=1}^{\infty} \frac{t^{n\kappa-1}}{\Gamma(n\kappa)}, \end{aligned} \tag{1.25}$$

where $t > 0$. Only distributional properties which are relevant to the theoretical justification of the results of this thesis are provided. The proof of the claims made in this section is deferred to Appendix A.

This section is organized as follows. In Subsection 1.8.1, we introduce the first order density and the functional form of the variance-covariance function of the IGP. Furthermore, in Subsection 1.8.2, we provide some asymptotic results of the IGP. Lastly, in Subsection 1.8.3, we present some distributional properties of the IGP for the particular case of a positive integer shape parameter.

1.8.1 Some First and Second Order Density and Moment Properties of the Inhomogeneous Gamma Process with Baseline Intensity Function $\lambda_1(t)$ and Shape Parameter $\kappa > 0$

In the notation and assumptions set down in the introduction of Section 1.8, we introduce the first order density and the functional form of the variance-covariance function of the IGP.

For all $n \in \mathbb{N}$, the **probability density function of T_n** is given by[9]

$$f_{T_n}(t) = \frac{\lambda_1(t)}{\Gamma(n\kappa)} \{\Lambda_1(t)\}^{n\kappa-1} \exp\{-\Lambda_1(t)\}\, I_{\{t>0\}}. \tag{1.26}$$

[9]The proof of equation (1.26) is provided in the Appendix A.3.1.1.

The **probability density function of** T_{n+1} **conditional on** $\{T_1 = t_1,\ \ldots\ ,\ T_n = t_n\}$ is given by[10]

$$f(t \mid t_1,\ \ldots,\ t_n) = \frac{\lambda_1(t)}{\Gamma(\kappa)} \left[\Lambda_1(t) - \Lambda_1(t_n)\right]^{\kappa-1} \exp\left\{-\left(\Lambda_1(t) - \Lambda_1(t_n)\right)\right\} I_{\{0<t_1<\cdots<t_n<t\}}. \tag{1.27}$$

For $t > 0$, the **variance function of the IGP** is given by[11]

$$\operatorname{var}\{N_G(t)\} = 2\int_0^{\Lambda_1(t)} m_1(u)M_1(\Lambda_1(t)-u)du + M_1(\Lambda_1(t)) - \left[M_1(\Lambda_1(t))\right]^2. \tag{1.28}$$

For $0 < t_1 \leq t_2 < \infty$, the **covariance function of the IGP** is given by[12]

$$\begin{aligned}\operatorname{cov}\{N_G(t_1),\ N_G(t_2)\} &= \int_0^{\Lambda_1(t_1)} m_1(u)\left[M_1(\Lambda_1(t_2)-u) + M_1(\Lambda_1(t_1)-u)\right]du \\ &\quad + M_1(\Lambda_1(t_1))\left[1 - M_1(\Lambda_1(t_2))\right]. \end{aligned} \tag{1.29}$$

For $0 < t_1 \leq t_2 < \infty$, the **variance of the increment process** is given by[13]

$$\begin{aligned}\operatorname{var}\{N_G(t_1,\ t_2)\} &= 2\int_{\Lambda_1(t_1)}^{\Lambda_1(t_2)} m_1(u)\left[M_1(\Lambda_1(t_2)-u)\right]du \\ &\quad + \left[\int_{\Lambda_1(t_1)}^{\Lambda_1(t_2)} m_1(u)du\right]\left[1 - \int_{\Lambda_1(t_1)}^{\Lambda_1(t_2)} m_1(u)du\right]. \end{aligned} \tag{1.30}$$

[10]The proof of equation (1.27) is provided in the Appendix A.3.1.2.
[11]The proof of equation (1.28) is provided in the Appendix A.3.1.3.
[12]The proof of equation (1.29) is provided in the Appendix A.3.1.3.
[13]The proof of equation (1.30) is provided in the Appendix A.3.1.3.

For $0 \leq t_1 < t_2 \leq t_3 < t_4 < \infty$, the **covariance between two disjoint intervals of the IGP** is given by[14]

$$\operatorname{cov}\{N_G(t_1,\ t_2),\ N_G(t_3,\ t_4)\} =$$

$$\int_{\Lambda_1(t_1)}^{\Lambda_1(t_2)} m_1(u)\left[M_1(\Lambda_1(t_4)-u)-M_1(\Lambda_1(t_3)-u)\right]du$$
$$-\left[M_1(\Lambda_1(t_2))-M_1(\Lambda_1(t_1))\right]\left[M_1(\Lambda_1(t_4))-M_1(\Lambda_1(t_3))\right]. \qquad (1.31)$$

The **first order probability structure of the IGP counting process** is given by[15]

$$P\{N_G(t)=0\} = \int_t^{\infty} \frac{\lambda_1(u)}{\Gamma(\kappa)}\{\Lambda_1(u)\}^{\kappa-1}\exp\{-\Lambda_1(u)\}\,du \qquad (1.32)$$

$$P\{N_G(t)=n\} = \int_0^{t} \frac{\lambda_1(u)}{\Gamma(n\kappa)}\{\Lambda_1(u)\}^{n\kappa-1}\exp\{-\Lambda_1(u)\}\,du - \int_0^{t} \frac{\lambda_1(u)}{\Gamma((n+1)\kappa)}\{\Lambda_1(u)\}^{(n+1)\kappa-1}\exp\{-\Lambda_1(u)\}\,du, \qquad (1.33)$$

where $n \in \mathbb{N}$ and $t > 0$.

1.8.2 Some Asymptotic Results for the Inhomogeneous Gamma Process with Baseline Intensity Function $\lambda_1(t)$ and Shape Parameter $\kappa > 0$

In the notation and assumptions set down in the introduction of Section 1.8, we introduce some asymptotic results of the IGP.

[14] The proof of equation (1.31) is provided in the Appendix A.3.1.3.

[15] The proof of equations (1.32) and (1.33) are provided in the Appendix A.3.1.4.

As $t \to \infty$, we have

$$\frac{N_G(t) - E[N_G(t)]}{\sqrt{\mathrm{var}\left\{N_G(t)\right\}}} \xrightarrow{\mathcal{L}} Z, \tag{1.34}$$

where Z is a standard normal random variable[16] and $t > 0$. Bandyopadhyay and Sen (2005) establish that as $t \to \infty$, we have

$$M(t) = \begin{cases} \frac{\Lambda_1(t)}{\kappa} + \frac{1-\kappa}{2\kappa} + O\left(\exp\left\{-a\Lambda_1\left(t\right)\right\}\right) & \text{if} \quad \kappa \in \mathbb{N} \\ \frac{\Lambda_1(t)}{\kappa} + \frac{1-\kappa}{2\kappa} + O\left(\exp\left\{-a\Lambda_1\left(t\right)\right\}\left(\Lambda_1\left(t\right)\right)^{-\kappa-1}\right) & \text{if} \quad \kappa \in \mathbb{R}^{+}\diagdown\mathbb{N} \end{cases} \tag{1.35}$$

and

$$\lambda_2(t) = \begin{cases} \frac{\lambda_1(t)}{\kappa} + O\left(\lambda_1(t)\exp\left\{-a\Lambda_1\left(t\right)\right\}\right) & \text{if} \quad \kappa \in \mathbb{N} \\ \frac{\lambda_1(t)}{\kappa} + O\left(\lambda_1(t)\exp\left\{-a\Lambda_1\left(t\right)\right\}\left(\Lambda_1\left(t\right)\right)^{-\kappa-1}\right) & \text{if} \quad \kappa \in \mathbb{R}^{+}\diagdown\mathbb{N}, \end{cases} \tag{1.36}$$

where $M(t)$ is the mean value function of the IGP, $a \in (0,\ 2]$, $\lambda_2(t)$ is the intensity function of the IGP (1.13), and $t > 0$. Using a result from Cox (1962), we show that as $t \to \infty$, we have[17]

$$\mathrm{var}\left\{N_G(t)\right\} = \frac{\Lambda_1\left(t\right)}{\kappa^2} + \frac{1}{12} + \frac{5}{4}\frac{1}{\kappa^2} - \frac{4}{3}\frac{1}{\kappa} + o(1), \tag{1.37}$$

[16]The proof of the asymptotic normality of the IGP is provided in the Appendix A.3.2.1.

[17]The proof of equation (1.37) is provided in the Appendix A.3.2.2.

where $t > 0$.

1.8.3 Some Distributional Properties of the Inhomogeneous Gamma Process with baseline intensity function $\lambda_1(t)$ and shape parameter $\kappa \in \mathbb{N}$

In the notation and assumptions set down in the introduction of Section 1.8, we only introduce some distributional properties of the IGP when the shape parameter κ is restricted to be a positive integer.

For $\kappa \in \mathbb{N}$ and $t > 0$, the intensity function of the IGP (1.13) reduces to[18]

$$\lambda_2(t) = \lambda_1(t) \exp\{-\Lambda_1(t)\} \sum_{n=1}^{\infty} \frac{\{\Lambda_1(t)\}^{n\kappa-1}}{(n\kappa-1)!}. \tag{1.38}$$

And for the realization $\left\{T_1 = t_1,\ T_2 = t_2,\ \ldots,\ T_{N(t)} = t_{n(t)} \leq t\right\}$, Hurley (1992) showed that for $t_{n(t)} < t \leq t_{n(t)+1}$ the conditional intensity function (1.16) reduces to

$$\begin{aligned}
\lambda_2(t \mid H_t) &= \frac{\lambda_1(t)}{(\kappa-1)!} \frac{\left\{\Lambda_1(t) - \Lambda_1(t_{n(t)})\right\}^{\kappa-1}}{\sum_{i=0}^{\kappa-1} \frac{\left\{\Lambda_1(t) - \Lambda_1(t_{n(t)})\right\}^{i}}{i!}} \\
&= \lambda_1(t) P\{W(t) = \kappa - 1 \mid W(t) \leq \kappa - 1\}, \qquad (1.39)
\end{aligned}$$

where $H_t = \{N(s),\ 0 < s \leq t\}$ and $W(t)$ is a Poisson random variable with mean $\Lambda_1(t) - \Lambda_1(t_{n(t)}) = \int_{t_{n(t)}}^{t} \lambda_1(u)du$. Now, when the shape parameter is $\kappa \in \mathbb{N}$, the IGP can be viewed as a process which samples every κ-th event of a nonhomogeneous Poisson process with intensity function $\lambda_1(t)$. It then follows that for $\kappa \in \mathbb{N}$, $n =$

[18] The proof of equation (1.38) is provided in the Appendix A.3.3.1.

$0,\ 1,\ 2,\ \ldots$, and $t > 0$, we have[19]

$$P\left\{N_G(t) = n\right\} = \exp\left\{-\Lambda_1(t)\right\} \sum_{j=n\kappa}^{(n+1)\kappa-1} \frac{\left\{\Lambda_1(t)\right\}^j}{j!}. \tag{1.40}$$

For $t > 0$ and small $h > 0$, the probability of no event in an infinitely small time interval (1.8) reduces to

$$P\left\{dN_G(t) = 0\right\} = 1 - \lambda_1(t) \exp\left\{-\Lambda_1(t)\right\} \sum_{n=1}^{\infty} \frac{\left[\Lambda_1(t)\right]^{\kappa n-1}}{(\kappa n - 1)!} h + o(h). \tag{1.41}$$

For $t > 0$ and small $h > 0$, the probability of the occurrence of one event in an infinitely small time interval (1.9) reduces to

$$P\left\{dN_G(t) = 1\right\} = \lambda_1(t) \exp\left\{-\Lambda_1(t)\right\} \sum_{n=1}^{\infty} \frac{\left[\Lambda_1(t)\right]^{\kappa n-1}}{(\kappa n - 1)!} h + o(h). \tag{1.42}$$

[19]The proof of equation (1.40) is provided in the Appendix A.3.3.2.

Chapter 2

An Inhomogeneous Gamma Process Model with a Periodic or Almost Periodic Baseline Intensity Function and Shape Parameter $\kappa > 0$

2.1 Introduction

The goal of this chapter is to present a model for an inhomogeneous Gamma process (IGP) with a periodic or almost periodic baseline intensity function and shape parameter greater than zero and to provide a method of estimating unknown parameters for this model. The proposed model deals with nonstationary and non-Poisson point events which show a pattern of periodicity or almost periodicity. Consistent estimators of the baseline intensity function are constructed mainly by the Bartlett periodogram (1.20). A method of forecasting the one step ahead point event is presented. Simulation results which support theoretical findings are provided. There are many real world applications of point processes which exhibit a pattern of periodicity or almost periodicity, such as in the study of seismicity where periodic patterns of earthquakes have been detected in certain geographic regions (Vere-Jones and Ozaki (1982)), in the study of meteorology where periodic storm patterns have been observed in the Arctic Sea (Lee et al. (1991)), in study of finance where the periodic patterns of stock transactions are observed throughout the trading day (Engle (2000)), or in medical science where the periodic arrival times of emergency room patients have been observed (Lewis (1970, 1972)).

As explained in Section 1.3, the intensity function of a point process, if it exists, can be used to describe the occurrence patterns of events. If a point process has a large intensity function over a given time interval, then one should expect to observe a lot of events over this time interval and vice versa. So, if a point process data set exhibits a pattern of periodicity, the intensity function should be modeled as an almost periodic function. References which discuss modeling periodicity in an IGP are given in Section 1.7, all of which have not been in the almost periodic context. For a concise literature review of some references which have discussed parametric and nonparametric approaches of modeling periodicity of a nonhomogeneous Poisson process (which is an IGP with shape parameter equal to one), we refer to Shao and Lii (2011). In this research, we propose a more general model which includes both the periodic and almost periodic Poisson process (the work of Shao and Lii (2011)) and the gamma renewal process with shape parameter $\kappa > 0$ and the scale parameter $\lambda > 0$, as particular cases. The concept of almost periodicity and our model are introduced in the next section.

The rest of this chapter is organized as follows. In Section 2.2, we introduce the proposed model, some definitions, regularity conditions, a method for parameter estimation, and some distributional properties. In Section 2.3, we propose a method of forecasting the one step ahead point events in the framework of our model. In Section 2.4, a simulation study which supports the theoretical findings is provided. In Section 2.5, we summarize our conclusions and discuss some potential future research. Appendix B contains the proofs of the theoretical results.

2.2 The Proposed Inhomogeneous Gamma Process Model

2.2.1 An Almost Periodic Function

In this section, we give two equivalent definitions of an almost periodic function. The following description of an almost periodic function can be found in Corduneanu (1989).

Definition 6. A complex valued function $f(x)$ defined for $-\infty < x < +\infty$ is called almost periodic, if for any $\epsilon > 0$, there exists a trigonometric polynomial $T_\epsilon(x)$, such that

$$|f(x) - T_\epsilon(x)| < \epsilon, \quad -\infty < x < +\infty,$$

where the trigonometric polynomial is of the form $T(x) = \sum_{k=1}^{n} c_k \exp\{i\lambda_k x\}$, c_k are complex numbers, and λ_k are real numbers.

From the above definition, we see that almost periodic functions are those functions on the real number line which can be uniformly approximated by trigonometric polynomials. It then follows that any trigonometric polynomial is an almost periodic function. Also, any periodic function which has a Fourier series representation is just a particular case of an almost periodic function. An equivalent definition of an almost periodic function can be found in Bohr (1947), and we refer to Corduneanu (1989) for the proof of the equivalence between the two definitions.

Definition 7. Assume that the function $f(\cdot)$ is continuous on the whole real line. If for any $\epsilon > 0$, there exists a number $l(\epsilon) > 0$ with the property that any interval of length $l(\epsilon)$ of the real line contains at least one point with abscissa ξ, such that

$$|f(x+\xi) - f(x)| < \epsilon, \quad -\infty < x < +\infty,$$

then $f(x)$ is said to be an almost periodic function.

From the above definition, we see that almost periodic functions are those functions which have a particular pattern of periodicity, but there exists no period τ for which the function repeats itself exactly.

2.2.2 An Almost Periodic Inhomogeneous Gamma Process Model

When modeling point process data which exhibits a pattern of periodicity, it is more realistic to assume that the parametric form of the intensity function of the point process is an almost periodic function of time $t > 0$ as opposed to a strictly periodic function of time $t > 0$. For instance, a particular configuration which occurs once may reoccur not exactly, but within some level of accuracy. By Definition 6 of Section 2.2.1, we know that any almost periodic function can be uniformly approximated by trigonometric polynomials; therefore, we propose an inhomogeneous Gamma process (IGP) model with shape parameter $\kappa > 0$ and baseline intensity function of the form

$$\lambda_1(t) \coloneqq \sum_{k=1}^{K} A_k \cos(\omega_k t + \phi_k) + B, \tag{2.1}$$

where $A_1 > A_2 > \cdots > A_K > 0$, $-\frac{\pi}{2} \leq \phi_k < \frac{3\pi}{2}$, $\omega_k > 0$, and $t > 0$. The constant B is introduced to guarantee that $\lambda_1(t) > 0$ for all $t > 0$. A sufficient condition to guarantee that $\lambda_1(t) > 0$ for all $t > 0$ is to assume that $B > \sum_{k=1}^{K} A_k$. With a baseline intensity function of the form (2.1), equation (1.13) implies that the intensity function of the IGP takes the form

$$\begin{aligned} \lambda_2(t) \quad = \quad & \left(\sum_{k=1}^{K} A_k \cos(\omega_k t + \phi_k) + B \right) \exp\left\{ - \int_0^t \left(\sum_{k=1}^{K} A_k \cos(\omega_k u + \phi_k) + B \right) du \right\} \\ & \times \sum_{n=1}^{\infty} \frac{1}{\Gamma(n\kappa)} \left\{ \int_0^t \left(\sum_{k=1}^{K} A_k \cos(\omega_k u + \phi_k) + B \right) du \right\}^{n\kappa - 1} . \end{aligned} \tag{2.2}$$

And conditional on the realization $H_t = \{T_1 = t_1, \ \ldots \ , \ T_{n-1} = t_{n-1}, \ N_G(t) = n - 1\}$, equation (1.16) implies that for $t_{n-1} < t \leq t_n$, the conditional intensity function takes the form

$\lambda_2(t \mid H_t) =$

$$\frac{\frac{\sum_{k=1}^{K} A_k \cos(\omega_k t+\phi_k)+B}{\Gamma(\kappa)}[\int_{t_{n-1}}^{t}(\sum_{k=1}^{K} A_k \cos(\omega_k u+\phi_k)+B)du]^{\kappa-1}e^{-\int_{t_{n-1}}^{t}(\sum_{k=1}^{K} A_k \cos(\omega_k u+\phi_k)+B)du}}{\int_t^{\infty}\frac{\sum_{k=1}^{K} A_k \cos(\omega_k z+\phi_k)+B}{\Gamma(\kappa)}[\int_{t_{n-1}}^{z}(\sum_{k=1}^{K} A_k \cos(\omega_k u+\phi_k)+B)du]^{\kappa-1}e^{-\int_{t_{n-1}}^{z}(\sum_{k=1}^{K} A_k \cos(\omega_k u+\phi_k)+B)du}dz}, \tag{2.3}$$

where $t_0 = 0$ and $t > 0$. We notice that $\lambda_2(t) = \lambda_1(t)$ and $\lambda_2(t \mid H_t) = \lambda_1(t)$, for all $t > 0$, if and only if $\kappa = 1$. For an observational time period $(0,\ T]$, we wish to provide a method of estimating the unknown parameters in equations (2.1)-(2.3). To achieve this goal, we use the time truncated joint likelihood function (1.17) of the IGP and not the event truncated joint likelihood function (1.3) of the IGP. Unless some good initial conditions are specified, traditional gradient based computer optimization algorithms will generally locate a local maximum as opposed to a global maximum of equation (1.17). Therefore, a different approach of estimating the unknown parameters must be proposed. Under some regularity conditions specified in the next section, we propose a mostly Bartlett periodogram based method of estimating unknown parameters in equations (2.1)-(2.3).

2.2.3 Some Assumptions and the Proposed Method of Estimation

In this section, we propose a method for estimating most of the unknown parameters in equations (2.1)-(2.3) (A method of estimating $\kappa \in \mathbb{N}$ and $K \in \{0\} \cup \mathbb{N}$ is introduced in Chapter 3). We begin by setting down some assumptions and introducing some notation. After which, we propose a mostly Bartlett periodogram based approach of parameter estimation. Lastly, we establish the asymptotic variance-covariance structure for the proposed estimators.

Assumption 1

Assume that $\{N_G(t),\ t > 0\}$ is an inhomogeneous Gamma process (IGP) with baseline intensity function (2.1) and shape parameter $\kappa > 0$, which is observed over the time interval $(0,\ T]$. Here, the parameters $\kappa > 0$ and $K = 1,\ 2,\ \ldots$ are assumed to be known and the parameters $\boldsymbol{\theta} := \{A,\ \omega,\ \phi,\ B\}$, where $\boldsymbol{A} := \{A_1,\ \ldots,\ A_K\}$, $\boldsymbol{\omega} := \{\omega_1,\ \ldots,\ \omega_K\}$, and $\boldsymbol{\phi} := \{\phi_1,\ \ldots,\ \phi_K\}$, are assumed to be unknown.

Under a certain minimum separation condition and frequency range restrictions described below, we define the frequency estimators, $\hat{\boldsymbol{\omega}}_T := \{\hat{\omega}_{1,T},\ \ldots,\ \hat{\omega}_{K,T}\}$ of $\boldsymbol{\omega}$, as the first K local maxima of the Bartlett periodogram (1.20). It follows directly from the properties of almost periodic functions that no matter which epochs occur, there will be arbitrary large values of ω for which the Bartlett periodogram approaches arbitrarily close to its theoretical maximum of $\frac{1}{2\pi T}\left|N_G(T)\right|^2$ (Vere-Jones (1982)). Hence, the maxima of the Bartlett periodogram over too large of a frequency range would be unrelated to the existence of the periodic effects, therefore, some bounds on the frequency range must be imposed. In a paper by Vere-Jones (1982), a wide range frequency upper bound, say Ω_T, which increases sufficiently slowly with T was suggested as a suitable frequency upper bound. The need to bound the frequency interval away from 0 arises because the Bartlett periodogram will generally have a peak at the origin and some other peaks near the origin caused by leakage. Therefore, removing a neighborhood about 0 prevents the frequency estimates from converging to

0. Also, for a fixed observational time period $(0,\ T]$, it is possible for there to exist a cosinusoid with a large period and for the Bartlett periodogram not to detect it. Therefore, a frequency lower bound which decreases sufficiently slowly with T must be imposed. Without such restrictions, the search for the first K local maxima of the Bartlett periodogram becomes meaningless, so we set down the following assumption.

Assumption 2

For the observational time period $(0,\ T]$, we assume that for each $k = 1,\ 2,\ \ldots,\ K$,

$$O(T^{\delta'-1}) \leq \omega_k \leq \Omega_T,$$

where $0 < \delta' < 1$, Ω_T is an upper bound possibly determined by observations on the process in the interval $(0,\ T)$ with $E[\Omega_T] = O(T^{1-\delta})$, and $0 < \delta < 1$.

Analogous to the estimation of several harmonic components in ordinary time series, some condition must be imposed on the angular frequencies which prevent them from being too close together. Such a restriction will prevent the estimators of two angular frequencies from converging in probability to the same value (Walker (1971)). Therefore, we set down the following minimum separation restrictions.

Assumption 3

For the observational time period $(0,\ T]$, we assume that

$$\lim_{T\to\infty}\left\{\min_{1\le k\ne k'\le K} T\,|\omega_k-\omega_{k'}|\right\}=\infty.$$

In summary, in the search for the local maxima of the Bartlett periodogram, we search in a frequency range which is defined by Assumption 2 and subject to the minimum separation constraints of Assumption 3. It then follows that the shortest distance between any two frequencies can not decrease faster than $O(T^{-1})$. So for a given local maximum, $\hat{\omega}_{i,T}$ $(i=1,\ \ldots,\ K-1)$ of the Bartlett periodogram $I_T(\omega)$, we search for the next local maximum by excluding the neighborhood $|\hat{\omega}_{i,T}-\omega| = O(T^{-1+\gamma})$, where $\gamma > 0$, from the set of possible frequencies. We then define the frequencies corresponding to the first K local maxima of the Bartlett periodogram, $\hat{\boldsymbol{\omega}}_T$, as the frequency estimates of $\boldsymbol{\omega}$. Given our definition of the first K local maxima of the Bartlett periodogram, to efficiently search for the frequency estimates, one would have to sample the Bartlett periodogram more finely than $O(T^{-1})$, namely $o(T^{-1})$.

To establish the asymptotic behavior of the frequency estimates, we first begin by decomposing the infinitesimal forward increment process in terms of a deterministic component and a stochastic component

$$dN_G(t) \coloneqq E[dN_G(t)] + dZ_G(t), \tag{2.4}$$

where $dZ_G(t) := dN_G(t) - E[dN_G(t)]$ and $t > 0$. In the decomposition, the deterministic component takes the functional form of equation (1.7). So, for all $t > 0$ and as $dt \to 0^+$, we have $E[dN_G(t)] = \lambda_2(t)dt + o(dt)$, where $\lambda_2(t)$ is the intensity function of the IGP and takes the functional form of equation (2.1). By definition, it is clear that $E[dZ_G(t)] = 0$, for all $t > 0$. By Lemma 20 of Appendix B, it follows that for $0 < s < t < \infty$, $\text{cov}\{dZ_G(s),\, dZ_G(t)\} \to 0$ as $|t-s| \to \infty$ and $\text{var}\{dZ_G(t)\} \approx \frac{1}{\kappa^2}\lambda_1(t)dt$, where $\lambda_1(t)$ is the baseline intensity function (2.1) of the IGP with shape parameter $\kappa > 0$. Next, we continue by establishing a bound on the absolute value of the finite Fourier-Stieltjes transform $\frac{1}{T^m}\int_0^T t^{m-1}e^{-i\omega t}dZ_G(t)$ subject to the constraints of Assumptions 1-3, where $m \geq 1$.

Lemma 8. [1] *Let $\{N_G(t),\ t > 0\}$ be an IGP with baseline intensity function (2.1) and shape parameter $\kappa > 0$, which satisfies Assumptions 1-3, that is observed over the time interval $(0,\ T]$. Let Ω_T be a frequency upper bound, possibly determined by observations on the process in the interval $(0,\ T)$, and for $t > 0$, set*

$$dZ_G(t) := dN_G(t) - E[dN_G(t)]. \tag{2.5}$$

Then for $0 < \delta < 1$, $E[\Omega_T] = O(T^{1-\delta})$, and $m \geq 1$, we have

$$\lim_{T\to\infty} \frac{1}{T^m} \sup_{0\leq\omega\leq\Omega_T} \left| \int_0^T t^{m-1}e^{-i\omega t}dZ_G(t) \right| = 0 \qquad \text{(a.s.)}.$$

[1] The proof of Lemma 8 is provided in the Appendix B.1.1.1.

For $m \geq 1$, Lemma 8 implies that in the decomposition

$$\begin{aligned} J_T(\omega) &:= \frac{1}{T^m}\int_0^T t^{m-1}e^{-i\omega t}dN_G(t) \\ &= \frac{1}{T^m}\int_0^T t^{m-1}e^{-i\omega t}\lambda_2(t)dt + \frac{1}{T^m}\int_0^T t^{m-1}e^{-i\omega t}dZ_G(t) \\ &= J_T^{(\lambda_2)}(\omega) + J_T^{(Z_G)}(\omega), \end{aligned} \tag{2.6}$$

$J_T^{(Z_G)}(\omega)$ converges to 0 uniformly for all $\omega \in (0,\ \Omega_T]$, and equivalently, $J_T^{(\lambda_2)}(\omega)$ is the dominant term in $J_T(\omega)$. Next, we use Lemma 8 to establish the super efficiency of the frequency estimators.

Proposition 9. [2] *Under Assumptions 1-3, $\hat{\boldsymbol{\omega}}_T$ is a consistent estimator of $\boldsymbol{\omega}$, and for each $k = 1,\ 2,\ \ldots,\ K$, we have*

$$(\hat{\omega}_{T,k} - \omega_k) = o(T^{-1}) \ \ \text{(a.s.)}.$$

To investigate the asymptotic behavior of the parameter estimates, we define the random variables

$$U := T^{-\frac{1}{2}}\int_0^T dZ_G(t),$$

$$V_k := T^{-\frac{1}{2}}\int_0^T \cos(\omega_k t)dZ_G(t), \qquad W_k := T^{-\frac{1}{2}}\int_0^T \sin(\omega_k t)dZ_G(t),$$

[2]The proof of Proposition 9 is provided in the Appendix B.1.1.2, and a finer rate of convergence of the frequency estimators is provided in Proposition 11.

$$X_k := T^{-\frac{3}{2}} \int_0^T t\cos(\omega_k t) dZ_G(t), \qquad Y_k := T^{-\frac{3}{2}} \int_0^T t\sin(\omega_k t) dZ_G(t), \tag{2.7}$$

where $k = 1,\ 2,\ \ldots,\ K$.

Under the conditions placed on the angular frequencies, we use Lemma 8 to establish the asymptotic first and second order moment properties of the random variables given in equation (2.7). These asymptotic results will be used to establish the asymptotic first and second order moment properties of all the parameter estimators. For simplicity, we use the following notations $\delta_{k,k'} := I_{\{\omega_k=\omega_{k'}\}}$, $\delta_{j,k+k'} := I_{\{\omega_j=\omega_k+\omega_{k'}\}}$, $\delta_{j,k-k'} := I_{\{\omega_j=\omega_k-\omega_{k'}\}}$, and $\delta_{j,k'-k} := I_{\{\omega_j=\omega_{k'}-\omega_k\}}$, where $I_{\{\cdot\}}$ is the indicator function.

Proposition 10. *Under Assumptions 1-3 and as the observational time $T > 0$ increases, the random vector $(U,\ V_1, \ldots, V_K,\ W_1, \ldots, W_K,\ \ X_1, \ldots, X_K,\ Y_1, \ldots, Y_K)'$ has an asymptotic mean* 0 *and an asymptotic variance-covariance matrix*

$\lim_{T\to\infty} \operatorname{cov}\left\{(U,\ V_k,\ W_k,\ X_k,\ Y_k)',\ (U,\ V_{k'},\ W_{k'},\ X_{k'},\ Y_{k'})\right\}$

$$= \begin{bmatrix} \frac{1}{\kappa^2}B & \frac{A_{k'}}{2\kappa^2}\cos(\phi_{k'}) & -\frac{A_{k'}}{2\kappa^2}\sin(\phi_{k'}) & \frac{A_{k'}}{4\kappa^2}\cos(\omega_{k'}) & -\frac{A_{k'}}{4\kappa^2}\sin(\phi_{k'}) \\ \frac{A_k}{2\kappa^2}\cos(\phi_k) & E_1(k,\ k') & E_3(k,\ k') & \frac{1}{2}E_1(k,\ k') & \frac{1}{2}E_3(k,\ k') \\ -\frac{A_k}{2\kappa^2}\sin(\phi_k) & E_3(k',\ k) & E_2(k,\ k') & \frac{1}{2}E_3(k',\ k) & \frac{1}{2}E_2(k,\ k') \\ \frac{A_k}{4\kappa^2}\cos(\phi_k) & \frac{1}{2}E_1(k',\ k) & \frac{1}{2}E_3(k,\ k') & \frac{1}{3}E_1(k,\ k') & \frac{1}{3}E_3(k,\ k') \\ -\frac{A_k}{4\kappa^2}\sin(\phi_k) & \frac{1}{2}E_3(k',\ k) & \frac{1}{2}E_2(k',\ k) & \frac{1}{3}E_3(k',\ k) & \frac{1}{3}E_2(k,\ k') \end{bmatrix},$$

where

$$
\begin{aligned}
E_1(k,\ k') &:= \lim_{T\to\infty} \operatorname{cov}\{V_k,\ V_{k'}\} \\
&= \frac{1}{4\kappa^2}\sum_{j=1}^{K} A_j \cos(\phi_j)\left\{\delta_{j,\ k+k'} + \delta_{j,\ k-k'} + \delta_{j,\ k'-k}\right\} + \frac{B}{2\kappa^2}\delta_{k,\ k'}, \\
E_2(k,\ k') &:= \lim_{T\to\infty} \operatorname{cov}\{W_k,\ W_{k'}\} \\
&= \frac{1}{4\kappa^2}\sum_{j=1}^{K} A_j \cos(\phi_j)\left\{-\delta_{j,k'+k} + \delta_{j,k-k'} + \delta_{j,k'-k}\right\} + \frac{B}{2\kappa^2}\delta_{k,k'}, \\
E_3(k,\ k') &:= \lim_{T\to\infty} \operatorname{cov}\{V_k,\ W_{k'}\} \\
&= \frac{1}{4\kappa^2}\sum_{j=1}^{K} A_j \sin(\phi_j)\left\{-\delta_{j,k+k'} + \delta_{j,k-k'} - \delta_{j,k'-k}\right\},
\end{aligned}
$$

and $k,\ k' = 1,\ \ldots,\ K$. Here, the rows of the variance-covariance matrix correspond to random variables with subscript k and the columns correspond to random variables with subscript k' [3].

For each $k = 1,\ 2,\ \ldots,\ K$, the Bartlett periodogram is a twice continuously differentiable function of ω_k and $\hat{\omega}_{k,T}$ is the kth largest local maximum of the Bartlett periodogram; therefore, the first order Taylor series expansion of the derivative of the Bartlett periodogram about $\hat{\omega}_{k,T}$ is

$$
\begin{aligned}
I'_T(\omega_k) &= I'_T(\hat{\omega}_{k,T}) + I''_T(\bar{\omega}_{k,T})\left(\omega_k - \hat{\omega}_{k,T}\right) \\
&= I''_T(\bar{\omega}_{k,T})\left(\omega_k - \hat{\omega}_{k,T}\right), \qquad (2.8)
\end{aligned}
$$

for some frequency $\bar{\omega}_{k,T}$ such that $0 \le |\bar{\omega}_{k,T} - \omega_k| \le |\hat{\omega}_{k,T} - \omega_k|$. It then follows that for each $k = 1,\ 2,\ \ldots,\ K$, we have

[3] The proof of Proposition 10 is provided in the Appendix B.1.1.3.

$$T^{\frac{3}{2}}\left(\hat{\omega}_{k,T}-\omega_k\right)=-\frac{2\pi T^{-\frac{3}{2}}I_T'(\omega_k)}{2\pi T^{-3}I_T''(\bar{\omega}_{k,T})}. \tag{2.9}$$

In the notation of the random variables (2.7), we show that for each $k = 1,\ 2,\ \ldots,\ K$, we have

$$2\pi T^{-\frac{3}{2}}I_T'(\omega_k)=\frac{A_k}{\kappa}\left\{V_k\frac{1}{2}\sin(\phi_k)+W_k\frac{1}{2}\cos(\phi_k)-X_k\sin(\phi_k)-Y_k\cos(\phi_k)\right\}+o(1), \tag{2.10}$$

and using the result $|\bar{\omega}_{k,T}-\omega_k| = o(T^{-1})$ implied by Proposition 9, we show that

$$2\pi T^{-3}I_T''(\bar{\omega}_{k,T})\to-\frac{A_k^2}{24\kappa^2}\ \text{(a.s.)}, \tag{2.11}$$

as $T \to \infty$ [4]. It then follows from equations (2.10) and (2.11), that for each $k = 1,\ 2,\ \ldots,\ K$, equation (2.9) becomes

$$T^{\frac{3}{2}}\left(\hat{\omega}_{k,T}-\omega_k\right)=\frac{24\kappa}{A_k}\left\{\frac{V_k}{2}\sin(\phi_k)+\frac{W_k}{2}\cos(\phi_k)-X_k\sin(\phi_k)-Y_k\cos(\phi_k)\right\}+o(1). \tag{2.12}$$

From equation (2.12) and Proposition 10, we obtain the asymptotic variance-covariance structure of $\hat{\boldsymbol{\omega}}_T$.

Proposition 11. *Under Assumptions 1-3 and as the observational time $T > 0$ increases, $T^{\frac{3}{2}}\left(\hat{\boldsymbol{\omega}}_T-\boldsymbol{\omega}\right)$ has an asymptotic mean 0 and an asymptotic variance*

[4]The proof equation (2.11) is provided in the Appendix B.1.1.4.

$$\lim_{T\to\infty} \mathrm{var}\left\{T^{\frac{3}{2}}\left(\hat{\omega}_{k,T}-\omega_k\right)\right\} = \frac{12}{A_k^2}\left\{2B-\sum_{j=1}^{K} A_j \cos(2\phi_k-\phi_j)\delta_{j,\,k+k}\right\},$$

for each $k=1,\ \ldots,\ K$, *and an asymptotic covariance*

$$\lim_{T\to\infty} \mathrm{cov}\left\{T^{\frac{3}{2}}\left(\hat{\omega}_{k,T}-\omega_k\right),\ T^{\frac{3}{2}}\left(\hat{\omega}_{k',T}-\omega_{k'}\right)\right\}$$

$$= \frac{12}{A_k A_{k'}}\sum_{j=1}^{K} A_j\{-\cos\left(-\phi_k-\phi_{k'}+\phi_j\right)\delta_{j,k+k'} + \cos\left(\phi_k-\phi_{k'}+\phi_j\right)\delta_{j,k'-k} + \cos\left(-\phi_k+\phi_{k'}+\phi_j\right)\delta_{j,k-k'}\},$$

for each $k,\ k'=1,\ \ldots,\ K$ *and* $k\neq k'$ [5].

We proceed to define the estimators $\hat{\boldsymbol{A}}_T := \left(\hat{A}_{1,T},\ \ldots,\ \hat{A}_{K,T}\right)$ of $\boldsymbol{A}$. In the proof of Proposition 9, we established that for each $k=1,\ \ldots,\ K$,

$$\lim_{T\to\infty} |J_T(\hat{\omega}_{k,T})| = \frac{A_k}{2\kappa}, \tag{2.13}$$

where $J_T(\cdot)$ is the finite Fourier-Stieltjes transform (2.6) with $m=1$. Therefore, an estimator of A_k can be defined as

$$\hat{A}_{k,T} := 2\kappa\,|J_T(\hat{\omega}_{k,T})| = \sqrt{\frac{8\kappa^2\pi}{T} I_T(\hat{\omega}_{k,T})}, \tag{2.14}$$

[5] The proof of Proposition 11 is provided in the Appendix B.1.1.5.

where $I_T(\cdot)$ is the Bartlett periodogram (1.20) and $J_T(\cdot)$ is the finite Fourier-Stieltjes transform (2.6) with $m = 1$. To establish the asymptotic properties of $\hat{\boldsymbol{A}}_T$, for each $k = 1, \ldots, K$, we use the decomposition[6]

$$T^{\frac{1}{2}} \left(\widehat{A}^2_{k,T} - A^2_k \right) = -T^{-\frac{1}{2}} 8\kappa^2 \pi \left(I_T(\omega_k) - I_T(\hat{\omega}_{k,T}) \right) + T^{\frac{1}{2}} \left(\frac{8\kappa^2\pi}{T} I_T(\omega_k) - A^2_k \right). \quad (2.15)$$

To evaluate expression (2.15), we show that for each $k = 1, \ldots, K$,

$$\frac{I_T(\omega_k)}{T} = \frac{A^2_k}{8\pi\kappa^2} + \frac{A_k}{2\pi\kappa} \cos(\phi_k) T^{-\frac{1}{2}} V_k - \frac{A_k}{2\pi\kappa} \sin(\phi_k) T^{-\frac{1}{2}} W_k + o(1), \quad (2.16)$$

and that the second order Taylor series expansion of $I_T(\omega_k)$ about the frequency estimate $\hat{\omega}_{k,T}$ is given by

$$\begin{aligned} I_T(\omega_k) &= I_T(\hat{\omega}_{k,T}) + I'_T(\hat{\omega}_{k,T}) \left(\omega_k - \hat{\omega}_{k,T} \right) + \frac{I''_T(\bar{\omega}_{k,T})}{2!} \left(\omega_k - \hat{\omega}_{k,T} \right)^2 \\ &= I_T(\hat{\omega}_{k,T}) + \frac{I''_T(\bar{\omega}_{k,T})}{2!} \left(\omega_k - \hat{\omega}_{k,T} \right)^2, \quad (2.17) \end{aligned}$$

for some frequency $\bar{\omega}_{k,T}$, such that $0 \leq |\bar{\omega}_{k,T} - \omega_k| \leq |\hat{\omega}_{k,T} - \omega_k|$. From equations

[6]The proof of equation (2.15) is provided in the Appendix B.1.1.6.

(2.11), (2.12), (2.15), (2.16), and (2.17) it follows that for each $k = 1, \ldots, K$ [7],

$$T^{\frac{1}{2}}\left(\widehat{A}_{k,T}^2 - A_k^2\right) = 4\kappa A_k \left\{\cos(\phi_k)V_k - \sin(\phi_k)W_k\right\} + o(1). \tag{2.18}$$

From Proposition 10 and expression (2.18), we can derive the asymptotic variance-covariance structure of $\hat{\boldsymbol{A}}_T$.

Proposition 12. *Under Assumptions 1-3 and as the observational time $T > 0$ increases, $\sqrt{T}(\hat{\mathbf{A}}_T - \mathbf{A})$ has an asymptotic mean 0 and an asymptotic variance*

$$\lim_{T\to\infty} \operatorname{var}\left\{T^{\frac{1}{2}}\left(\widehat{A}_{k,T} - A_k\right)\right\} = 2B + \sum_{j=1}^{K} A_j \cos(2\phi_k - \phi_j)\delta_{j,k+k},$$

for each $k = 1, \ldots, K$, and an asymptotic covariance

$$\begin{aligned}
&\lim\nolimits_{T\to\infty} \operatorname{cov}\left\{T^{\frac{1}{2}}\left(\widehat{A}_{k,T} - A_k\right),\ T^{\frac{1}{2}}\left(\widehat{A}_{k',T} - A_{k'}\right)\right\} \\
&\qquad = \sum_{j=1}^{K} A_j\{\cos(-\phi_k - \phi_{k'} + \phi_j)\delta_{j,\,k+k'} \\
&\qquad\qquad + \cos(-\phi_k + \phi_{k'} + \phi_j)\delta_{j,\,k-k'} + \cos(\phi_k - \phi_{k'} + \phi_j)\delta_{j,\,k'-k}\},
\end{aligned}$$

for each $k,\ k' = 1, \ldots, K$ and $k \neq k'$ [8].

Next, we proceed to define the estimators $\hat{\boldsymbol{\phi}}_T := \left(\hat{\phi}_{1,T}, \ldots, \hat{\phi}_{K,T}\right)$ of $\boldsymbol{\phi}$. For each $k = 1, \ldots, K$, we first consider the case when $\phi_k \neq \pm\frac{\pi}{2}$. From the useful integral

[7] The proof of equation (2.18) is provided in the Appendix B.1.1.6.

[8] The proof of Proposition 12 is provided in the Appendix B.1.1.7.

section of the Appendix B and Lemma 8, it follows that for each $k = 1, \ldots, K$ and as $T \to \infty$, $\frac{1}{T}\int_0^T \cos(\hat{\omega}_{k,T}t)dN_G(t) \to \frac{A_k}{2\kappa}\cos(\phi_k)$ and $-\frac{1}{T}\int_0^T \sin(\hat{\omega}_{k,T}t)dN_G(t) \to \frac{A_k}{2\kappa}\sin(\phi_k)$. Therefore, for each $k = 1, \ldots, K$ and $\phi_k \neq \pm\frac{\pi}{2}$ we have the relation

$$\tan(\hat{\phi}_{k,T}) := \frac{-\frac{1}{T}\int_0^T \sin(\hat{\omega}_{k,T}t)dN_G(t)}{\frac{1}{T}\int_0^T \cos(\hat{\omega}_{k,T}t)dN_G(t)}, \tag{2.19}$$

as $T \to \infty$. On the other hand, for each $k = 1, \ldots, K$ and $\phi_k = -\frac{\pi}{2}$ or $\phi_k = \frac{\pi}{2}$, it follows from the useful integral section of the Appendix B and from Lemma 8 that $\frac{1}{T}\int_0^T \cos(\hat{\omega}_{k,T}t)dN_G(t) \to 0$ and

$$-\frac{1}{T}\int_0^T \sin(\hat{\omega}_{k,T}t)dN_G(t) \quad \to \frac{A_k}{2\kappa}\sin(\phi_k) = \begin{cases} -\frac{A_k}{2\kappa} & \text{if } \ \phi_k = -\frac{\pi}{2} \\ \\ \frac{A_k}{2\kappa} & \text{if } \ \phi_k = \frac{\pi}{2}, \end{cases} \tag{2.20}$$

as $T \to \infty$. Therefore, for each $k = 1, \ldots, K$, a natural estimator of ϕ_k is

$$\hat{\phi}_{k,T} := \begin{cases} \tan^{-1}\left\{\frac{-\frac{1}{T}\int_0^T \sin(\hat{\omega}_{k,T}t)dN_G(t)}{\frac{1}{T}\int_0^T \cos(\hat{\omega}_{k,T}t)dN_G(t)}\right\} & \text{if } \ \frac{1}{T}\int_0^T \cos(\hat{\omega}_{k,T}t)dN_G(t) > 0 \\ \tan^{-1}\left\{\frac{-\frac{1}{T}\int_0^T \sin(\hat{\omega}_{k,T}t)dN_G(t)}{\frac{1}{T}\int_0^T \cos(\hat{\omega}_{k,T}t)dN_G(t)}\right\} + \pi & \text{if } \ \frac{1}{T}\int_0^T \cos(\hat{\omega}_{k,T}t)dN_G(t) < 0 \\ \frac{\pi}{2}\mathrm{sgn}\left\{-\frac{1}{T}\int_0^T \sin(\hat{\omega}_{k,T}t)dN_G(t)\right\} & \text{if } \ \frac{1}{T}\int_0^T \cos(\hat{\omega}_{k,T}t)dN_G(t) = 0. \end{cases} \tag{2.21}$$

To establish the asymptotic variance-covariance structure of $\hat{\boldsymbol{\phi}}_T$, for each $k = 1, \ldots, K$, we use the decomposition

$$
\begin{aligned}
T^{\frac{1}{2}}\left\{\tan(\hat{\phi}_{k,T})-\tan(\phi_k)\right\} &= T^{\frac{1}{2}}\left\{\tan(\hat{\phi}_{k,T})+\frac{\frac{1}{T}\int_0^T \sin(\omega_k t)dN_G(t)}{\frac{1}{T}\int_0^T \cos(\omega_k t)dN_G(t)}\right\} \\
&\quad +T^{\frac{1}{2}}\left\{\frac{-\frac{1}{T}\int_0^T \sin(\omega_k t)dN_G(t)}{\frac{1}{T}\int_0^T \cos(\omega_k t)dN_G(t)}-\tan(\phi_k)\right\}. \quad (2.22)
\end{aligned}
$$

Then, we show that for each $k = 1, \ldots, K$, we have [9]

$$
\begin{aligned}
T^{\frac{1}{2}}\left\{\tan(\hat{\phi}_{k,T})+\frac{\frac{1}{T}\int_0^T \sin(\omega_k t)dN_G(t)}{\frac{1}{T}\int_0^T \cos(\omega_k t)dN_G(t)}\right\} &= -\frac{12\kappa}{A_k\cos^2(\phi_k)}\{\frac{V_k}{2}\sin(\phi_k)+\frac{W_k}{2}\cos(\phi_k) \\
&\quad -X_k\sin(\phi_k)-Y_k\cos(\phi_k)\}+o(1) \quad (2.23)
\end{aligned}
$$

and

$$
\begin{aligned}
&T^{\frac{1}{2}}\left\{\frac{-\frac{1}{T}\int_0^T \sin(\omega_k t)dN_G(t)}{\frac{1}{T}\int_0^T \cos(\omega_k t)dN_G(t)}-\tan(\phi_k)\right\} \\
&\qquad = -\frac{2\kappa}{A_k\cos^2(\phi_k)+o(1)}\left\{\cos(\phi_k)W_k+\sin(\phi_k)V_k\right\}+o(1). \quad (2.24)
\end{aligned}
$$

Therefore, from relations (2.23) and (2.24) it follows that

$$
\begin{aligned}
T^{\frac{1}{2}}\left\{\tan(\hat{\phi}_{k,T})-\tan(\phi_k)\right\} &= -\frac{4\kappa}{A_k\cos^2(\phi_k)}\{2\sin(\phi_k)V_k+2\cos(\phi_k)W_k \\
&\quad -3X_k\sin(\phi_k)-3Y_k\cos(\phi_k)\}+o(1). \quad (2.25)
\end{aligned}
$$

We use relation (2.25) to establish the asymptotic variance-covariance structure of $\hat{\boldsymbol{\phi}}_T$.

[9] The proof of equations (2.23) and (2.24) are provided within the proof of Proposition 13 in the Appendix B.1.1.8.

Proposition 13. *Under Assumptions 1-3 and as the observational time $T > 0$ increases, $\sqrt{T}(\hat{\phi}_T - \phi)$ has an asymptotic mean 0 and an asymptotic variance*

$$\lim_{T\to\infty} \mathrm{var}\left\{T^{\frac{1}{2}}\left(\hat{\phi}_{k,T} - \phi_k\right)\right\} = \frac{4}{A_k^2}\left\{2B - \sum_{j=1}^{K} A_j \cos\left(-2\phi_k + \phi_j\right)\delta_{j,\, k+k}\right\}$$

for each $k = 1, \ldots, K$ and an asymptotic covariance

$$\begin{aligned}
&\lim\nolimits_{T\to\infty} \mathrm{cov}\left\{T^{\frac{1}{2}}\left(\hat{\phi}_{k,T} - \phi_k\right),\, T^{\frac{1}{2}}\left(\hat{\phi}_{k',T} - \phi_{k'}\right)\right\} \\
&\quad = \frac{4}{A_k A_{k'}} \sum_{j=1}^{K} A_j \{-\cos\left(-\phi_k - \phi_{k'} + \phi_j\right)\delta_{j,\, k+k'} \\
&\qquad + \cos\left(-\phi_k + \phi_{k'} + \phi_j\right)\delta_{j,\, k-k'} + \cos\left(\phi_k - \phi_{k'} + \phi_j\right)\delta_{j,\, k'-k}\},
\end{aligned}$$

for each $k,\ k' = 1, \ldots, K$ and $k \neq k'$ [10].

Lastly, we propose an estimator $\hat{\boldsymbol{B}}_T$ of B. Given the functional form of the baseline intensity function (2.1), it follows from equation (1.35) that

$$\lim_{T\to\infty} \frac{1}{T} E\left[N_G(T)\right] = \lim_{T\to\infty} \frac{1}{T}\frac{1}{\kappa}\int_0^T \left(\sum_{k=1}^{K} A_k \cos(\omega_k u + \phi_k) + B\right) du = \frac{B}{\kappa}. \tag{2.26}$$

Therefore, we define

$$\hat{\boldsymbol{B}}_T \;\; := \;\; \frac{1}{T} N_G(T)\kappa \tag{2.27}$$

[10]The proof of Proposition 13 is provided in the Appendix B.1.1.8.

as an estimator of B. We note that Lemma 18 of Appendix B implies that $\hat{\boldsymbol{B}}_T \to B$ almost surely as $T \to \infty$. Using (1.34), we can obtain a central limit theorem for $\hat{B}_T$.

Proposition 14. *Under Assumptions 1-3 and as the observational time $T > 0$ increases,*

$$T^{\frac{1}{2}} \left(\hat{B}_T - B \right) \xrightarrow{\mathcal{L}} ND(0,\ B), \tag{2.28}$$

where $ND(0,\ B)$ is a normal distribution with mean 0 *and variance $B > 0$* [11].

Using the Bartlett periodogram estimates, we show that the estimator of the baseline intensity function is $\hat{\lambda}_{1,T}(T) = \lambda_1(T) + O(T^{-\frac{1}{2}})$, so for large $T > 0$, $\hat{\lambda}_{1,T}(T)$ is asymptotically non-negative[12]. For a finite sample, the estimate $\hat{\boldsymbol{B}}_T = \frac{1}{T} N_G(T)\kappa$ may lead to a negative $\hat{\lambda}_{1,T}(t)$, for some values of $t \in (0,\ T]$. Since we made the assumption that $B > \sum_{k=1}^{K} A_k$, defining $\hat{\boldsymbol{B}}_T := \max\left\{\frac{1}{T} N_G(T)\kappa,\ \sum_{k=1}^{K} \hat{A}_k\right\}$ would guarantee that $\hat{\lambda}_{1,T}(t) > 0$ for all $t \in (0,\ T]$. Such an estimator of B will be asymptotically equal to $\frac{1}{T} N_G(T)\kappa$. In our simulation study, we use the estimator $\hat{\boldsymbol{B}}_T = \max\left\{\frac{N_G(T)}{T}\kappa,\ \sum_{k=1}^{K} \hat{A}_k\right\}$. We close this section by presenting the correlations between all of the parameter estimators.

Proposition 15. *Under Assumptions 1-3 and as the observational time $T > 0$ increases, $T^{\frac{3}{2}}(\hat{\boldsymbol{\omega}}_T - \boldsymbol{\omega})$, $\sqrt{T}\left(\hat{\mathbf{A}}_T - \mathbf{A}\right)$, $\sqrt{T}\left(\hat{\boldsymbol{\phi}}_T - \boldsymbol{\phi}\right)$, and $\sqrt{T}\left(\hat{B}_T - B\right)$ have an asymptotic mean* 0 *and an asymptotic variance-covariance*

[11] The proof of Proposition 14 follows from result (1.34).

[12] The proof of the claim that $\hat{\lambda}_{1,T}(T) = \lambda_1(T) + O(T^{-\frac{1}{2}})$ is provided in the Appendix B.1.1.10.

$$\lim_{T\to\infty} \mathrm{cov}\left\{T^{\frac{3}{2}}\left(\hat{\omega}_{k,T}-\omega_k\right),\ \sqrt{T}\left(\hat{\phi}_{k',T}-\phi_{k'}\right)\right\}$$

$$= \frac{6}{A_k A_{k'}}\{-2B\cos(\phi_k-\phi_{k'})\delta_{k,k'} + \sum_{j=1}^{K} A_j[\cos\left(-\phi_k-\phi_{k'}+\phi_j\right)\delta_{j,k+k'} - \cos\left(-\phi_k+\phi_{k'}+\phi_j\right)\delta_{j,k-k'} - \cos\left(\phi_k-\phi_{k'}+\phi_j\right)\delta_{j,k'-k}]\},$$

$$\lim_{T\to\infty} \mathrm{cov}\left\{\sqrt{T}\left(\hat{A}_{k,T}-A_k\right),\ \sqrt{T}\left(\hat{\phi}_{k',T}-\phi_{k'}\right)\right\}$$

$$=\frac{1}{A_{k'}}\sum_{j=1}^{K} A_j\{\sin\left(-\phi_k-\phi_{k'}+\phi_j\right)\delta_{j,\,k+k'} - \sin\left(-\phi_k+\phi_{k'}+\phi_j\right)\delta_{j,\,k-k'} + \sin\left(\phi_k-\phi_{k'}+\phi_j\right)\delta_{j,\,k'-k}\},$$

$$\lim_{T\to\infty} \mathrm{cov}\left\{\sqrt{T}\left(\widehat{A}_{k,T}-A_k\right),\ \sqrt{T}\left(\hat{B}_T-B\right)\right\} = A_k,$$
$$\lim_{T\to\infty} \mathrm{cov}\left\{T^{\frac{3}{2}}\left(\hat{\omega}_{k,T}-\omega_k\right),\ \sqrt{T}\left(\hat{A}_{k',T}-A_{k'}\right)\right\} = 0,$$
$$\lim_{T\to\infty} \mathrm{cov}\left\{T^{\frac{3}{2}}\left(\hat{\omega}_{k,T}-\omega_k\right),\ \sqrt{T}\left(\hat{B}_T-B\right)\right\} = 0,$$
$$\lim_{T\to\infty} \mathrm{cov}\left\{\sqrt{T}\left(\hat{\phi}_{k,T}-\phi_k\right),\ \sqrt{T}\left(\hat{B}_T-B\right)\right\} = 0,$$

where $k,\ k' = 1,\ \ldots,\ K$ [13].

2.3 Forecasting

Let $\{N_G(t),\ t>0\}$ be an inhomogeneous Gamma process (IGP) which satisfies Assumptions 1-3 of Section 2.2. In this section, we first investigate the problem of forecasting the one step ahead point event, say $T_{N_G(T)+1} = t_{n(T)+1}$, conditional on the history, $H_T = \left\{T_1 = t_1,\ \ldots\ ,\ T_{N_G(T)} = t_{n(T)}\right\}$, of the (IGP) up to and including the current time $T>0$. Furthermore, we describe how to construct a $100\,(1-\alpha)\,\%$ upper prediction bound a for the one step ahead point event forecast, where α is

[13] The proof of Proposition 15 is provided in the Appendix B.1.1.9.

the probability of a type one error and $a > T > 0$. Lastly, under the assumption that the shape parameter $\kappa \in \mathbb{N}$ and conditional on the first $n \in \mathbb{N}$ point events $T_1 = t_1, \ldots, T_n = t_n$, we present a method of predicting the one step ahead point event $T_{n+1} = t_{n+1}$.

We begin by considering the prediction for the one step ahead point event, $T_{N_G(T)+1} = t_{n(T)+1}$, conditional on the history, $H_T = \left\{T_1 = t_1, \ldots, T_{N_G(T)} = t_{n(T)}\right\}$, of the (IGP) up to and including the current time $T > 0$. For $T > 0$, the **forward waiting time**, say $\mathbf{w_T}$, is defined to be the time to the next epoch measured from the current time T. For $w \geq 0$, it follows from Pulcini (2003) that the cumulative distribution function of $\mathbf{w_T}$ is given by

$$P\left\{\mathbf{w_T} \leq w \mid H_T\right\} = 1 - \exp\left\{-\int_T^{T+w} \lambda_2(u \mid H_u)du\right\}, \tag{2.29}$$

where $H_T = \left\{T_1 = t_1, \ldots, T_{N_G(T)} = t_{n(T)}\right\}$ is the history of the IGP at the current time $T > 0$, $\lambda_2(t \mid H_T)$ is the conditional intensity function defined in equation (2.3), and $t \geq T$. To account for the elapsed time between the current time $T > 0$ and the last event time before or at the current time T, we define the one step ahead point event forecast as the expected value of the forward waiting time $\mathbf{w_T}$ plus the current time T.

Proposition 16. *Under Assumptions 1-3 of Section 2.2 and conditional on the history, say $H_T = \{T_1 = t_1, \ldots, T_{N_G(T)} = t_{n(T)}\}$, of the IGP at the current time $T > 0$,* *the one step ahead point event forecast of* $T_{n(T)+1} = t_{n(T)+1}$*, say* $\hat{T}_{n(T)+1}$*, is given by*

$$\begin{aligned}\hat{T}_{n(T)+1} &\coloneqq T + E\left[\mathbf{w_T} \mid H_T\right] \\ &= T + \int_0^\infty \exp\left\{-\int_0^w \lambda_2(T+y \mid H_{T+y})dy\right\} dw \qquad (2.30)\end{aligned}$$

and its mean squared error (MSE) is given by

$$\begin{aligned}\nu_{n(T)} &\coloneqq E\left[\left(T_{n(T)+1} - \hat{T}_{n(T)+1}\right)^2\right] \\ &= E_{H_T}[2\int_0^\infty w \exp\left\{-\int_0^w \lambda_2(T+y \mid H_{T+y})dy\right\} dw \\ &\quad -\left[\int_0^\infty \exp\left\{-\int_0^w \lambda_2(T+y \mid H_{T+y})dy\right\} dw\right]^2], \qquad (2.31)\end{aligned}$$

where $N_G(T) = n(T)$ *is the observed count at the current time* $T > 0$*,* $\lambda_2(t \mid H_t)$ *is the conditional intensity function defined in equation (2.3), and* $t > 0$ [14].

The calculation of the MSE, $\nu_{n(T)}$, is carried out by Monte Carlo integration with the following steps.

Step 1. For an observational time period $(0,\ T]$, generate a large sample of realizations of the IGP,

$$H_T^i = \left\{T_1^i = t_1^i,\ \ldots,\ T_{N_{G_i}(T)}^i = t_{n_i(T)}^i\right\},$$

[14] The proof of Proposition 16 is provided in the Appendix B.1.2.1.

where $i = 1,\ 2, \ldots$ is the i-th realization.

Step 2. For each realization, calculate

$$2 \int_0^\infty w \exp\left\{-\int_0^w \lambda_2(T + y \mid H^i_{T+y}) dy\right\} dw \\ - \left[\int_0^\infty \exp\left\{-\int_0^w \lambda_2(T + y \mid H^i_{T+y}) dy\right\} dw\right]^2,$$

and average over the number of realizations generated.

Suppose that instead of predicting $T_{n(T)+1} = t_{n(T)+1}$ with an IGP which satisfies Assumptions 1-3 of Section 2.2, we predict $t_{n(T)+1}$ with a homogeneous Poisson process (HPP) with intensity function $\widetilde{\lambda}_1(t) = \frac{B}{\kappa} > 0$, where $t > 0$. Denote such a predictor of $t_{n(T)+1}$ with $\widetilde{T}^{HPP}_{n(T)+1}$, where $\widetilde{T}^{HPP}_{n(T)+1} = T + \frac{\kappa}{B}$. In terms of MSE, the improvement in predicting $t_{n(T)+1}$ with $\hat{T}_{n(T)+1}$, as opposed to predicting $t_{n(T)+1}$ with $\widetilde{T}^{HPP}_{n(T)+1}$, is

$$\begin{aligned} \mu^{HPP}_{n(T)} &:= E\left[\left(T_{n(T)+1} - \widetilde{T}^{HPP}_{n(T)+1}\right)^2\right] - E\left[\left(T_{n(T)+1} - \hat{T}_{n(T)+1}\right)^2\right] \\ &= E_{H_T}\left[\left(\int_0^\infty \exp\left\{-\int_0^w \lambda_2(T + y \mid H_{T+y}) dy\right\} dw - \frac{\kappa}{B}\right)^2\right], \end{aligned} \tag{2.32}$$

and can be calculated by Monte Carlo integration with a procedure similar to that discussed above[15]. We notice that the improvement is $\mu^{HPP}_{n(T)} = 0$ if and only if $\kappa = 1$ and for each $k = 1,\ 2,\ \ldots,\ K$, $A_k = 0$.

Suppose that instead of predicting $T_{n(T)+1} = t_{n(T)+1}$ with an IGP which satisfies

[15]The proof of equation (2.32) is provided in the Appendix B.1.2.2.

Assumptions 1-3 of Section 2.2, we predict $t_{n(T)+1}$ with a nonhomogeneous Poisson process (NHPP) with intensity function $\widetilde{\lambda}_1(t) = \frac{1}{\kappa}\lambda_1(t) > 0$. Denote such a predictor of $t_{n(T)+1}$ with $\widetilde{T}_{n(T)+1}^{NHPP}$, where $\widetilde{T}_{n(T)+1}^{NHPP} = T + \int_0^\infty \exp\{-\frac{1}{\kappa}\int_0^w \lambda_1(T+y)dy\}dw$. In terms of MSE, the improvement in predicting $t_{n(T)+1}$ with $\hat{T}_{n(T)+1}$, as opposed to predicting $t_{n(T)+1}$ with $\widetilde{T}_{n(T)+1}^{NHPP}$, is

$$\begin{aligned}
\mu_{n(T)}^{NHPP} &:= E\left[\left(T_{n(T)+1} - \widetilde{T}_{n(T)+1}^{NHPP}\right)^2\right] - E\left[\left(T_{n(T)+1} - \hat{T}_{n(T)+1}\right)^2\right] \\
&= E_{H_T}[(\int_0^\infty \exp\{-\int_0^w \lambda_2(T+y \mid H_{T+y})dy\}dw \\
&\qquad - \int_0^\infty \exp\{-\frac{1}{\kappa}\int_0^w \lambda_1(T+y)dy\}dw)^2], \quad (2.33)
\end{aligned}$$

and can be calculated by Monte Carlo integration with a procedure similar to that discussed above[16]. We notice that the improvement is $\mu_{n(T)}^{NHPP} = 0$ if and only if $\kappa = 1$.

Next, we describe how to construct a $100\,(1-\alpha)\,\%$ upper prediction bound a for the one step ahead point event forecast, where α is the probability of a type one error and $a > T > 0$. From equation (2.29), it follows that for $a > T > 0$, $P\left\{\mathbf{w_T} \le a - T \mid H_T\right\} = 1-\alpha$ when $1 - \exp\left\{-\int_T^a \lambda_2(y \mid H_y)dy\right\} = 1-\alpha$. Therefore, a one-sided $(1-\alpha)\,100\%$ upper prediction bound for $T_{n(T)+1} = t_{n(T)+1}$ is of the form $(T,\ a]$, where a is the solution to the equation $\exp\left\{-\int_T^a \lambda_2(y \mid H_y)dy\right\} = \alpha$. In a similar fashion, one can use the conditional density (2.29) to construct two-sided prediction intervals.

[16]The proof of equation (2.33) is provided in the Appendix B.1.2.2.

We now present a method of forecasting the one step ahead point event, say $T_{n+1} = t_{n+1}$, from an event time $T_n = t_n$ given $T_1 = t_1, \ldots, T_n = t_n$, where $n = 1, 2, \ldots$ and the shape parameter of the IGP is a positive integer. We define the one step ahead point event forecast of t_{n+1} as $\hat{T}_{n+1} \coloneqq E\left[T_{n+1} \mid T_1, \ldots, T_n\right]$.

Proposition 17. *Upon observing the first n point events, $T_1 = t_1, \ldots, T_n = t_n$, of an IGP with baseline intensity function $\lambda_1(\cdot) > 0$, defined as in equation (2.1), with given shape parameter $\kappa = 1, 2, \ldots$, which satisfies Assumptions 1-3 of Section 2.2, the one step ahead point event forecast of $T_{n+1} = t_{n+1}$, say $\hat{T}_{n+1}$, is given by*

$$\begin{aligned}
\hat{T}_{n+1} &\coloneqq E\left[T_{n+1} \mid T_1 = t_1, \ldots, T_n = t_n\right] \\
&= t_n + \int_{t_n}^{\infty} \exp\left\{-\int_{t_n}^{s} \lambda_1(x)dx\right\} \sum_{i=0}^{\kappa-1} \frac{\left[\int_{t_n}^{s} \lambda_1(x)dx\right]^i}{i!} ds \\
&= t_n + \int_{t_n}^{\infty} P\left\{W(s) - W(t_n) \le \kappa - 1\right\} ds, \qquad (2.34)
\end{aligned}$$

where $\{W(t),\ t > 0\}$ is a nonhomogeneous Poisson process with intensity function $\lambda_1(\cdot) > 0$ [17].

2.4 A Simulation Study

In this section, we evaluate the performance of our method of parameter estimation through simulation. We consider sixteen different inhomogeneous Gamma process

[17] The proof of Proposition 17 is provided in the Appendix B.1.2.3.

(IGP) models with a given periodic or almost periodic baseline intensity function of the form

$$\begin{aligned}
\text{Case} \quad 1: \lambda_1(t) &= 1.6 + \cos\left(\frac{\pi}{4\sqrt{3}}t\right) + \frac{1}{2}\cos\left(\frac{\pi}{3\sqrt{2}}t + \frac{\pi}{4}\right), \\
\text{Case} \quad 2: \lambda_1(t) &= \sqrt{3.1 + 3\cos\left(\frac{\pi}{3\sqrt{2}}t\right)}, \\
\text{Case} \quad 3: \lambda_1(t) &= 0.1 + \frac{1}{2}\text{mod}\,[t,\ 2\pi], \\
\text{Case} \quad 4: \lambda_1(t) &= 1.3\exp\left\{\cos\left(\frac{\pi}{3\sqrt{2}}t + \frac{\pi}{4}\right)\right\},
\end{aligned}$$

and with a given shape parameter $\kappa \in \{2,\ 5,\ 10,\ 15\}$, where $t > 0$.

Each of the above baseline intensity functions was considered in Shao and Lii (2011) in the context of a nonhomogeneous Poisson process (NHPP) (an IGP with shape parameter $\kappa = 1$). The intensity function in Case 1 is almost periodic but is not periodic since the ratio of the two frequencies, $\frac{\pi}{4\sqrt{3}}$ and $\frac{\pi}{3\sqrt{2}}$, is not a rational number, so the function never repeats itself exactly. The baseline intensity functions of Cases 2-4 are not of the same functional form of equation (2.1), but can be well approximated by a functional of the form given in equation (2.1). In particular, Case 4 has a similar functional form as equation (1.22) and was considered in Lewis (1970, 1972) and in Vere-Jones (1982) in the context of a NHPP.

We generate each IGP model by using the Lewis and Shedler (1979) Thinning Algorithm to simulate a NHPP with a given baseline intensity function, then sample each κ event of the simulated NHPP. The sub-sampled NHPP epochs are then defined

	Case 1	Case 2	Case 3	Case 4
T	1000	1000	1000	1000
$N_G(T)$	[737, 837]	[764, 873]	[769, 888]	[779, 872]
κ	2	2	2	2
T	2500	2500	2500	2500
$N_G(T)$	[769, 834]	[777, 827]	[805, 870]	[779, 849]
κ	5	5	5	5
T	5000	5000	5000	5000
$N_G(T)$	[775, 824]	[781, 826]	[809, 857]	[795, 844]
κ	10	10	10	10
T	8000	8000	8000	8000
$N_G(T)$	[833, 867]	[841, 880]	[874, 913]	[858, 905]
κ	15	15	15	15

Table 2.1: For each of the 100 independently simulated replicates of the inhomogeneous Gamma process, this table contains the baseline intensity function case along with the corresponding observational length $T > 0$, observed sample size $N_G(T) = n(T)$, and the true shape parameter $\kappa > 0$. For example, the values in the upper left hand corner of this table correspond to the 100 Case 1 replicates which had observational length $T = 1000$, observed sample size $737 \leq N_G(T) \leq 837$, and shape parameter 2.

to be the epochs of the IGP model. There are 100 independent replicates of each baseline intensity function case and shape parameter combination. Table 2.1 describes the observational length $T > 0$, observed sample size $N_G(T) = n(T)$, and shape parameter $\kappa > 0$ for each of the simulated IGP models. For example, the values in the upper left hand corner of this table, correspond to the 100 Case 1 replicates which had observational length $T = 1000$, observed sample size $737 \leq N_G(T) \leq 837$, and shape parameter 2. For a given baseline intensity function and for a shape parameter that is $\kappa \geq 1$, as κ increases, the rate of occurrence decreases. Therefore, to maintain a similar sample size in each of the simulations, as we increase κ, we increase the observational time period $T > 0$. We estimate each baseline intensity function in the framework of our model and compare the estimated baseline intensity function with the true baseline intensity function. For the estimation procedure of Case 1, we fit our model assuming that we knew the true κ and the true K parameter values a priori, where K is the number of periodic components in the baseline intensity function. In Chapter 3, we propose the Akaike information criterion (AIC) and the Bayesian information criterion (BIC) method of selecting candidate values for the $\kappa \in \mathbb{N}$ and $K \in \{0\} \cup \mathbb{N}$ parameters. Likewise, for the estimation procedure of Cases 2-4, we fit our model assuming we knew the true κ parameter value a priori. However, we used the AIC and the BIC model selection results provided in Tables 3.1-3.4 to propose a parameter value for K. The details of the estimation procedure of the κ and K parameters values are provided in Chapter 3. More explicitly, based on the model selection results of Table 3.2, we fit the simulated Case 2 models assuming $K = 1$. Likewise, based on the model selection results of Table 3.3, we fit the simulated Case 3 models assuming $K = 2$. Finally, based on the model selection results of Table 3.4, we fit the simulated Case 4 models assuming $K = 1$. In Figures 2.1-2.4, plots (a)-(d) display the true baseline intensity function in solid black and the 100 estimated baseline intensity functions from the 100 replicates (the gray curves) for Cases 1-4, respectively. This gives a rough idea of the distribution of the estimated baseline intensity function over the time interval $t \in (0,\ T]$. More explicitly, in Figures 2.1-2.4 plots (a)-(d) display the estimated baseline intensity functions with plot (a) displaying the case when the true $\kappa = 2$, plot (b) displaying the case when the true $\kappa = 5$, plot (c) displaying the case when the true $\kappa = 10$, and plot (d) displaying the case when the true $\kappa = 15$.

We also conduct the out of sample one step ahead point forecast by using the estimated baseline intensity function in conjunction with the forecasting procedures of Section 2.3. That is, based on the observational period $T > 0$, we use the observed data $\left\{T_1 = t_1,\ \ldots,\ T_{N_G(T)} = t_{n(T)}\right\}$ to estimate the unknown baseline intensity function. Then, using Proposition 16, we forecast the out of sample point event $T_{N_G(T)+1} = t_{n(T)+1}$ from time $T > 0$. After that, for each $i = 2,\ 3,\ \ldots,\ 50$, we again use Proposition 16 to forecast the out of sample point events $T_{N_G(T)+i} = t_{n(T)+i}$ from the true point event $T_{N_G(T)+i-1} = t_{n(T)+i-1}$. Next, we compare the one step ahead point event forecast mean square error (MSE) of the predictions made based on the fitted IGP model to the one step ahead point event forecast MSE of the predictions made based on fitting a NHPP model with intensity function (2.1) (an IGP with shape parameter $\kappa = 1$). Likewise, we compare the one step ahead point event forecast MSE of the predictions made based on the fitted IGP model to the one step ahead point event forecast MSE of the predictions made based on fitting a HPP model with intensity function $\lambda_1(t) = \lambda$ (an IGP with baseline intensity function $\lambda_1(t) = \lambda$ and shape parameter $\kappa = 1$), where $t > 0$. That is, for each $i = 1,\ 2,\ \ldots,\ 50$, we compare the MSE ratios

$$\begin{aligned} MSE_{NHPP}^{IGP} &:= \frac{\frac{1}{100}\sum_{j=1}^{100}\left(t_{n_j(T)+i} - \hat{T}_{n_j(T)+i}\right)^2}{\frac{1}{100}\sum_{j=1}^{100}\left(t_{n_j(T)+i} - \tilde{T}_{n_j(T)+i}\right)^2} \\ MSE_{HPP}^{IGP} &:= \frac{\frac{1}{100}\sum_{j=1}^{100}\left(t_{n_j(T)+i} - \hat{T}_{n_j(T)+i}\right)^2}{\frac{1}{100}\sum_{j=1}^{100}\left(t_{n_j(T)+i} - \check{T}_{n_j(T)+i}\right)^2}, \end{aligned} \tag{2.35}$$

where $t_{n_j(T)+i}$ ($i = 1,\ 2,\ \ldots,\ 50$) is the true $(n_j(T) + i)$-th point event of the j-th realization, and $\hat{T}_{n_j(T)+i}$, $\tilde{T}_{n_j(T)+i}$, and $\check{T}_{n_j(T)+i}$ are the out of sample one step ahead predictions of $t_{n_j(T)+i}$ under the IGP, NHPP, and HPP models, respectively. In Figures 2.5-2.8, plots (a)-(d) display the 50 out of sample point forecast MSE ratios of equation (2.35) for Cases 1-4, respectively. That is, in Figures 2.5-2.8 plots (a)-(d) display the 50 out of sample point forecast MSE ratios with plot (a) displaying the case when the true $\kappa = 2$, plot (b) displaying the case when the true $\kappa = 5$, plot (c) displaying the case when the true $\kappa = 10$, and plot (d) displaying the case when the true $\kappa = 15$. In each of the plots (a)-(b), the horizontal dashed line represents a MSE ratio equal to 1. Asymptotically, the MSE ratio is expected to be below one for every $n \geq 1$. The peaks in the MSE ratio plots which are greater than 1 are caused by random variation of the processes. Table 2.2 gives the average forecast MSE reduction of using our model as opposed to using a NHPP or a HPP model. Overall, the simulation results demonstrate that our model can capture most of the variation of any periodic or almost periodic baseline intensity function of an IGP with shape parameter $\kappa > 0$.

To verify the theoretical results of Section 2.2, for each $\kappa \in \{2, 5, 10, 15\}$, we calculate the sample means and standard errors of the parameter estimates from the 100 independent replicates of Case 1 and display them in Table 2.3. As one can see, the sample means are close to the true parameter values and the sample standard deviations are close to the asymptotic standard deviation results of Section 2.2.

2.5 Discussion and Conclusion

In this chapter, we have proposed a very general model for an inhomogeneous Gamma process (IGP) which can have a baseline intensity function that can be periodic or almost periodic in any shape. Through simulation, we demonstrated the ability of our model to capture the form of various periodic or almost periodic baseline intensity functions. The parameter estimation was based on the Bartlett periodogram. Other estimation procedure, such as the method of maximum likelihood estimation (MLE), can be considered but may be too computationally intensive. The parameter

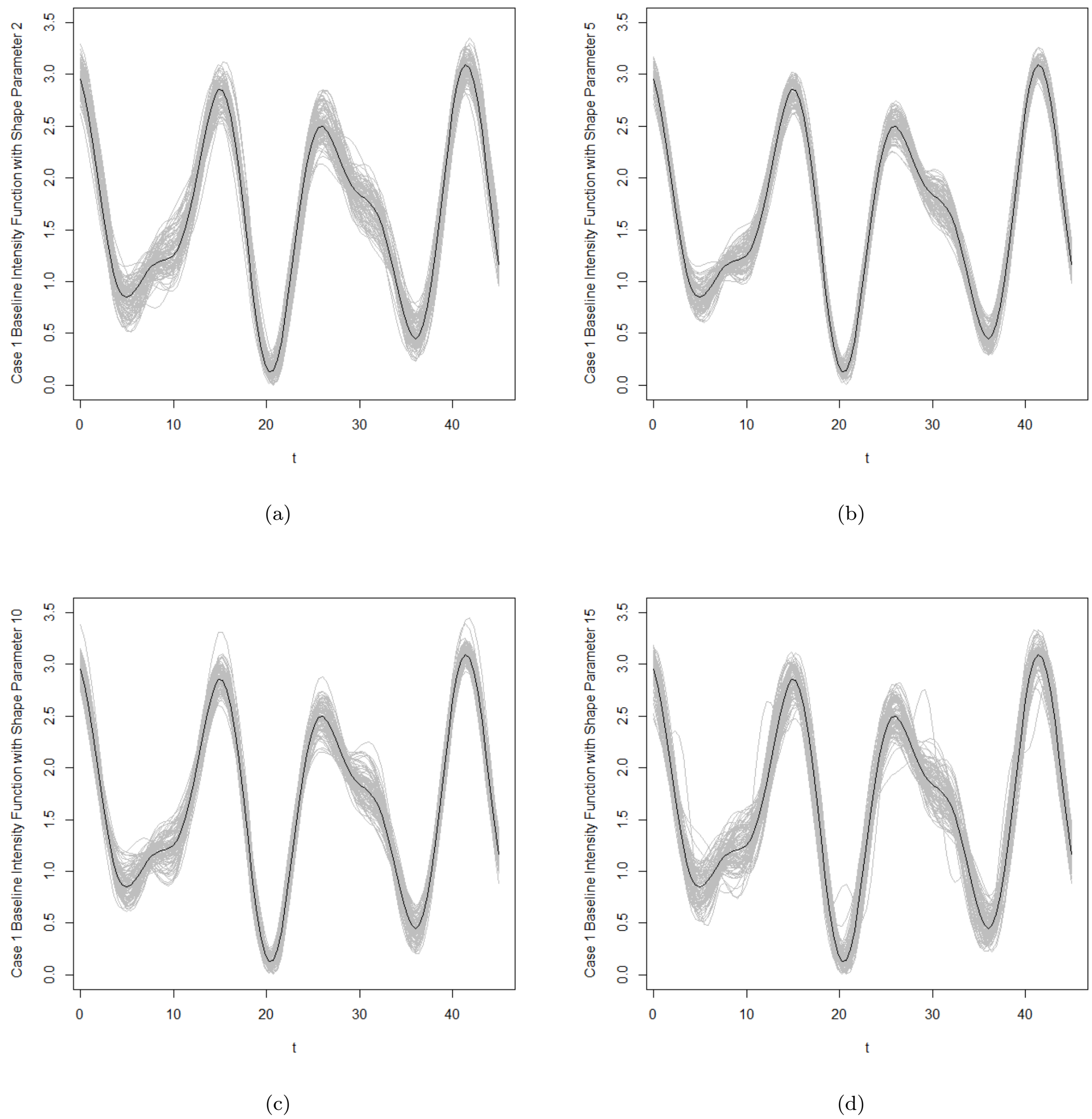

Figure 2.1: Based on the 100 replicated inhomogeneous Gamma process (IGP) models with the Case 1 baseline intensity function $\lambda_1(t) = 1.6 + \cos\left(\frac{\pi}{4\sqrt{3}}t\right) + \frac{1}{2}\cos\left(\frac{\pi}{3\sqrt{2}}t + \frac{\pi}{4}\right)$, where $t > 0$, this figure contains the estimated baseline intensity functions. Plots (a)-(d) display the true baseline intensity function in solid black and the 100 estimated baseline intensity functions in gray. Each estimation procedure was conducted assuming both the true κ and the true K parameter values were known a priori. Plot (a) displays the case when the true $\kappa = 2$, plot (b) displays the case when the true $\kappa = 5$, plot (c) displays the case when the true $\kappa = 10$, and plot (d) displays the case when the true $\kappa = 15$.

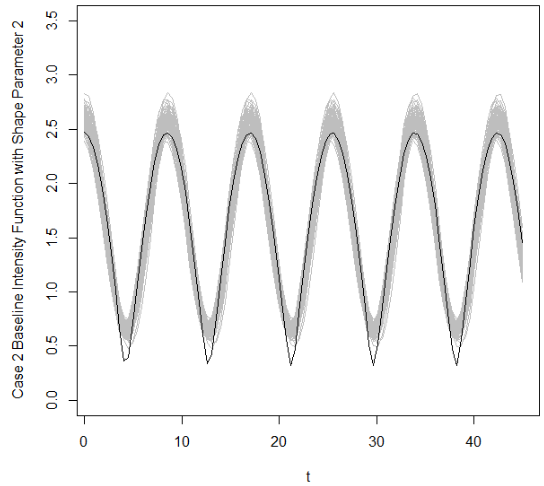

(a)

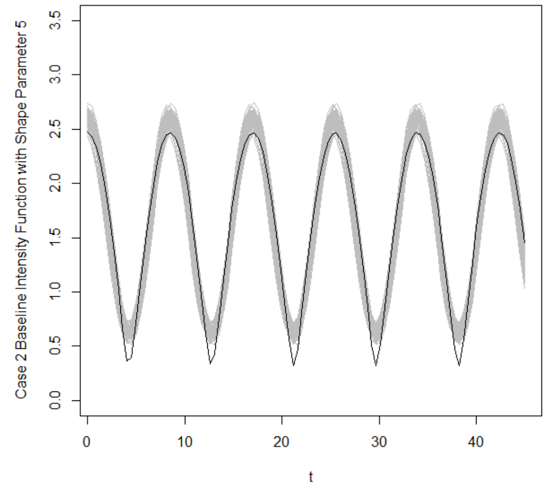

(b)

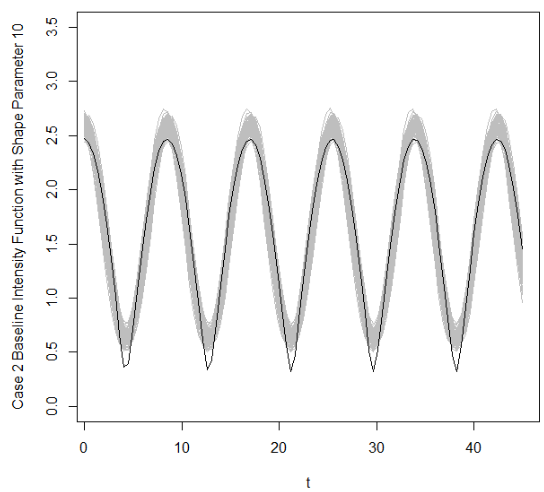

(c)

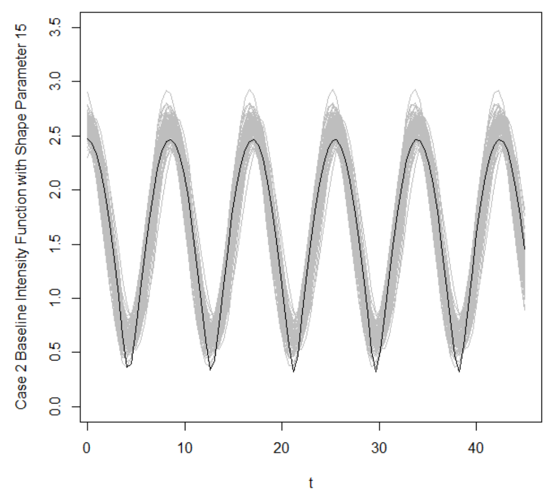

(d)

Figure 2.2: Based on the 100 replicated inhomogeneous Gamma process (IGP) models with the Case 2 baseline intensity function $\lambda_1(t) = \sqrt{3.1 + 3\cos\left(\frac{\pi}{3\sqrt{2}}t\right)}$, where $t > 0$, this figure contains the estimated baseline intensity functions. Plots (a)-(d) display the true baseline intensity function in solid black and the 100 estimated baseline intensity functions in gray. The Case 2 baseline intensity function does not have the same functional form of equation (2.1), and does not have a true K parameter value. Each estimation procedure was conducted assuming that the true κ parameter value was known a priori, and based on the Table 3.2 model selection results, we fit all of the IGP models assuming that $K = 1$. Plot (a) displays the case when the true $\kappa = 2$, plot (b) displays the case when the true $\kappa = 5$, plot (c) displays the case when the true $\kappa = 10$, plot (d) displays the case when the true $\kappa = 15$.

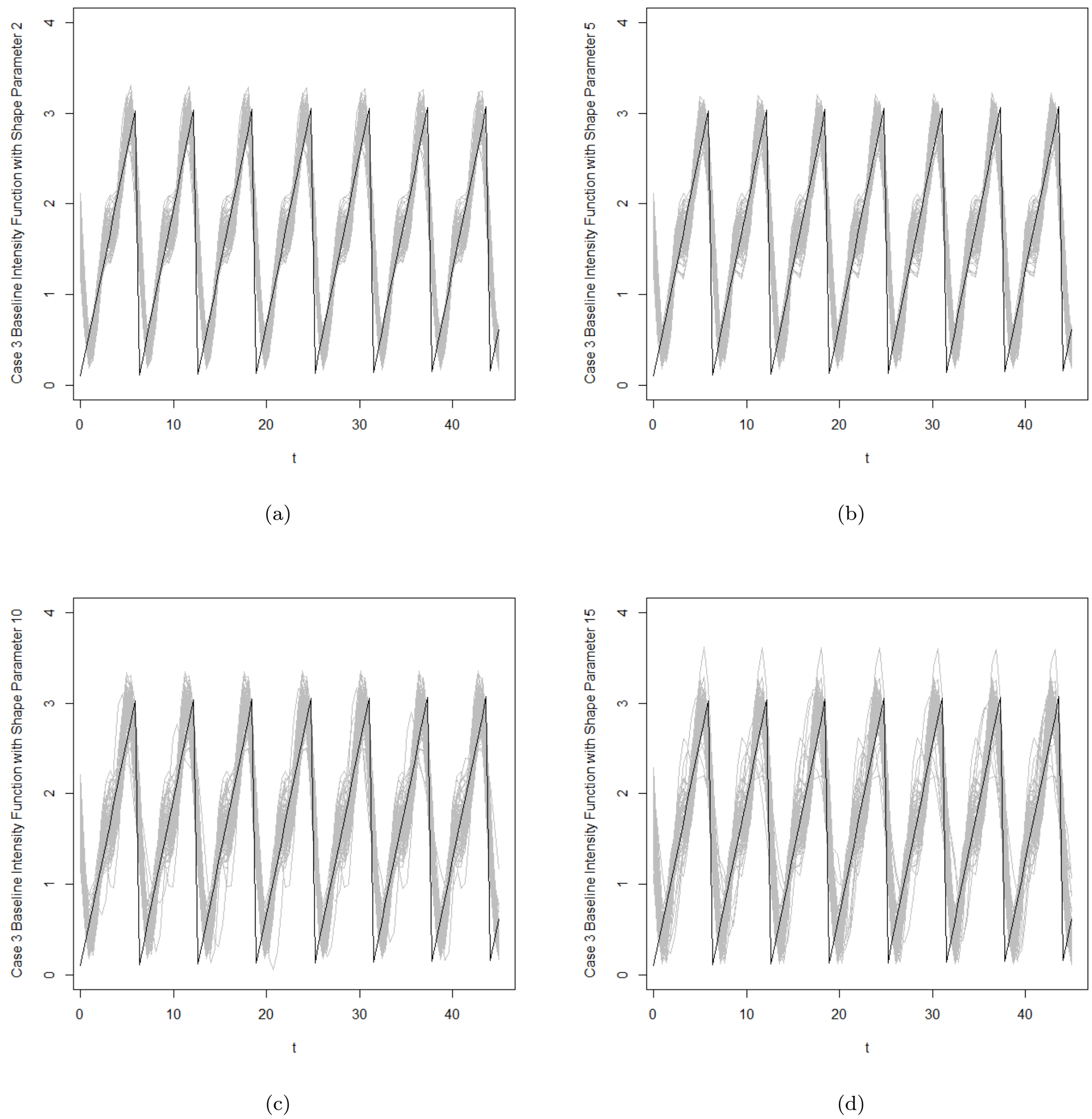

Figure 2.3: Based on the 100 replicated inhomogeneous Gamma process (IGP) models with the Case 3 baseline intensity function $\lambda_1(t) = 0.1 + \frac{1}{2}\text{mod}\,[t,\ 2\pi]$, where $t > 0$, this figure contains the estimated baseline intensity functions. Plots (a)-(d) display the true baseline intensity function in solid black and the 100 estimated baseline intensity functions in gray. The Case 3 baseline intensity function does not have the same functional form of equation (2.1), and does not have a true K parameter value. Each estimation procedure was conducted assuming that the true κ parameter value was known a priori, and based on the Table 3.3 model selection results, we fit all of the IGP models assuming that $K = 2$. Plot (a) displays the case when the true $\kappa = 2$, plot (b) displays the case when the true $\kappa = 5$, plot (c) displays the case when the true $\kappa = 10$, plot (d) displays the case when the true $\kappa = 15$.

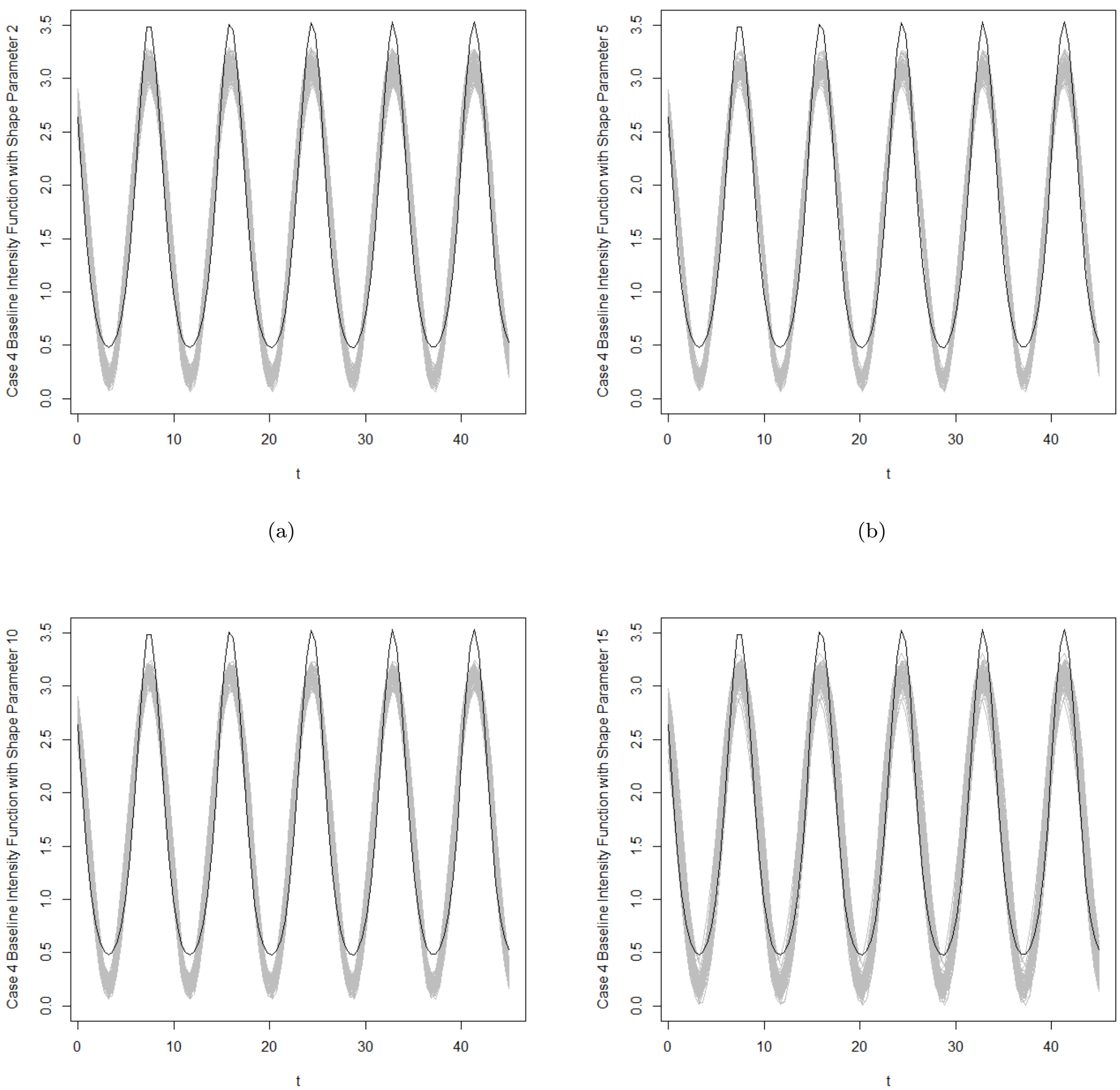

(a) (b) (c) (d)

Figure 2.4: Based on the 100 replicated inhomogeneous Gamma process (IGP) models with the Case 4 baseline intensity function $\lambda_1(t) = 1.3 \exp\left\{\cos\left(\frac{\pi}{3\sqrt{2}}t + \frac{\pi}{4}\right)\right\}$, where $t > 0$, this figure contains the estimated baseline intensity functions. Plots (a)-(d) display the true baseline intensity function in solid black and the 100 estimated baseline intensity functions in gray. The Case 4 baseline intensity function does not have the same functional form of equation (2.1), and does not have a true K parameter value. Each estimation procedure was conducted assuming that the true κ parameter value was known a priori, and based on the Table 3.4 model selection results, we fit all of the IGP models assuming that $K = 1$. Plot (a) displays the case when the true $\kappa = 2$, plot (b) displays the case when the true $\kappa = 5$, plot (c) displays the case when the true $\kappa = 10$, plot (d) displays the case when the true $\kappa = 15$.

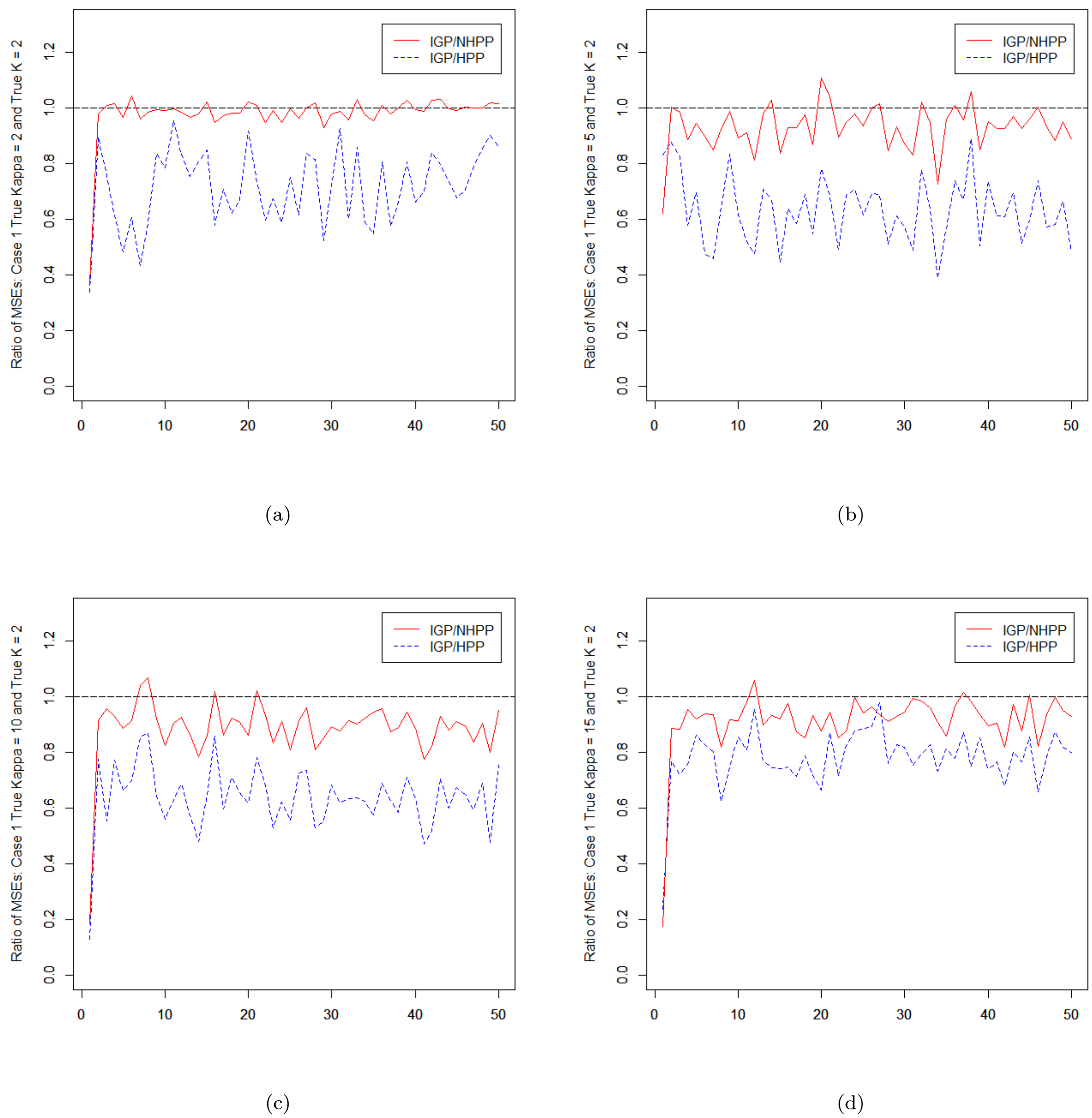

Figure 2.5: Based on the 100 replicated inhomogeneous Gamma process (IGP) models with the Case 1 baseline intensity function $\lambda_1(t) = 1.6 + \cos\left(\frac{\pi}{4\sqrt{3}}t\right) + \frac{1}{2}\cos\left(\frac{\pi}{3\sqrt{2}}t + \frac{\pi}{4}\right)$, where $t > 0$, plots (a)-(d) display the 50 out of sample point forecast MSE ratios of equation (2.35). In each of the plots (a)-(b), the dashed line represents a MSE ratio equal to 1. Asymptotically, the MSE ratio is expected to be below one for every $n \geq 1$. The peaks in the MSE ratio plots which are greater than 1 are caused by random variation of the processes. Plot (a) displays the case when the true $\kappa = 2$, plot (b) displays the case when the true $\kappa = 5$, plot (c) displays the case when the true $\kappa = 10$, plot (d) displays the case when the true $\kappa = 15$.

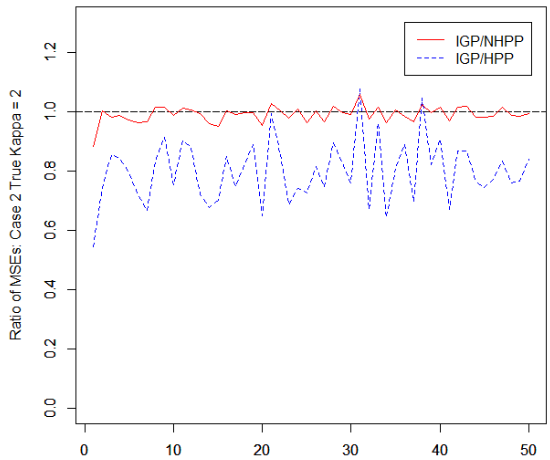

(a)

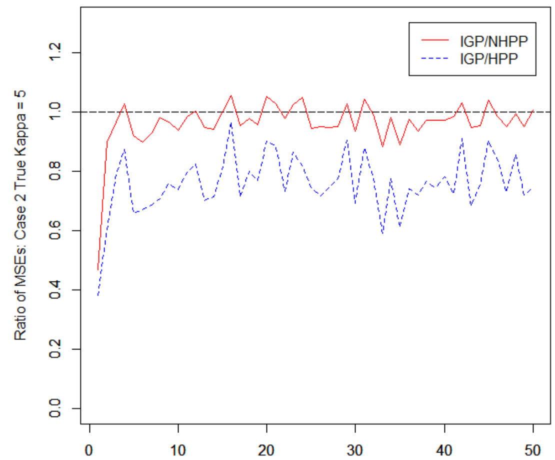

(b)

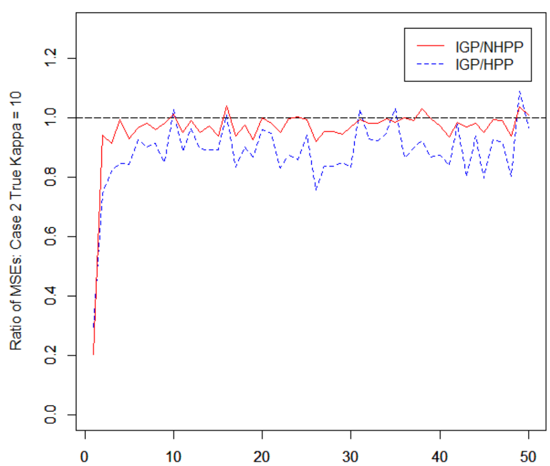

(c)

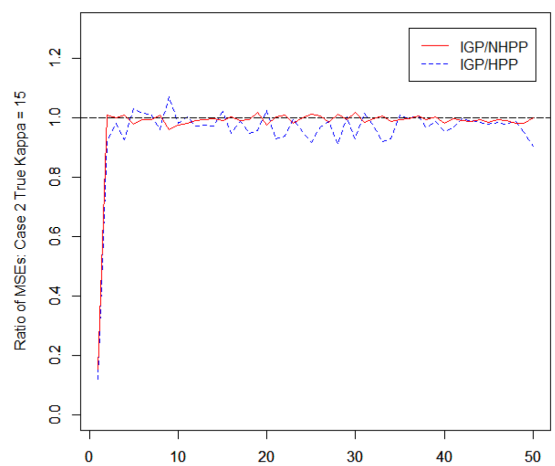

(d)

Figure 2.6: Based on the 100 replicated inhomogeneous Gamma process (IGP) models with the Case 2 baseline intensity function $\lambda_1(t) = \sqrt{3.1 + 3\cos\left(\frac{\pi}{3\sqrt{2}}t\right)}$, where $t > 0$, plots (a)-(d) display the 50 out of sample point forecast MSE ratios of equation (2.35). In each of the plots (a)-(b), the dashed line represents a MSE ratio equal to 1. Asymptotically, the MSE ratio is expected to be below one for every $n \geq 1$. The peaks in the MSE ratio plots which are greater than 1 are caused by random variation of the processes. Plot (a) displays the case when the true $\kappa = 2$, plot (b) displays the case when the true $\kappa = 5$, plot (c) displays the case when the true $\kappa = 10$, plot (d) displays the case when the true $\kappa = 15$.

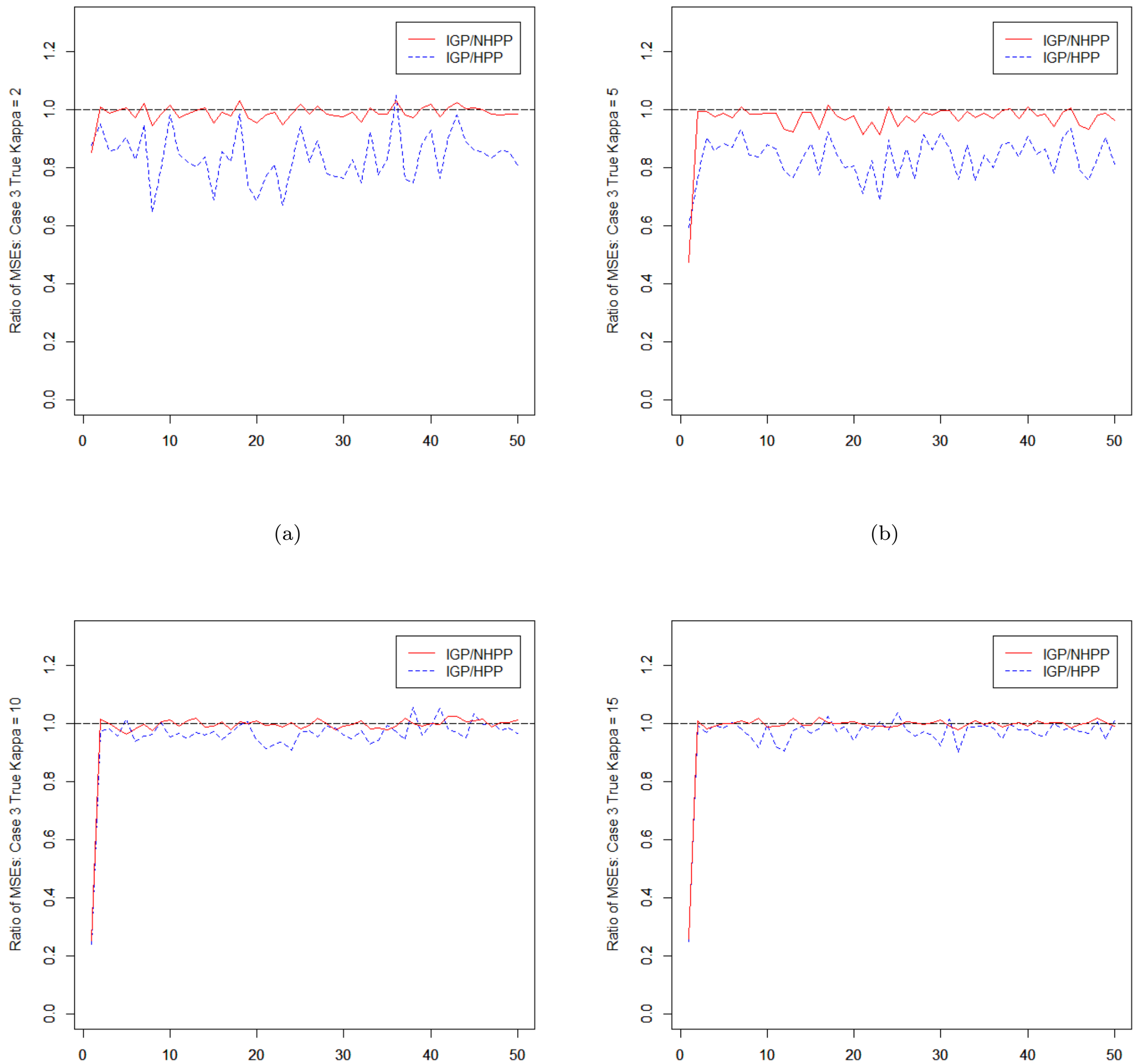

(a) (b)

(c) (d)

Figure 2.7: Based on the 100 replicated inhomogeneous Gamma process (IGP) models with the Case 3 baseline intensity function $\lambda_1(t) = 0.1 + \frac{1}{2}\text{mod}\,[t,\ 2\pi]$, where $t > 0$, plots (a)-(d) display the 50 out of sample point forecast MSE ratios of equation (2.35). In each of the plots (a)-(b), the dashed line represents a MSE ratio equal to 1. Asymptotically, the MSE ratio is expected to be below one for every $n \geq 1$. The peaks in the MSE ratio plots which are greater than 1 are caused by random variation of the processes. Plot (a) displays the case when the true $\kappa = 2$, plot (b) displays the case when the true $\kappa = 5$, plot (c) displays the case when the true $\kappa = 10$, plot (d) displays the case when the true $\kappa = 15$.

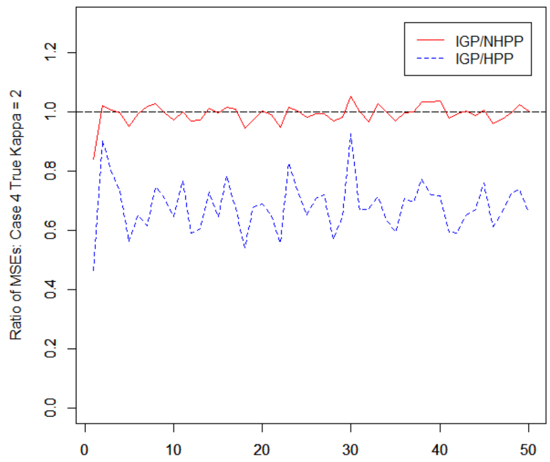

(a)

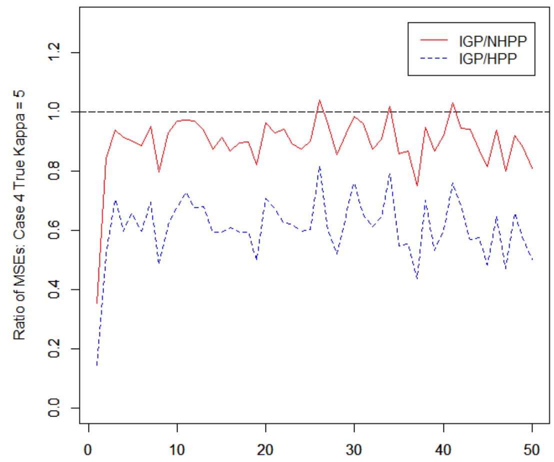

(b)

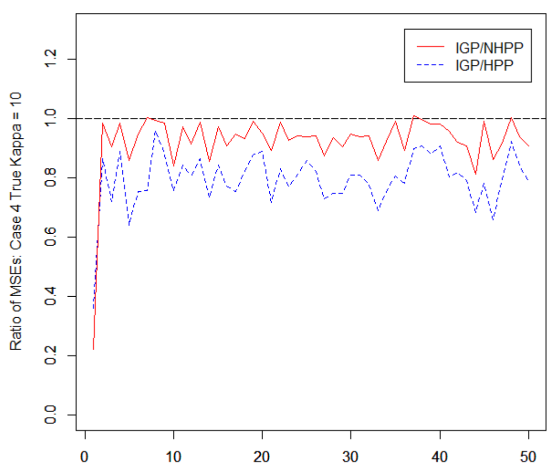

(c)

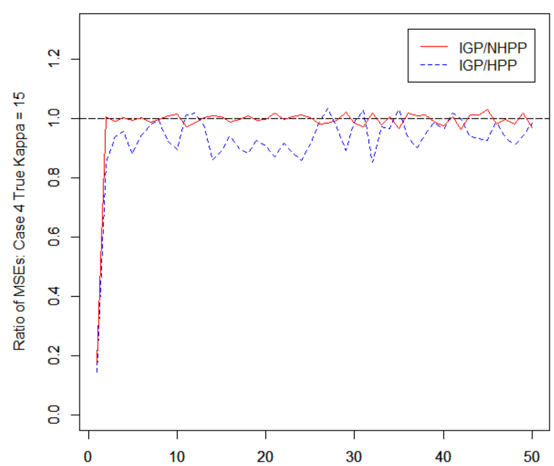

(d)

Figure 2.8: Based on the 100 replicated inhomogeneous Gamma process (IGP) models with the Case 4 baseline intensity function $\lambda_1(t) = 1.3 \exp\left\{\cos\left(\frac{\pi}{3\sqrt{2}}t + \frac{\pi}{4}\right)\right\}$, where $t > 0$, plots (a)-(d) display the 50 out of sample point forecast MSE ratios of equation (2.35). In each of the plots (a)-(b), the dashed line represents a MSE ratio equal to 1. Asymptotically, the MSE ratio is expected to be below one for every $n \geq 1$. The peaks in the MSE ratio plots which are greater than 1 are caused by random variation of the processes. Plot (a) displays the case when the true $\kappa = 2$, plot (b) displays the case when the true $\kappa = 5$, plot (c) displays the case when the true $\kappa = 10$, plot (d) displays the case when the true $\kappa = 15$.

	Case 1	Case 2	Case 3	Case 4
Φ	2.231952%	1.056035%	1.36506%	0.8013656%
Ψ	28.56207%	20.18019%	16.41724%	31.91568%
κ	2	2	2	2
Φ	7.102561%	3.786789%	3.602002%	10.43899%
Ψ	36.84359%	24.11509%	13.70757%	39.25226%
κ	5	5	5	5
Φ	10.67907%	4.200295%	1.776125%	7.786045%
Ψ	34.76953%	11.74642%	4.522555%	20.65559%
κ	10	10	10	10
Φ	8.826937%	2.32156%	1.651595%	2.027092%
Ψ	22.06252%	4.432919%	4.002103%	7.520595%
κ	15	15	15	15

Table 2.2: The table displays the average out of sample forecast MSE (equation (2.35)) reduction when forecasting with an IGP model as opposed to forecasting with a NHPP or a HPP model. In the table, we denote the average out of sample forecast MSE reduction when forecasting with an IGP model as opposed to forecasting with a NHPP model with Φ. And we denote the average out of sample forecast MSE reduction when forecasting with an IGP model as opposed to forecasting with a HPP model with Ψ. Overall, the simulation results demonstrate that our model can capture most of the variation of any periodic or almost periodic baseline intensity function of an IGP with shape parameter $\kappa > 0$.

	Parameter	ω_1	ω_2	A_1	A_2	ϕ_1	ϕ_2	B
	true value	0.45345	0.74048	1	0.5	0	0.78540	1.6
	sample mean	0.4534802	0.7406488	0.9983265	0.4965859	-0.0167732	0.6962794	1.600871
$\kappa = 2$	asymptotic sd	0.0001959592	0.0003919184	0.056569	0.056569	0.113137	0.226274	0.04
	sample sd	0.0001696883	0.0004164992	0.05892142	0.0612599	0.1081249	0.2530019	0.03873855
	sample mean	0.45353	0.7404956	1.000081	0.4970598	-0.004946407	0.7625446	1.599897
$\kappa = 5$	asymptotic sd	4.957419e-05	9.914837e-05	0.035777	0.035777	0.071554	0.143108	0.025298
	sample sd	5.886384e-05	0.0001283016	0.03671624	0.450818	0.08131632	0.1794645	0.02666738
	sample mean	0.453454	0.7404788	1.00017	0.5154577	-0.01323348	0.7824436	1.602232
$\kappa = 10$	asymptotic sd	1.752712e-05	3.505424e-05	0.025298	0.025298	0.0505964	0.101192	0.017889
	sample sd	3.107952e-05	9.12409e-05	0.04148636	0.05265325	0.09041378	0.2533043	0.02417023
	sample mean	0.4534489	0.7472944	1.003666	0.5087409	0.006010876	0.7916847	1.603827
$\kappa = 15$	asymptotic sd	8.660254e-06	1.732051e-05	0.02	0.02	0.04	0.08	0.014142
	sample sd	2.114341e-05	0.06817231	0.04495507	0.07304213	0.09746041	0.3345349	0.01969764

Table 2.3: The means and standard errors of the parameter estimates from the 100 replicates of the inhomogeneous Gamma process models with the Case 1 baseline intensity function $\lambda_1(t) = 1.6 + \cos\left(\frac{\pi}{4\sqrt{3}}t\right) + \frac{1}{2}\cos\left(\frac{\pi}{3\sqrt{2}}t + \frac{\pi}{4}\right)$, where $t > 0$, displayed by the true $\kappa = 2,\ 5,\ 10,\ 15$ parameter values. The estimation procedure was conducted assuming that both the true κ and the true K parameter values were known a priori.

estimates proposed in this chapter can be potentially used as the initial values for a computational MLE procedure. The selection of K, where K is the number of periodic components in the model, and the selection of the shape parameter κ, for the particular case when $\kappa \in \mathbb{N}$, will be discussed in Chapter 3.

Chapter 3

Determining κ and K by the AIC and the BIC Model Selection Criteria

3.1 Introduction

Let $\{N_G(t),\ t > 0\}$ be an inhomogeneous Gamma process (IGP) with baseline intensity function $\lambda_1(\cdot) > 0$ and shape parameter $\kappa \in \mathbb{N}$, which satisfies the Chapter 2 Assumptions 1-3. In this chapter, we propose a method for estimating the positive integer shape parameter κ and the number of periodic components, K, of the IGP $\{N_G(t),\ t > 0\}$. The proposed method of selecting the κ and the K parameter values is similar to the order selection of an ARMA process in time series: there is no unique and "best" or "correct" model selection method, and practitioners usually consider multiple model selection criteria. Analogous to time series analysis, we propose to consider different model selection criteria to produce candidates for the κ and the K parameter values in the framework of our model, and then examine the model fitting to select the best κ and K parameter values.

This chapter is organized as follows. In Section 3.2, we propose that the Akaike information criterion (AIC, Akaike 1974) and the Bayesian information criterion (BIC, Schwarz 1978) be used as procedures for obtaining candidate values for the κ and the K parameters. In Section 3.3, we combine the Bartlett periodogram estimation procedure of Section 2.2 with the AIC and the BIC estimation procedure of Section 3.2 and apply them to all the simulated IGP models of Section 2.4. Lastly, in Section 3.4, we apply our estimation procedure to a real data set.

3.2 The AIC and the BIC Procedure for Selecting the κ and the K Parameter Values

Let $\{N_G(t),\ t > 0\}$ be an inhomogeneous Gamma process (IGP) with baseline intensity function $\lambda_1(\cdot\,) > 0$ and shape parameter $\kappa \in \mathbb{N}$, which satisfies the Chapter 2 Assumptions 1-3. For the special case of an IGP with shape parameter $\kappa = 1$ (a nonhomogeneous Poisson process (NHPP)), Shao (2010) proposed that with the known value of K, where K is the number of periodic components of $\lambda_1(\cdot\,) > 0$, one can use the Bartlett periodogram parameter estimates of $\lambda_1(\cdot\,) > 0$ as "good" initial values for a computational maximum likelihood estimation (MLE) procedure of estimating $\lambda_1(\cdot\,) > 0$. Under the assumption that K is known, Shao (2010) showed that if we use the Bartlett periodogram estimates of $\lambda_1(\cdot\,) > 0$ as the initial values for a MLE method of estimating $\lambda_1(\cdot\,) > 0$, then the corresponding MLE are asymptotically consistent and normally distributed. Therefore, for a NHPP (an IGP with $\kappa = 1$)

with intensity function $\lambda_1(\cdot\,) > 0$, the regularity conditions for the Akaike information criterion (AIC, Akaike 1974) and the Bayesian information criterion (BIC, Schwarz 1978) model selection procedures are satisfied. Hence, for the NHPP with intensity function $\lambda_1(\cdot\,) > 0$, one can use the AIC and the BIC model section criteria to produce candidate values for K. Based on the fact that when $\kappa \in \mathbb{N}$ the IGP can be viewed as a process which samples every κ event of a NHPP (Berman (1981)) and based on the Chapter 3 theoretical findings of Shao (2010), we propose the AIC and the BIC model selection procedures for producing candidate values for κ and K.

We now describe the proposed method of producing candidate values for the shape parameter $\kappa \in \mathbb{N}$ and the number of periodic components, K, in the framework of our model. For candidate values of $\kappa \in \mathbb{N}$ and $K \in \{0\} \cup \mathbb{N}$, use the Bartlett periodogram estimation procedure of Section 2.2 to estimate the unknown parameter values of the baseline intensity function $\lambda_1(\cdot\,) > 0$, defined as in equation (2.1). After that, use the resulting parameter estimates as the initial values for a computational maximum likelihood method of estimating the unknown parameters of $\lambda_1(\cdot\,) > 0$. We applied the above estimation procedure to the simulated IGP models of Section 2.2.

We begin by describing our empirical findings from the above estimation procedure to the simulated IGP models of Section 2.2, which had the Case 1 baseline intensity function and a given shape parameter of the form $\kappa = 2,\ 5,\ 10,\ 15$. For these simulated data sets, we applied the above estimation procedure by assuming different κ and K parameter values, then producing the corresponding Bartlett periodogram estimates of $\lambda_1(\cdot\,) > 0$ as the initial values for the MLE procedure of estimating the unknown parameters of $\lambda_1(\cdot\,) > 0$. When the true $\kappa = 2$, we applied the procedure with $\kappa \in \{1,\ 2,\ \ldots,\ 5\}$ as candidate values for κ; when the true $\kappa = 5$, we applied the procedure with $\kappa \in \{1,\ 2,\ \ldots,\ 10\}$ as candidate values for κ; when the true $\kappa = 10$, we applied the procedure with $\kappa \in \{1,\ 2,\ \ldots,\ 15\}$ as candidate values for κ; and when the true $\kappa = 15$, we applied the procedure with $\kappa \in \{1,\ 2,\ \ldots,\ 20\}$ as candidate values for κ. In each case, we applied the procedure with $K \in \{0,\ 1,\ \ldots,\ 4\}$ as candidate values for K. We only considered small values for κ because as κ gets large, the shape of the joint density function (1.3), and hence the log-likelihood values for a given data set, varies slowly with increasing values of κ. Since there are two periodic components in the Case 1 baseline intensity function, we only considered small values for K in the estimation procedure. We did this because we defined the estimate of B as $\hat{\boldsymbol{B}}_T := \max\left\{\frac{1}{T}N_G(T)\kappa,\ \sum_{k=1}^{K}\hat{A}_k\right\}$, where $T > 0$ is the observational length of the IGP, the $\hat{A}_k$'s are the estimated amplitudes of $\lambda_1(\cdot\,) > 0$, and $N_G(T)$ is the count at observational time T. So, the larger the candidate K value, the more likely the overestimate of the B parameter value. When using the Bartlett periodogram estimates, with the true κ and the true K values of the Case 1 baseline intensity function as the initial values for a MLE procedure, the absolute error between the initial values and the MLE values approaches 0 as the observation time increases. Otherwise, when we use different κ and K values, the absolute error between the initial values and the MLE values did not approach 0 as the observation time increased.

The small absolute error between our proposed method of parameter estimation and the MLE method of parameter estimation, along with the fact that when $\kappa \in \mathbb{N}$ the IGP can be viewed as a process which samples very κ event of a NHPP, lead us to conjecture that the MLE's of the unknown parameters of $\lambda_1(\cdot) > 0$ in the IGP frame work are consistent and are asymptotically normally distributed as the observation time $T > 0$ increases. Therefore, the AIC and the BIC method of model selection can potentially be justified (establishing the consistency and the asymptotic normality of the MLE is an ongoing research problem) and we propose to define the AIC and the BIC as in Chapter 3 of Shao (2010). More explicitly, we propose to define $AIC := -2\mathcal{L}\left(\hat{\theta}^{MLE}\right) + 2\left(3K+1\right)$ and $BIC := -2\mathcal{L}\left(\hat{\theta}^{MLE}\right) + \left(5K+1\right)\log\left(T\right)$, where $\log(\cdot)$ is the natural logarithm, $\hat{\theta}^{MLE}$ is the MLE parameter estimates of $\lambda_1(\cdot) > 0$, and $\mathcal{L}\left(\cdot\right)$ is the log-likelihood of the data. In both the AIC and the BIC model selection procedures, the model which yields the smallest AIC/BIC value, respectively, is considered the best approximation of the true model in question. The proposed model selection procedure is described below.

For a given set of data, consider the candidate values $\kappa = \kappa_1,\ \kappa_2,\ \ldots,\ \kappa_{\tilde{\kappa}}$ and $K = K_1,\ K_2,\ \ldots,\ K_{\tilde{K}}$, where $\kappa_{\tilde{\kappa}}$ and $K_{\tilde{K}}$ are the largest of the κ and the K candidate values under consideration. Let θ denote the unknown parameter values of the baseline intensity function $\lambda_1(\cdot) > 0$ (not including the unknown κ and K parameter values), let $\hat{\theta}^{BP}_{\kappa_i,\,K_j}$ denote the Bartlett periodogram estimates for θ which were produced under the assumption that the true $\kappa = \kappa_i$ and the true $K = K_j$, and let $\hat{\theta}^{MLE}_{\kappa_i,\, K_j}$ denote the maximum likelihood estimates of θ which were produced using $\hat{\theta}^{BP}_{\kappa_i,\, K_j}$ as the initial values for the MLE procedure.

Step 1 Initialize $i = 1$ and $j = 1$.

Step 2 Fix $\kappa = \kappa_i$.

Step 3 Fix $K = K_j$ and let $\hat{\theta}^{BP}_{\kappa_i,\, K_j}$ be the corresponding Bartlett periodogram estimates of θ.

Step 4 Let $\hat{\theta}^{BP}_{\kappa_i,\, K_j}$ be the initial values for a MLE procedure and let $\hat{\theta}^{MLE}_{\kappa_i,\, K_j}$ be the corresponding MLE of θ.

Step 5 Calculate the AIC and the BIC values using the MLE $\hat{\theta}^{MLE}_{\kappa_i,\, K_j}$.

Step 6 If $i = \tilde{\kappa}$ and $j = \tilde{K}$, go to Step 7. Else if $i < \tilde{\kappa}$ and $j = \tilde{K}$, update $i = i + 1$ and go to Step 2. Else if $i \neq \tilde{\kappa}$ and $j \neq \tilde{K}$, update $j = j + 1$ and go to Step 3.

Step 7 Using the parameter estimates $\hat{\theta}^{MLE}_{\kappa_i,\, K_j}$, where $i \in \{1,\ 2,\ \ldots,\ \tilde{\kappa}\}$ and $j \in \{1,\ 2,\ \ldots,\ \tilde{K}\}$, select the κ and K parameter values based on the following two criteria. If the AIC and the BIC select the same κ and K values, then define the κ and the K estimates as these values. If the AIC and the BIC criteria select different κ and K values, then conduct out of sample predictions and select the model with the smaller (averaged) squared prediction error.

3.3 Simulation

In this section, we consider the same Cases 1-4 periodic or almost periodic baseline intensity functions of Section 2.4:

$$
\begin{aligned}
\text{Case} \quad 1: \lambda_1(t) &= 1.6 + \cos\left(\frac{\pi}{4\sqrt{3}}t\right) + \frac{1}{2}\cos\left(\frac{\pi}{3\sqrt{2}}t + \frac{\pi}{4}\right), \\
\text{Case} \quad 2: \lambda_1(t) &= \sqrt{3.1 + 3\cos\left(\frac{\pi}{3\sqrt{2}}t\right)}, \\
\text{Case} \quad 3: \lambda_1(t) &= 0.1 + \frac{1}{2}\text{mod}\left[t,\ 2\pi\right], \\
\text{Case} \quad 4: \lambda_1(t) &= 1.3\exp\left\{\cos\left(\frac{\pi}{3\sqrt{2}}t + \frac{\pi}{4}\right)\right\},
\end{aligned}
$$

with shape parameters $\kappa \in \{2,\ 5,\ 10,\ 15\}$, where $t > 0$. We use the same simulated inhomogeneous Gamma process (IGP) data sets described in Section 2.4 and are summarized in Table 2.1. We recall that there are 100 independent IGP realizations for each baseline intensity function and shape parameter combination. For each simulated data set, we simulate 50 out-of-sample data points accordingly to assess the out-of-sample predictions. We perform the estimation analysis using the procedures described in Section 3.2. Tables 3.1-3.4 summarize the candidate values for the shape parameter κ and the number of periodic components K.

We begin by summarizing the proposed candidate values for the shape parameter κ and the number of frequency components K. For each simulated data set, the candidate values for $K = 0,\ 1, \ldots, 4$, where $K = 0$ implies a gamma renewal process model. For a data set with the true $\kappa = 2$, the candidate values for κ were $\kappa = 1,\ 2,\ \ldots,\ 5$. For a data set with the true $\kappa = 5$, the candidate values for κ were $\kappa = 1,\ 2,\ \ldots,\ 10$. For a data set with the true $\kappa = 10$, the candidate values for κ were $\kappa = 1,\ 2,\ \ldots,\ 15$. Lastly, for a data set with the true $\kappa = 15$, the candidate values for κ were $\kappa = 1,\ 2,\ \ldots,\ 20$.

We now summarize the estimated values for the shape parameter κ and the estimated values for the number of frequency components K. Tables 3.1-3.4 contain the exact counts of the number of times that a particular $(\kappa,\ K)$ combination was chosen for a particular IGP model that was simulated 100 times. Table 3.1 contains the counts for all the Case 1 data sets, Table 3.2 contains the counts for all the Case 2 data sets, Table 3.3 contains the counts for all the Case 3 data sets, and Table 3.4 contains the counts for all the Case 4 data sets. For Tables 3.1-3.4, in each cell of sub-tables (a)-(d), the top value corresponds to the number of times the AIC selected the particular $(\kappa,\ K)$ combination, the middle value corresponds to the number of times the BIC selected the particular $(\kappa,\ K)$ combination, and the bottom value corresponds to the number of times that our model selection procedure (as defined in Step 7 of Section 3.2) selected the particular $(\kappa,\ K)$ combination.

For all the simulated Case 1 data sets, the estimation procedure estimated the correct κ and K values most often. When the true $\kappa = 2$ and the true $K = 2$, the AIC estimation procedure had a 96% success rate and the BIC estimation procedure had a 100% success rate. The final model selection procedure had an overall success rate of 99%. When the true $\kappa = 5$ and the true $K = 2$, the AIC estimation procedure had a 94% success rate and the BIC estimation procedure had a 95% success rate. The final model selection procedure had an overall success rate of 95%. When the true $\kappa = 10$ and the true $K = 2$, the AIC, the BIC, and the final estimation procedure each had a 78% success rate. When the true $\kappa = 15$ and the true $K = 2$, the AIC, the BIC, and the final estimation procedure each had a 47% success rate. We notice that in all the simulations, K is estimated with an almost 100% success rate. However, we notice that as κ increases, the variability among the κ estimates increases. A possible explanation for this is because as κ gets large, the shape of the joint density function (1.3), and hence the log-likelihood values for a given data set, varies slowly with increasing values of κ. For a comparison of the estimation procedure when the true $\kappa = 15$, we pool together the number of times the estimation procedures estimated $K = 2$, $\kappa = 14,\ 15$, and 16, and we get the following estimation results. The AIC estimation procedure had an overall success rate of 97%, and the BIC and the final model selection procedure had an overall success rate of 96% for estimating $\kappa \in \{14,\ 15,\ 16\}$ and $K = 2$. Overall, Table 3.1 demonstrates that for an IGP model with baseline intensity function of the form (2.1) and with shape parameter of the form $\kappa \in \mathbb{N}$, our estimation procedure produced reasonable estimates for the shape parameter κ and excellent estimates for the number of periodic components K.

All the simulated IGP models of Section 2.2 with the baseline intensity function of the forms given in Cases 2-4 do not have a true K parameter value. However, the

Cases 2-4 baseline intensity functions can be well approximated by a functional of the form (2.1), which does have a K parameter value. So we estimated the Cases 2-4 baseline intensity functions with a functional of the form (2.1) and the results are presented below.

Per Table 3.2, for the Case 2 data sets, when the true $\kappa = 2$, the AIC, the BIC, and the final estimation procedure had a 100% success rate for estimating κ. When the true $\kappa = 5$, the AIC, the BIC, and the final estimation procedure had a 94% success rate for estimating κ. When the true $\kappa = 10$, the AIC estimation procedure had a 60% success rate for estimating κ and the BIC estimation procedure had a 63% success rate for estimating κ. The final model selection procedure had an overall success rate of 64% for estimating κ. When the true $\kappa = 15$, the AIC estimation procedure had a 39% success rate for estimating κ and the BIC estimation procedure had a 52% success rate for estimating κ. The final model selection procedure had an overall success rate of 47% for estimating κ. We notice that as κ increases, the variability among the κ estimates increases. A possible explanation for this is because as κ gets large, the shape of the joint density function (1.3), and hence the log-likelihood values for a given data set, varies slowly with increasing values of κ. For a comparison of the estimation procedure when the true $\kappa = 15$, we pool together the number of times the estimation procedures estimated $\kappa = 14,\ 15$, and 16, and we get the following estimation results. The AIC estimation procedure had a 89% success rate for estimating $\kappa \in \{14,\ 15,\ 16\}$ and the BIC estimation procedure had a 95%

success rate for estimating $\kappa \in \{14,\ 15,\ 16\}$. The final model selection procedure had an overall success rate of 91% for estimating $\kappa \in \{14,\ 15,\ 16\}$.

Per Table 3.3, for the Case 3 data sets, when the true $\kappa = 2$, the AIC, the BIC, and the final estimation procedure each had a 100% success rate for estimating κ. When the true $\kappa = 5$, the AIC, the BIC, and the final estimation procedure each had a 93% success rate for estimating κ. When the true $\kappa = 10$, the AIC estimation procedure had a 67% success rate for estimating κ and the BIC estimation procedure had a 69% success rate for estimating κ. The final model selection procedure had an overall success rate of 67% for estimating κ. When the true $\kappa = 15$, the AIC estimation procedure had a 50% success rate for estimating κ and the BIC estimation procedure had a 57% success rate for estimating κ. The final model selection procedure had an overall success rate of 53% for estimating κ. We notice that as κ increases, the variability among the κ estimates increases. A possible explanation for this is because as κ gets large, the shape of the joint density function (1.3), and hence the log-likelihood values for a given data set, varies slowly with increasing values of κ. For a comparison of the estimation procedure when the true $\kappa = 15$, we pool together the number of times the estimation procedures estimated $\kappa = 14,\ 15$, and 16, and we get the following estimation results. The AIC estimation procedure had a 94% success rate for estimating $\kappa \in \{14,\ 15,\ 16\}$ and the BIC estimation procedure had a 97% success rate for estimating $\kappa \in \{14,\ 15,\ 16\}$. The final model selection procedure had an overall success rate of 96% for estimating $\kappa \in \{14,\ 15,\ 16\}$.

Per Table 3.4, for the Case 4 data sets, when the true $\kappa = 2$, the AIC, the BIC, and the final model selection procedure has a 100% success rate for estimating κ. When the true $\kappa = 5$, the AIC estimation procedure had a 93% success rate for estimating κ and the BIC estimation procedure had a 95% success rate for estimating κ. The final model selection procedure had an overall success rate of 95% for estimating κ. When the true $\kappa = 10$, the AIC estimation procedure had a 64% success rate for estimating κ and the BIC estimation procedure had a 69% success rate for estimating κ. The final model selection procedure had an overall success rate of 68% for estimating κ. When the true $\kappa = 15$, the AIC estimation procedure had a 57% success rate for estimating κ and the BIC estimation procedure had a 59% success rate for estimating κ. The final model selection procedure had an overall success rate of 59% for estimating κ. We notice that as κ increases, the variability among the κ estimates increases. A possible explanation for this is because as κ gets large, the shape of the joint density function (1.3), and hence the log-likelihood values for a given data set, varies slowly with increasing values of κ. For a comparison of the estimation procedure when the true $\kappa = 15$, we pool together the number of times the estimation procedures estimated $\kappa = 14,\ 15,$ and 16, and we get the following estimation results. The AIC estimation procedure had a 97% success rate for estimating $\kappa \in \{14,\ 15,\ 16\}$ and the BIC estimation procedure had a 99% success rate for estimating $\kappa \in \{14,\ 15,\ 16\}$. The final model selection procedure had an overall success rate of 99% for estimating $\kappa \in \{14,\ 15,\ 16\}$.

Overall, Tables 3.2-3.4 demonstrate that our estimation procedure produced reasonable estimates for the shape parameter κ when the true baseline intensity function is periodic and not of the same functional form as (2.1).

3.4 A Bedload Transport Example

In this section, we reanalyze the occurrence times of bedload movements (defined below) in two streams which were initially described in Carling and Hurley (1987) and analyzed in Hurley (1992). As stated in Hurley (1992), when modeling event occurrences in time, the homogeneous Poisson process (HPP) model is a natural first choice. However, when it is evident from the data that the rate of occurrence has fluctuated over the observational period, the nonhomogeneous Poisson process (NHPP) is a sensible second choice model. The inhomogeneous Gamma process (IGP) is a valuable third choice model because it is a natural extension of both the HPP and NHPP. The IGP model rarely has been fitted to point process data because of the awkward form of the conditional intensity function of the IGP. However, in Hurley's (1992) paper, the occurrence of bedload movements was modeled as an IGP with a purely periodic baseline intensity function and we attempt to model the bedload movement occurrence data as an IGP with an almost periodic baseline intensity function which satisfies the Chapter 2 Assumptions 1-3. We organize the rest of this section as follows. First, we describe the bedload movement occurrence data which were analyzed in Hurley (1992). Second, we summarize the periodic IGP

$\kappa \setminus K$	$K=2$	$K=3$
$\kappa=2$	96 100 99	4 0 1

True $\kappa=2$, True $K=2$

(a)

$\kappa \setminus K$	$K=2$	$K=3$
$\kappa=5$	94 95 95	1 0 0
$\kappa=6$	5 5 5	0 0 0

True $\kappa=5$, True $K=2$

(b)

$\kappa \setminus K$	$K=2$
$\kappa=9$	10 10 10
$\kappa=10$	78 78 78
$\kappa=11$	12 12 12

True $\kappa=10$, True $K=2$

(c)

$\kappa \setminus K$	$K=1$	$K=2$
$\kappa=14$	0 1 1	22 21 21
$\kappa=15$	0 0 0	47 47 47
$\kappa=16$	0 0 0	28 28 28
$\kappa=17$	0 0 0	3 3 3

True $\kappa=15$, True $K=2$

(d)

Table 3.1: This table contains the counts of the number of times that a particular $(\kappa,\ K)$ combination was chosen out of the 100 simulated IGP with baseline intensity function of the form $\lambda_1(t)$=$1.6+\cos\left(\frac{\pi}{4\sqrt{3}}t\right)+\frac{1}{2}\cos\left(\frac{\pi}{3\sqrt{2}}t+\frac{\pi}{4}\right)$, where $0 < t \leq T$. In each cell of sub-tables (a)-(d), the top value corresponds to the number of times the AIC selected the particular $(\kappa,\ K)$ combination, the middle value corresponds to the number of times the BIC selected the particular $(\kappa,\ K)$ combination, and the bottom value corresponds to the number of times that the model selection procedure selected the particular $(\kappa,\ K)$ combination. In each cell of Tables (a)-(d), the top value corresponds to the AIC counts, the middle value corresponds to the BIC counts, and the bottom value corresponds to the final model selection counts. In each simulation, the number of periodic components was $K=2$, and the candidate values for K were $0,\ 1,\ldots,4$. In Table (a), the true value of κ is 2, and the candidate values for κ were $1,\ 2,\ \ldots,5$. In Table (b), the true value of κ is 5, and the candidate values for κ were $1,\ 2,\ \ldots,10$. In Table (c), the true value of κ is 10, and the candidate values for κ were $1,\ 2,\ \ldots,15$. In Table (d), the true value of κ is 15, and the candidate values for κ were $1,\ 2,\ \ldots,20$.

$\kappa \backslash K$	$K=1$	$K=2$	$K=3$
	2	16	82
$\kappa=2$	100	0	0
	65	11	24

True $\kappa=2$

(a)

$\kappa \backslash K$	$K=1$	$K=2$	$K=3$
	0	0	2
$\kappa=4$	2	0	0
	1	0	1
	9	36	49
$\kappa=5$	94	0	0
	51	20	23
	0	4	0
$\kappa=6$	4	0	0
	2	2	0

True $\kappa=5$

(b)

$\kappa \backslash K$	$K=1$	$K=2$	$K=3$
	0	1	0
$\kappa=8$	1	0	0
	0	1	0
	0	6	10
$\kappa=9$	13	0	0
	7	2	4
	6	40	14
$\kappa=10$	63	0	0
	38	22	4
	0	21	2
$\kappa=11$	23	0	0
	13	8	1

True $\kappa=10$

(c)

$\kappa \backslash K$	$K=1$	$K=2$	$K=3$
	1	3	2
$\kappa=13$	4	0	0
	4	0	1
	5	17	2
$\kappa=14$	23	1	0
	14	9	1
	9	23	7
$\kappa=15$	51	1	0
	35	10	2
	5	20	1
$\kappa=16$	19	0	0
	13	7	0
	0	5	0
$\kappa=17$	1	0	0
	1	3	0

True $\kappa=15$

(d)

Table 3.2: This table contains the counts of the number of times that a particular $(\kappa,\ K)$ combination was chosen out of the 100 simulated IGP with baseline intensity function $\lambda_1(t) = \sqrt{3.1 + 3\cos(\frac{\pi}{3\sqrt{2}}t)}$, where $0 < t \leq T$. In each cell of sub-tables (a)-(d), the top value corresponds to the number of times the AIC selected the particular $(\kappa,\ K)$ combination, the middle value corresponds to the number of times the BIC selected the particular $(\kappa,\ K)$ combination, and the bottom value corresponds to the number of times that the model selection procedure selected the particular $(\kappa,\ K)$ combination. For each simulation, the candidate values for K were $0,\ 1, \ldots, 4$. In Table (a), the true value of κ is 2, and the candidate values for κ were $1,\ 2,\ \ldots, 5$. In Table (b), the true value of κ is 5, and the candidate values for κ were $1,\ 2,\ \ldots, 10$. In Table (c), the true value of κ is 10, and the candidate values for κ were $1,\ 2,\ \ldots, 15$. In Table (d), the true value of κ is 15, and the candidate values for κ were $1,\ 2,\ \ldots, 20$.

$\kappa \backslash K$	$K=2$	$K=3$
	69	31
$\kappa=2$	100	0
	91	9

True $\kappa = 2$

(a)

$\kappa \backslash K$	$K=1$	$K=2$	$K=3$
	0	2	0
$\kappa=4$	0	2	0
	0	2	0
	0	83	10
$\kappa=5$	2	91	0
	1	91	1
	0	5	0
$\kappa=6$	0	5	0
	0	5	0

True $\kappa = 5$

(b)

$\kappa \backslash K$	$K=1$	$K=2$	$K=3$
	0	12	2
$\kappa=9$	2	11	0
	2	11	1
	0	66	1
$\kappa=10$	8	61	0
	3	64	0
	0	19	0
$\kappa=11$	0	18	0
	0	19	0

True $\kappa = 10$

(c)

$\kappa \backslash K$	$K=1$	$K=2$	$K=3$
	0	1	2
$\kappa=13$	1	0	0
	1	0	0
	9	12	4
$\kappa=14$	27	0	0
	20	5	0
	14	32	4
$\kappa=15$	56	1	0
	36	17	0
	4	12	3
$\kappa=16$	13	0	0
	11	7	0
	1	2	0
$\kappa=17$	2	0	0
	2	1	0

True $\kappa = 15$

(d)

Table 3.3: This table contains the counts of the number of times that a particular $(\kappa,\ K)$ combination was chosen out of the 100 simulated IGP with baseline intensity function $\lambda_1(t) = 0.1 + \frac{1}{2}\text{mod}\,[t,\ 2\pi]$, where $0 < t \leq T$. In each cell of sub-tables (a)-(d), the top value corresponds to the number of times the AIC selected the particular $(\kappa,\ K)$ combination, the middle value corresponds to the number of times the BIC selected the particular $(\kappa,\ K)$ combination, and the bottom value corresponds to the number of times that the model selection procedure selected the particular $(\kappa,\ K)$ combination. For each simulation, the candidate values for K were $0,\ 1, \ldots, 4$. In Table (a), the true value of κ is 2, and the candidate values for κ were $1,\ 2,\ \ldots, 5$. In Table (b), the true value of κ is 5, and the candidate values for κ were $1,\ 2,\ \ldots, 10$. In Table (c), the true value of κ is 10, and the candidate values for κ were $1,\ 2,\ \ldots, 15$. In Table (d), the true value of κ is 15, and the candidate values for κ were $1,\ 2,\ \ldots, 20$.

$\kappa \backslash K$	$K = 1$	$K = 2$
	53	47
$\kappa = 2$	100	0
	90	10

True $\kappa = 2$

(a)

$\kappa \backslash K$	$K = 1$	$K = 2$
	0	6
$\kappa = 4$	1	3
	1	3
	82	11
$\kappa = 5$	95	0
	94	1
	1	0
$\kappa = 6$	1	0
	1	0

True $\kappa = 5$

(b)

$\kappa \backslash K$	$K = 1$	$K = 2$
	0	5
$\kappa = 8$	0	1
	0	2
	18	0
$\kappa = 9$	19	0
	19	0
	63	1
$\kappa = 10$	69	0
	68	0
	10	2
$\kappa = 11$	10	0
	10	0
	1	0
$\kappa = 12$	1	0
	1	0

True $\kappa = 10$

(c)

$\kappa \backslash K$	$K = 1$	$K = 2$
	0	1
$\kappa = 13$	1	0
	1	0
	21	0
$\kappa = 14$	23	0
	23	0
	53	4
$\kappa = 15$	59	0
	59	0
	15	4
$\kappa = 16$	16	1
	16	1
	0	1
$\kappa = 17$	0	0
	0	0
	0	1
$\kappa = 18$	0	0
	0	0

True $\kappa = 15$

(d)

Table 3.4: This table contains the counts of the number of times that a particular $(\kappa,\ K)$ combination was chosen out of the 100 simulated IGP with baseline intensity function $\lambda_1(t) = 1.3 \exp\left\{\cos\left(\frac{\pi}{3\sqrt{2}}t + \frac{\pi}{4}\right)\right\}$, where $0 < t \leq T$. In each cell of sub-tables (a)-(d), the top value corresponds to the number of times the AIC selected the particular $(\kappa,\ K)$ combination, the middle value corresponds to the number of times the BIC selected the particular $(\kappa,\ K)$ combination, and the bottom value corresponds to the number of times that the model selection procedure selected the particular $(\kappa,\ K)$ combination. For each simulation, the candidate values for K were $0,\ 1, \ldots, 4$. In Table (a), the true value of κ is 2, and the candidate values for κ were $1,\ 2,\ \ldots, 5$. In Table (b), the true value of κ is 5, and the candidate values for κ were $1,\ 2,\ \ldots, 10$. In Table (c), the true value of κ is 10, and the candidate values for κ were $1,\ 2,\ \ldots, 15$. In Table (d), the true value of κ is 15, and the candidate values for κ were $1,\ 2,\ \ldots, 20$.

models considered in Hurley (1992) and his empirical findings. Lastly, we reanalyze Hurley's (1992) bedload movement occurrence data in the framework of our almost periodic IGP model.

We now describe the bedload movement occurrence data which were analyzed in Hurley (1992). As part of a larger study to investigate the effects of human activities, such as impounding water in regulatory reservoirs on salmonid fish (Salmo trutta), the Great Eggleshope Beck and the Carl Beck streams (which are two small unregulated streams located in Upper Teesdale, UK) were selected for the monitoring of bedload throughput. Hurley (1992) argues that studies on unregulated streams, such as these two, permit for future comparisons with streams that have been affected by human activities. The features of the two lakes are described in Carling and Reader (1982). A pit-type bedload trap was dug in each stream across the width of the bed and close to the catchment outlets. A bedload movement event was defined as any discharge which transported coarse sand and granules, greater than 2mm, into the trap. Salmonids bury their eggs in the top 20 cm of the gravel bed and an event of this size would cause disturbance of the bed where the eggs lie. Thus, usually during heavy rainfall, the times of bedload movement events may influence the spawning success of salmonid fish. The occurrence times of 78 events in Great Eggleshope and 82 events in Carl Beck over a six year period were recorded and are provided in Appendix A of Hurley (1992). For both the Great Eggleshope Beck and the Carl Beck data, Hurley (1992) states that the histograms of monthly frequencies of events show a seasonal cycle with winter peaks, summer lows, and a possible small spring peak.

We now present the IGP models which were considered in Hurley (1992) and summarize his empirical findings. In his paper, Hurley proposed to fit an IGP model using an iterative reweighted least-squares regression procedure for the maximum likelihood estimation. However, Hurley's procedure does not estimate κ, so he performs his estimation procedure by substituting in candidate values for κ. He then performs some log-likelihood ratio test within nested models to determine the appropriate number of periodic and trend components to include in his models. Then he defines the estimate of κ as the κ value which gave rise to the IGP model with the largest maximum likelihood among the candidate models. Fifteen IGP models were fitted to the data, with candidate shape parameter $\kappa = 1$ (the nonhomogeneous Poisson process), $\kappa = 2$, and $\kappa = 3$, each with the following baseline intensity functions:

Case 1 $\lambda_1(t) := \exp\{\beta_0\}$

Case 2 $\lambda_1(t) := \exp\{\beta_0 + A_1 \cos(\omega_1 t) + B_1 \sin(\omega_1 t)\}$

Case 3 $\lambda_1(t) := \exp\{\beta_0 + A_1 \cos(\omega_1 t) + B_1 \sin(\omega_1 t) + \beta_1 t\}$

Case 4 $\lambda_1(t) := \exp\{\beta_0 + A_1 \cos(\omega_1 t) + B_1 \sin(\omega_1 t) + \beta_1 t + A_2 \cos(\omega_2 t) + B_2 \sin(\omega_2 t)\}$

Case 5 $\lambda_1(t) := \exp\{\beta_0 + A_1 \cos(\omega_1 t) + B_1 \sin(\omega_1 t) + \beta_1 t + A_2 \cos(\omega_2 t) + B_2 \sin(\omega_2 t)$

$$+ A_3 \cos(\omega_3 t) + B_3 \sin(\omega_3 t)\},$$

where $t > 0$, the frequencies $\omega_1 = \frac{2\pi}{365.25}$, $\omega_2 = 2\frac{2\pi}{365.25}$, and $\omega_3 = 3\frac{2\pi}{365.25}$ are assumed known a priori, and the parameters A_i ($i = 1,\ 2,\ 3$), B_i ($i = 1,\ 2,\ 3$), and β_1 are unknown. The frequencies correspond to a cycle of period 1 year, to a cycle of period $\frac{1}{2}$ year, and to a cycle of period $\frac{1}{3}$ year, respectively. Hurley (1992) uses his iterative reweighted least squares procedure to fit a given IGP model to each data set individually. After fitting the above models to the data sets, Hurley (1992) concludes that the log-likelihood ratio tests between nested models suggests that the baseline intensity function should include a linear trend and include cycles of period 1 year and $\frac{1}{2}$ year. The cycle of period $\frac{1}{3}$ year is not required. Furthermore, he states that maximization of the likelihood function of the data suggest that the Cases 1-3 models should have a shape parameter $\kappa = 1$ and the Cases 4 and 5 models should have a shape parameter $\kappa = 2$. Therefore, among the models considered, Hurley (1992) chooses the IGP model with the Case 4 baseline intensity function and shape parameter $\kappa = 2$. When fitting an IGP model with the Case 4 baseline intensity function and shape parameter $\kappa = 2$ to the Great Eggleshope Beck data, the maximum log-likelihood of the model is -307.16. Similarly, for the Carl Beck data, the maximum log-likelihood of the model is -324.84.

We now reanalyze Hurley's (1992) bedload movement occurrence data in the framework of our model. We begin by describing the assumptions imposed on the Great Eggleshope Beck data set. When observing an IGP, we must define the first observation as the time origin, and after that, we must set the first event after the time origin as the first IGP epoch and so on. The time origin for the Great Eggleshope Beck data set is December 8, 1978. For the Great Eggleshope Beck data, the observational time is $T = 6$ years, and the data is given in units of days, so the total observational time is $T = 2191.5$ days. However, for computational tractability we use the time truncated joint density function (1.3) in the MLE procedure, so we define the observational time as the last bedload transport occurrence, namely $T = 2007$ days. The data set has a total of 78 observations. Therefore, if we define the first observation as the time origin, then there are a total of 77 events. Now, our estimation procedure requires that the angular frequencies satisfy the Chapter 2 Assumptions 2-3; therefore, we set down the following frequency range restrictions. The maximum considered period is 1 year, so the minimum considered frequency is $\frac{2\pi}{365.25} = 0.01720242$. Observations were made every day, so we assumed that the smallest period is 1 week. Therefore, the maximum frequency is assumed to be $\frac{2\pi}{7} = 0.8975979$. The minimum separation period between two frequencies is assumed to be $\frac{6\pi}{T} = 0.009392$. Given the small sample size, we apply the Section 3.2 estimation procedure without conducting the out of sample forecast to assess the model validity. Instead, we check the goodness of fit of our model using Ogata's (1988) Residual Analysis method, which we described in Section 1.4. Furthermore, we introduce a linear trend component to the baseline intensity function (2.1) when conducting a computational MLE procedure. We do this by using the Bartlett periodogram estimates of the baseline intensity function (2.1), without the linear trend component included, as the initial values for a MLE procedure for estimating the baseline intensity function (2.1). Next, we use the corresponding MLE of the baseline intensity function (2.1) as the initial values for a MLE procedure for estimating the baseline intensity function (2.1) plus a linear trend component and we use $\left(N_G(T/2)/(T/2) + N_G(T/2,\ T)/(T/2)\right)/2$ as the initial value for the MLE of the coefficient of the linear trend component. In our estimation procedure, the candidate values for the shape parameter were $\kappa = 1,\ 2,\ \ldots,\ 10$ and the candidate values for the number of periodic components were $K = 0,\ 1, \ldots,\ 7$, where $K = 0$ implies a gamma renewal process model. We describe the performance of our model on the Great Eggleshope Beck data set below.

The parameter estimates of the baseline intensity function (2.1) are provided in Table 3.5. The Bartlett periodogram estimates of the baseline intensity function (2.1) when using the AIC estimates for κ and K are provided under the heading "The AIC and the Bartlett Periodogram Estimates." The estimated periodic component corresponds to a $\frac{2\pi}{0.0174647} = 359.77$ day cycle (a yearly cycle). Similarly, the Bartlett periodogram estimates of the baseline intensity function (2.1) when using the BIC estimates for κ and K are provided under the heading "The BIC and the Bartlett Periodogram Estimates." Out of the models considered, the AIC model selection procedure estimates $\kappa = 2$ and $K = 1$ and the BIC model selection procedure estimates $\kappa = 2$ and $K = 0$. The Bartlett periodogram of the Great Eggleshope Beck data is provided in Figure 3.1 and is labeled as Figure (a) which indicates that the 359.77 day cycle (a yearly cycle) is the most significant cycle of the data. The corresponding Q-Q plot of the residual process, when fitting the data set with the AIC estimates

$\kappa = 2$ and $K = 1$, is provided in Figure 3.2 and is labeled as Figure (a). The Q-Q plot indicates that the IGP model with $\kappa = 2$ and $K = 1$ adequately describes the data. The corresponding Q-Q plot of the residual process, when fitting the data set with the BIC estimates $\kappa = 2$ and $K = 0$, is provided in Figure 3.4, and is labeled as Figure (a). The Q-Q plot indicates that the IGP model with $\kappa = 2$ and $K = 0$ adequately describes the data. The corresponding MLE of the baseline intensity function (2.1), when using the AIC estimates $\kappa = 2$ and $K = 1$, are provided under the heading "The Corresponding MLE when using the AIC Estimates $\kappa = 2$ and $K = 1$." The estimated periodic component corresponds to a $\frac{2\pi}{0.017655} = 355.87$ day cycle (a yearly cycle). The log-likelihood of this model is -316.394 and is slightly smaller than Hurley's (1992) Case 4 fitted model which had a log-likelihood of -307.16. Similarly, the MLE of the baseline intensity function (2.1), when using the BIC estimates for κ and K, is provided under the heading "The Corresponding MLE when using the BIC Estimates $\kappa = 2$ and $K = 0$." There is no frequency component for this model. The log-likelihood of this model is -326.435 and is larger than Hurley's (1992) Case 4 fitted model which had a log-likelihood of -307.16. The corresponding Q-Q plot of the residual process, when fitting the data with the AIC estimates $\kappa = 2$ and $K = 1$ and the MLE of the baseline intensity function (2.1), indicates that the MLE based IGP model with $\kappa = 2$ and $K = 1$ is not an adequate model for the data. The MLE of the baseline intensity function (2.1) plus a linear trend component, when using the AIC estimates $\kappa = 2$ and $K = 1$, is provided under the heading "The Corresponding

MLE with Trend Component when using the AIC Estimates $\kappa = 2$ and $K = 1$." The estimated periodic component corresponds to a $\frac{2\pi}{0.0176503} = 355.98$ day cycle. The log-likelihood of this model is -325.1825. The corresponding Q-Q plot of the residual process, when fitting the data with the AIC estimates $\kappa = 2$ and $K = 1$ and the MLE of the baseline intensity function (2.1) plus linear trend component, indicates that the MLE with the added trend component IGP model with $\kappa = 2$ and $K = 1$ is not an adequate model for the data. In conclusion, among the fitted IGP models, the IGP model with $\kappa = 2$, $K = 1$, and with the Bartlett periodogram based estimates is the better model.

We now describe the assumptions imposed on the Carl Beck data set. The time origin for the Carl Beck data set is October 5, 1978. For the Carl Beck data, the observation time is $T = 6$ years, and the data is given in units of days, so the total observational time is $T = 2191.5$ days. However, for computational tractability we use the time truncated joint density function (1.3) in the MLE procedure, so we define the observational time as the last bedload transport occurrence time, namely $T = 1999$ days. The data set has a total of 82 observations. Therefore, if we define the first observation as the time origin, then there are a total of 81 events. Now, our estimation procedure requires that the angular frequencies satisfy the Chapter 2 Assumptions 2-3; therefore, we set down the following frequency range restrictions. The maximum considered period is 1 year so the minimum assumed frequency is $\frac{2\pi}{365.25} = 0.01720242$. Observations were made every day so we assumed that the smallest period is 1 week.

Therefore, the maximum frequency is assumed to be $\frac{2\pi}{7} = 0.8975979$. The minimum separation period between two frequencies is assumed to be $\frac{6\pi}{T} = 0.009429$. Given the small sample size, we apply the Section 3.2 estimation procedure without conducting the out of sample forecast. Furthermore, we introduce a linear trend component to the baseline intensity function (2.1) when conducting a computational MLE procedure. We do this by using the Bartlett periodogram estimates of the baseline intensity function (2.1), without the linear trend component included, as the initial values for a MLE procedure for estimating the baseline intensity function (2.1). Next, we use the corresponding MLE of the baseline intensity function (2.1) as the initial values for a MLE procedure for estimating the baseline intensity function (2.1) plus a linear trend component and we use $\left(N_G(T/2)/(T/2) + N_G(T/2,\ T)/(T/2)\right)/2$ as the initial value for the MLE of the coefficient of the linear trend component. In our estimation procedure, the candidate values for the shape parameter were $\kappa = 1,\ 2,\ \ldots,\ 10$ and the candidate values for the number of periodic components were $K = 0,\ 1, \ldots,\ 7$, where $K = 0$ implies a gamma renewal process model. We describe the performance of our model on the Carl Beck data set below.

The parameter estimates of the baseline intensity function (2.1) are provided in Table 3.6. The Bartlett periodogram estimates of the baseline intensity function (2.1) when using the AIC estimates for κ and K are provided under the heading "The AIC and the Bartlett Periodogram Estimates." The estimated periodic component corresponds to a $\frac{2\pi}{0.01720242} = 365.25$ day cycle (a yearly cycle). Similarly, the Bartlett periodogram estimates of the baseline intensity function (2.1) when using the BIC estimates for κ and K are provided under the heading "The BIC and the Bartlett Periodogram Estimates." Out of the models considered, the AIC model selection procedure estimates $\kappa = 1$ and $K = 1$, and the BIC model selection procedure estimates $\kappa = 1$ and $K = 0$. The Bartlett periodogram of the Carl Beck data is provided in Figure 3.1 and is labeled as Figure (b), and indicates that the $\frac{2\pi}{0.01720242} =$ 365.25 day cycle (a yearly cycle) and the $\frac{2\pi}{0.804734594} = 7.80$ day cycle are the most significant cycles of the data. The corresponding Q-Q plot of the residual process, when fitting the data set with the AIC estimates $\kappa = 1$ and $K = 1$, is provided in Figure 3.3 and is labeled as Figure (a). The Q-Q plot indicates that the IGP model with $\kappa = 1$ and $K = 1$ adequately describes the data. The corresponding Q-Q plot of the residual process, when fitting the data set with the BIC estimates $\kappa = 1$ and $K = 0$, is provided in Figure 3.4 and is labeled as Figure (b). The Q-Q plot indicates that the IGP model with $\kappa = 1$ and $K = 0$ adequately describes the data. The corresponding MLE of the baseline intensity function (2.1), when using the AIC estimates $\kappa = 1$ and $K = 1$, is provided under the heading "The Corresponding MLE when using the AIC Estimates $\kappa = 1$ and $K = 1$." The estimated periodic component corresponds to a $\frac{2\pi}{0.0171994} = 365.314$ day cycle (a yearly cycle). The log-likelihood of this model is -333.8368 and is slightly smaller than Hurley's (1992) Case 4 fitted model which had a log-likelihood of -324.84. Similarly, the MLE of the baseline intensity function (2.1) is provided under the heading "The Corresponding MLE when using the

BIC Estimates $\kappa = 1$ and $K = 0$." There is no frequency component for this model. The log-likelihood of this model is -339.0792 and is slightly smaller than Hurley's (1992) corresponding model with a log-likelihood of -324.84. The corresponding Q-Q plot of the residual process, when fitting the data with the AIC estimates $\kappa = 1$ and $K = 1$ and the MLE of the baseline intensity function (2.1), indicates that the MLE based IGP model with $\kappa = 1$ and $K = 1$ is not an adequate model for the data. The MLE of the baseline intensity function (2.1) plus a linear trend component, when using the AIC estimates $\kappa = 1$ and $K = 1$, is provided under the heading "The Corresponding MLE with Trend Component when using the AIC Estimates $\kappa = 1$ and $K = 1$." The estimated periodic component corresponds to a $\frac{2\pi}{0.034574} = 181.732$ day cycle. The log-likelihood of this model is -340.6279. The corresponding Q-Q plot of the residual process, when fitting the data with the AIC estimates $\kappa = 1$ and $K = 1$ and the MLE of the baseline intensity function (2.1) plus linear trend component, indicates that the MLE with the added trend component IGP model with $\kappa = 1$ and $K = 1$ is not an adequate model for the data. In conclusion, among the fitted IGP models, the IGP model with $\kappa = 1$, $K = 1$, and with the Bartlett periodogram based estimates is the better model.

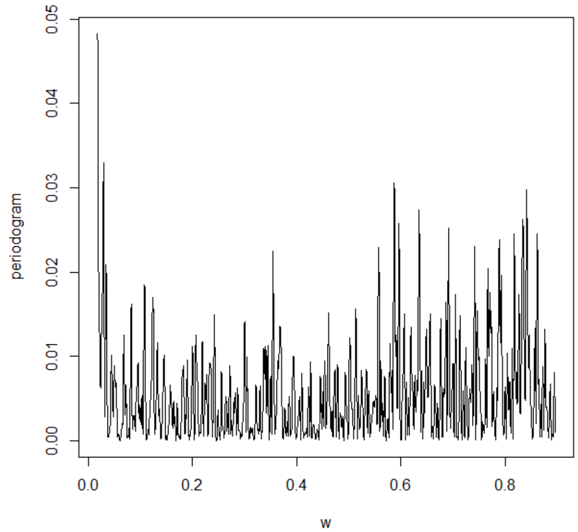

(a)

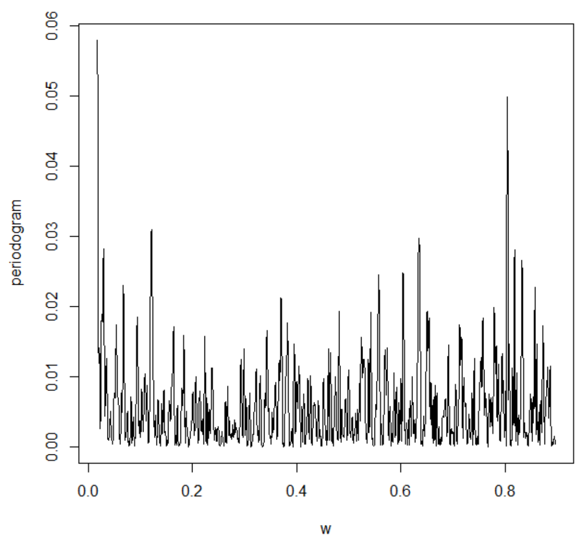

(b)

Figure 3.1: The empirical Bartlett periodogram of the Great Eggleshope Beck and Carl Beck bedload transport occurrence data. Figure (a) contains the empirical Bartlett periodogram of the Great Eggleshope Beck data set, with the time origin set at December 8, 1978. Figure (b) provides the empirical Bartlett periodogram of the Carl Beck data set, with the time origin set at October 5, 1978.

The AIC and the Bartlett Periodogram Estimates					
A_1	ω_1	ϕ_1	B	κ	K
0.0496383	0.0174647	0.0174647	0.0767314	2	1

The BIC and the Bartlett Periodogram Estimates		
B	κ	K
0.0767314	2	0

The Corresponding MLE when using the AIC Estimates $\kappa = 2$ and $K = 1$					
A_1	ω_1	ϕ_1	B	AIC	Log-likelihood
0.0440188	0.017655	-0.70303	0.0761464	640.788	-316.394

The Corresponding MLE when using the BIC Estimates $\kappa = 2$ and $K = 0$		
B	BIC	Log-likelihood
0.0767314	660.4748	-326.435

The Corresponding MLE with Trend Component when using the AIC Estimates $\kappa = 2$ and $K = 1$				
A_1	ω_1	ϕ_1	B	C
0.0495719	0.0176503	-0.712924	0.078174	2.70173e-09

AIC	Log-likelihood
652.365	-325.1825

Table 3.5: The estimated parameters for the baseline intensity function (2.1) based on the Great Eggleshope Beck bedload transport data set. The time origin is December 8, 1978. The Bartlett periodogram based estimates of the baseline intensity function (2.1) when using the AIC estimates for κ and K are provided under the heading "The AIC and the Bartlett Periodogram Estimates." The Bartlett periodogram based estimates of the baseline intensity function (2.1) when using the BIC estimates for κ and K are provided under the heading "The BIC and the Bartlett Periodogram Estimates." The MLE of the baseline intensity function (2.1), when using the AIC estimates $\kappa = 2$ and $K = 1$, is provided under the heading "The Corresponding MLE when using the AIC Estimates $\kappa = 2$ and $K = 1$." The MLE of the baseline intensity function (2.1), when using the BIC estimates $\kappa = 2$ and $K = 0$, is provided under the heading "The Corresponding MLE when using the BIC Estimates $\kappa = 2$ and $K = 0$." The MLE of the baseline intensity function (2.1) plus a linear trend component, say C, when using the AIC estimates $\kappa = 2$ and $K = 1$, is provided under the heading "The Corresponding MLE with Trend Component when using the AIC Estimates $\kappa = 2$ and $K = 1$."

The AIC and the Bartlett Periodogram Estimates					
A_1	ω_1	ϕ_1	B	κ	K
0.02697619	0.01720242	4.705694	0.04052026	1	1

The BIC and the Bartlett Periodogram Estimates		
B	κ	K
0.0767314	1	0

The Corresponding MLE when using the AIC Estimates $\kappa = 1$ and $K = 1$					
A_1	ω_1	ϕ_1	B	AIC	Log-likelihood
0.0235210	0.0171994	4.50283	0.0392126	675.6737	-333.8368

The Corresponding MLE when using the BIC Estimates $\kappa = 1$ and $K = 0$		
B	BIC	Log-likelihood
0.0767314	685.7589	-339.0792

The Corresponding MLE with Trend Component when using the AIC Estimates $\kappa = 1$ and $K = 1$				
A_1	ω_1	ϕ_1	B	C
0.0269743	0.034574	4.70571	0.0446683	4.07505e-12

AIC	Log-likelihood
689.256	-340.6279

Table 3.6: The estimated parameters for the baseline intensity function (2.1) based on the Carl Beck bedload transport data set. The time origin is October 5, 1978. The Bartlett periodogram estimates of the baseline intensity function (2.1) when using the AIC estimates for κ and K are provided under the heading "The AIC and the Bartlett Periodogram Estimates." The Bartlett periodogram estimates of the baseline intensity function (2.1) when using the BIC estimates for κ and K are provided under the heading "The BIC and the Bartlett Periodogram Estimates." The MLE of the baseline intensity function (2.1), when using the AIC estimates $\kappa = 1$ and $K = 1$, is provided under the heading "The Corresponding MLE when using the AIC Estimates $\kappa = 1$ and $K = 1$." The MLE of the baseline intensity function (2.1), when using the BIC estimates $\kappa = 1$ and $K = 0$, is provided under the heading "The Corresponding MLE when using the BIC Estimates $\kappa = 1$ and $K = 0$." The MLE of the baseline intensity function (2.1) plus a linear trend component, when using the AIC estimates $\kappa = 1$ and $K = 1$, is provided under the heading "The Corresponding MLE with Trend Component when using the AIC Estimates $\kappa = 1$ and $K = 1$."

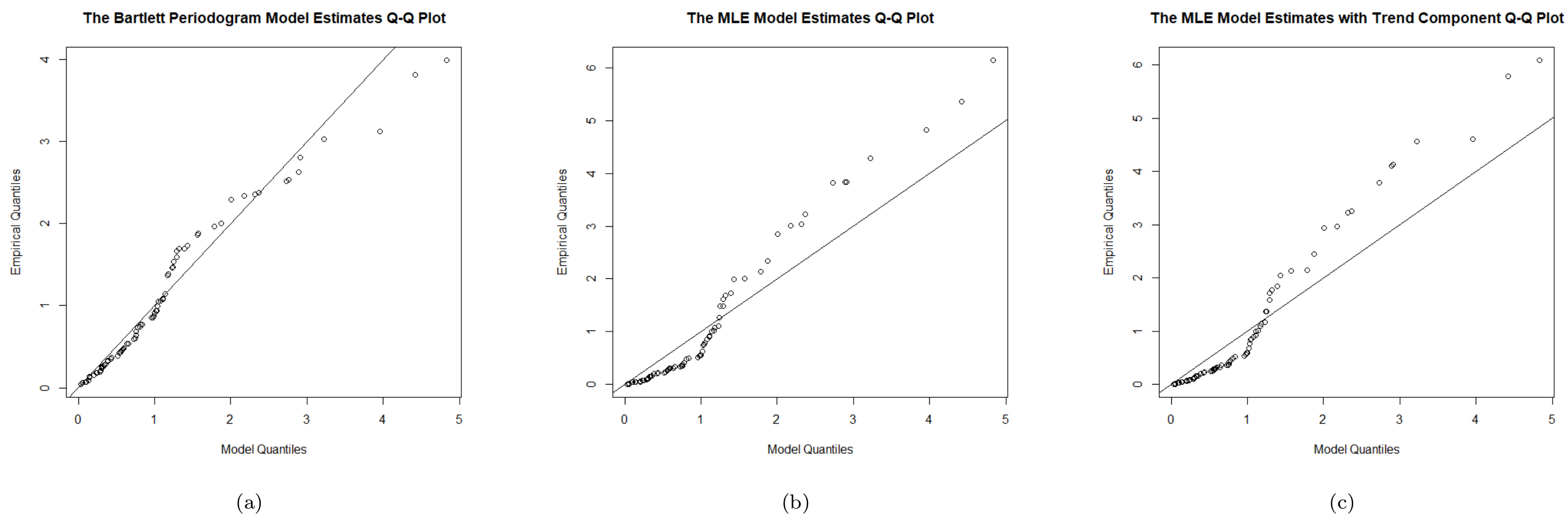

Figure 3.2: The Q-Q plots of the fitted residual process for the Great Eggleshope Beck data set, when using the AIC estimates for κ and K. Plot (a) is the corresponding Q-Q plots of the fitted residual process when using the fitted model with the Bartlett periodogram estimates of the baseline intensity function (2.1). Plot (b) is the corresponding Q-Q plots of the fitted residual process when using the fitted model with the MLEs of the baseline intensity function (2.1). Plot (c) is the corresponding Q-Q plots of the fitted residual process when using the fitted model with the MLEs of the baseline intensity function (2.1) plus a trend component.

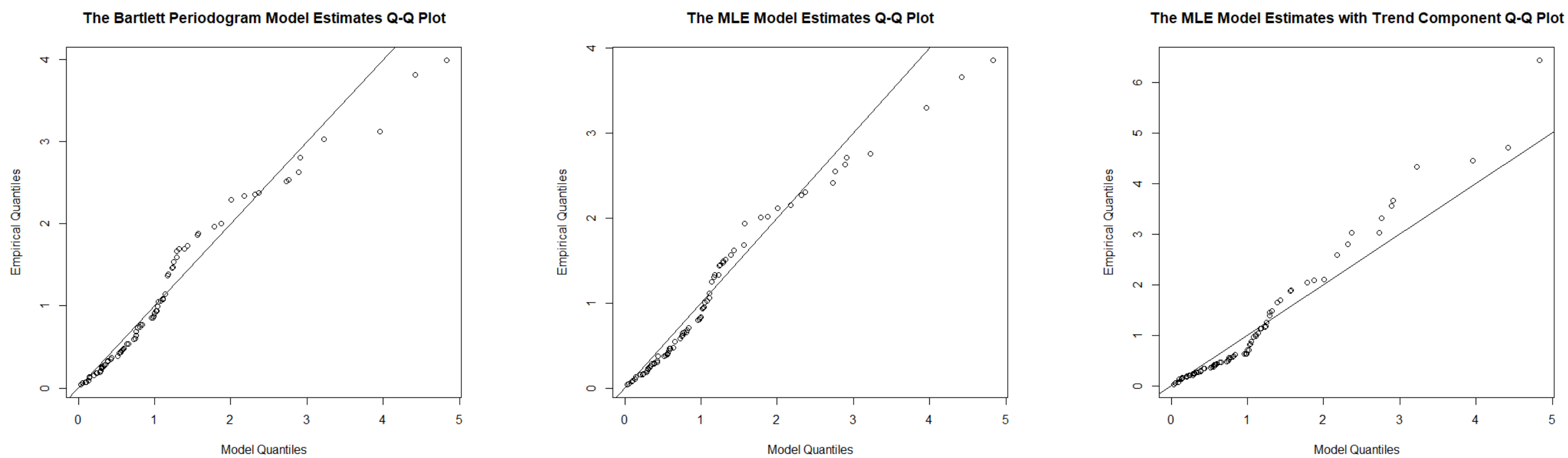

(a) (b) (c)

Figure 3.3: The Q-Q plots of the fitted residual process for the Carl Beck data set, when using the AIC estimates for κ and K. Plot (a) is the corresponding Q-Q plots of the fitted residual process when using the fitted model with the Bartlett periodogram estimates of the baseline intensity function (2.1). Plot (b) is the corresponding Q-Q plots of the fitted residual process when using the fitted model with the MLEs of the baseline intensity function (2.1). Plot (c) is the corresponding Q-Q plots of the fitted residual process when using the fitted model with the MLEs of the baseline intensity function (2.1) plus a trend component.

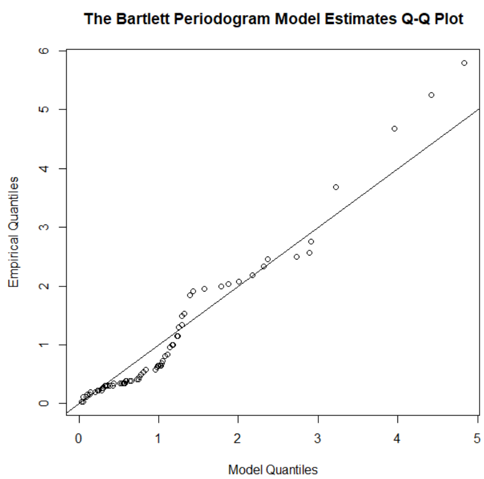

(a)

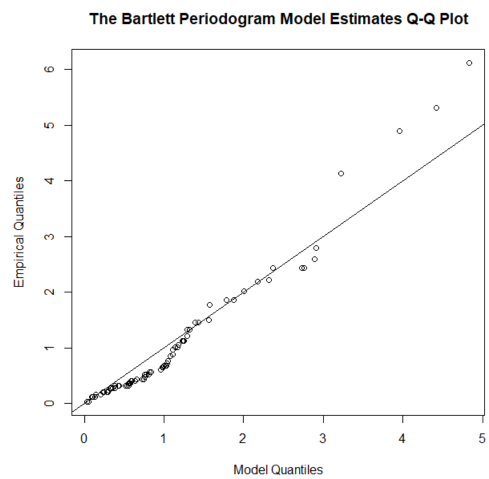

(b)

Figure 3.4: The Q-Q plots of the fitted residual process for the Great Eggleshope Beck and Carl Beck data sets, when using the BIC estimates for κ and K. Plot (a) corresponds to the Great Eggleshope Beck data with $\kappa = 2$ and $K = 0$. Plot (b) corresponds to the Carl Beck data with $\kappa = 1$ and $K = 0$.

Chapter 4

Summary and Future Work

4.1 Summary

In this thesis, a general model for the baseline intensity function of an inhomogeneous Gamma process is proposed and investigated. The proposed model deals with non-stationary and non-Poisson point events which show a pattern of periodicity or almost periodicity, such as in the study of meteorology where periodic storm patterns have been observed in the Arctic Sea (Lee et al. (1991)). The proposed inhomogeneous Gamma process model with almost periodic baseline intensity function, which includes the purely periodic baseline intensity function as a particular case, is much more general and useful than the existing models such as those provided in Berman (1981) and Hurley (1992). We demonstrate this by both a simulation study and a real life data set analysis.

The basic concepts of point processes on the nonnegative real line are introduced in Chapter 1. The gamma renewal process, homogeneous Poisson process, nonhomogeneous Poisson process, and inhomogeneous Gamma process are introduced in Section 1.2. The literature review on the current progress of modeling periodicity in an inhomogeneous Gamma process is provided in Section 1.7. In Chapter 2, the concept of an almost periodic function is introduced. In Section 2.2, the almost periodic inhomogeneous Gamma process model is introduced. Since purely periodic functions are special cases of almost periodic functions, we argue that almost periodic inhomogeneous Gamma process models should always be considered over the purely periodic models. The prediction of the one step ahead point event in the framework of our model is considered in Section 2.3. Lastly, we demonstrate the usefulness of our model through simulation.

The proposed inhomogeneous Gamma process model is a class of models indexed by the shape parameter $\kappa > 0$ and the number of cosinusoidal terms in the baseline intensity function K. In Chapter 2, the parameter estimators are defined for known κ and K. In the data analysis, both κ and K are usually unknown, and we need to select the best κ and K so that the corresponding model can best approximate the unknown true model. So in Chapter 3, we propose to use the AIC and the BIC model selection criteria to determine the κ and K values. The estimation procedure of the κ and K parameters is provided in Section 3.2 and then we follow the procedures to reanalyze the simulated data set.

4.2 Future Work

This thesis proposes a parametric model for the baseline intensity function of an inhomogeneous Gamma process (IGP) with shape parameter $\kappa > 0$. A future direction of research is in extending our IGP model to a marked point IGP with a periodic or almost periodic baseline intensity function model. For instance, the stock transaction process tends to exhibit a higher volume of transactions during the opening and the closing of a trading day and much less during the lunch hour, and this pattern repeats daily. Therefore, the stock transaction process can be modeled as an IGP with a periodic or almost periodic baseline intensity function. However, a question of practical interest is whether the time of a stock transaction influences the transaction type and quantity, and a stochastic process which can model such behavior is a marked point IGP with a periodic or almost periodic baseline intensity function. Another field of study which models physical phenomena with marked point processes is Seismology. The occurrence time of an earth quake process has been shown to exhibit periodic occurrence patterns Vere-Jones (1982). Therefore, the occurrence time of an earth quake process can be modeled as an IGP with a periodic or almost periodic baseline intensity function. However, a question of practical interest is whether the time of an earthquake influences the location and magnitude of the earthquake, and a stochastic process which can model such behavior is a marked point IGP with a periodic or almost periodic baseline intensity function. Therefore, extending our model to a marked point IGP with a periodic or almost period baseline intensity function is a problem worth pursuing.

Appendix A

Proofs for Chapter 1

A.1 Proofs for Chapter 1 Section 2

A.1.1 The random variables $0 < T_1 < T_2 < \cdots < T_n < \infty$ are the random epoch times of an inhomogeneous Gamma process with baseline intensity function $0 < \lambda_1(t) \leq M < \infty$ $(0 < t < \infty)$ and shape parameter $\kappa > 0$ if and only if for each $i = 1,\ 2,\ \ldots,\ n$, the random variables $Y_i = \Lambda_1(T_i) - \Lambda_1(T_{i-1})$ are independent and identically distributed $\mathit{\Gamma}(\kappa,\ 1)$ random variables, where $\Lambda_1(t) := \int_0^t \lambda_1(u)du$, $\Lambda_1(\infty) = \infty$, and $T_0 = 0$.

Proof. By the one-to-one correspondence between the random epochs $0 < T_1 < T_2 < \cdots < T_n < \infty$ and the transformation $Y_i = \Lambda_1(T_i) - \Lambda_1(T_{i-1})$, where $n,\ i = 1,\ 2,\ \ldots$ and $T_0 = 0$, it suffices to show that if $0 < T_1 < T_2 < \cdots < T_n < \infty$ are the random epoch times of an inhomogeneous Gamma process (IGP), then $Y_i = \Lambda_1(T_i) - \Lambda_1(T_{i-1})$ are independent and identically distributed $\mathit{\Gamma}(\kappa,\ 1)$ random variables, where $\kappa > 0$

is the shape parameter and 1 is the scale parameter.

For $t > 0$, let $0 < \lambda_1(t) \leq M < \infty$ be the baseline intensity function of an inhomogeneous Gamma process (IGP) with shape parameter $\kappa > 0$, and let $\Lambda_1(t) := \int_0^t \lambda_1(u)du$, where $\Lambda_1(\infty) = \infty$. Let $0 < T_1 < T_2 < \cdots < T_n < \infty$ be the random epoch times of the IGP, then by equation (1.3) for each $n \in \mathbb{N}$ the joint density function of $\{T_i\}_{i=1}^n$ is given by

$$f_n(t_1, \ldots, t_n) = \frac{1}{\Gamma(\kappa)^n} \left\{ \prod_{i=1}^{n} \lambda_1(t_i) \left[\Lambda_1(t_i) - \Lambda_1(t_{i-1})\right]^{\kappa-1} \right\} e^{-\Lambda_1(t_n)} I_{(0<t_1<\cdots<t_n<\infty)},$$

where $t_0 = 0$. Since for each $i = 1, \ldots, n$, we defined $Y_i := \Lambda_1(T_i) - \Lambda_1(T_{i-1})$, where $T_0 = 0$, it then follows that $\Lambda_1(T_n) = \sum_{i=1}^n Y_i = \sum_{i=1}^n (\Lambda_1(T_i) - \Lambda_1(T_{i-1}))$ and

$$\begin{array}{rcccc} Y_1 & = & \Lambda_1(T_1) - \Lambda_1(T_0) & = & \Lambda_1(T_1) \\ Y_2 & = & \Lambda_1(T_2) - \Lambda_1(T_1) & = & \Lambda_1(T_2) - Y_1 \\ Y_3 & = & \Lambda_1(T_3) - \Lambda_1(T_2) & = & \Lambda_1(T_3) - (Y_1 + Y_2) \\ \vdots & \vdots & \vdots & \vdots & \vdots \\ Y_n & = & \Lambda_1(T_n) - \Lambda_1(T_{n-1}) & = & \Lambda_1(T_n) - \left(\sum_{i=1}^{n-1} Y_i\right). \end{array}$$

Since for $t > 0$, $\Lambda_1(t) = \int_0^t \lambda_1(u)du$ is a strictly increasing continuous function, a unique inverse exists, and $\frac{d}{dt}\Lambda_1^{-1}(t) = \frac{1}{\lambda_1(\Lambda_1^{-1}(t))}$, where $\Lambda_1^{-1}(\cdot)$ is the inverse function of $\Lambda_1(\cdot)$. We then notice that

$$
\begin{aligned}
T_1 &= \Lambda_1^{-1}(Y_1) \\
T_2 &= \Lambda_1^{-1}(Y_1 + Y_2) \\
T_3 &= \Lambda_1^{-1}(Y_1 + Y_2 + Y_3) \\
&\vdots \\
T_n &= \Lambda_1^{-1}\left(\sum_{i=1}^{n} Y_i\right).
\end{aligned}
$$

The Jacobian of this transformation, with lower triangular portion omitted, is

$$
|J| = \begin{vmatrix}
\frac{1}{\lambda_1(\Lambda_1^{-1}(y_1))} & 0 & \cdots & & 0 \\
* & \frac{1}{\lambda_1(\Lambda_1^{-1}(y_1+y_2))} & \ddots & & \vdots \\
* & * & \frac{1}{\lambda_1(\Lambda_1^{-1}(y_1+y_2+y_3))} & \ddots & \\
* & * & * & \ddots & 0 \\
* & * & * & * & \frac{1}{\lambda_1(\Lambda_1^{-1}(y_1+\cdots+y_n))}
\end{vmatrix}
$$

and

$$
\begin{aligned}
|J| &= \frac{1}{\lambda_1(\Lambda_1^{-1}(y_1))} \frac{1}{\lambda_1(\Lambda_1^{-1}(y_1+y_2))} \cdots \frac{1}{\lambda_1(\Lambda_1^{-1}(y_1+\cdots+y_n))} \\
&= \frac{1}{\prod_{i=1}^{n} \lambda_1(\Lambda_1^{-1}\left(\sum_{j=1}^{i} y_j\right))}.
\end{aligned}
$$

Therefore, we have

$f_n(y_1, \ldots,\ y_n)$

$$= \frac{1}{\Gamma(\kappa)^n}\left[\prod_{i=1}^{n} \lambda_1\left(\Lambda_1^{-1}(\sum_{j=1}^{i} y_j)\right) y_i^{\kappa-1}\right] \frac{\exp\{-\sum_{i=1}^{n} y_i\}}{\prod_{i=1}^{n} \lambda_1\left(\Lambda_1^{-1}(\sum_{j=1}^{i} y_j)\right)} \prod_{i=1}^{n} I_{(0<y_i<\infty)}$$

$$= \frac{1}{\Gamma(\kappa)^n}\left[\prod_{i=1}^{n} y_i^{\kappa-1}\right] \exp\left\{-\sum_{i=1}^{n} y_i\right\} \prod_{i=1}^{n} I_{(0<y_i<\infty)}. \tag{A.1}$$

We notice that equation (A.1) is the joint density function of $n \in \mathbb{N}$ independent and identically distributed $\Gamma(\kappa,\ 1)$ random variables, and the result follows.

□

A.2 Proofs for Chapter 1 Section 3

A.2.1 Proof of Equations (1.5) and (1.13)

Proof. Using the tautology $\{N_G(t) \geq n\} \Leftrightarrow \{T_n \leq t\}$, where $n \in \mathbb{N}$ and $t > 0$, it follows that $M(t) \coloneqq E[N_G(t)] = \sum_{n=1}^{\infty} P\{N_G(t) \geq n\} = \sum_{n=1}^{\infty} P\{T_n \leq t\} = \sum_{n=1}^{\infty} F_{T_n}(t)$, where $F_{T_n}(\cdot)$ is the cumulative distribution function of the n-th epoch. Therefore, it follows that $\lambda_2(t) = \frac{d}{dt}M(t) = \sum_{n=1}^{\infty} f_{T_n}(t)$ for all $t > 0$, where $f_{T_n}(\cdot)$ is the density function of the n-th epoch. Equations (1.5) and (1.13) then follow from equation (1.26). □

A.2.2 Proof of Equations (1.8)-(1.10)

Proof. We first establish the claim that

$$P\left\{N_G(t,\ t+h)=1\right\}=\sum_{n=1}^{\infty}\frac{\lambda_1(t)}{\Gamma(n\kappa)}\left\{\Lambda_1(t)\right\}^{n\kappa-1}\exp\left\{-\Lambda_1(t)\right\}h+o(h),$$

where $t>0$, $h>0$, and $h\to 0$. The event $\{N_G(t,\ t+h)=1\}$ will occur if and only if there is one event in the time interval $(t,\ t+h]$, where $t>0$, $h>0$, and $h\to 0$. Since at time $t>0$, no event could have occurred, one event could have occurred, two events could have occurred, and so on, it follows from equation (1.26), and the fact that the IGP is regular and orderly that for $t>0$, $h>0$, and $h\to 0$, we have

$$\begin{aligned}
P\left\{N_G(t,\ t+h)=1\right\} &= \sum_{n=1}^{\infty}P\left\{t<T_n\le t+h\right\}\\
&= \sum_{n=1}^{\infty}\int_t^{t+h}\frac{\lambda_1(u)}{\Gamma(n\kappa)}\left\{\Lambda_1(u)\right\}^{n\kappa-1}\exp\left\{-\Lambda_1(u)\right\}du\\
&= \sum_{n=1}^{\infty}\frac{\lambda_1(t)}{\Gamma(n\kappa)}\left\{\Lambda_1(t)\right\}^{n\kappa-1}\exp\left\{-\Lambda_1(t)\right\}h+o(h), \quad \text{(A.2)}
\end{aligned}$$

and the result follows.

Next, we establish the claim that $P\left\{N(t,\ t+h)\ge 2\right\}=o(h)$, where $t>0$, $h>0$, and $h\to 0$. The event $\{N_G(t,\ t+h)\ge 2\}$ will occur if and only if there are two or more events in the time interval $(t,\ t+h]$, where $t>0$, $h>0$, and $h\to 0$. Since at time $t>0$, no event could have occurred, one event could have occurred, two events could have occurred, and so on, it follows from equation (1.26), and the fact that the point process is regular and orderly that for $t > 0$, $h > 0$, and $h \to 0$, we have

$$\begin{aligned} P\{N(t,\ t+h) \geq 2\} &= \sum_{j=1}^{\infty}\sum_{n=1}^{\infty} P\{t < T_n < \cdots < T_{n+j} \leq t+h\} \\ &= o(h), \end{aligned} \tag{A.3}$$

and the result follows.

Lastly, we establish the claim that

$$P\{N_G(t,\ t+h) = 0\} = 1 - \sum_{n=1}^{\infty} \frac{\lambda_1(t)}{\Gamma(n\kappa)} \{\Lambda_1(t)\}^{n\kappa-1} \exp\{-\Lambda_1(t)\}h + o(h),$$

where $t > 0$, $h > 0$, and $h \to 0$. From equations (A.2) and (A.3), it follows that for $t > 0$, $h > 0$, and $h \to 0$, we have

$$\begin{aligned} P\{N_G(t,\ t+h) = 0\} &= 1 - P\{N_G(t,\ t+h) \geq 1\} \\ &= 1 - P\{N_G(t,\ t+h) = 1\} - P\{N_G(t,\ t+h) \geq 2\} \\ &= 1 - \sum_{n=1}^{\infty} \frac{\lambda_1(t)}{\Gamma(n\kappa)} \{\Lambda_1(t)\}^{n\kappa-1} \exp\{-\Lambda_1(t)\}h + o(h), \end{aligned} \tag{A.4}$$

and the result follows. $\square$

A.2.3 Proof of Equation (1.11)

Proof. From equation (1.26), for all $t > 0$, we have

$$\begin{aligned} E[N_G(t)] &= \sum_{n=1}^{\infty} P\left\{N_G(t) \geq n\right\} \\ &= \sum_{n=1}^{\infty} P\left\{T_n \leq t\right\} \\ &= \sum_{n=1}^{\infty} \int_0^t \frac{\lambda_1(u)}{\Gamma(n\kappa)} \left\{\Lambda_1(u)\right\}^{n\kappa-1} \exp\left\{-\Lambda_1(u)\right\} du \\ &= \int_0^t \sum_{n=1}^{\infty} \frac{\lambda_1(u)}{\Gamma(n\kappa)} \left\{\Lambda_1(u)\right\}^{n\kappa-1} \exp\left\{-\Lambda_1(u)\right\} du. \end{aligned} \tag{A.5}$$

Therefore, for all $t > 0$, we have

$$\begin{aligned} \lim_{h\to 0^+} \frac{E[N_G(t+h) - N_G(t)]}{h} &= \lim_{h\to 0^+} \frac{E[N_G(t+h)] - E[N_G(t)]}{h} \\ &= \lim_{h\to 0^+} \frac{\int_t^{t+h} \sum_{n=1}^{\infty} \frac{\lambda_1(u)}{\Gamma(n\kappa)} \left\{\Lambda_1(u)\right\}^{n\kappa-1} \exp\left\{-\Lambda_1(u)\right\} du}{h} \\ &= \sum_{n=1}^{\infty} \frac{\lambda_1(t)}{\Gamma(n\kappa)} \left\{\Lambda_1(t)\right\}^{n\kappa-1} \exp\left\{-\Lambda_1(t)\right\}. \end{aligned} \tag{A.6}$$

From equations (1.9), (1.10), and (1.13), it follows that for all $t > 0$, we have

$$\begin{aligned} \lim_{h\to 0^+} \frac{P\left\{N_G(t,\ t+h) \geq 1\right\}}{h} &= \lim_{h\to 0^+} \frac{\sum_{n=1}^{\infty} \frac{\lambda_1(t)}{\Gamma(n\kappa)} \left\{\Lambda_1(t)\right\}^{n\kappa-1} \exp\left\{-\Lambda_1(t)\right\} h + o(h)}{h} \\ &= \sum_{n=1}^{\infty} \frac{\lambda_1(t)}{\Gamma(n\kappa)} \left\{\Lambda_1(t)\right\}^{n\kappa-1} \exp\left\{-\Lambda_1(t)\right\}. \end{aligned} \tag{A.7}$$

Therefore, for all $t > 0$, we have

$$\lim_{h \to 0^+} \frac{P\{N_G(t,\ t+h) \geq 1\}}{h} = \lim_{h \to 0^+} \frac{E[N_G(t+h) - N_G(t)]}{h}. \tag{A.8}$$

$\square$

A.3 Proofs for Chapter 1 Section 8

A.3.1 Proofs for Chapter 1 Section 8 Subsection 1

A.3.1.1 Proof of Equation (1.26)

Proof. From the proof of A.1.1, we know that the random epoch sequence of the IGP, say $\{T_n,\ n \in \mathbb{N}\}$, has a joint density function of equation (1.3) if and only if for each $i = 1,\ 2,\ \ldots,\ n$, the random variables $\Lambda_1(T_i) - \Lambda_1(T_{i-1})$ are independent and identically distributed $\Gamma(\kappa,\ 1)$, where $T_0 = 0$. Therefore, for each $n = 1,\ 2,\ \ldots,\ \Lambda_1(T_n) = \sum_{i=1}^{n} \{\Lambda_1(T_i) - \Lambda_1(T_{i-1})\} \sim \Gamma(n\kappa,\ 1)$ with density function $f_{\Lambda_1(T_n)}(t) = \frac{1}{\Gamma(n\kappa)} t^{n\kappa-1} \exp\{-t\} I_{\{t>0\}}$. Since $\Lambda_1(t) = \int_0^t \lambda_1(u)du$, it follows that $f_{T_n}(t)$ $= f_{\Lambda_1(t)}(\Lambda_1(t)) \frac{d}{dt}[\Lambda_1(t)] = \frac{\lambda_1(t)}{\Gamma(n\kappa)} \{\Lambda_1(t)\}^{n\kappa-1} \exp\{-\Lambda_1(t)\} I_{\{t>0\}}$. $\square$

A.3.1.2 Proof of Equation (1.27)

Proof. From equation (1.3), it follows that

$$
\begin{aligned}
f(t_{n+1} \mid t_1, \ldots, t_n) &= \frac{f_{n+1}(t_1, \ldots, t_{n+1})}{f_n(t_1, \ldots, t_n)} \\
&= \frac{\frac{1}{\Gamma(\kappa)^{n+1}} \left\{\prod_{i=1}^{n+1} \lambda_1(t_i) \left[\Lambda_1(t_i) - \Lambda_1(t_{i-1})\right]^{\kappa-1}\right\} e^{-\Lambda_1(t_{n+1})}}{\frac{1}{\Gamma(\kappa)^{n}} \left\{\prod_{i=1}^{n} \lambda_1(t_i) \left[\Lambda_1(t_i) - \Lambda_1(t_{i-1})\right]^{\kappa-1}\right\} e^{-\Lambda_1(t_{n})}} \\
&= \frac{\lambda_1(t_{n+1})}{\Gamma(\kappa)} \left[\Lambda_1(t_{n+1}) - \Lambda_1(t_n)\right]^{\kappa-1} e^{-(\Lambda(t_{n+1})-\Lambda(t_n))} \prod_{i=1}^{n+1} I_{(0<t_i<\infty).}
\end{aligned}
$$

□

A.3.1.3 Proof of Equations (1.28)-(1.31)

Proof. For $t > 0$, let $0 < \lambda_1(t) \leq M < \infty$ be the baseline intensity function of an inhomogeneous Gamma process (IGP), say $\{N_G(t),\ t > 0\}$, with shape parameter $\kappa > 0$. For $t > 0$, let $\Lambda_1(t) = \int_0^t \lambda_1(u)du < \infty$ and $\Lambda_1(\infty) = \infty$. Denote the corresponding random epochs of the IGP with $0 < T_1^G < T_2^G < \cdots < T_n^G < \infty$. Let $\{N_R(t),\ t > 0\}$ be a gamma renewal process (GRP) with independent and identically $\Gamma(\kappa,\ 1)$ distributed interarrival times, and let $0 < T_1^R < T_2^R < \cdots < T_n^R < \infty$ denote the random epochs of the GRP. From the proof of A.1.1, we know that for each $n = 1,\ 2,\ \ldots,\ \Lambda_1(T_n^G) \sim \Gamma(n\kappa,\ 1)$ and $T_n^R \sim \Gamma(n\kappa,\ 1)$. If we transform the time scale of the IGP from t to $\Lambda_1^{-1}(t)$, where $\Lambda_1^{-1}(\cdot)$ denotes the inverse function of $\Lambda_1(\cdot)$, then for $t > 0$ and $n \in \mathbb{N}$ we have $P\left\{N_G(\Lambda_1^{-1}(t)) \geq n\right\}$ $= P\left\{T_n^G \leq \Lambda_1^{-1}(t)\right\} = P\left\{\Lambda_1(T_n^G) \leq t\right\} = P\left\{T_n^R \leq t\right\} = P\left\{N_R(t) \geq n\right\}$. Therefore, if we transform the time scale of the IGP from t to $\Lambda_1^{-1}(t)$, then the IGP is transformed into a GRP. Likewise, if we transform the time scale of a GRP from t to $\Lambda_1(t)$, then for $t > 0$ we have $P\left\{N_R(\Lambda_1(t)) \geq n\right\} = P\left\{T_n^R \leq \Lambda_1(t)\right\} = P\left\{\Lambda_1(T_n^G) \leq \Lambda_1(t)\right\}=$ $P\left\{\Lambda_1^{-1}((\Lambda_1(T_n^G)) \leq \Lambda_1^{-1}(\Lambda_1(t))\right\} = P\left\{T_n^G \leq t\right\} = P\left\{N_G(t) \geq n\right\}$. Hence, if we transform the time scale of a GRP from t to $\Lambda_1(t)$, then the GRP is transformed into an IGP. We use these results to derive some moment properties of the IGP which will be used to establish the variance-covariance structure of the IGP. For $0 < s < t < \infty$, we have

$$
\begin{aligned}
E\left[N_G(t)\right] &= \sum_{n=1}^{\infty} P\left\{N_G(t) \geq n\right\} \\
&= \sum_{n=1}^{\infty} P\left\{N_R(\Lambda_1(t)) \geq n\right\} \\
&= E\left[N_R(\Lambda_1(t))\right], \\
E\left[N_G(s)N_G(t)\right] &= \sum_{m=1}^{\infty}\sum_{n=1}^{\infty} P\left\{N_G(s) \geq m,\ N_G(t) \geq n\right\} \\
&= \sum_{m=1}^{\infty}\sum_{n=1}^{\infty} P\left\{N_R(\Lambda_1(s)) \geq m,\ N_R(\Lambda_1(t)) \geq n\right\} \\
&= E\left[N_R(\Lambda_1(s))N_R(\Lambda_1(t))\right].
\end{aligned}
\tag{A.9}
$$

Next, we apply the renewal process variance-covariance results of Gakis and Sivazlian (1993) to the GRP $\{N_R(t),\ t > 0\}$. For $t > 0$, define $M_1(t) \coloneqq E\left[N_R(t)\right]$ and $m_1(t) \coloneqq \frac{d}{dt}E\left[N_R(t)\right]$. Then from Gakis and Sivazlian (1993), for $0 < t_1 \leq t_2 < \infty$, we know that

$$\text{cov}\left\{N_R(t_1),\ N_R(t_2)\right\} = \int_0^{t_1} m_1(u)\left[M_1(t_2-u)+M_1(t_1-u)\right]du + M_1(t_1)\left[1-M_1(t_2)\right], \tag{A.10}$$

and for $0 < t < \infty$,

$$\text{var}\left\{N_R(t)\right\} = 2\int_0^{t} m_1(u)M_1(t-u)du + M_1(t) - \left[M_1(t)\right]^2. \tag{A.11}$$

From equations (A.10) and (A.11), we can use the relationship (A.9) between the IGP and the GRP to argue that for $0 < t_1 \leq t_2 < \infty$,

$$\begin{aligned} \text{cov}\left\{N_G(t_1),\ N_G(t_2)\right\} &= \int_0^{\Lambda_1(t_1)} m_1(u)\left[M_1(\Lambda_1(t_2)-u)+M_1(\Lambda_1(t_1)-u)\right]du \\ &\quad + M_1(\Lambda_1(t_1))\left[1-M_1(\Lambda_1(t_2))\right], \end{aligned} \tag{A.12}$$

and for $0 < t < \infty$,

$$\text{var}\left\{N_G(t)\right\} = 2\int_0^{\Lambda_1(t)} m_1(u)M_1(\Lambda_1(t)-u)du + M_1(\Lambda_1(t)) - \left[M_1(\Lambda_1(t))\right]^2. \tag{A.13}$$

Now, from equations (A.12) and (A.13), it follows that for $0 < t_1 \leq t_2 < \infty$,

$$\begin{aligned}
\operatorname{var}\{N_G(t_1,\ t_2)\} &= \operatorname{var}\{N_G(t_2)\} + \operatorname{var}\{N_G(t_1)\} - 2\operatorname{cov}\{N_G(t_1),\ N_G(t_2)\} \\
&= 2\int_{\Lambda_1(t_1)}^{\Lambda_1(t_2)} m_1(u) M_1(\Lambda_1(t_2) - u) du \\
&\quad + \left[\int_{\Lambda_1(t_1)}^{\Lambda_1(t_2)} m_1(u) du\right]\left[1 - \int_{\Lambda_1(t_1)}^{\Lambda_1(t_2)} m_1(u) du\right]. \qquad \text{(A.14)}
\end{aligned}$$

Lastly, from equation (A.12), it follows that for $0 < t_t < t_2 \leq t_3 < t_4 < \infty$,

$$\begin{aligned}
&\operatorname{cov}\{N_G(t_1,\ t_2),\ N_G(t_3,\ t_4)\} \\
&= \operatorname{cov}\{N_G(t_4),\ N_G(t_2)\} - \operatorname{cov}\{N_G(t_4),\ N_G(t_1)\} \\
&\quad -\operatorname{cov}\{N_G(t_3),\ N_G(t_2)\} + \operatorname{cov}\{N_G(t_3),\ N_G(t_1)\} \\
&= \int_{\Lambda_1(t_1)}^{\Lambda_1(t_2)} m_1(u) M_1(\Lambda_1(t_4) - u) du - \int_{\Lambda_1(t_1)}^{\Lambda_1(t_2)} m_1(u) M_1(\Lambda_1(t_3) - u) du \\
&\quad - \left[M_1(\Lambda_1(t_2)) - M_1(\Lambda_1(t_1))\right]\left[M_1(\Lambda_1(t_4)) - M_1(\Lambda_1(t_3))\right]. \qquad \text{(A.15)}
\end{aligned}$$

□

A.3.1.4 Proof of Equations (1.32) and (1.33)

Proof. Since $\{N_G(t) = 0\} \Leftrightarrow \{T_1 > t\}$ and for each $n \in \mathbb{N}$ $\{N_G(t) \geq n\} \Leftrightarrow \{T_n \leq t\}$, it follows that $P\{N_G(t) = 0\} = P\{T_1 > t\}$ and $P\{N_G(t) = n\} = P\{N_G(t) \geq n\} - P\{N_G(t) \geq n+1\} = P\{T_n \leq t\} - P\{T_{n+1} \leq t\}$. Therefore, equations (1.32) and (1.33) follow from equation (1.26). □

A.3.2 Proofs for Chapter 1 Section 8 Subsection 2

A.3.2.1 A Central Limit Theorem for the Inhomogeneous Gamma Process, Equation (1.34)

Proof. From the proof of A.1.1, we know that the random epoch sequence of the IGP, say $\{T_n,\ n \in \mathbb{N}\}$, has the joint density function of equation (1.3) if and only if for each $i = 1,\ 2,\ \ldots,\ n$, the random variables $Y_i := \Lambda_1(T_i) - \Lambda_1(T_{i-1})$ are independent and identically distributed $\Gamma(\kappa,\ 1)$, where $\kappa > 0$ is the shape parameter, 1 is the scale parameter, and $T_0 = 0$. Therefore, for each $i = 1,\ \ldots, n$, $\Lambda_1(T_i) = \sum_{j=1}^{i} Y_j$ is a sum of independent and identically distributed random variables, where $E\left[|Y_j|\right] < \infty$ and $E\left[Y_j^2\right] < \infty$. It then follows from the Lindeberg-Feller central limit theorem that as $n \to \infty$,

$$\frac{1}{\sqrt{n}} \sum_{j=1}^{n} \left(\frac{Y_j - \kappa}{\sqrt{\kappa}}\right) = \frac{1}{\sqrt{n}} \left(\frac{\sum_{j=1}^{n} Y_j - n\kappa}{\sqrt{\kappa}}\right) = \frac{1}{\sqrt{n}} \left(\frac{\Lambda_1(T_n) - n\kappa}{\sqrt{\kappa}}\right) \to Z, \quad \text{(A.16)}$$

where Z is a standard normal random variable. For a fixed $x > 0$ and all $t > 0$, define $n(t) := \lfloor E\left[N_G(t)\right] + x\sqrt{\operatorname{var}\left\{N_G(t)\right\}}\rfloor$, $\epsilon(t) := E\left[N_G(t)\right] + x\sqrt{\operatorname{var}\left\{N_G(t)\right\}} - n(t)$, and $Z_{n(t)} = \frac{1}{\sqrt{\kappa n(t)}}(\Lambda_1(T_{n(t)}) - n(t)\kappa)$, where $\lfloor \cdot \rfloor$ is the floor function and $\epsilon(t) \in [0, 1)$. From equation (A.16), we notice that as $t \to \infty$, $Z_{n(t)} \to Z$ in distribution. Then for $n(t) \in \mathbb{N}$ and as $t \to \infty$,

$$P\left\{\frac{N_G(t) - E[N_G(t)]}{\sqrt{\operatorname{var}[N_G(t)]}} < x\right\} = P\left\{N_G(t) < E\left[N_G(t)\right] + x\sqrt{\operatorname{var}\left\{N_G(t)\right\}}\right\}$$

$$= P\left\{N_G(t) < n(t) + \epsilon(t)\right\}$$

$$= P\left\{N_G(t) < n(t)\right\} \quad (\text{Since } \ \epsilon(t) \in [0,1) \ \text{ and } \ N_G(t) \in \mathbb{Z}^+.)$$

$$= P\left\{T_{n(t)} > t\right\}$$

$$= P\left\{\Lambda_1\left(T_{n(t)}\right) > \Lambda_1(t)\right\}$$

$$= P\left\{\frac{1}{\sqrt{n(t)}}\left(\frac{\Lambda_1(T_{n(t)}) - n(t)\kappa}{\sqrt{\kappa}}\right) > \frac{1}{\sqrt{n(t)}}\left(\frac{\Lambda_1(t) - n(t)\kappa}{\sqrt{\kappa}}\right)\right\}$$

$$= P\left\{Z_{n(t)} > \frac{1}{\sqrt{n(t)}}\left(\frac{\Lambda_1(t) - n(t)\kappa}{\sqrt{\kappa}}\right)\right\}$$

$$= P\left\{Z_{n(t)} > \frac{1}{\sqrt{\kappa}}\frac{\Lambda_1(t) - (E\left[N_G(t)\right] + x\sqrt{\mathrm{var}\left\{N_G(t)\right\}} - \epsilon(t))\kappa}{\sqrt{E\left[N_G(t)\right] + x\sqrt{\mathrm{var}\left\{N_G(t)\right\}} - \epsilon(t)}}\right\}.$$

From equations (1.35) and (1.37), it follows that as $t \to \infty$,

$$P\left\{\frac{N_G(t) - E[N_G(t)]}{\sqrt{\mathrm{var}[N_G(t)]}} < x\right\}$$

$$= P\left\{Z_{n(t)} > \frac{1}{\sqrt{\kappa}}\frac{\Lambda_1(t) - \left(\Lambda_1(t) + \frac{1-\kappa}{2} + o(1) + x\kappa\sqrt{var\left\{N_G(t)\right\}} - \epsilon(t)\kappa\right)}{\sqrt{E\left[N_G(t)\right] + x\sqrt{\mathrm{var}\left\{N_G(t)\right\}} - \epsilon(t)}}\right\}$$

$$= P\left\{Z_{n(t)} > \frac{1}{\sqrt{\kappa}}\frac{-x\kappa\sqrt{\mathrm{var}\left\{N_G(t)\right\}} - \frac{1-\kappa}{2} + \epsilon(t)\kappa + o(1)}{\sqrt{E\left[N_G(t)\right] + x\sqrt{\mathrm{var}\left\{N_G(t)\right\}} - \epsilon(t)}}\right\}$$

$$= P\left\{Z_{n(t)} > \frac{1}{\sqrt{\kappa}}\frac{-x\kappa - \frac{\frac{1-\kappa}{2} - \epsilon(t)\kappa + o(1)}{\sqrt{\mathrm{var}\{N_G(t)\}}}}{\frac{\sqrt{E[N_G(t)] + x\sqrt{\mathrm{var}\{N_G(t)\}} - \epsilon(t)}}{\sqrt{\mathrm{var}\{N_G(t)\}}}}\right\}$$

$$= P\left\{Z_{n(t)} > \frac{\kappa}{\sqrt{\kappa}}\frac{-x - \frac{1}{\kappa}\frac{\frac{1-\kappa}{2} - \epsilon(t)\kappa + o(1)}{\sqrt{\mathrm{var}\{N_G(t)\}}}}{\sqrt{\frac{E[N_G(t)]}{\mathrm{var}\{N_G(t)\}} + x\frac{\sqrt{\mathrm{var}\{N_G(t)\}}}{\mathrm{var}\{N_G(t)\}} - \frac{\epsilon(t)}{\mathrm{var}\{N_G(t)\}}}}\right\}$$

$$
\begin{aligned}
&= P\left\{ Z_{n(t)} > \sqrt{\kappa}\frac{-x-\frac{1}{\kappa}\frac{\frac{1-\kappa}{2}-\epsilon(t)\kappa+o(1)}{\sqrt{\frac{\Lambda_1(t)}{\kappa^2}+\frac{1}{12}+\frac{5}{4}\frac{1}{\kappa^2}-\frac{4}{3}\frac{1}{\kappa}+o(1)}}}{\sqrt{\frac{\frac{\Lambda_1(t)}{\kappa}+\frac{1-\kappa}{2\kappa}+o(1)}{\frac{\Lambda_1(t)}{\kappa^2}+\frac{1}{12}+\frac{5}{4}\frac{1}{\kappa^2}-\frac{4}{3}\frac{1}{\kappa}+o(1)}+x\frac{\sqrt{\frac{\Lambda_1(t)}{\kappa^2}+\frac{1}{12}+\frac{5}{4}\frac{1}{\kappa^2}-\frac{4}{3}\frac{1}{\kappa}+o(1)}}{\frac{\Lambda_1(t)}{\kappa^2}+\frac{1}{12}+\frac{5}{4}\frac{1}{\kappa^2}-\frac{4}{3}\frac{1}{\kappa}+o(1)}-\frac{\epsilon(t)}{\mathrm{var}\{N_G(t)\}}}} \right\} \\
&= P\left\{ Z_{n(t)} > \frac{-x-\frac{1}{\kappa}\frac{\frac{1-\kappa}{2}-\epsilon(t)\kappa+o(1)}{\sqrt{\frac{\Lambda_1(t)}{\kappa^2}+\frac{1}{12}+\frac{5}{4}\frac{1}{\kappa^2}-\frac{4}{3}\frac{1}{\kappa}+o(1)}}}{\sqrt{\frac{\frac{\Lambda_1(t)}{\kappa^2}+\frac{1-\kappa}{2\kappa^2}+o(1)}{\frac{\Lambda_1(t)}{\kappa^2}+\frac{1}{12}+\frac{5}{4}\frac{1}{\kappa^2}-\frac{4}{3}\frac{1}{\kappa}+o(1)}+\frac{x}{\kappa}\frac{\sqrt{\frac{\Lambda_1(t)}{\kappa^2}+\frac{1}{12}+\frac{5}{4}\frac{1}{\kappa^2}-\frac{4}{3}\frac{1}{\kappa}+o(1)}}{\frac{\Lambda_1(t)}{\kappa^2}+\frac{1}{12}+\frac{5}{4}\frac{1}{\kappa^2}-\frac{4}{3}\frac{1}{\kappa}+o(1)}}-\frac{\epsilon(t)}{\mathrm{var}\{N_G(t)\}}} \right\} \\
&\to P\left\{Z > -x\right\} \quad (\text{Since } \ \Lambda_1(t) \to \infty \ \text{ as } \ t \to \infty.) \\
&= P\left\{Z \le x\right\},
\end{aligned}
$$

where Z is a standard normal random variable. Therefore, as $t \to \infty$, we have

$$
\frac{N_G(t) - E[N_G(t)]}{\sqrt{\mathrm{var}[N_G(t)]}} \to Z.
$$

□

A.3.2.2 Proof of Equation (1.37)

Proof. Let f and F be the probability density function (pdf) and the cumulative distribution function (cdf) of a continuous random variable X, respectively, such that $P(X \ge 0) = 1$, $\mu = E[X] < \infty$, $\sigma^2 = \mathrm{var}\{\mathrm{X}\} < \infty$, and $\mu_3 = E[(X-\mu)^3] < \infty$. Let $\{N_R(t),\ t > 0\}$ be a renewal process with interarrival times which are independent and identically distributed with cdf F. From Cox (1962), we know that for such a renewal process $\{N_R(t),\ t > 0\}$, we have

$$E[N_R(t)] = \frac{t}{\mu} + \frac{\sigma^2 - \mu^2}{2\mu^2} + o(1), \tag{A.17}$$

and

$$\mathrm{var}\,\{N_R(t)\} = \frac{\sigma^2}{\mu^3}t - \frac{2\mu_3}{3\mu^3} + \frac{5\sigma}{4\mu^4} + \frac{1}{12} + o(1), \tag{A.18}$$

as $t \to \infty$. If $X \sim \Gamma(\kappa,\ 1)$, it then follows from equations (A.17) and (A.18) that as $t \to \infty$,

$$E[N_R(t)] = \frac{t}{\kappa} + \frac{1-\kappa}{2\kappa} + o(1), \tag{A.19}$$

and

$$\mathrm{var}\,\{N_R(t)\} = \frac{t}{\kappa^2} + \frac{1}{12} + \frac{5}{4}\frac{1}{\kappa^2} - \frac{4}{3}\frac{1}{\kappa} + o(1). \tag{A.20}$$

Let $\{N_R(t),\ t > 0\}$ be a renewal process with interarrival times which are independent and identically distributed $\Gamma(\kappa,\ 1)$ random variables. If $\{N_G(t),\ t > 0\}$ is an IGP with baseline intensity function $0 < \lambda_1(t) \leq M < \infty$ and shape parameter $\kappa > 0$, such that $\Lambda_1(t) = \int_0^t \lambda_1(u)du$ and $\Lambda_1(\infty) = \infty$, then from equation (A.9) it follows that as $t \to \infty$,

$$E\left[N_G(t)\right] = \frac{\Lambda_1(t)}{\kappa} + \frac{1-\kappa}{2\kappa} + o(1) \tag{A.21}$$

and

$$\operatorname{var}\{N_G(t)\} = \frac{\Lambda_1(t)}{\kappa^2} + \frac{1}{12} + \frac{5}{4}\frac{1}{\kappa^2} - \frac{4}{3}\frac{1}{\kappa} + o(1). \tag{A.22}$$

$\square$

A.3.3 Proofs for Chapter 1 Section 8 Subsection 3

A.3.3.1 Proof of Equation (1.38)

Proof. If $n\kappa \in \mathbb{N}$, then $\Gamma(n\kappa) = (n\kappa - 1)!$. Therefore, equation (1.38) follows from equation (1.13). $\square$

A.3.3.2 Proof of Equation (1.40)

Proof. Let $\{N(t),\ t > 0\}$ be a nonhomogeneous Poisson process with intensity function $\lambda_1(t) > 0$ and let $\Lambda_1(t) \coloneqq \int_0^t \lambda_1(u)du$, where $\Lambda_1(\infty) = \infty$. Let $\{N_G(t),\ t > 0\}$ be an inhomogeneous Gamma process which samples every κ event of $\{N(t),\ t > 0\}$. Then for each $n = 0,\ 1,\ 2,\ \ldots$ and $t > 0$, $\{N_G(t) = n\} = \{N(t) = \kappa n\} \cup \{N(t) = \kappa n + 1\}$ $\cup \cdots \cup \{N(t) = \kappa(n+1) - 1\}$. Therefore, $P\{N_G(t) = n\} = \sum_{j=n\kappa}^{(n+1)\kappa-1} P\{N(t) = j\}$ $= \exp\{-\Lambda_1(t)\} \sum_{j=n\kappa}^{(n+1)\kappa-1} \frac{\{\Lambda_1(t)\}^j}{j!}$. $\square$

Appendix B

Proofs for Chapter 2

B.1 Some Useful Asymptotic Integrals and Trigonometric Identities

In this section, we present some asymptotic integrals which are used for proofs throughout Chapter 2. For each asymptotic integral, we use the following assumptions $k,\ k' = 1, 2\ \ldots,\ K$, $\omega_k > 0$, $\omega > 0$, $\gamma > 0$, $T \to \infty$, and $c \neq 0$, where c is a constant. Lastly, we assume that the angular frequencies follow the Chapter 2 Assumptions 2 and 3.

$$\frac{1}{T}\int_0^T \sin(\omega t)dt = \frac{1}{\omega T}(1-\cos(\omega T))$$

$$= \begin{cases} \frac{1}{cT^{-\gamma}}(1-\cos(cT^{-\gamma})) & \text{if} \quad \omega \quad = \quad cT^{-1-\gamma} \\ \frac{1}{c}(1-\cos(c)) & \text{if} \quad \omega \quad = \quad cT^{-1} \\ \frac{1}{cT^{\gamma}}(1-\cos(cT^{\gamma})) & \text{if} \quad \omega \quad = \quad cT^{-1+\gamma} \\ \frac{1}{\omega T}(1-\cos(\omega T)) & \text{if} \quad \omega \quad \text{is} \quad \text{fixed} \end{cases}$$

$$= \begin{cases} \frac{1}{cT^{-\gamma}}(1-(1-\frac{c^2T^{-2\gamma}}{2!}+\frac{c^4T^{-4\gamma}}{4!}-\frac{c^6T^{-6\gamma}}{6!}+\cdots)) & \text{if} \quad \omega \quad = \quad cT^{-1-\gamma} \\ \frac{1}{c}(1-\cos(c)) & \text{if} \quad \omega \quad = \quad cT^{-1} \\ o(1) & \text{if} \quad \omega \quad = \quad cT^{-1+\gamma} \\ o(1) & \text{if} \quad \omega \quad \text{is} \quad \text{fixed} \end{cases}$$

$$= \begin{cases} o(1) & \text{if} \quad \omega \quad = \quad cT^{-1-\gamma} \\ \frac{1}{c}(1-\cos(c)) & \text{if} \quad \omega \quad = \quad cT^{-1} \\ o(1) & \text{if} \quad \omega \quad = \quad cT^{-1+\gamma} \\ o(1) & \text{if} \quad \omega \quad \text{is} \quad \text{fixed.} \end{cases} \tag{B.1}$$

$$
\begin{aligned}
\frac{1}{T}\int_0^T \cos(\omega t)dt &= \frac{1}{\omega T}\sin(\omega T) \\
&= \begin{cases}
\frac{1}{cT^{-\gamma}}\sin(cT^{-\gamma}) & \text{if} \quad \omega \quad = \quad cT^{-1-\gamma} \\
\frac{1}{c}\sin c & \text{if} \quad \omega \quad = \quad cT^{-1} \\
\frac{1}{cT^{\gamma}}\sin(cT^{\gamma}) & \text{if} \quad \omega \quad = \quad cT^{-1+\gamma} \\
\frac{1}{\omega T}\sin(\omega T) & \text{if} \quad \omega \quad \text{is} \quad \text{fixed}
\end{cases} \\
&= \begin{cases}
\frac{1}{cT^{-\gamma}}(cT^{-\gamma} - \frac{c^3T^{-3\gamma}}{3!} + \frac{c^5T^{-5\gamma}}{5!} - \frac{c^7T^{-7\gamma}}{7!} + \cdots) & \text{if} \quad \omega \quad = \quad cT^{-1-\gamma} \\
\frac{1}{c}\sin c & \text{if} \quad \omega \quad = \quad cT^{-1} \\
o(1) & \text{if} \quad \omega \quad = \quad cT^{-1+\gamma} \\
o(1) & \text{if} \quad \omega \quad \text{is} \quad \text{fixed}
\end{cases} \\
&= \begin{cases}
1 + o(1) & \text{if} \quad \omega \quad = \quad cT^{-1-\gamma} \\
\frac{1}{c}\sin c & \text{if} \quad \omega \quad = \quad cT^{-1} \\
o(1) & \text{if} \quad \omega \quad = \quad cT^{-1+\gamma} \\
o(1) & \text{if} \quad \omega \quad \text{is} \quad \text{fixed.}
\end{cases}
\end{aligned}
\tag{B.2}
$$

$$
\begin{aligned}
\frac{1}{T^2}\int_0^T t\sin(\omega t)dt &= \frac{-1}{\omega^2 T^2}(\omega T\cos(\omega T)-\sin(\omega T)) \\
&= \begin{cases}
\frac{-1}{c^2T^{-2\gamma}}(cT^{-\gamma}\cos(cT^{-\gamma})-\sin(cT^{-\gamma})) & \text{if} \quad \omega \;=\; cT^{-1-\gamma} \\
\frac{-1}{c^2}(c\cos(c)-\sin(c)) & \text{if} \quad \omega \;=\; cT^{-1} \\
\frac{-1}{c^2T^{2\gamma}}(cT^{\gamma}\cos(cT^{\gamma})-\sin(cT^{\gamma})) & \text{if} \quad \omega \;=\; cT^{-1+\gamma} \\
\frac{-1}{\omega^2T^2}(\omega T\cos(\omega T)-\sin(\omega T)) & \text{if} \quad \omega \;\text{is}\; \text{fixed}
\end{cases} \\
&= \begin{cases}
\frac{-1}{c^2T^{-2\gamma}}(-\frac{c^3T^{-3\gamma})}{3}+\frac{c^5T^{-5\gamma})}{30}-\frac{c^7T^{-7\gamma})}{840}+\cdots) & \text{if} \quad \omega \;=\; cT^{-1-\gamma} \\
\frac{-1}{c^2}(c\cos(c)-\sin(c)) & \text{if} \quad \omega \;=\; cT^{-1} \\
o(1) & \text{if} \quad \omega \;=\; cT^{-1+\gamma} \\
o(1) & \text{if} \quad \omega \;\text{is}\; \text{fixed}
\end{cases} \\
&= \begin{cases}
o(1) & \text{if} \quad \omega \;=\; cT^{-1-\gamma} \\
\frac{-1}{c^2}(c\cos(c)-\sin(c)) & \text{if} \quad \omega \;=\; cT^{-1} \\
o(1) & \text{if} \quad \omega \;=\; cT^{-1+\gamma} \\
o(1) & \text{if} \quad \omega \;\text{is}\; \text{fixed.}
\end{cases}
\end{aligned} \tag{B.3}
$$

$$
\frac{1}{T^2}\int_0^T t\cos(\omega t)dt = \frac{1}{\omega^2 T^2}(\cos(\omega T) + \omega T\sin(\omega T) - 1)
$$

$$
= \begin{cases}
\frac{1}{c^2T^{-2\gamma}}(\cos(cT^{-\gamma}) + cT^{-\gamma}\sin(cT^{-\gamma}) - 1) & \text{if} \quad \omega = cT^{-1-\gamma} \\
\frac{1}{c^2}(\cos(c) + c\sin(c) - 1) & \text{if} \quad \omega = cT^{-1} \\
\frac{1}{c^2T^{2\gamma}}(\cos(cT^{\gamma}) + cT^{\gamma}\sin(cT^{\gamma}) - 1) & \text{if} \quad \omega = cT^{-1+\gamma} \\
\frac{1}{\omega^2T^2}(\cos(\omega T) + \omega T\sin(\omega T) - 1) & \text{if} \quad \omega \text{ is fixed}
\end{cases}
$$

$$
= \begin{cases}
\frac{1}{c^2T^{-2\gamma}}(\frac{c^2T^{-2\gamma}}{2} - \frac{c^4T^{-4\gamma}}{8} + \frac{c^6T^{-6\gamma}}{144} + \cdots) & \text{if} \quad \omega = cT^{-1-\gamma} \\
\frac{1}{c^2}(\cos(c) + c\sin(c) - 1) & \text{if} \quad \omega = cT^{-1} \\
o(1) & \text{if} \quad \omega = cT^{-1+\gamma} \\
o(1) & \text{if} \quad \omega \text{ is fixed}
\end{cases}
$$

$$
= \begin{cases}
\frac{1}{2} + o(1) & \text{if} \quad \omega = cT^{-1-\gamma} \\
\frac{1}{c^2}(\cos(c) + c\sin(c) - 1) & \text{if} \quad \omega = cT^{-1} \\
o(1) & \text{if} \quad \omega = cT^{-1+\gamma} \\
o(1) & \text{if} \quad \omega \text{ is fixed.}
\end{cases} \tag{B.4}
$$

$$
\begin{aligned}
\frac{1}{T^3}\int_0^T t^2\sin(\omega t)dt &= -\frac{(\omega^2T^2-2)\cos(\omega T)-2(\omega T\sin(\omega T)-1)}{T^3\omega^3} \\
&= \begin{cases}
-\frac{(c^2T^{-2\gamma}-2)\cos(cT^{-\gamma})-2(cT^{-\gamma}\sin(cT^{-\gamma})-1)}{c^3T^{-3\gamma}} & \text{if} \quad \omega = cT^{-1-\gamma} \\
-\frac{(c^2-2)\cos(c)-2(c\sin(c)-1)}{c^3} & \text{if} \quad \omega = cT^{-1} \\
-\frac{(c^2T^{2\gamma}-2)\cos(cT^{\gamma})-2(cT^{\gamma}\sin(cT^{\gamma})-1)}{c^3T^{3\gamma}} & \text{if} \quad \omega = cT^{-1+\gamma} \\
-\frac{(\omega^2T^2-2)\cos(\omega T)-2(\omega T\sin(\omega T)-1)}{T^3\omega^3} & \text{if} \quad \omega \text{ is fixed}
\end{cases} \\
&= \begin{cases}
-(-\frac{cT^{-\gamma}}{4}+\frac{c^3T^{-3\gamma}}{36}+\cdots) & \text{if} \quad \omega = cT^{-1-\gamma} \\
-\frac{(c^2-2)\cos(c)-2(c\sin(c)-1)}{c^3} & \text{if} \quad \omega = cT^{-1} \\
o(1) & \text{if} \quad \omega = cT^{-1+\gamma} \\
o(1) & \text{if} \quad \omega \text{ is fixed}
\end{cases} \\
&= \begin{cases}
o(1) & \text{if} \quad \omega = cT^{-1-\gamma} \\
-\frac{(c^2-2)\cos(c)-2(c\sin(c)-1)}{c^3} & \text{if} \quad \omega = cT^{-1} \\
o(1) & \text{if} \quad \omega = cT^{-1+\gamma} \\
o(1) & \text{if} \quad \omega \text{ is fixed.}
\end{cases} \qquad \text{(B.5)}
\end{aligned}
$$

$$
\begin{aligned}
\frac{1}{T^3}\int_0^T t^2\cos(\omega t)dt &= \frac{2\omega T\cos(\omega T)+(\omega^2T^2-2)\sin(\omega T)}{T^3\omega^3} \\
&= \begin{cases}
\frac{2cT^{-\gamma}\cos(cT^{-\gamma})+(c^2T^{-2\gamma}-2)\sin(cT^{-\gamma})}{c^3T^{-3\gamma}} & \text{if} \quad \omega \;=\; cT^{-1-\gamma} \\
\frac{2c\cos(c)+(c^2-2)\sin(c)}{c^3} & \text{if} \quad \omega \;=\; cT^{-1} \\
\frac{2cT^{\gamma}\cos(cT^{\gamma})+(c^2T^{2\gamma}-2)\sin(cT^{\gamma})}{c^3T^{3\gamma}} & \text{if} \quad \omega \;=\; cT^{-1+\gamma} \\
\frac{2\omega T\cos(\omega T)+(\omega^2T^2-2)\sin(\omega T)}{T^3\omega^3} & \text{if} \quad \omega \;\text{is}\; \text{fixed}
\end{cases} \\
&= \begin{cases}
\frac{1}{3}-\frac{c^2T^{-2\gamma}}{10}+\frac{c^4T^{-4\gamma}}{168}+\cdots & \text{if} \quad \omega \;=\; cT^{-1-\gamma} \\
\frac{2c\cos(c)+(c^2-2)\sin(c)}{c^3} & \text{if} \quad \omega \;=\; cT^{-1} \\
o(1) & \text{if} \quad \omega \;=\; cT^{-1+\gamma} \\
o(1) & \text{if} \quad \omega \;\text{is}\; \text{fixed}
\end{cases} \\
&= \begin{cases}
\frac{1}{3}+o(1) & \text{if} \quad \omega \;=\; cT^{-1-\gamma} \\
\frac{2c\cos(c)+(c^2-2)\sin(c)}{c^3} & \text{if} \quad \omega \;=\; cT^{-1} \\
o(1) & \text{if} \quad \omega \;=\; cT^{-1+\gamma} \\
o(1) & \text{if} \quad \omega \;\text{is}\; \text{fixed.}
\end{cases} \qquad \text{(B.6)}
\end{aligned}
$$

Next, we use the asymptotic integrals (B.1)-(B.6), along with the trigonometric identities

$$\begin{aligned}\cos(\alpha)\cos(\beta) &= \frac{1}{2}\left[\cos(\alpha+\beta)+\cos(\alpha-\beta)\right] \\ \cos(\alpha)\sin(\beta) &= \frac{1}{2}\left[\sin(\alpha+\beta)-\sin(\alpha-\beta)\right], \end{aligned} \tag{B.7}$$

to establish the asymptotic integrals (B.10)-(B.15). For completeness, we work out the details of the derivation of the asymptotic integral (B.10), and in a similar way we can derive the other asymptotic integrals.

Using the trigonometric identities (B.7), we have

$\frac{1}{T}\int_0^T \cos(\omega_k t + \phi_k)\cos(\omega t)dt$

$$\begin{aligned} &= \frac{1}{2T}\int_0^T [\cos((\omega_k+\omega)t+\phi_k)+\cos((\omega_k-\omega)t+\phi_k)]dt \\ &= \frac{1}{2T}\int_0^T [\cos((\omega_k+\omega)t)\cos(\phi_k)-\sin((\omega_k+\omega)t)\sin(\phi_k)]dt \\ &\quad +\frac{1}{2T}\int_0^T \cos((\omega_k-\omega)t+\phi_k)dt. \end{aligned} \tag{B.8}$$

To evaluate $\frac{1}{2T}\int_0^T[\cos((\omega_k+\omega)t)\cos(\phi_k)-\sin((\omega_k+\omega)t)\sin(\phi_k)]dt$, as $T\to\infty$, we recall that under the conditions imposed on the angular frequencies, we have $\omega_k \geq O(T^{\delta'-1})$, where $0<\delta'<1$. Therefore, a lower bound for $\omega_k+\omega$, where $\omega>0$ is some fixed angular frequency, can not decrease to 0 faster than $O(T^{\delta'-1})$. It then follows that a lower bound for $(\omega_k+\omega)T$ is of order $O(T^{\delta'})$, where $0<\delta'<1$. Therefore, from the asymptotic integrals (B.1) and (B.2), we have $\frac{1}{2T}\int_0^T[\cos((\omega_k+\omega)t)\cos(\phi_k)-$

$\sin((\omega_k+\omega)t)\sin(\phi_k)]dt = o(1)$. It then follows that

$\frac{1}{T}\int_0^T \cos(\omega_k t+\phi_k)\cos(\omega t)dt$

$$\begin{aligned} &= \frac{1}{2T}\int_0^T \cos((\omega_k-\omega)t+\phi_k)dt + o(1) \\ &= \frac{1}{2T}\int_0^T [\cos((\omega_k-\omega)t)\cos(\phi_k) - \sin((\omega_k-\omega)t)\sin(\phi_k)]dt + o(1). \end{aligned} \quad \text{(B.9)}$$

Therefore, from integrals (B.1) and (B.2), we have

$$\frac{1}{T}\int_0^T \cos(\omega_k t+\phi_k)\cos(\omega t)dt = \begin{cases} \frac{1}{2}\cos(\phi_k)+o(1) & \text{if } |\omega-\omega_k| = cT^{-1-\gamma} \\ \frac{1}{2}\frac{\sin(c+\phi_k)-\sin(\phi_k)}{c}+o(1) & \text{if } |\omega-\omega_k| = cT^{-1} \\ o(1) & \text{if } |\omega-\omega_k| = cT^{-1+\gamma}. \end{cases} \quad \text{(B.10)}$$

Similarly, we can show that

$\frac{1}{T}\int_0^T \cos(\omega_k t+\phi_k)\sin(\omega t)dt$

$$= \begin{cases} -\frac{1}{2}\sin(\phi_k)+o(1), & \text{if } |\omega-\omega_k| = cT^{-1-\gamma} \\ \frac{1}{2}\frac{\cos(c+\phi_k)-\cos(\phi_k)}{c}+o(1) & \text{if } |\omega-\omega_k| = cT^{-1} \\ o(1) & \text{if } |\omega-\omega_k| = cT^{-1+\gamma}, \end{cases} \quad \text{(B.11)}$$

$\frac{1}{T^2}\int_0^T t\cos(\omega_k t+\phi_k)\cos(\omega t)dt$

$$= \begin{cases} \frac{1}{4}\cos(\phi_k)+o(1) & \text{if } |\omega-\omega_k| = cT^{-1-\gamma} \\ \frac{1}{2}[\frac{\cos(c+\phi_k)-\cos(\phi_k)}{c^2}+\frac{\sin(c+\phi_k)}{c}]+o(1) & \text{if } |\omega-\omega_k| = cT^{-1} \\ o(1) & \text{if } |\omega-\omega_k| = cT^{-1+\gamma}, \end{cases} \quad \text{(B.12)}$$

$\frac{1}{T^2}\int_0^T t\cos(\omega_k t+\phi_k)\sin(\omega t)dt$

$$= \begin{cases} -\frac{1}{4}\sin(\phi_k)+o(1) & \text{if } |\omega-\omega_k| = cT^{-1-\gamma} \\ -\frac{1}{2}\left[\frac{\sin(c+\phi_k)-\sin(\phi_k)}{c^2}-\frac{\cos(c+\phi_k)}{c}\right]+o(1) & \text{if } |\omega-\omega_k| = cT^{-1} \\ o(1) & \text{if } |\omega-\omega_k| = cT^{-1+\gamma}, \end{cases} \quad \text{(B.13)}$$

$\frac{1}{T^3}\int_0^T t^2\cos(\omega_k t+\phi_k)\cos(\omega t)dt$

$$= \begin{cases} \frac{1}{6}\cos(\phi_k) + o(1) & \text{if} \quad |\omega - \omega_k| \;=\; cT^{-1-\gamma} \\ \frac{1}{2}[-2\frac{\sin(c+\phi_k)-\sin(\phi_k)}{c^3} + 2\frac{\cos(c+\phi_k)}{c^2} & \text{if} \quad |\omega - \omega_k| \;=\; cT^{-1} \\ \quad +\frac{\sin(c+\phi_k)}{c}] + o(1) & \\ o(1) & \text{if} \quad |\omega - \omega_k| \;=\; cT^{-1+\gamma}, \end{cases} \quad \text{(B.14)}$$

and

$$\frac{1}{T^3}\int_0^T t^2\cos(\omega_k t + \phi_k)\sin(\omega t)dt$$

$$= \begin{cases} -\frac{1}{6}\sin(\phi_k) + o(1) & \text{if} \quad |\omega - \omega_k| \;=\; cT^{-1-\gamma} \\ -\frac{1}{2}[2\frac{\cos(c+\phi_k)-\cos(\phi_k)}{c^3} + 2\frac{\sin(c+\phi_k)}{c^2} & \text{if} \quad |\omega - \omega_k| \;=\; cT^{-1} \\ \quad -\frac{\cos(c+\phi_k)}{c}] + o(1) & \\ o(1) & \text{if} \quad |\omega - \omega_k| \;=\; cT^{-1+\gamma}. \end{cases} \quad \text{(B.15)}$$

Next, we present the asymptotic integrals (B.18)-(B.26), which can all be derived in a similar fashion. For completeness, we derive the asymptotic integral (B.18), and in a similar way we can derive the other asymptotic integrals.

From the trigonometric identities (B.7), it follows that if $\omega_k \neq \omega_{k'}$, we have

$$\frac{1}{T}\int_0^T \cos(\omega_k t)\cos(\omega_{k'} t)dt \;=\; \frac{1}{2T}\int_0^T \left[\cos((\omega_k + \omega_{k'})t) + \cos((\omega_k - \omega_{k'})t)\right] dt. \quad \text{(B.16)}$$

From the Chapter 2 Assumptions 2 and 3, we know that $|\omega_k - \omega_{k'}| = cT^{-1+\gamma}$, and $(\omega_k + \omega_{k'})$ has a lower bound that can not decrease to 0 faster than $O(T^{\delta'-1})$, where $0 < \delta' < 1$. It then follows that $|\omega_k - \omega_{k'}|\, T = cT^{\gamma}$ and that $(\omega_k + \omega_{k'})T$ has a lower bound that is of order $O(T^{\delta'})$. Therefore, from integral (B.2) we have

$$\frac{1}{T}\int_0^T \cos(\omega_k t)\cos(\omega_{k'} t)dt = o(1). \tag{B.17}$$

On the other hand, if $\omega_k = \omega_{k'}$, we have

$$\begin{aligned}\frac{1}{T}\int_0^T \cos(\omega_k t)\cos(\omega_k t)dt &= \frac{1}{2T}\int_0^T \left[\cos(2\omega_k t) + 1\right] dt \\ &= \frac{1}{2}\left[\frac{\sin(2\omega_k T)}{2\omega_k T} + 1\right] \\ &= \frac{1}{2} + o(1). \end{aligned} \tag{B.18}$$

Similarly, for the asymptotic integrals of equations (B.18)-(B.26), if $\omega_k \neq \omega_{k'}$, each of the asymptotic integrals is of order $o(1)$. On the other hand, if $\omega_k = \omega_{k'}$, then we have

$$\frac{1}{T}\int_0^T \cos(\omega_k t)\sin(\omega_{k'} t)dt = o(1), \tag{B.19}$$

$$\frac{1}{T}\int_0^T \sin(\omega_k t)\sin(\omega_{k'} t)dt = \frac{1}{2} + o(1), \tag{B.20}$$

$$\frac{1}{T^2}\int_0^T t\cos(\omega_k t)\cos(\omega_{k'} t)dt = \frac{1}{4} + o(1), \tag{B.21}$$

$$\frac{1}{T^2}\int_0^T t\cos(\omega_k t)\sin(\omega_{k'} t)dt = o(1), \tag{B.22}$$

$$\frac{1}{T^2}\int_0^T t\sin(\omega_k t)\sin(\omega_{k'} t)dt = \frac{1}{4} + o(1), \tag{B.23}$$

$$\frac{1}{T^3}\int_0^T t^2\cos(\omega_k t)\cos(\omega_{k'} t)dt = \frac{1}{6} + o(1), \tag{B.24}$$

$$\frac{1}{T^3}\int_0^T t^2\cos(\omega_k t)\sin(\omega_{k'} t)dt = o(1), \tag{B.25}$$

and

$$\frac{1}{T^3}\int_0^T t^2\sin(\omega_k t)\sin(\omega_{k'} t)dt = \frac{1}{6} + o(1). \tag{B.26}$$

The following trigonometric identities are useful for establishing the variance-covariance structure of the integrals defined in equation (2.7). The derivation of the below trigonometric identities all follow a similar approach. Therefore, we only derive the trigonometric identity (B.27). Let α, β, and γ be real numbers, then

$$\begin{aligned}
\sin(\alpha)\sin(\beta)\sin(\gamma) &= -\frac{1}{8i}\left[e^{i\alpha} - e^{-i\alpha}\right]\left[e^{i\beta} - e^{-i\beta}\right]\left[e^{i\gamma} - e^{-i\gamma}\right] \\
&= -\frac{1}{8i}\left[e^{i\alpha+i\beta} - e^{-i\alpha+i\beta} - e^{i\alpha-i\beta} + e^{-i\alpha-i\beta}\right]\left[e^{i\gamma} - e^{-i\gamma}\right] \\
&= -\frac{1}{8i}\{e^{i\alpha+i\beta+i\gamma} - e^{-i\alpha+i\beta+i\gamma} - e^{i\alpha-i\beta+i\gamma} + e^{-i\alpha-i\beta+i\gamma} \\
&\quad -e^{i\alpha+i\beta-i\gamma} + e^{-i\alpha+i\beta-i\gamma} + e^{i\alpha-i\beta-i\gamma} - e^{-i\alpha-i\beta-i\gamma}\} \\
&= -\frac{1}{4}\{\sin(\alpha+\beta+\gamma) - \sin(-\alpha+\beta+\gamma) \\
&\quad -\sin(\alpha-\beta+\gamma) + \sin(-\alpha-\beta+\gamma)\},
\end{aligned} \tag{B.27}$$

$$\cos(\alpha)\cos(\beta)\cos(\gamma) = \frac{1}{4}\{\cos(\alpha+\beta+\gamma) + \cos(-\alpha+\beta+\gamma)$$
$$+ \cos(\alpha-\beta+\gamma) + \cos(-\alpha-\beta+\gamma)\}, \tag{B.28}$$

$$\cos(\alpha)\sin(\beta)\sin(\gamma) = \frac{1}{4}\{-\cos(\alpha+\beta+\gamma) - \cos(-\alpha+\beta+\gamma)$$
$$+ \cos(\alpha-\beta+\gamma) + \cos(-\alpha-\beta+\gamma)\}, \tag{B.29}$$

and

$$\sin(\alpha)\cos(\beta)\cos(\gamma) = \frac{1}{4}\{\sin(\alpha+\beta+\gamma) - \sin(-\alpha+\beta+\gamma)$$
$$+ \sin(\alpha-\beta+\gamma) - \sin(-\alpha-\beta+\gamma)\}. \tag{B.30}$$

B.1.1 Proofs for Chapter 2 Section 2

B.1.1.1 Proof of Chapter 2 Lemma 8

Proof. First we consider the case when $m = 1$. For $t > 0$, let $0 < \epsilon_1 \leq \lambda_1(t) \leq J_1 < \infty$, $0 < \epsilon_2 \leq \lambda_2(t) \leq J_1^G < \infty$, $\epsilon = \min\{\epsilon_1, \epsilon_2\}$, $J = \max\left\{J_1, J_1^G\right\}$, and define $M_T := \sup_{0 \leq \omega \leq \Omega_T} \left|\int_0^T e^{i\omega t} dZ_G(t)\right|$. In this proof, we employ the Borel Cantelli

Lemma to show that as $T \to \infty$, $\frac{1}{T} M_T \to 0$ almost surely. To do this, we placed an upper bound on $\frac{1}{T} E[M_T]$ which tends to 0 as $T \to \infty$. We begin by decomposing the integral $\int_0^T e^{i\omega t} dZ_G(t)$ into two separate integrals by partitioning the observational time interval $(0,\ T]$ into L (to be fixed later), equally spaced and mutually exclusive sub-intervals of length $\triangle > 0$, so that $T = L\triangle$, where $\triangle = O(T^{-v})$ and $\frac{1}{3} < v < 1$.

$$
\begin{aligned}
\int_0^T e^{i\omega t} dZ_G(t) &= \sum_{l=0}^{L-1} \int_{l\triangle}^{(l+1)\triangle} \left(e^{i\omega l\triangle} + e^{i\omega l\triangle}\left(e^{i\omega(t-l\triangle)} - 1\right)\right) dZ_G(t) \\
&= \sum_{l=0}^{L-1} \int_{l\triangle}^{(l+1)\triangle} e^{i\omega l\triangle} dZ_G(t) + \sum_{l=0}^{L-1} \int_{l\triangle}^{(l+1)\triangle} e^{i\omega l\triangle}\left(e^{i\omega(t-l\triangle)} - 1\right) dZ_G(t) \\
&= \sum_{l=0}^{L-1} e^{i\omega l\triangle} \int_{l\triangle}^{(l+1)\triangle} dZ_G(t) + \sum_{l=0}^{L-1} e^{i\omega l\triangle} \int_{l\triangle}^{(l+1)\triangle} \left(e^{i\omega(t-l\triangle)} - 1\right) dZ_G(t) \\
&= \sum_{l=0}^{L-1} e^{i\omega l\triangle} Z_l + \sum_{l=0}^{L-1} e^{i\omega l\triangle} \int_0^{\triangle} \left(e^{i\omega u} - 1\right) dZ_G(u + l\triangle) \\
&:= S_1(\omega,\ T) + S_2(\omega,\ T), \qquad \text{(B.31)}
\end{aligned}
$$

where

$$
Z_l := \int_{l\triangle}^{(l+1)\triangle} dZ_G(t). \qquad \text{(B.32)}
$$

It then follows that

$$
\sup_{0\le\omega\le\Omega_T} \left|\int_0^T e^{i\omega t} dZ_G(t)\right| \le \sup_{0\le\omega\le\Omega_T} |S_1(\omega,\ T)| + \sup_{0\le\omega\le\Omega_T} |S_2(\omega,\ T)|. \qquad \text{(B.33)}
$$

From here, we place an upper bound on

$$\frac{1}{T}E\left[M_T\right] \leq \frac{1}{T}E\left[\sup_{0\leq\omega\leq\Omega_T}|S_1(\omega,\ T)|\right] + \frac{1}{T}E\left[\sup_{0\leq\omega\leq\Omega_T}|S_2(\omega,\ T)|\right]. \tag{B.34}$$

We begin by expressing the squared modulus of $S_1(\omega,\ T)$ as

$$|S_1(\omega,\ T)|^2 \ = \ \sum_{l=0}^{L-1} Z_l^2 + 2\sum_{r=1}^{L-1}\cos(\omega r\triangle)\sum_{l=0}^{L-1-r} Z_l Z_{l+r}. \tag{B.35}$$

Then, using the moment results of Z_l, provided in equations (B.66)-(B.68) of Appendix B Lemma 20, we see that the expected value of equation (B.35) becomes

$$\begin{aligned}
E\left[|S_1(\omega,\ T)|^2\right] &= \sum_{l=0}^{L-1} E[Z_l^2] + 2\sum_{r=1}^{L-1}\cos(\omega r\triangle)\sum_{l=0}^{L-1-r} E[Z_l Z_{l+r}] && \text{(B.36)}\\
&= \sum_{l=0}^{L-1}\{E[Z_l^2] - (E[Z_l])^2\} && \text{(B.37)}\\
&\quad + 2\sum_{r=1}^{L-1}\cos(\omega r\triangle)\sum_{l=0}^{L-1-r}\{E[Z_l Z_{l+r}] - E[Z_l]E[Z_{l+r}]\} && \text{(B.38)}\\
&= \sum_{l=0}^{L-1}\operatorname{var}\{Z_l\} + 2\sum_{r=1}^{L-1}\cos(\omega r\triangle)\sum_{l=0}^{L-1-r}\operatorname{cov}\{Z_l,\ Z_{l+r}\} && \text{(B.39)}\\
&\leq \sum_{l=0}^{L-1}\operatorname{var}\{Z_l\} + 2\sum_{r=1}^{L-1}\sum_{l=0}^{L-1-r}|\operatorname{cov}\{Z_l,\ Z_{l+r}\}| && \text{(B.40)}
\end{aligned}$$

$$
\begin{aligned}
&= \sum_{l=0}^{L-1}\left[\frac{1}{\kappa^2}\lambda_1(l\triangle)\triangle + O\left(\exp\left\{-a(\Lambda_1(l\triangle)\triangle)\right\}\lambda_1(l\triangle)\triangle\right)\right] && \text{(B.41)}\\
&\quad +2\sum_{r=1}^{L-1}\sum_{l=0}^{L-1-r} O\left(\exp\left\{-a\int_{l\triangle}^{(l+r)\triangle}\lambda_1(u)du\right\}\lambda_1(l\triangle)\triangle\right) && \text{(B.42)}\\
&\leq \frac{1}{\kappa^2}JL\triangle + O\left(L\triangle\right) + 2\sum_{r=1}^{L-1}(L-r)O\left(\exp\left\{-a\epsilon r\triangle\right\}J\triangle\right) && \text{(B.43)}\\
&= \frac{1}{\kappa^2}JT + O\left(T\right) + 2\sum_{r=1}^{L-1}(L-r)O\left(\exp\left\{-a\epsilon r\triangle\right\}\triangle\right) && \text{(B.44)}\\
&\leq \frac{1}{\kappa^2}JT + O\left(T\right) + O\left(\left[\frac{\exp\left\{-a\epsilon L\triangle\right\}}{(a\epsilon\triangle)^2} + \frac{a\epsilon L\triangle - 1}{(a\epsilon\triangle)^2}\right]\triangle\right) && \text{(B.45)}\\
&= \frac{1}{\kappa^2}JT + O\left(T\right) + O\left(\frac{\exp\left\{-a\epsilon T\right\}}{(a\epsilon)^2T^{-\nu}} + \frac{a\epsilon T - 1}{(a\epsilon)^2T^{-\nu}}\right) && \text{(B.46)}\\
&= O(T^{1+\nu}), && \text{(B.47)}
\end{aligned}
$$

where equation (B.37) follows since $E[Z_l] = 0$, equations (B.41) and (B.42) follow from the variance-covariance results given in equations (B.67) and (B.68) and from the approximation $\Lambda_1((l+1)\triangle) - \Lambda_1(l\triangle) \approx \lambda_1(l\triangle)\triangle$, equation (B.43) follows since $0 < \epsilon \leq \lambda_1(l\triangle) \leq J < \infty$ and $\int_{l\triangle}^{(l+r)\triangle}\lambda_1(u)du \geq \epsilon r\triangle$, equation (B.44) follows since $T = L\triangle$, equation (B.45) follows by using the inequality $\sum_{r=1}^{L-1}(L-r)\exp\{-cr\} \leq \int_0^L (L-r)\exp\{-cr\}\,dr$ $(c > 0)$, equation (B.46) follows since $T = L\triangle$ and $\triangle = O(T^{-\nu})$, and $a \in (0,\ 2]$. It then follows from equation (B.47) that

$$
\frac{1}{T}E\left[\sup_{\omega}|S_1(\omega,\ T)|\right] \leq \frac{1}{T}\sqrt{E\left[\sup_{\omega}|S_1(\omega,\ T)|^2\right]} \leq O(T^{-\frac{1}{2}+\frac{1}{2}\nu}), \tag{B.48}
$$

and we notice that $\frac{1}{T}E\left[\sup_{\omega}|S_1(\omega,\ T)|\right] \to 0$ as $T \to \infty$ when $0 < v < 1$. Next, we place an upper bound on

$$E\left[\sup_{0\leq\omega\leq\Omega_T}|S_2(\omega,\ T)|\right] = E\left[\sup_{0\leq\omega\leq\Omega_T}\left|\sum_{l=0}^{L-1} e^{i\omega l\triangle}\int_0^{\triangle}\left(e^{i\omega u}-1\right)dZ_G(u+l\triangle)\right|\right]. \tag{B.49}$$

First, we notice that for $u \geq 0$,

$$\left|e^{i\omega u}-1\right|^2 = \left(e^{i\omega u}-1\right)\left(e^{-i\omega u}-1\right) = 2-\left(e^{-i\omega u}+e^{i\omega u}\right) = 2\left[1-\cos(\omega u)\right] = 4\sin^2\left(\frac{\omega u}{2}\right). \tag{B.50}$$

Also, since we assumed that $0 \leq \omega \leq \Omega_T$, it then follows from (B.50) that for all $u\omega \geq 0$,

$$\left|e^{i\omega u}-1\right| = 2\left|\sin\left(\frac{\omega u}{2}\right)\right| \leq \omega u \leq \Omega_T u. \tag{B.51}$$

Second, we notice that for $t > 0$,

$$E\left[|dZ_G(t)|\right] = E\left[|dN_G(t)-E[dN_G(t)]|\right] \leq E\left[|dN_G(t)|\right] + |E[dN_G(t)]| \leq 2Jdt. \tag{B.52}$$

Therefore, from equations (B.51) and (B.52) it follows that

$$\frac{1}{T}E\left[\sup_{0\leq\omega\leq\Omega_T}|S_2(\omega,\ T)|\right] = \frac{1}{T}E\left[\sup_{0\leq\omega\leq\Omega_T}\left|\sum_{l=0}^{L-1} e^{i\omega l\triangle}\int_0^{\triangle}\left(e^{i\omega u}-1\right)dZ_G(u+l\triangle)\right|\right]$$

$$
\begin{aligned}
&\leq \frac{1}{T}E\left[\sup_{0\leq\omega\leq\Omega_T}\sum_{l=0}^{L-1}\int_0^{\triangle}\left|\left(e^{i\omega u}-1\right)dZ_G(u+l\triangle)\right|\right] \\
&\leq \frac{1}{T}\sum_{l=0}^{L-1}\int_0^{\triangle}E\left[\Omega_T\right]u2Jdu \\
&= \frac{1}{T}JL\triangle^2E\left[\Omega_T\right] \\
&= \frac{1}{T}JT\triangle E\left[\Omega_T\right],\ \text{since } T=L\triangle \\
&= O(T^{-v+1-\delta}),\ \text{since } \triangle=O(T^{-v}) \text{ and } E\left[\Omega_T\right]=O(T^{1-\delta}), \qquad \text{(B.53)}
\end{aligned}
$$

which goes to 0 as $T\to\infty$ when $1<\nu+\delta$. Combining results (B.48) and (B.53), we have

$$
\begin{aligned}
\frac{1}{T}E\left[M_T\right] &\leq \frac{1}{T}E\left[\sup_{0\leq\omega\leq\Omega_T}\left|S_1(\omega,\ T)\right|\right]+\frac{1}{T}E\left[\sup_{0\leq\omega\leq\Omega_T}\left|S_2(\omega,\ T)\right|\right] \\
&= O(T^{-\frac{1}{2}+\frac{1}{2}\nu})+O(T^{-v+1-\delta}). \qquad \text{(B.54)}
\end{aligned}
$$

From result (B.54), we find that the optimum choice of ν is $1-\frac{2}{3}\delta$, where $0<\delta<1$. This choice implies that

$$
\frac{1}{T}E\left[M_T\right]=O(T^{-\frac{1}{3}\delta}). \qquad \text{(B.55)}
$$

We complete the proof by using equation (B.55) in conjunction with the Borel Cantelli Lemma to show that $\frac{1}{T}M_T\to 0$ almost surely, as $T\to\infty$. Let α_k and T_k be a sequence of positive numbers such that $T_k\to\infty$, $\frac{T_{k+1}}{T_k}\to 1$, and $\alpha_k\to 0$. For example, let $\alpha_k=k^{-\beta}$ and $T_k=k^{\gamma}$, where $\beta>0$ and $\gamma>\frac{3(\beta+1)}{\delta}$, then

$$P\left\{\frac{1}{T_k}M_{T_k} > \alpha_k\right\} \ \ \le \tfrac{1}{\alpha_k}\tfrac{1}{T_k}E\left[M_{T_k}\right] \ \ = O(k^{-\frac{1}{3}\gamma\delta+\beta}), \tag{B.56}$$

and

$$\sum_{k=1}^{\infty} P\left\{\frac{1}{T_k}M_{T_k} > \alpha_k\right\} < \infty. \tag{B.57}$$

By the Borel Cantelli Lemma, it then follows that

$$P\left\{\frac{1}{T_k}M_{T_k} > \alpha_k, \ \ \text{infinitely} \ \ \text{often}\right\} = 0,$$

which implies that

$$P\left\{\frac{1}{T_k}M_{T_k} \le \alpha_k, \ \ \text{infinitely} \ \ \text{often}\right\} = 1. \tag{B.58}$$

Therefore, for such a choice of α_k and T_k, we have shown that

$$\frac{1}{T_k}M_{T_k} \to 0 \ \ \text{(a.s.)} \ \ \text{as} \ \ T \to \infty. \tag{B.59}$$

For intervening values of T, $T_k < T \le T_{k+1}$, we have

$$
\begin{aligned}
\frac{1}{T}M_T &= \frac{1}{T}\sup_{0\le\omega\le\Omega_T}\left|\int_0^T e^{i\omega t}dZ_G(t)\right| \\
&= \frac{1}{T}\sup_{0\le\omega\le\Omega_T}\left|\int_0^{T_k} e^{i\omega t}dZ_G(t)+\int_{T_k}^T e^{i\omega t}dZ_G(t)\right| \\
&\le \frac{1}{T_k}\sup_{0\le\omega\le\Omega_T}\left|\int_0^{T_k} e^{i\omega t}dZ_G(t)\right|+\frac{1}{T_k}\sup_{0\le\omega\le\Omega_T}\left|\int_{T_k}^T e^{i\omega t}dZ_G(t)\right| \\
&= \frac{1}{T_k}M_{T_k}+\frac{1}{T_k}\sup_{0\le\omega\le\Omega_T}\left|\int_{T_k}^T e^{i\omega t}dZ_G(t)\right| \\
&\le \frac{1}{T_k}M_{T_k}+\frac{1}{T_k}\sup_{0\le\omega\le\Omega_T}\left|\int_{T_k}^T e^{i\omega t}dN_G(t)\right|+\frac{1}{T_k}\sup_{0\le\omega\le\Omega_T}\left|\int_{T_k}^T e^{i\omega t}\lambda_2(u)du\right| \\
&\le \frac{1}{T_k}M_{T_k}+\frac{1}{T_k}\int_{T_k}^T dN_G(t)+\frac{1}{T_k}\int_{T_k}^T \lambda_2(u)du \\
&\le \frac{1}{T_k}M_{T_k}+\frac{1}{T_k}\left(N_G(T)-N_G(T_k)\right)+\frac{1}{T_k}J\left(T-T_k\right) \\
&\le \frac{1}{T_k}M_{T_k}+\left(\frac{N_G(T_{k+1})}{T_{k+1}}\frac{T_{k+1}}{T_k}-\frac{N_G(T_k)}{T_k}\right)+\frac{1}{T_k}J\left(T_{k+1}-T_k\right) \\
&\to 0 \text{ (a.s.) as } T\to\infty, \qquad \text{(B.60)}
\end{aligned}
$$

where the fact that as $T \to \infty$, $\frac{N_G(T_{k+1})}{T_{k+1}}\frac{T_{k+1}}{T_k} - \frac{N_G(T_k)}{T_k} \to 0$ almost surely follows from Appendix B Lemma 18 below. Therefore, as $T \to \infty$, $\frac{1}{T}M_T \to 0$ almost surely, and this completes the proof for the case when $m = 1$. Next, we consider the case when $m > 1$. Since

$$
\begin{aligned}
\frac{1}{T^m}\sup_{0\le\omega\le\Omega_T}\left|\int_0^T t^{m-1}e^{i\omega t}dZ_G(t)\right| &= \frac{1}{T}\sup_{0\le\omega\le\Omega_T}\left|\int_0^T\left(\frac{t}{T}\right)^{m-1}e^{i\omega t}dZ_G(t)\right| \\
&\le \frac{1}{T}\sup_{0\le\omega\le\Omega_T}\left|\int_0^T e^{i\omega t}dZ_G(t)\right|,
\end{aligned}
$$

the result follows. $\square$

Lemma 18. *For $t > 0$, let $\lambda_1(\cdot)$ be the baseline intensity function of an inhomogeneous Gamma process (IGP), say $\{N_G(t),\ t > 0\}$, with shape parameter $\kappa > 0$ that satisfies Assumptions 1-3 of Section 2.2. Then,*

$$\frac{N_G(t)}{t} \to \frac{B}{\kappa} \ \text{(a.s.)} \ \text{as} \ t \to \infty, \tag{B.61}$$

where $B > 0$ is the baseline constant defined in equation (2.1).

Proof. For $t > 0$, let $\lambda_1(\cdot)$ be the baseline intensity function of an inhomogeneous Gamma process (IGP), say $\{N_G(t),\ t > 0\}$, with shape parameter $\kappa > 0$ that satisfies Assumptions 1-3 of Section 2.2. For $t > 0$, let $\Lambda_1(t) := \int_0^t \lambda_1(u)du < \infty$, where $\Lambda_1(\infty) = \infty$. Furthermore, let $\{N_R(t),\ t > 0\}$ be a gamma renewal process (GRP) with independent and identically $\Gamma(\kappa,\ 1)$ distributed interarrival times. In the proof of A.3.1.3, provided in Appendix A, we showed that if we transform the time scale of the IGP from t to $\Lambda_1^{-1}(t)$, where $\Lambda_1^{-1}(\cdot)$ is the inverse function of $\Lambda_1(\cdot)$, then the IGP is transformed into a GRP. Likewise, if we transform the time scale of a GRP from t to $\Lambda_1(t)$, then the GRP is transformed into an IGP. Since $\{N_R(t),\ t > 0\}$ is a GRP, it follows from the Strong Law of Large Numbers for renewal processes that as $t \to \infty$, and hence as $\Lambda_1(t) \to \infty$, we have

$$\frac{N_R(\Lambda_1(t))}{\Lambda_1(t)} \to \frac{1}{\kappa} \ \text{(a.s.)}.$$

Also, in the notation of equation (2.1), it follows that for $t > 0$, we have

$$\begin{aligned}
\frac{\Lambda_1(t)}{t} &= \frac{\int_0^t \left[\sum_{k=1}^{K} A_k \cos(\omega_k u + \phi_k) + B\right] du}{t} \\
&\to B \text{ as } t \to \infty.
\end{aligned}$$

It then follows that

$$\begin{aligned}
\frac{N_G(t)}{t} &\overset{d}{=} \frac{N_R(\Lambda_1(t))}{t} \\
&= \frac{N_R(\Lambda_1(t))}{\Lambda_1(t)} \frac{\Lambda_1(t)}{t} \\
&\to \frac{1}{\kappa} B \text{ (a.s.) as } t \to \infty.
\end{aligned}$$

□

Lemma 19. *Let $\kappa > 0$ and $t > 0$, then*

$$\int_0^t \sum_{n=1}^{\infty} \frac{u^{n\kappa-1}}{\Gamma(n\kappa)} \exp\{-u\}\, du = \begin{cases} \frac{t}{\kappa} + \frac{1-\kappa}{2\kappa} + O\left(\exp\{-at\}\right) & \text{if } \kappa \in \mathbb{N} \\ \frac{t}{\kappa} + \frac{1-\kappa}{2\kappa} + O\left(\exp\{-at\} t^{-\kappa-1}\right) & \text{if } \kappa \in \mathbb{R}^+ \setminus \mathbb{N}, \end{cases} \tag{B.62}$$

and

$$\exp\{-t\} \sum_{n=1}^{\infty} \frac{t^{n\kappa-1}}{\Gamma(n\kappa)} = \begin{cases} \frac{1}{\kappa} + O\left(\exp\{-at\}\right) & \text{if } \kappa \in \mathbb{N} \\ \frac{1}{\kappa} + O\left(\exp\{-at\} t^{-\kappa-1}\right) & \text{if } \kappa \in \mathbb{R}^+ \setminus \mathbb{N}, \end{cases} \tag{B.63}$$

where $a \in (0, 2]$.

Proof. Let $\{N_G(t),\ t > 0\}$ be an inhomogeneous Gamma process (IGP) with baseline intensity function $\lambda_1(\cdot) > 0$ and shape parameter $\kappa > 0$. Assume that for all $t > 0$, $\Lambda_1(t) := \int_0^t \lambda_1(u) du < \infty$ and $\Lambda_1(\infty) = \infty$. From equations (1.4), (1.5), and (1.35), we have

$$E[N_G(t)] = \int_0^t \sum_{n=1}^{\infty} \frac{\lambda_1(u)}{\Gamma(n\kappa)} \{\Lambda_1(u)\}^{n\kappa-1} \exp\{-\Lambda_1(u)\}\, du$$
$$= \begin{cases} \frac{\Lambda_1(t)}{\kappa} + \frac{1-\kappa}{2\kappa} + O\left(\exp\{-a\Lambda_1(t)\}\right) & \text{if} \quad \kappa \in \mathbb{N} \\ \frac{\Lambda_1(t)}{\kappa} + \frac{1-\kappa}{2\kappa} + O\left(\exp\{-a\Lambda_1(t)\}\left(\Lambda_1(t)\right)^{-\kappa-1}\right) & \text{if} \quad \kappa \in \mathbb{R}^+ \diagdown \mathbb{N}, \end{cases} \tag{B.64}$$

where $t > 0$. From equations (1.6) and (1.36), we have

$$\frac{d}{dt}\left[E[N_G(t)]\right] = \lambda_2(t)$$
$$= \sum_{n=1}^{\infty} \frac{\lambda_1(t)}{\Gamma(n\kappa)} \{\Lambda_1(t)\}^{n\kappa-1} \exp\{-\Lambda_1(t)\}$$
$$= \begin{cases} \frac{\lambda_1(t)}{\kappa} + O\left(\lambda_1(t)\exp\{-a\Lambda_1(t)\}\right) & \text{if} \quad \kappa \in \mathbb{N} \\ \frac{\lambda_1(t)}{\kappa} + O\left(\lambda_1(t)\exp\{-a\Lambda_1(t)\}\left(\Lambda_1(t)\right)^{-\kappa-1}\right) & \text{if} \quad \kappa \in \mathbb{R}^+ \diagdown \mathbb{N}, \end{cases} \tag{B.65}$$

where $t > 0$. Assume that for all $t > 0$, $\lambda_1(t) = 1$, then $\Lambda_1(t) = t > 0$. It then follows from equations (B.64) and (B.65) that for all $t > 0$ and some $a \in (0,\ 2]$, we have

$$\int_0^t \sum_{n=1}^{\infty} \frac{u^{n\kappa-1}}{\Gamma(n\kappa)} \exp\{-u\}\, du = \begin{cases} \frac{t}{\kappa} + \frac{1-\kappa}{2\kappa} + O\left(\exp\{-at\}\right) & \text{if} \quad \kappa \in \mathbb{N} \\ \frac{t}{\kappa} + \frac{1-\kappa}{2\kappa} + O\left(\exp\{-at\}\, t^{-\kappa-1}\right) & \text{if} \quad \kappa \in \mathbb{R}^+ \diagdown \mathbb{N}, \end{cases}$$

and

$$\exp\{-t\}\sum_{n=1}^{\infty}\frac{t^{n\kappa-1}}{\Gamma(n\kappa)}=\begin{cases}\frac{1}{\kappa}+O\left(\exp\{-at\}\right) & \text{if} \quad \kappa\in\mathbb{N}\\ \frac{1}{\kappa}+O\left(\exp\{-at\}\,t^{-\kappa-1}\right) & \text{if} \quad \kappa\in\mathbb{R}^{+}\diagdown\mathbb{N}.\end{cases}$$

$\square$

Lemma 20. *Let $\{dZ_G(t),\ t>0\}$ be the stochastic process defined in Chapter 2 Lemma 8, $Z_l := \int_{l\triangle}^{(l+1)\triangle} dZ_G(t)$, where $\triangle = O(T^{-v})$, $T>0$, $0<v<\infty$, $l\in\{0,\ 1,\ 2,\ \ldots,\ L-1\}$, and L is a fixed positive integer such that $T=L\triangle$. Let $\lambda_1(\cdot)$ be defined as in equation (2.1) and define $\Lambda_1(t) := \int_0^t \lambda_1(u)du$, where $t>0$, then*

$$E[Z_l]=0, \tag{B.66}$$

$$\operatorname{var}\{Z_l\}=\frac{1}{\kappa^2}(\Lambda_1((l+1)\triangle)-\Lambda_1(l\triangle))+O\left(\exp\{-a\Lambda_1(l\triangle)\}\left(\Lambda_1((l+1)\triangle)-\Lambda_1(l\triangle)\right)\right), \tag{B.67}$$

and

$$\operatorname{cov}\{Z_l,\ Z_{l+r}\}=O\left(\exp\left\{-a\int_{l\triangle}^{(l+r)\triangle}\lambda_1(u)du\right\}\left[\exp\left\{a\int_{l\triangle}^{(l+1)\triangle}\lambda_1(u)du\right\}-1\right]\right), \tag{B.68}$$

where $r\in\{1,\ 2,\ \ldots,\ L-1\}$ and $a\in(0,2]$.

Proof. From equation (2.5) of Chapter 2 Lemma 8, we recall that $dZ_G(t) := dN_G(t) - E[dN_G(t)]$, where $t>0$. Therefore, for each $l\in\{0,\ 1,\ 2,\ \ldots,\ L-1\}$, we have $Z_l=\int_{l\triangle}^{(l+1)\triangle} dZ_G(t)=\int_{l\triangle}^{(l+1)\triangle}(dN_G(t)-E[dN_G(t)])$. It then follows that

$$E[Z_l]=\int_{l\triangle}^{(l+1)\triangle}E[dZ_G(t)]=0, \tag{B.69}$$

which completes the proof of equation (B.66).

We now establish the variance-covariance structure of Z_l. In establishing the variance-covariance structure of Z_l, we first notice that for each $l \in \{0,\ 1,\ 2,\ \ldots,\ L-1\}$, we have

$$
\begin{aligned}
\operatorname{var}\{Z_l\} &= \operatorname{var}\left\{\int_{l\triangle}^{(l+1)\triangle} dN_G(t)\right\} \\
&= \operatorname{var}\{N_G((l+1)\triangle) - N_G(l\triangle)\} \\
&= \operatorname{var}\{N_G(l\triangle,\ (l+1)\triangle)\}\,, \qquad \text{(B.70)}
\end{aligned}
$$

and for each $r \in \{1,\ 2,\ \ldots,\ L-1\}$, we have

$$
\begin{aligned}
\operatorname{cov}\{Z_l,\ Z_{l+r}\} &= \operatorname{cov}\left\{\int_{l\triangle}^{(l+1)\triangle} dN_G(t),\ \int_{(l+r)\triangle}^{(l+r+1)\triangle} dN_G(t)\right\} \\
&= \operatorname{cov}\{N_G((l+1)\triangle) - N_G(l\triangle),\ N_G((l+r+1)\triangle) - N_G((l+r)\triangle)\} \\
&= \operatorname{cov}\{N_G(l\triangle,\ (l+1)\triangle),\ N_G((l+r)\triangle,\ (l+r+1)\triangle)\}\,. \qquad \text{(B.71)}
\end{aligned}
$$

Therefore, we can use the variance-covariance results (1.30) and (1.31) to establish the variance-covariance structure of Z_l. However, when using these results, we need to use the functions $M_1(\cdot)$ and $m_1(\cdot)$ defined in equation (1.25), and we find it more convenient to use the asymptotic form of the functions $M_1(\cdot)$ and $m_1(\cdot)$. From lemma 19, it follows that the asymptotic form of the functions $M_1(\cdot)$ and $m_1(\cdot)$ can be expressed as

$$
\begin{aligned}
M_1(t) \;&:=\; \int_0^t \sum_{n=1}^{\infty} \frac{u^{n\kappa-1}}{\Gamma(n\kappa)} \exp\{-u\}\, du \\
&= \begin{cases} \frac{t}{\kappa} + \frac{1-\kappa}{2\kappa} + O\left(\exp\{-at\}\right) & \text{if} \quad \kappa \in \mathbb{N} \\ \frac{t}{\kappa} + \frac{1-\kappa}{2\kappa} + O\left(\exp\{-at\}\, t^{-\kappa-1}\right) & \text{if} \quad \kappa \in \mathbb{R}^{+} \diagdown \mathbb{N}, \end{cases}
\end{aligned}
\tag{B.72}
$$

and

$$
\begin{aligned}
m_1(t) \;&:=\; \exp\{-t\} \sum_{n=1}^{\infty} \frac{t^{n\kappa-1}}{\Gamma(n\kappa)} \\
&= \begin{cases} \frac{1}{\kappa} + O\left(\exp\{-at\}\right) & \text{if} \quad \kappa \in \mathbb{N} \\ \frac{1}{\kappa} + O\left(\exp\{-at\}\, t^{-\kappa-1}\right) & \text{if} \quad \kappa \in \mathbb{R}^{+} \diagdown \mathbb{N}, \end{cases}
\end{aligned}
\tag{B.73}
$$

where $a \in (0, 2]$ and $0 < t \leq T$. Therefore, from equations (1.30), (B.72), and (B.73) it follows that for $l \in \{0,\ 1,\ 2,\ \ldots,\ L-1\}$, the variance of Z_l can be expressed as

$$
\begin{aligned}
\operatorname{var}\{Z_l\} =& 2\int_{\Lambda_1(l\triangle)}^{\Lambda_1((l+1)\triangle)} m_1(u) M_1(\Lambda_1((l+1)\triangle) - u) du \\
&+ \int_{\Lambda_1(l\triangle)}^{\Lambda_1((l+1)\triangle)} m_1(u) du - \left[\int_{\Lambda_1(l\triangle)}^{\Lambda_1((l+1)\triangle)} m_1(u) du\right]^2
\end{aligned}
$$

$$
\begin{aligned}
=&2\int_{\Lambda_1(l\triangle)}^{\Lambda_1((l+1)\triangle)}\left[\frac{1}{\kappa}+O\left(\exp\{-au\}\right)\right]\{\frac{\Lambda_1((l+1)\triangle)-u}{\kappa}\\
&+\frac{1-\kappa}{2\kappa}+O\left(\exp\{-a(\Lambda_1((l+1)\triangle)-u)\}\right)\}du\\
&+\int_{\Lambda_1(l\triangle)}^{\Lambda_1((l+1)\triangle)}\left[\frac{1}{\kappa}+O\left(\exp\{-au\}\right)\right]du\\
&-\left[\int_{\Lambda_1(l\triangle)}^{\Lambda_1((l+1)\triangle)}\left[\frac{1}{\kappa}+O\left(\exp\{-au\}\right)\right]du\right]^2\\
=&2\int_{\Lambda_1(l\triangle)}^{\Lambda_1((l+1)\triangle)}[\frac{1}{\kappa^2}(\Lambda_1((l+1)\triangle)-u)+O\left(\frac{1}{\kappa}\exp\{-au\}\{\Lambda_1((l+1)\triangle)-u\}\right)\\
&+\frac{1}{\kappa}\frac{1-\kappa}{2\kappa}+O\left(\exp\{-au\}\frac{1-\kappa}{2\kappa}\right)\\
&+O\left(\frac{1}{\kappa}\exp\{-a(\Lambda_1((l+1)\triangle)-u)\}\right)+O\left(\exp\{-a\Lambda_1((l+1)\triangle)\}\right)]du\\
&+\frac{1}{\kappa}(\Lambda_1((l+1)\triangle)-\Lambda_1(l\triangle))+O\left(\frac{\exp\{-a\Lambda_1(l\triangle)\}}{a}-\frac{\exp\{-a\Lambda_1((l+1)\triangle)\}}{a}\right)\\
&-\left[\frac{1}{\kappa}(\Lambda_1((l+1)\triangle)-\Lambda_1(l\triangle))+O\left(\frac{\exp\{-a\Lambda_1(l\triangle)\}}{a}-\frac{\exp\{-a\Lambda_1((l+1)\triangle)\}}{a}\right)\right]^2\\
=&2[\frac{1}{\kappa^2}(\Lambda_1((l+1)\triangle))(\Lambda_1((l+1)\triangle)-\Lambda_1(l\triangle))-\frac{1}{2\kappa^2}(\Lambda_1^2((l+1)\triangle)-\Lambda_1^2(l\triangle))\\
&+O(\frac{1}{a\kappa}\exp\{-a\Lambda_1(l\triangle)\}\left(\Lambda_1((l+1)\triangle)-\Lambda_1(l\triangle)\right)\\
&+\frac{1}{a^2\kappa}\left(\exp\{-a\Lambda_1((l+1)\triangle)\}-\exp\{-a\Lambda_1(l\triangle)\}\right))\\
&+\frac{1}{\kappa}\frac{1-\kappa}{2\kappa}(\Lambda_1((l+1)\triangle)-\Lambda_1(l\triangle))\\
&+O\left(\frac{1-\kappa}{2\kappa}\{\frac{\exp\{-a\Lambda_1(l\triangle)\}}{a}-\frac{\exp\{-a\Lambda_1((l+1)\triangle)\}}{a}\}\right)\\
&+O\left(\frac{1}{\kappa}\{\frac{1}{a}-\frac{\exp\{-a\left[\Lambda_1((l+1)\triangle)-\Lambda_1(l\triangle)\right]\}}{a}\}\right)\\
&+O\left(\exp\{-a\Lambda_1((l+1)\triangle)\}\left(\Lambda_1((l+1)\triangle)-\Lambda_1(l\triangle)\right)\right)]
\end{aligned}
$$

$$
\begin{aligned}
&+\frac{1}{\kappa}(\Lambda_1((l+1)\triangle)-\Lambda_1(l\triangle))+O\left(\frac{\exp\{-a\Lambda_1(l\triangle)\}}{a}-\frac{\exp\{-a\Lambda_1((l+1)\triangle)\}}{a}\right)\\
&-\left[\frac{1}{\kappa}(\Lambda_1((l+1)\triangle)-\Lambda_1(l\triangle))+O\left(\frac{\exp\{-a\Lambda_1(l\triangle)\}}{a}-\frac{\exp\{-a\Lambda_1((l+1)\triangle)\}}{a}\right)\right]^2\\
=&\frac{2}{\kappa^2}[\Lambda_1^2((l+1)\triangle))-\Lambda_1((l+1)\triangle)\Lambda_1(l\triangle)]-\frac{1}{\kappa^2}(\Lambda_1^2((l+1)\triangle)-\Lambda_1^2(l\triangle))\\
&+O(\frac{2}{a\kappa}\exp\{-a\Lambda_1(l\triangle)\}(\Lambda_1((l+1)\triangle)-\Lambda_1(l\triangle))\\
&+\frac{2}{a^2\kappa}(\exp\{-a\Lambda_1((l+1)\triangle)\}-\exp\{-a\Lambda_1(l\triangle)\}))\\
&+\frac{1-\kappa}{\kappa^2}(\Lambda_1((l+1)\triangle)-\Lambda_1(l\triangle))\\
&+O\left(\frac{1-\kappa}{\kappa}\{\frac{\exp\{-a\Lambda_1(l\triangle)\}}{a}-\frac{\exp\{-a\Lambda_1((l+1)\triangle)\}}{a}\}\right)\\
&+O\left(\frac{2}{\kappa}\{\frac{1}{a}-\frac{\exp\{-a\left[\Lambda_1((l+1)\triangle)-\Lambda_1(l\triangle)\right]\}}{a}\}\right)\\
&+O\left(2\exp\{-a\Lambda_1((l+1)\triangle)\}(\Lambda_1((l+1)\triangle)-\Lambda_1(l\triangle))\right)\\
&+\frac{1}{\kappa}(\Lambda_1((l+1)\triangle)-\Lambda_1(l\triangle))+O\left(\frac{\exp\{-a\Lambda_1(l\triangle)\}}{a}-\frac{\exp\{-a\Lambda_1((l+1)\triangle)\}}{a}\right)\\
&-\frac{1}{\kappa^2}(\Lambda_1((l+1)\triangle)-\Lambda_1(l\triangle))^2\\
&+O\left(-\frac{2}{\kappa}(\Lambda_1((l+1)\triangle)-\Lambda_1(l\triangle))\{\frac{\exp\{-a\Lambda_1(l\triangle)\}}{a}-\frac{\exp\{-a\Lambda_1((l+1)\triangle)\}}{a}\}\right)\\
&+O\left(-\left[\frac{\exp\{-a\Lambda_1(l\triangle)\}}{a}-\frac{\exp\{-a\Lambda_1((l+1)\triangle)\}}{a}\right]^2\right)
\end{aligned}
$$

$$
\begin{aligned}
=&\frac{2}{\kappa^2}[\Lambda_1^2((l+1)\triangle)) - \Lambda_1((l+1)\triangle)\Lambda_1(l\triangle)] - \frac{1}{\kappa^2}\Lambda_1^2((l+1)\triangle) + \frac{1}{\kappa^2}\Lambda_1^2(l\triangle) \\
&+ \frac{1-\kappa}{\kappa^2}(\Lambda_1((l+1)\triangle) - \Lambda_1(l\triangle)) + \frac{1}{\kappa}(\Lambda_1((l+1)\triangle) - \Lambda_1(l\triangle)) \\
&- \frac{1}{\kappa^2}\{\Lambda_1^2((l+1)\triangle) - 2\Lambda_1((l+1)\triangle)\Lambda_1(l\triangle) + \Lambda_1^2(l\triangle)\} \\
&+ O(\frac{2}{a\kappa}\exp\{-a\Lambda_1(l\triangle)\}(\Lambda_1((l+1)\triangle) - \Lambda_1(l\triangle)) \\
&+ \frac{2}{a^2\kappa}(\exp\{-a\Lambda_1((l+1)\triangle)\} - \exp\{-a\Lambda_1(l\triangle)\})) \\
&+ O\left(\frac{1-\kappa}{\kappa}\{\frac{\exp\{-a\Lambda_1(l\triangle)\}}{a} - \frac{\exp\{-a\Lambda_1((l+1)\triangle)\}}{a}\}\right) \\
&+ O\left(\frac{2}{\kappa}\{\frac{1}{a} - \frac{\exp\{-a[\Lambda_1((l+1)\triangle) - \Lambda_1(l\triangle)]\}}{a}\}\right) \\
&+ O(2\exp\{-a\Lambda_1((l+1)\triangle)\}(\Lambda_1((l+1)\triangle) - \Lambda_1(l\triangle))) \\
&+ O\left(\frac{\exp\{-a\Lambda_1(l\triangle)\}}{a} - \frac{\exp\{-a\Lambda_1((l+1)\triangle)\}}{a}\right) \\
&+ O\left(-\frac{2}{\kappa}(\Lambda_1((l+1)\triangle) - \Lambda_1(l\triangle))\{\frac{\exp\{-a\Lambda_1(l\triangle)\}}{a} - \frac{\exp\{-a\Lambda_1((l+1)\triangle)\}}{a}\}\right) \\
&+ O\left(-\left[\frac{\exp\{-a\Lambda_1(l\triangle)\}}{a} - \frac{\exp\{-a\Lambda_1((l+1)\triangle)\}}{a}\right]^2\right) \\
=&\frac{2}{\kappa^2}[\Lambda_1^2((l+1)\triangle)) - \Lambda_1((l+1)\triangle)\Lambda_1(l\triangle)] - \frac{1}{\kappa^2}\Lambda_1^2((l+1)\triangle) + \frac{1}{\kappa^2}\Lambda_1^2(l\triangle) \\
&+ \frac{1-\kappa}{\kappa^2}(\Lambda_1((l+1)\triangle) - \Lambda_1(l\triangle)) + \frac{\kappa}{\kappa^2}(\Lambda_1((l+1)\triangle) - \Lambda_1(l\triangle)) \\
&- \frac{1}{\kappa^2}\{\Lambda_1^2((l+1)\triangle) - 2\Lambda_1((l+1)\triangle)\Lambda_1(l\triangle) + \Lambda_1^2(l\triangle)\} \\
&+ O(\exp\{-a\Lambda_1(l\triangle)\}(\Lambda_1((l+1)\triangle) - \Lambda_1(l\triangle))) \\
=&\frac{1}{\kappa^2}(\Lambda_1((l+1)\triangle) - \Lambda_1(l\triangle)) + O(\exp\{-a\Lambda_1(l\triangle)\}(\Lambda_1((l+1)\triangle) - \Lambda_1(l\triangle))),
\end{aligned}
\tag{B.74}
$$

where $a \in (0, 2]$.

Next, we establish the covariance structure of Z_l and Z_{l+r}. From results (1.31), (B.72), and (B.73), it follows that for $l \in \{0,\ 1,\ 2,\ \ldots,\ L-1\}$ and $r \in \{1,\ 2,\ \ldots,\ L-1\}$, we have

$$\begin{aligned}
\operatorname{cov}\{Z_l,\ Z_{l+r}\} &= \int_{\Lambda_1(l\triangle)}^{\Lambda_1((l+1)\triangle)} m_1(u)[M_1(\Lambda_1((l+r+1)\triangle) - u) \\
&- M_1(\Lambda_1((l+r)\triangle) - u)]du \\
&- \left[\int_{\Lambda_1(l\triangle)}^{\Lambda_1((l+1)\triangle)} m_1(u)du\right]\left[\int_{\Lambda_1((l+r)\triangle)}^{\Lambda_1((l+r+1)\triangle)} m_1(u)du\right] \\
&= \int_{\Lambda_1(l\triangle)}^{\Lambda_1((l+1)\triangle)} \left[\frac{1}{\kappa} + O\left(\exp\{-au\}\right)\right][\frac{\Lambda_1((l+r+1)\triangle) - u}{\kappa} \\
&+ \frac{1-\kappa}{2\kappa} + O\left(\exp\{-a(\Lambda_1((l+r+1)\triangle) - u)\}\right) \\
&- \{\frac{\Lambda_1((l+r)\triangle) - u}{\kappa} + \frac{1-\kappa}{2\kappa} \\
&+ O\left(\exp\{-a(\Lambda_1((l+r)\triangle) - u)\}\right)\}]du \\
&- \left[\int_{\Lambda_1(l\triangle)}^{\Lambda_1((l+1)\triangle)} m_1(u)du\right]\left[\int_{\Lambda_1((l+r)\triangle)}^{\Lambda_1((l+r+1)\triangle)} m_1(u)du\right]
\end{aligned}$$

$$\begin{aligned}
&= \int_{\Lambda_1(l\triangle)}^{\Lambda_1((l+1)\triangle)} \left[\frac{1}{\kappa} + O\left(\exp\{-au\}\right)\right][\frac{1}{\kappa}\{\Lambda_1((l+r+1)\triangle) - \Lambda_1((l+r)\triangle)\} \\
&+ O\left(\exp\{-a(\Lambda_1((l+r+1)\triangle) - u)\}\right) \\
&+ O\left(-\exp\{-a(\Lambda_1((l+r)\triangle) - u)\}\right)]du \\
&- \left[\int_{\Lambda_1(l\triangle)}^{\Lambda_1((l+1)\triangle)} m_1(u)du\right]\left[\int_{\Lambda_1((l+r)\triangle)}^{\Lambda_1((l+r+1)\triangle)} m_1(u)du\right]
\end{aligned}$$

$$
\begin{aligned}
=&\int_{\Lambda_1(l\triangle)}^{\Lambda_1((l+1)\triangle)} [\frac{1}{\kappa^2}\{\Lambda_1((l+r+1)\triangle)-\Lambda_1((l+r)\triangle)\}\\
&+O\left(\frac{1}{\kappa}\{\Lambda_1((l+r+1)\triangle)-\Lambda_1((l+r)\triangle)\}\exp\{-au\}\right)\\
&+O\left(\frac{1}{\kappa}\exp\{-a(\Lambda_1((l+r+1)\triangle)-u)\}\right)+O\left(\exp\{-a\Lambda_1((l+r+1)\triangle)\}\right)\\
&+O\left(-\frac{1}{\kappa}\exp\{-a(\Lambda_1((l+r)\triangle)-u)\}\right)+O\left(-\exp\{-a\Lambda_1((l+r)\triangle)\}\right)]du\\
&-\left[\int_{\Lambda_1(l\triangle)}^{\Lambda_1((l+1)\triangle)} m_1(u)du\right]\left[\int_{\Lambda_1((l+r)\triangle)}^{\Lambda_1((l+r+1)\triangle)} m_1(u)du\right]\\
=&\frac{1}{\kappa^2}\{\Lambda_1((l+r+1)\triangle)-\Lambda_1((l+r)\triangle)\}\{\Lambda_1((l+1)\triangle)-\Lambda_1(l\triangle)\}\\
&+O(\frac{1}{a\kappa}\{\Lambda_1((l+r+1)\triangle)-\Lambda_1((l+r)\triangle)\}[\exp\{-a\Lambda_1(l\triangle)\}\\
&-\exp\{-a\Lambda_1((l+1)\triangle)\}])\\
&+O(\frac{1}{a\kappa}\exp\{-a(\Lambda_1((l+r+1)\triangle)-\Lambda_1((l+1)\triangle))\}\\
&-\frac{1}{a\kappa}\exp\{-a(\Lambda_1((l+r+1)\triangle)-\Lambda_1(l\triangle))\})\\
&+O\left(\exp\{-a\Lambda_1((l+r+1)\triangle)\}\left(\Lambda_1((l+1)\triangle)-\Lambda_1(l\triangle)\right)\right)\\
&+O(\frac{1}{a\kappa}\exp\{-a(\Lambda_1((l+r)\triangle)-\Lambda_1((l+1)\triangle))\}\\
&-\frac{1}{a\kappa}\exp\{-a(\Lambda_1((l+r)\triangle)-\Lambda_1(l\triangle))\})\\
&+O\left(-\exp\{-a\Lambda_1((l+r)\triangle)\}\left(\Lambda_1((l+1)\triangle)-\Lambda_1(l\triangle)\right)\right)\\
&-\left[\int_{\Lambda_1(l\triangle)}^{\Lambda_1((l+1)\triangle)} m_1(u)du\right]\left[\int_{\Lambda_1((l+r)\triangle)}^{\Lambda_1((l+r+1)\triangle)} m_1(u)du\right]
\end{aligned}
$$

$$
\begin{aligned}
=&\frac{1}{\kappa^2}\{\Lambda_1((l+r+1)\triangle)-\Lambda_1((l+r)\triangle)\}\{\Lambda_1((l+1)\triangle)-\Lambda_1(l\triangle)\}\\
&+O(\frac{1}{a\kappa}\{\Lambda_1((l+r+1)\triangle)-\Lambda_1((l+r)\triangle)\}[\exp\{-a\Lambda_1(l\triangle)\}\\
&-\exp\{-a\Lambda_1((l+1)\triangle)\}])\\
&+O(\frac{1}{a\kappa}\exp\{-a(\Lambda_1((l+r+1)\triangle)-\Lambda_1((l+1)\triangle))\}\\
&-\frac{1}{a\kappa}\exp\{-a(\Lambda_1((l+r+1)\triangle)-\Lambda_1(l\triangle))\})\\
&+O\left(\exp\{-a\Lambda_1((l+r+1)\triangle)\}\left(\Lambda_1((l+1)\triangle)-\Lambda_1(l\triangle)\right)\right)\\
&+O(\frac{1}{a\kappa}\exp\{-a(\Lambda_1((l+r)\triangle)-\Lambda_1((l+1)\triangle))\}\\
&-\frac{1}{a\kappa}\exp\{-a(\Lambda_1((l+r)\triangle)-\Lambda_1(l\triangle))\})\\
&+O\left(-\exp\{-a\Lambda_1((l+r)\triangle)\}\left(\Lambda_1((l+1)\triangle)-\Lambda_1(l\triangle)\right)\right)\\
&-[\frac{1}{\kappa}(\Lambda_1((l+1)\triangle)-\Lambda_1(l\triangle))\\
&+O\left(\frac{\exp\{-a\Lambda_1(l\triangle)\}}{a}-\frac{\exp\{-a\Lambda_1((l+1)\triangle)\}}{a}\right)]\times\\
&[\frac{1}{\kappa}(\Lambda_1((l+r+1)\triangle)-\Lambda_1((l+r)\triangle))\\
&+O\left(\frac{\exp\{-a\Lambda_1((l+r)\triangle)\}}{a}-\frac{\exp\{-a\Lambda_1((l+r+1)\triangle)\}}{a}\right)]
\end{aligned}
$$

$$
\begin{aligned}
=&\frac{1}{\kappa^2}\{\Lambda_1((l+r+1)\triangle)-\Lambda_1((l+r)\triangle)\}\{\Lambda_1((l+1)\triangle)-\Lambda_1(l\triangle)\}\\
&+O(\frac{1}{a\kappa}\{\Lambda_1((l+r+1)\triangle)-\Lambda_1((l+r)\triangle)\}[\exp\{-a\Lambda_1(l\triangle)\}\\
&-\exp\{-a\Lambda_1((l+1)\triangle)\}])\\
&+O(\frac{1}{a\kappa}\exp\{-a(\Lambda_1((l+r+1)\triangle)-\Lambda_1((l+1)\triangle))\}\\
&-\frac{1}{a\kappa}\exp\{-a(\Lambda_1((l+r+1)\triangle)-\Lambda_1(l\triangle))\})\\
&+O\left(\exp\{-a\Lambda_1((l+r+1)\triangle)\}\left(\Lambda_1((l+1)\triangle)-\Lambda_1(l\triangle)\right)\right)\\
&+O(\frac{1}{a\kappa}\exp\{-a(\Lambda_1((l+r)\triangle)-\Lambda_1((l+1)\triangle))\}\\
&-\frac{1}{a\kappa}\exp\{-a(\Lambda_1((l+r)\triangle)-\Lambda_1(l\triangle))\})\\
&+O\left(-\exp\{-a\Lambda_1((l+r)\triangle)\}\left(\Lambda_1((l+1)\triangle)-\Lambda_1(l\triangle)\right)\right)\\
&-\frac{1}{\kappa^2}\left\{(\Lambda_1((l+1)\triangle)-\Lambda_1(l\triangle))\right\}\left\{(\Lambda_1((l+r+1)\triangle)-\Lambda_1((l+r)\triangle))\right\}\\
&+O(-\frac{1}{\kappa}(\Lambda_1((l+r+1)\triangle)-\Lambda_1((l+r)\triangle))[\\
&\frac{\exp\{-a\Lambda_1(l\triangle)\}}{a}-\frac{\exp\{-a\Lambda_1((l+1)\triangle)\}}{a}])\\
&+O(-\frac{1}{\kappa}(\Lambda_1((l+1)\triangle)-\Lambda_1(l\triangle))[\\
&\frac{\exp\{-a\Lambda_1((l+r)\triangle)\}}{a}-\frac{\exp\{-a\Lambda_1((l+r+1)\triangle)\}}{a}])\\
&+O(-\frac{1}{a^2}\left[\exp\{-a\Lambda_1(l\triangle)\}-\exp\{-a\Lambda_1((l+1)\triangle)\}\right][\\
&\exp\{-a\Lambda_1((l+r)\triangle)\}-\exp\{-a\Lambda_1((l+r+1)\triangle)\}])
\end{aligned}
$$

$$
\begin{aligned}
=&O(\frac{1}{a\kappa}\{\Lambda_1((l+r+1)\triangle)-\Lambda_1((l+r)\triangle)\}[\\
&\exp\{-a\Lambda_1(l\triangle)\}-\exp\{-a\Lambda_1((l+1)\triangle)\}])\\
&+O(\frac{1}{a\kappa}\exp\{-a(\Lambda_1((l+r+1)\triangle)-\Lambda_1((l+1)\triangle))\}\\
&-\frac{1}{a\kappa}\exp\{-a(\Lambda_1((l+r+1)\triangle)-\Lambda_1(l\triangle))\})\\
&+O\left(\exp\{-a\Lambda_1((l+r+1)\triangle)\}\left(\Lambda_1((l+1)\triangle)-\Lambda_1(l\triangle)\right)\right)\\
&+O(\frac{1}{a\kappa}\exp\{-a(\Lambda_1((l+r)\triangle)-\Lambda_1((l+1)\triangle))\}\\
&-\frac{1}{a\kappa}\exp\{-a(\Lambda_1((l+r)\triangle)-\Lambda_1(l\triangle))\})\\
&+O\left(-\exp\{-a\Lambda_1((l+r)\triangle)\}\left(\Lambda_1((l+1)\triangle)-\Lambda_1(l\triangle)\right)\right)\\
&+O(-\frac{1}{\kappa}(\Lambda_1((l+r+1)\triangle)-\Lambda_1((l+r)\triangle))[\\
&\frac{\exp\{-a\Lambda_1(l\triangle)\}}{a}-\frac{\exp\{-a\Lambda_1((l+1)\triangle)\}}{a}])\\
&+O(-\frac{1}{\kappa}(\Lambda_1((l+1)\triangle)-\Lambda_1(l\triangle))[\\
&\frac{\exp\{-a\Lambda_1((l+r)\triangle)\}}{a}-\frac{\exp\{-a\Lambda_1((l+r+1)\triangle)\}}{a}])\\
&+O(-\frac{1}{a^2}\left[\exp\{-a\Lambda_1(l\triangle)\}-\exp\{-a\Lambda_1((l+1)\triangle)\}\right][\\
&\exp\{-a\Lambda_1((l+r)\triangle)\}-\exp\{-a\Lambda_1((l+r+1)\triangle)\}])
\end{aligned}
$$

$$
\begin{aligned}
&=O(\frac{1}{a\kappa}\exp\{-a(\Lambda_1((l+r)\triangle)-\Lambda_1((l+1)\triangle))\} \\
&\quad -\frac{1}{a\kappa}\exp\{-a(\Lambda_1((l+r)\triangle)-\Lambda_1(l\triangle))\}) \\
&=O(\frac{1}{a\kappa}[\exp\{-a(\Lambda_1((l+r)\triangle)\}\exp\{a\Lambda_1((l+1)\triangle)\} \\
&\quad -\exp\{-a(\Lambda_1((l+r)\triangle)\}\exp\{a\Lambda_1(l\triangle)\}]) \\
&=O\left(\frac{1}{a\kappa}\exp\{-a(\Lambda_1((l+r)\triangle)\}\left[\exp\{a\Lambda_1((l+1)\triangle)\}-\exp\{a\Lambda_1(l\triangle)\}\right]\right) \\
&=O\left(\frac{1}{a\kappa}\exp\{-a(\Lambda_1((l+r)\triangle)+a\Lambda_1(l\triangle)\}\left[\exp\left\{a\int_{l\triangle}^{(l+1)\triangle}\lambda_1(u)du\right\}-1\right]\right) \\
&=O\left(\frac{1}{a\kappa}\exp\left\{-a\int_{l\triangle}^{(l+r)\triangle}\lambda_1(u)du\right\}\left[\exp\left\{a\int_{l\triangle}^{(l+1)\triangle}\lambda_1(u)du\right\}-1\right]\right), \qquad \text{(B.75)}
\end{aligned}
$$

where $a \in (0, 2]$. □

B.1.1.2 Proof of Proposition 9

Proof. We first establish that $\hat{\omega}_{\mathbf{T}} \to \omega_{\mathbf{T}}$ (a.s), as $T \to \infty$, that is, $\hat{\omega}_{\mathbf{T}}$ is a consistent estimator of ω. For every $\omega \in \{\omega : \ O(T^{\delta'-1}) \leq \omega \leq \Omega_T, \ 0 < \delta' < 1\}$ and for each $k = 1, \ 2, \ \ldots, \ K$, Lemma 8 (of Section 2.2) and equation (1.36) imply that when $m = 1$ the integral (2.6) reduces to $J_T(\omega) = \frac{1}{T}\int_0^T e^{-i\omega t}\lambda_2(t)dt + \frac{1}{T}\int_0^T e^{-i\omega t}dZ_G(t)$ $= \frac{1}{T}\int_0^T e^{-i\omega t}\frac{1}{\kappa}\lambda_1(t)dt + o(1) = \frac{1}{T}\int_0^T e^{-i\omega t}\frac{1}{\kappa}\{\sum_{k=1}^K A_k\cos(\omega_k t + \phi_k) + B\}dt + o(1)$. Therefore, from the useful integral section of Appendix B, it then follows that for each frequency in the frequency range $\omega \in \{\omega : \ O(T^{\delta'-1}) \leq \omega \leq \Omega_T, \ 0 < \delta' < 1\}$, we have

$$J_T(\omega) = \begin{cases} \frac{A_k}{2\kappa} e^{i\phi_k} + o(1) & \text{if} \quad |\omega - \omega_k| = cT^{-1-\gamma} \\ \frac{A_k}{i2\kappa} e^{i\phi_k} \frac{1-\exp\{-ic\}}{c} + o(1) & \text{if} \quad |\omega - \omega_k| = cT^{-1} \\ o(1) & \text{if} \quad |\omega - \omega_k| = cT^{-1+\gamma}, \end{cases} \tag{B.76}$$

where $k = 1,\ 2,\ \ldots,\ K$, $c \neq 0$, and $\gamma > 0$. Therefore, the local maxima must occur in the neighborhood of ω_k ($k = 1,\ 2,\ \ldots,\ K$) where the width of this neighborhood is at most $O(T^{-1})$. It then follows that under Assumption 3 (of Section 2.2), these neighborhoods are disjoint for large T. By the definition of the K local maxima of $|J_T(\omega)|$, only one maximum should be considered in a neighborhood of length $O(T^{-1+\gamma})$, where $\gamma > 0$. Therefore, the K largest local maxima of $|J_T(\omega)|$ must occur in these neighborhood of $\omega_T = (\omega_1,\ \ldots,\ \omega_K)$, with each neighborhood containing one local maximum, namely, the frequency estimates $\hat{\omega}_{k,T}$, where $k = 1,\ 2,\ \ldots,\ K$. Since these neighborhoods tend to 0 as $T \to \infty$, it follows that $\hat{\omega}_{\mathbf{T}} \to \omega_{\mathbf{T}}$ (a.s), as $T \to \infty$, that is, $\hat{\omega}_{\mathbf{T}}$ is a consistent estimator of ω.

We now show that that for each $k = 1,\ 2,\ \ldots,\ K$, $(\hat{\omega}_{k,T} - \omega_k) = o(T^{-1})$ almost surely as $T \to \infty$. Using the notation of equation (2.6) and equation (B.76), we know that for each $k = 1,\ 2,\ \ldots,\ K$, $|J_T(\omega)|$ obtains its k-th local maximum at $\hat{\omega}_{k,T}$, while $\left|J_T^{(\lambda_2)}(\omega)\right|$ has its k-th local maximum at ω_k. So for all $\omega \in \{\omega :\ O(T^{\delta'-1}) \leq \omega \leq$

$\Omega_T, \quad 0 < \delta' < 1\}$, we have

$$\begin{aligned} |J_T(\hat{\omega}_{k,T})| &\geq |J_T(\omega_k)| \\ &\geq \left| \left| J_T^{(\lambda_2)}(\omega_k) \right| - \left| J_T^{(Z_G)}(\omega_k) \right| \right| \\ &= \left| J_T^{(\lambda_2)}(\omega_k) \right| - \left| J_T^{(Z_G)}(\omega_k) \right|, \end{aligned}$$

and

$$\begin{aligned} \left| J_T^{(\lambda_2)}(\omega_k) \right| &\geq \left| J_T^{(\lambda_2)}(\hat{\omega}_{k,T}) \right| \\ &\geq \left| \left| J_T^{(\lambda_2)}(\hat{\omega}_{k,T}) + J_T^{(Z_G)}(\hat{\omega}_{k,T}) \right| - \left| J_T^{(Z_G)}(\hat{\omega}_{k,T}) \right| \right| \\ &= |J_T(\hat{\omega}_{k,T})| - \left| J_T^{(Z_G)}(\hat{\omega}_{k,T}) \right|. \end{aligned}$$

Therefore, it follows that for each $k = 1,\ 2,\ \ldots,\ K$, we have

$$\left| J_T^{(\lambda_2)}(\omega_k) \right| - \left| J_T^{(Z_G)}(\omega_k) \right| \leq |J_T(\hat{\omega}_{k,T})| \leq \left| J_T^{(\lambda_2)}(\omega_k) \right| + \left| J_T^{(Z_G)}(\hat{\omega}_{k,T}) \right|.$$

Now from Lemma 8, we know that for each $k = 1,\ 2,\ \ldots,\ K$, we have

$$\lim_{T \to 0} \left| J_T^{(Z_G)}(\omega_k) \right| \to 0 \ \ \text{(a.s.)} \quad \text{and} \quad \lim_{T \to 0} \left| J_T^{(Z_G)}(\hat{\omega}_{k,T}) \right| \to 0 \ \ \text{(a.s.)},$$

and it then follows from equation (B.76) that

$$\lim_{T\to 0}|J_T(\hat{\omega}_{k,T})| \quad = \quad \lim_{T\to 0}\left|J_T^{(\lambda_2)}(\hat{\omega}_{k,T})\right| = \left|\frac{A_k}{2\kappa}e^{i\phi_k}\right| = \frac{A_k}{2\kappa}. \tag{B.77}$$

However, we know by direct computation that

$$|J_T(\hat{\omega}_{k,T})| = \frac{A_k}{2\kappa}\left|\frac{1-e^{-i\left(\hat{\omega}_{k,T}-\omega_k\right)T}}{i\left(\hat{\omega}_{k,T}-\omega_k\right)T}\right| + o(1). \tag{B.78}$$

Hence, from equations (B.77) and (B.78), it follows that as $T\to\infty$,

$$\left|\frac{1-e^{-i\left(\hat{\omega}_{k,T}-\omega_k\right)T}}{i\left(\hat{\omega}_{k,T}-\omega_k\right)T}\right| \to 1 \ \ (a.s.). \tag{B.79}$$

Therefore, for each $k = 1,\ 2,\ \ldots,\ K$, we have

$$(\hat{\omega}_{k,T}-\omega_k) = o(T^{-1}) \ \ \text{(a.s.)}, \tag{B.80}$$

as $T\to\infty$. □

B.1.1.3 The Derivation of the Asymptotic Variance-Covariance Matrix of the Random Variables of Equation (2.7)

Proof. The asymptotic variance-covariance matrix of the random variables $(U,\ V_1,\ldots,$ $V_K,\ W_1,\ldots,\ W_K,\ X_1,\ldots,X_K,\ Y_1,\ldots,Y_K)'$, defined in equation (2.7), can be obtained by direct calculation. We begin by establishing some asymptotic variance-covariance bounds which will be used throughout the derivation of the asymptotic variance-covariance matrix of the random variables $(U,\ V_1, \ldots, V_K,\ \ W_1, \ldots, W_K,\ X_1, \ldots, X_K,\ Y_1, \ldots, Y_K)'$. Let $\lambda_1(\cdot)$ be the baseline intensity function and $\lambda_2(\cdot)$ be the intensity function of an inhomogeneous Gamma process (IGP) which satisfies the Chapter 2 Assumptions 1-3. For the observational time period $T > 0$, let $0 < t \leq T$, $0 < \epsilon_1 \leq \lambda_1(t) \leq J_1 < \infty$, $0 < \epsilon_2 \leq \lambda_2(t) \leq J_1^G < \infty$, $\epsilon = \min\{\epsilon_1,\ \epsilon_2\}$, $J = \max\left\{J_1,\ J_1^G\right\}$, $\triangle = O(T^{-\nu})$, $\frac{1}{3} < v < 1$, and L be an integer such that $T = L\triangle$.

We now establish that

$$\frac{1}{T^m} \int\int\limits_{\substack{0<r<T \\ 0<l\leq T-r}} t^{m-1} \text{cov}\left\{dZ_G(r),\ dZ_G(r+l)\right\} \to 0 \ \text{ as }\ \mathrm{T} \to \infty, \tag{B.81}$$

where $m \geq 1$.

From equation (B.68), we know that for some $a \in (0,\ 2]$, there exists some $M \in (0,\ \infty)$, such that

$$\left|\frac{1}{T} \int\int\limits_{\substack{0<r<T \\ 0<l\leq T-r}} \text{cov}\left\{dZ_G(r),\ dZ_G(r+l)\right\}\right| \leq \frac{1}{T} \int\int\limits_{\substack{0<r<T \\ 0<l\leq T-r}} \left|\text{cov}\left\{dZ_G(r),\ dZ_G(r+l)\right\}\right|$$

$$
\begin{aligned}
&\leq \frac{M}{T}\sum_{r=1}^{L-1}\sum_{l=0}^{L-1-r}\left[\exp\left\{-a\int_{l\triangle}^{(l+r)\triangle}\lambda_1(u)du\right\}(\lambda_1(l\triangle)\triangle+o(\triangle))\right]\triangle\triangle \\
&\leq \frac{MJ}{T}\sum_{r=1}^{L-1}\sum_{l=0}^{L-1-r}\left[\exp\left\{-a\epsilon r\triangle\right\}\left(\triangle^3+o(\triangle^3)\right)\right] \\
&\leq \frac{c}{T}\sum_{r=1}^{L-1}(L-1-r)\exp\left\{-a\epsilon r\triangle\right\}\triangle^3 \quad \text{for some constant } c>0 \\
&\leq \frac{c\triangle^3}{T}\int_0^L (L-r)\exp\left\{-a\epsilon\triangle r\right\}dr \\
&= \frac{c\triangle^3}{T(a\epsilon\triangle)^2}\left[(a\epsilon\triangle r-a\epsilon\triangle L+1)\exp\left\{-a\epsilon\triangle r\right\}\right]_0^L \\
&= \frac{c\triangle}{T(a\epsilon)^2}\left[\exp\left\{-a\epsilon\triangle L\right\}+a\epsilon\triangle L-1\right] \\
&= \frac{c\triangle}{T(a\epsilon)^2}\left[\exp\left\{-a\epsilon T\right\}+a\epsilon T-1\right] \\
&= \frac{c\triangle}{(a\epsilon)^2}\left[\frac{\exp\left\{-a\epsilon T\right\}}{T}+a\epsilon-\frac{1}{T}\right] \\
&\to 0 \ \text{ as } \ T\to\infty. \qquad \text{(B.82)}
\end{aligned}
$$

From equation (B.82), it follows that for $m \geq 1$, we have

$$
\begin{aligned}
&\left|\frac{1}{T^m}\iint\limits_{\substack{0<r<T\\0<l\leq T-r}} l^{m-1}\operatorname{cov}\left\{dZ_G(r),\ dZ_G(r+l)\right\}\right| \\
&\qquad = \left|\frac{1}{T}\iint\limits_{\substack{0<r<T\\0<l\leq T-r}}\left(\frac{l}{T}\right)^{m-1}\operatorname{cov}\left\{dZ_G(r),\ dZ_G(r+l)\right\}\right| \\
&\qquad \leq \frac{1}{T}\iint\limits_{\substack{0<r<T\\0<l\leq T-r}}\left|\operatorname{cov}\left\{dZ_G(r),\ dZ_G(r+l)\right\}\right| \\
&\qquad \to 0 \ \text{ as } \ T\to\infty, \qquad \text{(B.83)}
\end{aligned}
$$

and equation (B.81) therefore follows.

We now show that

$$\lim_{T\to\infty}\frac{1}{T}\int_0^T \text{var}\left\{dZ_G(t)\right\} = \lim_{T\to\infty}\frac{1}{T\kappa^2}\int_0^T \lambda_1(u)du. \tag{B.84}$$

From equation (B.67), we know that there exists some $a \in (0,\ 2]$ such that

$$\begin{aligned}
\frac{1}{T}\int_0^T \text{var}\left\{dZ_G(t)\right\} =& \frac{1}{T}\sum_{l=0}^{L-1}\text{var}\left\{dZ_G(l\triangle)\right\}\triangle \\
=& \frac{1}{T}\sum_{l=0}^{L-1}[\frac{1}{\kappa^2}(\Lambda_1((l+1)\triangle)-\Lambda_1(l\triangle)) \\
&+ O\left(\exp\left\{-a\Lambda_1(l\triangle)\right\}(\Lambda_1((l+1)\triangle)-\Lambda_1(l\triangle))\right)]\triangle \\
=& \frac{1}{T}\sum_{l=0}^{L-1}[\frac{1}{\kappa^2}\int_{l\triangle}^{(l+1)\triangle}\lambda_1(u)du \\
&+ O\left(\exp\left\{-a\Lambda_1(l\triangle)\right\}(\Lambda_1((l+1)\triangle)-\Lambda_1(l\triangle))\right)]\triangle \\
=& \frac{1}{T}\sum_{l=0}^{L-1}[\frac{1}{\kappa^2}\lambda_1(l\triangle)\triangle + o(\triangle) \\
&+ O\left(\exp\left\{-a\Lambda_1(l\triangle)\right\}(\Lambda_1((l+1)\triangle)-\Lambda_1(l\triangle))\right)]\triangle \\
=& \frac{1}{T\kappa^2}\int_0^T\lambda_1(u)du + \frac{1}{T}\sum_{l=0}^{L-1}o(\triangle)\triangle \\
&+ \frac{1}{T}\sum_{l=0}^{L-1}O\left(\exp\left\{-a\Lambda_1(l\triangle)\right\}(\Lambda_1((l+1)\triangle)-\Lambda_1(l\triangle))\right)\triangle \\
=& \frac{1}{T\kappa^2}\int_0^T\lambda_1(u)du + o(\triangle) \\
&+ \frac{1}{T}\sum_{l=0}^{L-1}O\left(\exp\left\{-a\Lambda_1(l\triangle)\right\}(\Lambda_1((l+1)\triangle)-\Lambda_1(l\triangle))\right)\triangle
\end{aligned}$$

$$
\begin{aligned}
&\leq \frac{1}{T\kappa^2}\int_0^T \lambda_1(u)du + o(\triangle) + \frac{1}{T}\sum_{l=0}^{L-1} O\left(\exp\left\{-a\epsilon l\triangle\right\} J\triangle\right)\triangle \\
&\leq \frac{1}{T\kappa^2}\int_0^T \lambda_1(u)du + o(\triangle) + \frac{1}{T}\sum_{l=0}^{L-1} O\left(J\triangle^2\right) \\
&= \frac{1}{T\kappa^2}\int_0^T \lambda_1(u)du + o(\triangle) + \frac{1}{T}LO\left(J\triangle^2\right) \\
&= \frac{1}{T\kappa^2}\int_0^T \lambda_1(u)du + o(\triangle) + \frac{1}{T}O\left(JL\triangle\triangle\right) \\
&= \frac{1}{T\kappa^2}\int_0^T \lambda_1(u)du + o(\triangle) + \frac{1}{T}O\left(JT\triangle\right) \\
&= \frac{1}{T\kappa^2}\int_0^T \lambda_1(u)du + O\left(T^{-\nu}\right),
\end{aligned}
$$

and equation (B.84) therefore follows.

Using the equations (B.81) and (B.84), we derive the asymptotic variance-covariance matrix of the random variables $(U,\ V_1,\ldots,V_K,\ W_1,\ldots,W_K, X_1,\ldots,X_K, Y_1,\ldots,Y_K)'$. We begin by establishing

$$
\lim_{\mathrm{T}\to\infty} \mathrm{cov}\left\{\mathrm{U},\ \mathrm{U}\right\} = \frac{1}{\kappa^2}\mathrm{B}.
$$

Since

$$
\lim_{T\to\infty} \mathrm{cov}\left\{U,\ U\right\} = \lim_{T\to\infty}\frac{1}{T}\mathrm{var}\left\{\int_0^T dZ_G(s)\right\} = \lim_{T\to\infty}\frac{1}{T}\mathrm{var}\left\{Z_G(T)\right\},
$$

it follows from equation (1.37) that

$$\lim_{T\to\infty} \operatorname{cov}\{U,\ U\} = \frac{1}{\kappa^2} B.$$

Next, we establish

$$\lim_{\mathrm{T}\to\infty} \operatorname{cov}\{\mathrm{U},\ \mathrm{V_{k'}}\} = \frac{\mathrm{A_{k'}}}{2\kappa^2} \cos(\phi_{\mathrm{k'}}).$$

Since

$$\begin{aligned}
\lim_{T\to\infty} \operatorname{cov}\{U,\ V_{k'}\} &= \lim_{T\to\infty} \operatorname{cov}\left\{T^{-\frac{1}{2}} \int_0^T dZ_G(s),\ T^{-\frac{1}{2}} \int_0^T \cos(\omega_{k'} t) dZ_G(t)\right\} \\
&= \lim_{T\to\infty} \frac{1}{T} \int_0^T \int_0^T \cos(\omega_{k'} t) \operatorname{cov}\{dZ_G(s),\ dZ_G(t)\} \\
&= \lim_{T\to\infty} \frac{1}{T} [\int_0^T \cos(\omega_{k'} t) \operatorname{var}\{dZ_G(t)\} \\
&\quad +2 \int\!\!\int_{\substack{0<s<T \\ 0<t\leq T-s}} \cos(\omega_{k'}(s+t)) \operatorname{cov}\{dZ_G(s),\ dZ_G(s+t)\}],
\end{aligned}$$

it follows from the useful integral section of Appendix B, equations (B.66), (B.67), (B.81), (B.84), and the Chapter 2 Assumption 3 that

$$\begin{aligned}
\lim_{T\to\infty} \operatorname{cov}\{U,\ V_{k'}\} &= \lim_{T\to\infty} \frac{1}{T\kappa^2} \int_0^T \cos(\omega_{k'} t) \lambda_1(t) dt \\
&= \lim_{T\to\infty} \frac{1}{T\kappa^2} \int_0^T \cos(\omega_{k'} t) \left[\sum_{k=1}^{K} A_k \cos(\omega_k t + \phi_k) + B\right] dt
\end{aligned}$$

$$= \lim_{T\to\infty} \frac{1}{T\kappa^2} \int_0^T \cos(\omega_{k'}t) \sum_{k=1}^{K} A_k \cos(\omega_k t + \phi_k) dt + \lim_{T\to\infty} \frac{1}{T\kappa^2} \int_0^T \cos(\omega_{k'}t) B dt$$
$$= \lim_{T\to\infty} \frac{1}{T\kappa^2} \int_0^T \cos(\omega_{k'}t) \sum_{k=1}^{K} A_k \cos(\omega_k t + \phi_k) dt$$
$$= \frac{A_{k'}}{2\kappa^2} \cos(\phi_{k'}).$$

Likewise, we establish

$$\lim_{\mathrm{T}\to\infty} \operatorname{cov}\{\mathrm{U},\ \mathrm{W}_{\mathrm{k}'}\} = -\frac{\mathrm{A}_{\mathrm{k}'}}{2\kappa^2} \sin(\phi_{\mathrm{k}'}).$$

Since

$$\begin{aligned}
\lim_{T\to\infty} \operatorname{cov}\{U,\ W_{k'}\} &= \lim_{T\to\infty} \operatorname{cov}\left\{T^{-\frac{1}{2}} \int_0^T dZ_G(s),\ T^{-\frac{1}{2}} \int_0^T \sin(\omega_{k'}t) dZ_G(t)\right\} \\
&= \lim_{T\to\infty} \frac{1}{T} \int_0^T \int_0^T \sin(\omega_{k'}t) \operatorname{cov}\{dZ_G(s),\ dZ_G(t)\} \\
&= \lim_{T\to\infty} \frac{1}{T} [\int_0^T \sin(\omega_{k'}t) \operatorname{var}\{dZ_G(t)\} \\
&\quad +2 \int\int_{\substack{0<s<T \\ 0<t\le T-s}} \sin(\omega_{k'}(s+t)) \operatorname{cov}\{dZ_G(s),\ dZ_G(s+t)\}],
\end{aligned}$$

it follows from the useful integral section of Appendix B, equations (B.66), (B.67), (B.81), (B.84), and the Chapter 2 Assumption 3 that

$$\begin{aligned}
\lim_{T\to\infty} \operatorname{cov}\{U,\ W_{k'}\} &= \lim_{T\to\infty} \frac{1}{T\kappa^2} \int_0^T \sin(\omega_{k'}t) \lambda_1(t) dt \\
&= -\frac{A_{k'}}{2\kappa^2} \sin(\phi_{k'}).
\end{aligned}$$

Likewise, we establish

$$\lim_{\mathrm{T}\to\infty} \mathrm{cov}\left\{\mathrm{U},\ \mathrm{X}_{\mathrm{k}'}\right\} = \frac{\mathrm{A}_{\mathrm{k}'}}{4\kappa^2}\cos(\phi_{\mathrm{k}'}).$$

Since

$$\begin{aligned}
\lim_{T\to\infty} \mathrm{cov}\left\{U,\ X_{k'}\right\} &= \lim_{T\to\infty} \mathrm{cov}\left\{T^{-\frac{1}{2}}\int_0^T dZ_G(s),\ T^{-\frac{3}{2}}\int_0^T t\cos(\omega_{k'}t)dZ_G(t)\right\} \\
&= \lim_{T\to\infty} \frac{1}{T^2}\int_0^T\int_0^T t\cos(\omega_{k'}t)\mathrm{cov}\left\{dZ_G(s),\ dZ_G(t)\right\} \\
&= \lim_{T\to\infty} \frac{1}{T^2}[\int_0^T t\cos(\omega_{k'}t)\mathrm{var}\left\{dZ_G(t)\right\} \\
&\quad +2\int\int_{\substack{0<s<T\\0<t\leq T-s}} (s+t)\cos(\omega_{k'}(s+t))\mathrm{cov}\left\{dZ_G(s),\ dZ_G(s+t)\right\}],
\end{aligned}$$

it follows from the useful integral section of Appendix B, equations (B.66), (B.67), (B.81), (B.84), and the Chapter 2 Assumption 3 that

$$\begin{aligned}
\lim_{T\to\infty} \mathrm{cov}\left\{U,\ X_{k'}\right\} &= \lim_{T\to\infty} \frac{1}{T^2\kappa^2}\int_0^T t\cos(\omega_{k'}t)\lambda_1(t)dt \\
&= \frac{A_{k'}}{4\kappa^2}\cos(\phi_{k'}).
\end{aligned}$$

Likewise, we establish

$$\lim_{\mathrm{T}\to\infty} \mathrm{cov}\left\{\mathrm{U},\ \mathrm{Y}_{\mathrm{k}'}\right\} = -\frac{\mathrm{A}_{\mathrm{k}'}}{4\kappa^2}\sin(\phi_{\mathrm{k}'}).$$

Since

$$\lim_{T\to\infty} \mathrm{cov}\left\{U,\ Y_{k'}\right\} = \lim_{T\to\infty} \mathrm{cov}\left\{T^{-\frac{1}{2}}\int_0^T dZ_G(s),\ T^{-\frac{3}{2}}\int_0^T t\sin(\omega_{k'}t)dZ_G(t)\right\}$$

$$
\begin{aligned}
&= \lim_{T\to\infty} \frac{1}{T^2} \int_0^T \int_0^T t \sin(\omega_{k'} t) \mathrm{cov}\left\{dZ_G(s),\ dZ_G(t)\right\} \\
&= \lim_{T\to\infty} \frac{1}{T^2} [\int_0^T t \sin(\omega_{k'} t) \mathrm{var}\left\{dZ_G(t)\right\} \\
&\quad +2 \int\int_{\substack{0<s<T \\ 0<t\leq T-s}} (s+t) \sin(\omega_{k'}(s+t)) \mathrm{cov}\left\{dZ_G(s),\ dZ_G(s+t)\right\}],
\end{aligned}
$$

it follows from the useful integral section of Appendix B, equations (B.66), (B.67), (B.81), (B.84), and the Chapter 2 Assumption 3 that

$$
\begin{aligned}
\lim_{T\to\infty} \mathrm{cov}\left\{U,\ Y_{k'}\right\} &= \lim_{T\to\infty} \frac{1}{T^2 \kappa^2} \int_0^T t \sin(\omega_{k'} t) \lambda_1(t) dt \\
&= -\frac{A_{k'}}{4\kappa^2} \sin(\phi_{k'}).
\end{aligned}
$$

We now provide some extra details in establishing

$$
\lim_{\mathrm{T}\to\infty} \mathrm{cov}\left\{\mathrm{V_k},\ \mathrm{V_{k'}}\right\} = \frac{1}{4\kappa^2} \sum_{j=1}^{K} A_j \cos(\phi_j) \left\{\delta_{j,\, k+k'} + \delta_{j,\, k-k'} + \delta_{j,\, k'-k}\right\} + \frac{B}{2\kappa^2} \delta_{k,\, k'}.
$$

Since

$$
\begin{aligned}
\lim_{T\to\infty} \mathrm{cov}\left\{V_k,\ V_{k'}\right\} &= \lim_{T\to\infty} \mathrm{cov}\left\{T^{-\frac{1}{2}} \int_0^T \cos(\omega_k s) dZ_G(s),\ T^{-\frac{1}{2}} \int_0^T \cos(\omega_{k'} t) dZ_G(t)\right\} \\
&= \lim_{T\to\infty} \frac{1}{T} \int_0^T \int_0^T \cos(\omega_k s) \cos(\omega_{k'} t) \mathrm{cov}\left\{dZ_G(s),\ dZ_G(t)\right\}
\end{aligned}
$$

$$
\begin{aligned}
&= \lim_{T\to\infty} \frac{1}{T}[\int_0^T \cos(\omega_k t)\cos(\omega_{k'} t)\mathrm{var}\{dZ_G(t)\} \\
&\quad +2 \underset{\substack{0<s<T \\ 0<t\leq T-s}}{\int\int} \cos(\omega_k s)\cos(\omega_{k'}(s+t))\mathrm{cov}\{dZ_G(s),\ dZ_G(s+t)\}] \\
&= \lim_{T\to\infty} \frac{1}{T\kappa^2}\int_0^T \cos(\omega_k t)\cos(\omega_{k'} t)\lambda_1(t)dt \\
&\quad +2\lim_{T\to\infty} \frac{1}{T} \underset{\substack{0<s<T \\ 0<t\leq T-s}}{\int\int} \cos(\omega_k s)\cos(\omega_{k'}(s+t))\mathrm{cov}\{dZ_G(s),\ dZ_G(s+t)\},
\end{aligned}
$$

it then follows from the useful integral and trigonometric identity section of Appendix B, equations (B.66), (B.67), (B.81), (B.84), the assumption $\omega > 0$, and the Chapter 2 Assumption 3 that

$$
\begin{aligned}
\lim_{T\to\infty} \mathrm{cov}\{V_k,\ V_{k'}\} &= \lim_{T\to\infty} \frac{1}{T\kappa^2}\int_0^T \cos(\omega_k t)\cos(\omega_{k'} t)\lambda_1(t)dt \\
&= \lim_{T\to\infty} \frac{1}{T\kappa^2}\int_0^T \cos(\omega_k t)\cos(\omega_{k'} t)\left[\sum_{k=1}^{K} A_k\cos(\omega_k t+\phi_k)+B\right]dt \\
&= \lim_{T\to\infty} \frac{1}{T\kappa^2}\int_0^T \cos(\omega_k t)\cos(\omega_{k'} t)\sum_{k=1}^{K} A_k\cos(\omega_k t+\phi_k)dt \\
&\quad +\lim_{T\to\infty} \frac{1}{T\kappa^2}\int_0^T \cos(\omega_k t)\cos(\omega_{k'} t)Bdt \\
&= \lim_{T\to\infty} \frac{1}{T\kappa^2}\int_0^T \cos(\omega_k t)\cos(\omega_{k'} t)\sum_{k=1}^{K} A_k\cos(\omega_k t+\phi_k)dt
\end{aligned}
$$

$$=\frac{1}{4T\kappa^2}\int_0^T \sum_{j=1}^{K} A_j\{\cos((\omega_k+\omega_{k'}+\omega_j)t+\phi_j)+\cos((\omega_k-\omega_{k'}-\omega_j)t-\phi_j)$$

$$+\cos((\omega_k-\omega_{k'}+\omega_j)t+\phi_j)+\cos((\omega_k+\omega_{k'}-\omega_j)t-\phi_j)\}dt+\frac{B}{2\kappa^2}\delta_{k,\,k'}$$

$$=\frac{1}{4\kappa^2}\sum_{j=1}^{K} A_j\cos(\phi_j)\left\{\delta_{j,\,k+k'}+\delta_{j,\,k-k'}+\delta_{j,\,k'-k}\right\}+\frac{B}{2\kappa^2}\delta_{k,\,k'},$$

where the last equation follows since the only way the last integral is nonzero asymptotically is when

$$\begin{aligned}
\omega_k-\omega_{k'}-\omega_j &= 0\\
\omega_k-\omega_{k'}+\omega_j &= 0\\
\omega_k+\omega_{k'}-\omega_j &= 0.
\end{aligned}$$

Likewise, we establish

$$\lim_{\mathrm{T}\to\infty}\operatorname{cov}\left\{\mathrm{V_k},\ \mathrm{W_{k'}}\right\}=\frac{1}{4\kappa^2}\sum_{j=1}^{K} A_j\sin(\phi_j)\left\{-\delta_{j,k+k'}+\delta_{j,k-k'}-\delta_{j,k'-k}\right\}.$$

Since

$$\lim_{T\to\infty} \mathrm{cov}\left\{V_k,\ W_{k'}\right\} = \lim_{T\to\infty} \mathrm{cov}\left\{T^{-\frac{1}{2}} \int_0^T \cos(\omega_k s) dZ_G(s),\ T^{-\frac{1}{2}} \int_0^T \sin(\omega_{k'} t) dZ_G(t)\right\}$$

$$\begin{aligned}
&= \lim_{T\to\infty} \frac{1}{T} \int_0^T \int_0^T \cos(\omega_k s) \sin(\omega_{k'} t) \mathrm{cov}\left\{dZ_G(s),\ dZ_G(t)\right\} \\
&= \lim_{T\to\infty} \frac{1}{T} [\int_0^T \cos(\omega_k t) \sin(\omega_{k'} t) \mathrm{var}\left\{dZ_G(t)\right\} \\
&\quad +2 \int\!\!\int_{\substack{0<s<T \\ 0<t\leq T-s}} \cos(\omega_k s) \sin(\omega_{k'}(s+t)) \mathrm{cov}\left\{dZ_G(s),\ dZ_G(s+t)\right\}],
\end{aligned}$$

it then follows from the useful integral and trigonometric identity section of Appendix B, equations (B.66), (B.67), (B.81), (B.84), the assumption $\omega > 0$, and the Chapter 2 Assumption 3 that

$$\lim_{T\to\infty} \mathrm{cov}\left\{V_k,\ W_{k'}\right\} = \lim_{T\to\infty} \frac{1}{T\kappa^2} \int_0^T \cos(\omega_k t) \sin(\omega_{k'} t) \lambda_1(t) dt$$

$$\begin{aligned}
&= \frac{1}{4T\kappa^2} \int_0^T \sum_{j=1}^K A_j \{\sin((\omega_k + \omega_{k'} + \omega_j)t + \phi_j) - \sin((\omega_k - \omega_{k'} + \omega_j)t + \phi_j) \\
&\quad - \sin((\omega_k - \omega_{k'} - \omega_j)t - \phi_j) + \sin((\omega_k + \omega_{k'} - \omega_j)t - \phi_j)\} dt \\
&= \frac{1}{4\kappa^2} \sum_{j=1}^K A_j \sin(\phi_j) \left\{-\delta_{j,k+k'} + \delta_{j,k-k'} - \delta_{j,k'-k}\right\},
\end{aligned}$$

where the last equation follows since the only way the last integral is nonzero asymptotically is when

$$\begin{aligned}\omega_k - \omega_{k'} + \omega_j &= 0 \\ \omega_k - \omega_{k'} - \omega_j &= 0 \\ \omega_k + \omega_{k'} - \omega_j &= 0.\end{aligned}$$

Likewise, we establish

$$\lim_{\mathrm{T}\to\infty} \mathrm{cov}\left\{\mathrm{V_k},\ \mathrm{X_{k'}}\right\} = \frac{1}{8\kappa^2}\sum_{j=1}^{K} A_j\cos(\phi_j)\left\{\delta_{j,k+k'} + \delta_{j,k-k'} + \delta_{j,k'-k}\right\} + \frac{B}{4\kappa^2}\delta_{k,k'}.$$

Since

$$\lim_{T\to\infty} \mathrm{cov}\left\{V_k,\ X_{k'}\right\} = \lim_{T\to\infty} \mathrm{cov}\left\{T^{-\frac{1}{2}}\int_0^T \cos(\omega_k s)dZ_G(s),\ T^{-\frac{3}{2}}\int_0^T t\cos(\omega_{k'}t)dZ_G(t)\right\}$$

$$\begin{aligned}&= \lim_{T\to\infty}\frac{1}{T^2}\int_0^T\int_0^T t\cos(\omega_k s)\cos(\omega_{k'}t)\mathrm{cov}\left\{dZ_G(s),\ dZ_G(t)\right\} \\ &= \lim_{T\to\infty}\frac{1}{T^2}[\int_0^T t\cos(\omega_k t)\cos(\omega_{k'}t)\mathrm{var}\left\{dZ_G(t)\right\} \\ &\quad +2\iint\limits_{\substack{0<s<T \\ 0<t\leq T-s}}(s+t)\cos(\omega_k s)\cos(\omega_{k'}(s+t))\mathrm{cov}\left\{dZ_G(s),\ dZ_G(s+t)\right\}],\end{aligned}$$

it then follows from the useful integral and trigonometric identity section of Appendix B, equations (B.66), (B.67), (B.81), (B.84), the assumption $\omega > 0$, and the

Chapter 2 Assumption 3 that

$$\lim_{T\to\infty} \operatorname{cov}\{V_k,\ X_{k'}\} = \lim_{T\to\infty} \frac{1}{T^2\kappa^2}\int_0^T t\cos(\omega_k t)\cos(\omega_{k'}t)\lambda_1(t)dt$$

$$\begin{aligned} &= \frac{1}{4T^2\kappa^2}\int_0^T \sum_{j=1}^K A_j t\{\cos((\omega_k+\omega_{k'}+\omega_j)t+\phi_j)+\cos((\omega_k-\omega_{k'}+\omega_j)t+\phi_j) \\ &\quad +\cos((\omega_k-\omega_{k'}-\omega_j)t-\phi_j)+\cos((\omega_k+\omega_{k'}-\omega_j)t-\phi_j)\}dt+\frac{B}{4\kappa^2}\delta_{k,k'} \\ &= \frac{1}{8\kappa^2}\sum_{j=1}^K A_j\cos(\phi_j)\left\{\delta_{j,k+k'}+\delta_{j,k-k'}+\delta_{j,k'-k}\right\}+\frac{B}{4\kappa^2}\delta_{k,k'}, \end{aligned}$$

where the last equation follows since the only way the last integral is nonzero asymptotically is when

$$\begin{aligned} \omega_k-\omega_{k'}+\omega_j &= 0 \\ \omega_k-\omega_{k'}-\omega_j &= 0 \\ \omega_k+\omega_{k'}-\omega_j &= 0. \end{aligned}$$

Likewise, we establish

$$\lim_{\mathrm{T}\to\infty} \operatorname{cov}\{\mathrm{V_k},\ \mathrm{Y_{k'}}\} = \frac{1}{8\kappa^2}\sum_{j=1}^K A_j\sin(\phi_j)\left\{-\delta_{j,\,k+k'}+\delta_{j,\,k-k'}-\delta_{j,\,k'-k}\right\}.$$

Since

$$\lim_{T\to\infty} \text{cov}\{V_k,\ Y_{k'}\} = \lim_{T\to\infty} \text{cov}\left\{T^{-\frac{1}{2}} \int_0^T \cos(\omega_k s) dZ_G(s),\ T^{-\frac{3}{2}} \int_0^T t\sin(\omega_{k'} t) dZ_G(t)\right\}$$

$$\begin{aligned}
&= \lim_{T\to\infty} \frac{1}{T^2} \int_0^T \int_0^T t\cos(\omega_k s)\sin(\omega_{k'} t)\text{cov}\{dZ_G(s),\ dZ_G(t)\} \\
&= \lim_{T\to\infty} \frac{1}{T^2}[\int_0^T t\cos(\omega_k t)\sin(\omega_{k'} t)\text{var}\{dZ_G(t)\} \\
&\quad +2 \int\int_{\substack{0<s<T \\ 0<t\leq T-s}} (s+t)\cos(\omega_k s)\sin(\omega_{k'}(s+t))\text{cov}\{dZ_G(s),\ dZ_G(s+t)\}],
\end{aligned}$$

it then follows from the useful integral and trigonometric identity section of Appendix B, equations (B.66), (B.67), (B.81), (B.84), the assumption $\omega > 0$, and the Chapter 2 Assumption 3 that

$$\lim_{T\to\infty} \text{cov}\{V_k,\ Y_{k'}\} = \lim_{T\to\infty} \frac{1}{T^2\kappa^2} \int_0^T t\cos(\omega_k t)\sin(\omega_{k'} t)\lambda_1(t)dt$$

$$\begin{aligned}
&= \frac{1}{4T^2\kappa^2} \int_0^T \sum_{j=1}^{K} A_j t\{\sin((\omega_k+\omega_{k'}+\omega_j)t+\phi_j) - \sin((\omega_k-\omega_{k'}+\omega_j)t+\phi_j) \\
&\quad -\sin((\omega_k-\omega_{k'}-\omega_j)t-\phi_j) + \sin((\omega_k+\omega_{k'}-\omega_j)t-\phi_j)\}dt \\
&= \frac{1}{8\kappa^2} \sum_{j=1}^{K} A_j \sin(\phi_j)\left\{-\delta_{j,\,k+k'} + \delta_{j,\,k-k'} - \delta_{j,\,k'-k}\right\},
\end{aligned}$$

where the last equation follows since the only way the last integral is nonzero asymptotically is when

$$\begin{aligned}\omega_k - \omega_{k'} + \omega_j &= 0\\ \omega_k - \omega_{k'} - \omega_j &= 0\\ \omega_k + \omega_{k'} - \omega_j &= 0.\end{aligned}$$

Likewise, we establish

$$\lim_{\mathrm{T}\to\infty} \mathrm{cov}\left\{\mathrm{W_k},\ \mathrm{W_{k'}}\right\} = \frac{1}{4\kappa^2}\sum_{j=1}^{K} A_j \cos(\phi_j)\left\{-\delta_{j,k'+k} + \delta_{j,k-k'} + \delta_{j,k'-k}\right\} + \frac{B}{2\kappa^2}\delta_{k,k'}.$$

Since

$$\begin{aligned}\lim_{T\to\infty} \mathrm{cov}\left\{W_k,\ W_{k'}\right\} &= \lim_{T\to\infty} \mathrm{cov}\left\{T^{-\frac{1}{2}}\int_0^T \sin(\omega_k s) dZ_G(s),\ T^{-\frac{1}{2}}\int_0^T \sin(\omega_{k'} t) dZ_G(t)\right\}\\ &= \lim_{T\to\infty}\frac{1}{T}\int_0^T\int_0^T \sin(\omega_k s)\sin(\omega_{k'} t)\mathrm{cov}\left\{dZ_G(s),\ dZ_G(t)\right\}\\ &= \lim_{T\to\infty}\frac{1}{T}[\int_0^T \sin(\omega_k t)\sin(\omega_{k'} t)\mathrm{var}\left\{dZ_G(t)\right\}\\ &\quad +2\iint\limits_{\substack{0<s<T\\ 0<t\leq T-s}} \sin(\omega_k s)\sin(\omega_{k'}(s+t))\mathrm{cov}\left\{dZ_G(s),\ dZ_G(s+t)\right\}],\end{aligned}$$

it then follows from the useful integral and trigonometric identity section of Appendix B, equations (B.66), (B.67), (B.81), (B.84), the assumption $\omega > 0$, and the Chapter

2 Assumption 3 that

$$\lim_{T\to\infty} \operatorname{cov}\{W_k,\ W_{k'}\} = \lim_{T\to\infty} \frac{1}{T\kappa^2}\int_0^T \sin(\omega_k t)\sin(\omega_{k'} t)\lambda_1(t)dt$$

$$\begin{aligned}
&= -\frac{1}{4T\kappa^2}\int_0^T \sum_{j=1}^{K} A_j\{\cos((\omega_k+\omega_{k'}+\omega_j)t+\phi_j) - \cos((\omega_k-\omega_{k'}+\omega_j)t+\phi_j) \\
&\quad - \cos((\omega_k-\omega_{k'}-\omega_j)t-\phi_j) + \cos((\omega_k+\omega_{k'}-\omega_j)t-\phi_j)\}dt + \frac{B}{2\kappa^2}\delta_{k,k'} \\
&= \frac{1}{4\kappa^2}\sum_{j=1}^{K} A_j\cos(\phi_j)\{-\delta_{j,k'+k}+\delta_{j,k-k'}+\delta_{j,k'-k}\} + \frac{B}{2\kappa^2}\delta_{k,k'},
\end{aligned}$$

where the last equation follows since the only way the last integral is nonzero asymptotically is when

$$\begin{aligned}
\omega_k - \omega_{k'} + \omega_j &= 0 \\
\omega_k - \omega_{k'} - \omega_j &= 0 \\
\omega_k + \omega_{k'} - \omega_j &= 0.
\end{aligned}$$

Likewise, we establish

$$\lim_{\mathrm{T}\to\infty} \operatorname{cov}\{\mathrm{W_k},\ \mathrm{X_{k'}}\} = \frac{1}{8\kappa^2}\sum_{j=1}^{K} A_j\sin(\phi_j)\{-\delta_{j,\,k+k'}+\delta_{j,\,k'-k}-\delta_{j,\,k-k'}\}.$$

Since

$$\lim_{T\to\infty} \text{cov}\left\{W_k,\ X_{k'}\right\} = \lim_{T\to\infty} \text{cov}\left\{T^{-\frac{1}{2}} \int_0^T \sin(\omega_k s) dZ_G(s),\ T^{-\frac{3}{2}} \int_0^T t\cos(\omega_{k'} t) dZ_G(t)\right\}$$

$$\begin{aligned}
&= \lim_{T\to\infty} \frac{1}{T^2} \int_0^T \int_0^T t\sin(\omega_k s)\cos(\omega_{k'} t)\text{cov}\left\{dZ_G(s),\ dZ_G(t)\right\} \\
&= \lim_{T\to\infty} \frac{1}{T^2} [\int_0^T t\sin(\omega_k t)\cos(\omega_{k'} t)\text{var}\left\{dZ_G(t)\right\} \\
&\quad +2 \int\int_{\substack{0<s<T \\ 0<t\leq T-s}} (s+t)\sin(\omega_k s)\cos(\omega_{k'}(s+t))\text{cov}\left\{dZ_G(s),\ dZ_G(s+t)\right\}],
\end{aligned}$$

it then follows from the useful integral and trigonometric identity section of Appendix B, equations (B.66), (B.67), (B.81), (B.84), the assumption $\omega > 0$, and the Chapter 2 Assumption 3 that

$$\begin{aligned}
\lim_{T\to\infty} \text{cov}\left\{W_k,\ X_{k'}\right\} &= \lim_{T\to\infty} \frac{1}{T^2\kappa^2} \int_0^T t\sin(\omega_k t)\cos(\omega_{k'} t)\lambda_1(t)dt \\
&= \frac{1}{8\kappa^2} \sum_{j=1}^{K} A_j \sin(\phi_j)\left\{-\delta_{j,\ k+k'} + \delta_{j,\ k'-k} - \delta_{j,\ k-k'}\right\}.
\end{aligned}$$

Likewise, we establish

$$\lim_{\mathrm{T}\to\infty} \text{cov}\left\{\mathrm{W_k},\ \mathrm{Y_{k'}}\right\} = \frac{1}{8\kappa^2} \sum_{j=1}^{K} A_j \cos(\phi_j)\left\{-\delta_{j,\ k+k'} + \delta_{j,\ k-k'} + \delta_{j,\ k'-k}\right\} + \frac{B}{4\kappa^2}\delta_{k,\ k'}.$$

Since

$$\lim_{T\to\infty} \text{cov}\left\{W_k,\ Y_{k'}\right\} = \lim_{T\to\infty} \text{cov}\left\{T^{-\frac{1}{2}}\int_0^T \sin(\omega_k s)dZ_G(s),\ T^{-\frac{3}{2}}\int_0^T t\sin(\omega_{k'}t)dZ_G(t)\right\}$$

$$\begin{aligned}
&= \lim_{T\to\infty}\frac{1}{T^2}\int_0^T\int_0^T t\sin(\omega_k s)\sin(\omega_{k'}t)\text{cov}\left\{dZ_G(s),\ dZ_G(t)\right\} \\
&= \lim_{T\to\infty}\frac{1}{T^2}[\int_0^T t\sin(\omega_k t)\sin(\omega_{k'}t)\text{var}\left\{dZ_G(t)\right\} \\
&\quad +2\int\!\!\int_{\substack{0<s<T \\ 0<t\leq T-s}}(s+t)\sin(\omega_k s)\sin(\omega_{k'}(s+t))\text{cov}\left\{dZ_G(s),\ dZ_G(s+t)\right\}],
\end{aligned}$$

it then follows from the useful integral and trigonometric identity section of Appendix B, equations (B.66), (B.67), (B.81), (B.84), the assumption $\omega > 0$, and the Chapter 2 Assumption 3 that

$$\begin{aligned}
\lim_{T\to\infty} \text{cov}\left\{W_k,\ Y_{k'}\right\} &= \lim_{T\to\infty}\frac{1}{T^2\kappa^2}\int_0^T t\sin(\omega_k t)\sin(\omega_{k'}t)\lambda_1(t)dt \\
&= \frac{1}{8\kappa^2}\sum_{j=1}^{K}A_j\cos(\phi_j)\left\{-\delta_{j,\ k+k'}+\delta_{j,\ k-k'}+\delta_{j,\ k'-k}\right\}+\frac{B}{4\kappa^2}\delta_{k,\ k'}.
\end{aligned}$$

Likewise, we establish

$$\lim_{\mathrm{T}\to\infty} \text{cov}\left\{\mathrm{X_k},\ \mathrm{X_{k'}}\right\} = \frac{1}{12\kappa^2}\sum_{j=1}^{K}A_j\cos(\phi_j)\left\{\delta_{j,\ k+k'}+\delta_{j,\ k-k'}+\delta_{j,\ k'-k}\right\}+\frac{B}{6\kappa^2}\delta_{k,k'}.$$

Since

$$\lim_{T\to\infty} \operatorname{cov}\{X_k,\ X_{k'}\} = \lim_{T\to\infty} \operatorname{cov}\left\{T^{-\frac{3}{2}} \int_0^T s\cos(\omega_k s)dZ_G(s),\ T^{-\frac{3}{2}} \int_0^T t\cos(\omega_{k'} t)dZ_G(t)\right\}$$

$$\begin{aligned}
&= \lim_{T\to\infty} \frac{1}{T^3} \int_0^T \int_0^T st\cos(\omega_k s)\cos(\omega_{k'} t)\operatorname{cov}\{dZ_G(s),\ dZ_G(t)\} \\
&= \lim_{T\to\infty} \frac{1}{T^3}[\int_0^T t^2\cos(\omega_k t)\cos(\omega_{k'} t)\operatorname{var}\{dZ_G(t)\} \\
&\quad +2 \iint\limits_{\substack{0<s<T \\ 0<t\leq T-s}} s(s+t)\cos(\omega_k s)\cos(\omega_{k'}(s+t))\operatorname{cov}\{dZ_G(s),\ dZ_G(s+t)\}],
\end{aligned}$$

it then follows from the useful integral and trigonometric identity section of Appendix B, equations (B.66), (B.67), (B.81), (B.84), the assumption $\omega > 0$, and the Chapter 2 Assumption 3 that

$$\begin{aligned}
\lim_{T\to\infty} \operatorname{cov}\{X_k,\ X_{k'}\} &= \lim_{T\to\infty} \frac{1}{T^3\kappa^2} \int_0^T t^2\cos(\omega_k t)\cos(\omega_{k'} t)\lambda_1(t)dt \\
&= \frac{1}{12\kappa^2} \sum_{j=1}^{K} A_j\cos(\phi_j)\{\delta_{j,\ k+k'} + \delta_{j,\ k-k'} + \delta_{j,\ k'-k}\} + \frac{B}{6\kappa^2}\delta_{k,k'}.
\end{aligned}$$

Likewise, we establish

$$\lim_{\mathrm{T}\to\infty} \operatorname{cov}\{\mathrm{X_k},\ \mathrm{Y_{k'}}\} = \frac{1}{12\kappa^2} \sum_{j=1}^{K} A_j\sin(\phi_j)\{-\delta_{j,\ k+k'} + \delta_{j,\ k-k'} - \delta_{j,\ k'-k}\}.$$

Since

$$\lim_{T\to\infty} \operatorname{cov}\{X_k,\ Y_{k'}\} = \lim_{T\to\infty} \operatorname{cov}\left\{T^{-\frac{3}{2}}\int_0^T s\cos(\omega_k s)dZ_G(s),\ T^{-\frac{3}{2}}\int_0^T t\sin(\omega_{k'} t)dZ_G(t)\right\}$$

$$\begin{aligned}
&= \lim_{T\to\infty} \frac{1}{T^3}\int_0^T\int_0^T st\cos(\omega_k s)\sin(\omega_{k'} t)\operatorname{cov}\{dZ_G(s),\ dZ_G(t)\} \\
&= \lim_{T\to\infty} \frac{1}{T^3}[\int_0^T t^2\cos(\omega_k t)\sin(\omega_{k'} t)\operatorname{var}\{dZ_G(t)\} \\
&\quad +2\iint\limits_{\substack{0<s<T \\ 0<t\le T-s}} s(s+t)\cos(\omega_k s)\sin(\omega_{k'}(s+t))\operatorname{cov}\{dZ_G(s),\ dZ_G(s+t)\}],
\end{aligned}$$

it then follows from the useful integral and trigonometric identity section of Appendix B, equations (B.66), (B.67), (B.81), (B.84), the assumption $\omega > 0$, and the Chapter 2 Assumption 3 that

$$\begin{aligned}
\lim_{T\to\infty} \operatorname{cov}\{X_k,\ Y_{k'}\} &= \lim_{T\to\infty} \frac{1}{T^3\kappa^2}\int_0^T t^2\cos(\omega_k t)\sin(\omega_{k'} t)\lambda_1(t)dt \\
&= \frac{1}{12\kappa^2}\sum_{j=1}^K A_j\sin(\phi_j)\left\{-\delta_{j,\ k+k'} + \delta_{j,\ k-k'} - \delta_{j,\ k'-k}\right\}.
\end{aligned}$$

Likewise, we establish

$$\lim_{\mathrm{T}\to\infty} \operatorname{cov}\{\mathrm{Y_k},\ \mathrm{Y_{k'}}\} = \frac{1}{12\kappa^2}\sum_{j=1}^K A_j\cos(\phi_j)\left\{-\delta_{j,\ k+k'} + \delta_{j,\ k-k'} + \delta_{j,\ k'-k}\right\} + \frac{B}{6\kappa^2}\delta_{k,k'}.$$

Since

$$\lim_{T\to\infty} \operatorname{cov}\left\{Y_k,\ Y_{k'}\right\} = \lim_{T\to\infty} \operatorname{cov}\left\{T^{-\frac{3}{2}} \int_0^T s\sin(\omega_k s)dZ_G(s),\ T^{-\frac{3}{2}} \int_0^T t\sin(\omega_{k'} t)dZ_G(t)\right\}$$

$$\begin{aligned}
&= \lim_{T\to\infty} \frac{1}{T^3} \int_0^T \int_0^T st\sin(\omega_k s)\sin(\omega_{k'} t)\operatorname{cov}\left\{dZ_G(s),\ dZ_G(t)\right\} \\
&= \lim_{T\to\infty} \frac{1}{T^3}[\int_0^T t^2\sin(\omega_k t)\sin(\omega_{k'} t)\operatorname{var}\left\{dZ_G(t)\right\} \\
&\quad +2 \int\int_{\substack{0<s<T \\ 0<t\leq T-s}} s(s+t)\sin(\omega_k s)\sin(\omega_{k'}(s+t))\operatorname{cov}\left\{dZ_G(s),\ dZ_G(s+t)\right\}],
\end{aligned}$$

it then follows from the useful integral and trigonometric identity section of Appendix B, equations (B.66), (B.67), (B.81), (B.84), the assumption $\omega > 0$, and the Chapter 2 Assumption 3 that

$$\begin{aligned}
\lim_{T\to\infty} \operatorname{cov}\left\{Y_k,\ Y_{k'}\right\} &= \lim_{T\to\infty} \frac{1}{T^3\kappa^2} \int_0^T t^2\sin(\omega_k t)\sin(\omega_{k'} t)\lambda_1(t)dt \\
&= \frac{1}{12\kappa^2}\sum_{j=1}^{K} A_j\cos(\phi_j)\left\{-\delta_{j,\,k+k'} + \delta_{j,\,k-k'} + \delta_{j,\,k'-k}\right\} + \frac{B}{6\kappa^2}\delta_{k,k'}.
\end{aligned}$$

□

B.1.1.4 Proof of Equations (2.10), (2.11), and (2.16)

Proof. Here we establish equations (2.10), (2.11), and (2.16). We first establish equation (2.16), then equation (2.10), and conclude with equation (2.11). To establish equation (2.16), we begin by expanding the Bartlett Periodogram,

$$
\begin{aligned}
I_T(\omega) =& \frac{1}{2\pi T}\left|\int_0^T e^{-i\omega t} dN_G(t)\right|^2 \\
=& \frac{1}{2\pi T}\left\{\left[\int_0^T \cos(\omega t) dN_G(t)\right]^2 + \left[\int_0^T \sin(\omega t) dN_G(t)\right]^2\right\},
\end{aligned} \tag{B.85}
$$

where $\omega > 0$. Next, we take the first two derivatives, with respect to ω, of the Bartlett Periodogram components,

$$
\left[\int_0^T \cos(\omega t) dN_G(t)\right]^2 \quad \text{and} \quad \left[\int_0^T \sin(\omega t) dN_G(t)\right]^2,
$$

and we notice that

$$
\frac{d}{d\omega}\left[\int_0^T \cos(\omega t) dN_G(t)\right]^2 = -2\int_0^T \cos(\omega t) dN_G(t)\int_0^T t\sin(\omega t) dN_G(t), \tag{B.86}
$$

$$
\begin{aligned}
\frac{d^2}{d\omega^2}\left[\int_0^T \cos(\omega t) dN_G(t)\right]^2 &= -2\frac{d}{d\omega}\int_0^T \cos(\omega t) dN_G(t)\int_0^T t\sin(\omega t) dN_G(t) \\
&= -2\{-\int_0^T t\sin(\omega t) dN_G(t)\int_0^T t\sin(\omega t) dN_G(t) \\
&+ \int_0^T \cos(\omega t) dN_G(t)\int_0^T t^2\cos(\omega t) dN_G(t)\}
\end{aligned}
$$

$$
\begin{aligned}
&= -2\{-\left[\int_0^T t\sin(\omega t)dN_G(t)\right]^2 \\
&\quad + \int_0^T \cos(\omega t)dN_G(t)\int_0^T t^2\cos(\omega t)dN_G(t)\} \\
&= 2\{\left[\int_0^T t\sin(\omega t)dN_G(t)\right]^2 \\
&\quad - \int_0^T \cos(\omega t)dN_G(t)\int_0^T t^2\cos(\omega t)dN_G(t)\}, \qquad \text{(B.87)}
\end{aligned}
$$

$$
\frac{d}{d\omega}\left[\int_0^T \sin(\omega t)dN_G(t)\right]^2 = 2\int_0^T \sin(\omega t)dN_G(t)\int_0^T t\cos(\omega t)dN_G(t), \qquad \text{(B.88)}
$$

and

$$
\begin{aligned}
\frac{d^2}{d\omega^2}\left[\int_0^T \sin(\omega t)dN_G(t)\right]^2 &= 2\{\int_0^T t\cos(\omega t)dN_G(t)\int_0^T t\cos(\omega t)dN_G(t) \\
&\quad - \int_0^T \sin(\omega t)dN_G(t)\int_0^T t^2\sin(\omega t)dN_G(t)\} \\
&= 2\{\left[\int_0^T t\cos(\omega t)dN_G(t)\right]^2 \\
&\quad - \int_0^T \sin(\omega t)dN_G(t)\int_0^T t^2\sin(\omega t)dN_G(t)\}. \qquad \text{(B.89)}
\end{aligned}
$$

Using the decomposition defined in equation (2.4), equation (B.85) can be re-expressed as

$$
\begin{aligned}
2\pi T I_T(\omega) &= \left[\int_0^T \cos(\omega t) dN_G(t)\right]^2 + \left[\int_0^T \sin(\omega t) dN_G(t)\right]^2 \\
&= \left[\int_0^T \cos(\omega t) E\left[dN_G(t)\right] + \int_0^T \cos(\omega t) dZ_G(t)\right]^2 \\
&+ \left[\int_0^T \sin(\omega t) E\left[dN_G(t)\right] + \int_0^T \sin(\omega t) dZ_G(t)\right]^2
\end{aligned}
$$

$$
\begin{aligned}
= \; & \left[\int_0^T \cos(\omega t) E\left[dN_G(t)\right]\right]^2 + 2\int_0^T \cos(\omega t) E\left[dN_G(t)\right] \int_0^T \cos(\omega t) dZ_G(t) \\
& + \left[\int_0^T \cos(\omega t) dZ_G(t)\right]^2 + \left[\int_0^T \sin(\omega t) E\left[dN_G(t)\right]\right]^2 \\
& + 2\int_0^T \sin(\omega t) E\left[dN_G(t)\right] \int_0^T \sin(\omega t) dZ_G(t) + \left[\int_0^T \sin(\omega t) dZ_G(t)\right]^2, \quad \text{(B.90)}
\end{aligned}
$$

and using the notation of equation (2.7), we have

$$
\begin{aligned}
2\pi T I_T(\omega_k) \; = \; & \left[\int_0^T \cos(\omega_k t) E\left[dN_G(t)\right]\right]^2 + 2\int_0^T \cos(\omega_k t) E\left[dN_G(t)\right] \left(T^{\frac{1}{2}} V_k\right) \\
& + \left[T^{\frac{1}{2}} V_k\right]^2 + \left[\int_0^T \sin(\omega_k t) E\left[dN_G(t)\right]\right]^2 \\
& + 2\int_0^T \sin(\omega_k t) E\left[dN_G(t)\right] \left(T^{\frac{1}{2}} W_k\right) + \left[T^{\frac{1}{2}} W_k\right]^2. \quad \text{(B.91)}
\end{aligned}
$$

Therefore, it follows that

$$
\begin{aligned}
2\pi\frac{I_T(\omega_k)}{T} &= \frac{1}{T^2}\left[\int_0^T \cos(\omega_k t)E\left[dN_G(t)\right]\right]^2 + 2\frac{1}{T^2}\int_0^T \cos(\omega_k t)E\left[dN_G(t)\right]\left(T^{\frac{1}{2}}V_k\right) \\
&\quad + \left[T^{-\frac{1}{2}}V_k\right]^2 \\
&\quad + \frac{1}{T^2}\left[\int_0^T \sin(\omega_k t)E\left[dN_G(t)\right]\right]^2 + 2\frac{1}{T^2}\int_0^T \sin(\omega_k t)E\left[dN_G(t)\right]\left(T^{\frac{1}{2}}W_k\right) \\
&\quad + \left[T^{-\frac{1}{2}}W_k\right]^2 \\
&= \left[\frac{1}{T}\int_0^T \cos(\omega_k t)E\left[dN_G(t)\right]\right]^2 + 2\frac{1}{T}\int_0^T \cos(\omega_k t)E\left[dN_G(t)\right]\left(T^{-\frac{1}{2}}V_k\right) \\
&\quad + \left[T^{-\frac{1}{2}}V_k\right]^2 \\
&\quad + \left[\frac{1}{T}\int_0^T \sin(\omega_k t)E\left[dN_G(t)\right]\right]^2 + 2\frac{1}{T}\int_0^T \sin(\omega_k t)E\left[dN_G(t)\right]\left(T^{-\frac{1}{2}}W_k\right) \\
&\quad + \left[T^{-\frac{1}{2}}W_k\right]^2. \qquad \text{(B.92)}
\end{aligned}
$$

And since for $t > 0$, $E\left[dN_G(t)\right] = \lambda_2(t)dt + o(dt)$ and equation (1.36) implies that $\lambda_2(t) = \frac{1}{\kappa}\lambda_1(t) + O\left(\lambda_1(t)\exp\left\{-a\Lambda_1(t)\right\}\right)$, it then follows from the useful integral section of Appendix B that

$$
\begin{aligned}
2\pi\frac{I_T(\omega_k)}{T} = &\left[\frac{A_k}{2\kappa}\cos(\phi_k) + o(1)\right]^2 + 2\left[\frac{A_k}{2\kappa}\cos(\phi_k) + o(1)\right]\left(T^{-\frac{1}{2}}V_k\right) \\
&+ \left[T^{-\frac{1}{2}}V_k\right]^2 \\
&+ \left[-\frac{A_k}{2\kappa}\sin(\phi_k) + o(1)\right]^2 + 2\left[-\frac{A_k}{2\kappa}\sin(\phi_k) + o(1)\right]\left(T^{-\frac{1}{2}}W_k\right) \\
&+ \left[T^{-\frac{1}{2}}W_k\right]^2
\end{aligned}
$$

$$
\begin{aligned}
&= \frac{A_k^2}{4\kappa^2} + \frac{A_k}{\kappa}\cos(\phi_k)\left(T^{-\frac{1}{2}}V_k\right) - \frac{A_k}{\kappa}\sin(\phi_k)\left(T^{-\frac{1}{2}}W_k\right) + \left[T^{-\frac{1}{2}}V_k\right]^2 \\
&\quad + \left[T^{-\frac{1}{2}}W_k\right]^2 + o(1),
\end{aligned} \tag{B.93}
$$

and from the Chapter 2 Lemma 8, we conclude that

$$
\frac{I_T(\omega_k)}{T} = \frac{A_k^2}{8\pi\kappa^2} + \frac{A_k}{2\pi\kappa}\cos(\phi_k)\left(T^{-\frac{1}{2}}V_k\right) - \frac{A_k}{2\pi\kappa}\sin(\phi_k)\left(T^{-\frac{1}{2}}W_k\right) + o(1), \tag{B.94}
$$

which establishes equation (2.16).

Next, we establish equation (2.10). From equations (B.85)-(B.89), we notice that

$$
\begin{aligned}
2\pi T\frac{d}{d\omega}I_T(\omega) &= -2\left[\int_0^T \cos(\omega t)dN_G(t)\right]\left[\int_0^T t\sin(\omega t)dN_G(t)\right] \\
&\quad +2\left[\int_0^T \sin(\omega t)dN_G(t)\right]\left[\int_0^T t\cos(\omega t)dN_G(t)\right] \\
&= 2\{\left[\int_0^T \sin(\omega t)dN_G(t)\right]\left[\int_0^T t\cos(\omega t)dN_G(t)\right] \\
&\quad -\left[\int_0^T \cos(\omega t)dN_G(t)\right]\left[\int_0^T t\sin(\omega t)dN_G(t)\right]\} \\
&= 2\{\left[\int_0^T \sin(\omega t)E\left[dN_G(t)\right] + \int_0^T \sin(\omega t)dZ_G(t)\right] \\
&\quad \times\left[\int_0^T t\cos(\omega t)E\left[dN_G(t)\right] + \int_0^T t\cos(\omega t)dZ_G(t)\right] \\
&\quad -\left[\int_0^T \cos(\omega t)E\left[dN_G(t)\right] + \int_0^T \cos(\omega t)dZ_G(t)\right] \\
&\quad \times\left[\int_0^T t\sin(\omega t)E\left[dN_G(t)\right] + \int_0^T t\sin(\omega t)dZ_G(t)\right]\}
\end{aligned}
$$

$$
\begin{aligned}
= \quad & 2\{[\int_0^T \sin(\omega t) E\left[dN_G(t)\right] \int_0^T t\cos(\omega t) E\left[dN_G(t)\right] \\
& + \int_0^T \sin(\omega t) E\left[dN_G(t)\right] \int_0^T t\cos(\omega t) dZ_G(t)] \\
& +[\int_0^T \sin(\omega t) dZ_G(t) \int_0^T t\cos(\omega t) E\left[dN_G(t)\right] \\
& + \int_0^T \sin(\omega t) dZ_G(t) \int_0^T t\cos(\omega t) dZ_G(t)] \\
& -[\int_0^T \cos(\omega t) E\left[dN_G(t)\right] \int_0^T t\sin(\omega t) E\left[dN_G(t)\right] \\
& + \int_0^T \cos(\omega t) E\left[dN_G(t)\right] \int_0^T t\sin(\omega t) dZ_G(t)] \\
& -[\int_0^T \cos(\omega t) dZ_G(t) \int_0^T t\sin(\omega t) E\left[dN_G(t)\right] \\
& + \int_0^T \cos(\omega t) dZ_G(t) \int_0^T t\sin(\omega t) dZ_G(t)]\}. \qquad \text{(B.95)}
\end{aligned}
$$

Therefore, in the notation of equation (2.7), it follows that

$$
\begin{aligned}
2\pi T \tfrac{d}{d\omega} I_T(\omega)|_{\omega=\omega_k} = \quad & 2\{\int_0^T \sin(\omega_k t) E\left[dN_G(t)\right] \int_0^T t\cos(\omega_k t) E\left[dN_G(t)\right] \\
& + \int_0^T \sin(\omega_k t) E\left[dN_G(t)\right] \left(T^{\frac{3}{2}} X_k\right) \\
& + \left(T^{\frac{1}{2}} W_k\right) \int_0^T t\cos(\omega_k t) E\left[dN_G(t)\right] + \left(T^{\frac{1}{2}} W_k\right) \left(T^{\frac{3}{2}} X_k\right) \\
& - \int_0^T \cos(\omega_k t) E\left[dN_G(t)\right] \int_0^T t\sin(\omega_k t) E\left[dN_G(t)\right] \\
& - \int_0^T \cos(\omega_k t) E\left[dN_G(t)\right] \left(T^{\frac{3}{2}} Y_k\right) \\
& - \left(T^{\frac{1}{2}} V_k\right) \int_0^T t\sin(\omega_k t) E\left[dN_G(t)\right] - \left(T^{\frac{1}{2}} V_k\right) \left(T^{\frac{3}{2}} Y_k\right)\}. \quad \text{(B.96)}
\end{aligned}
$$

After grouping like terms together and using equation (1.36), we conclude that

$$\begin{aligned}
2\pi T\frac{d}{d\omega}I_T(\omega)|_{\omega=\omega_k} =2\{&\int_0^T \sin(\omega_k t)E\left[dN_G(t)\right]\int_0^T t\cos(\omega_k t)E\left[dN_G(t)\right]\\
&-\int_0^T \cos(\omega_k t)E\left[dN_G(t)\right]\int_0^T t\sin(\omega_k t)E\left[dN_G(t)\right]\\
&+\int_0^T \sin(\omega_k t)E\left[dN_G(t)\right]\left(T^{\frac{3}{2}}X_k\right)\\
&-\int_0^T \cos(\omega_k t)E\left[dN_G(t)\right]\left(T^{\frac{3}{2}}Y_k\right)\\
&+\left(T^{\frac{1}{2}}W_k\right)\int_0^T t\cos(\omega t)E\left[dN_G(t)\right]\\
&-\left(T^{\frac{1}{2}}V_k\right)\int_0^T t\sin(\omega t)E\left[dN_G(t)\right]\\
&+\left(T^{\frac{1}{2}}W_k\right)\left(T^{\frac{3}{2}}X_k\right)-\left(T^{\frac{1}{2}}V_k\right)\left(T^{\frac{3}{2}}Y_k\right)\}
\end{aligned}$$

$$\begin{aligned}
= \quad & 2\{\left[-T\frac{A_k}{2\kappa}\sin(\phi_k)+To(1)\right]\left[T^2\frac{A_k}{4\kappa}\cos(\phi_k)+T^2o(1)\right]\\
&-\left[T\frac{A_k}{2\kappa}\cos(\phi_k)+To(1)\right]\left[-T^2\frac{A_k}{4\kappa}\sin(\phi_k)+T^2o(1)\right]\\
&+\left[-T\frac{A_k}{2\kappa}\sin(\phi_k)+To(1)\right]\left(T^{\frac{3}{2}}X_k\right)-\left[T\frac{A_k}{2\kappa}\cos(\phi_k)+To(1)\right]\left(T^{\frac{3}{2}}Y_k\right)\\
&+\left(T^{\frac{1}{2}}W_k\right)\left[T^2\frac{A_k}{4\kappa}\cos(\phi_k)+T^2o(1)\right]\\
&-\left(T^{\frac{1}{2}}V_k\right)\left[-T^2\frac{A_k}{4\kappa}\sin(\phi_k)+T^2o(1)\right]\\
&+\left(T^{\frac{1}{2}}W_k\right)\left(T^{\frac{3}{2}}X_k\right)-\left(T^{\frac{1}{2}}V_k\right)\left(T^{\frac{3}{2}}Y_k\right)\}. \qquad \text{(B.97)}
\end{aligned}$$

Therefore, we have

$$
\begin{aligned}
2\pi T^{-\frac{3}{2}} I_T'(\omega_k) = 2\{ & T^{\frac{1}{2}} \left[-\frac{A_k}{2\kappa}\sin(\phi_k) + o(1) \right] \left[\frac{A_k}{4\kappa}\cos(\phi_k) + o(1) \right] \\
& - T^{\frac{1}{2}} \left[\frac{A_k}{2\kappa}\cos(\phi_k) + o(1) \right] \left[-\frac{A_k}{4\kappa}\sin(\phi_k) + o(1) \right] \\
& + \left[-\frac{A_k}{2\kappa}\sin(\phi_k) + o(1) \right] (X_k) - \left[\frac{A_k}{2\kappa}\cos(\phi_k) + o(1) \right] (Y_k) \\
& + (W_k) \left[\frac{A_k}{4\kappa}\cos(\phi_k) + o(1) \right] - (V_k) \left[-\frac{A_k}{4\kappa}\sin(\phi_k) + o(1) \right] \\
& + T^{-\frac{1}{2}} (W_k)(X_k) - T^{-\frac{1}{2}} (V_k)(Y_k)\} \\
=2\{ & \left[-\frac{A_k}{2\kappa}\sin(\phi_k) + o(1) \right] X_k - \left[\frac{A_k}{2\kappa}\cos(\phi_k) + o(1) \right] Y_k \\
& + W_k \left[\frac{A_k}{4\kappa}\cos(\phi_k) + o(1) \right] - V_k \left[-\frac{A_k}{4\kappa}\sin(\phi_k) + o(1) \right] \\
& + T^{-\frac{1}{2}} (W_k)(X_k) - T^{-\frac{1}{2}} (V_k)(Y_k)\}
\end{aligned}
$$

$$
\begin{aligned}
= \quad & 2\left\{ -\frac{A_k}{2\kappa}\sin(\phi_k)X_k - \frac{A_k}{2\kappa}\cos(\phi_k)Y_k + W_k\frac{A_k}{4\kappa}\cos(\phi_k) + V_k\frac{A_k}{4\kappa}\sin(\phi_k) \right\} \\
& +o(1) \\
= \quad & \frac{A_k}{\kappa}\left\{ V_k\frac{1}{2}\sin(\phi_k) + W_k\frac{1}{2}\cos(\phi_k) - X_k\sin(\phi_k) - Y_k\cos(\phi_k) \right\} \\
& +o(1), \qquad \text{(B.98)}
\end{aligned}
$$

which establishes equation (2.10).

Next, we establish equation (2.11). From equations (B.85)-(B.89), we notice that

$$
\begin{aligned}
2\pi T I_T''(\omega) = {} & 2\left\{\left[\int_0^T t\sin(\omega t)dN_G(t)\right]^2 - \left[\int_0^T \cos(\omega t)dN_G(t)\right]\left[\int_0^T t^2\cos(\omega t)dN_G(t)\right]\right\} \\
& + 2\left\{\left[\int_0^T t\cos(\omega t)dN_G(t)\right]^2 - \left[\int_0^T \sin(\omega t)dN_G(t)\right]\left[\int_0^T t^2\sin(\omega t)dN_G(t)\right]\right\} \\
& = 2\{\left[\int_0^T t\sin(\omega t)dN_G(t)\right]^2 + \left[\int_0^T t\cos(\omega t)dN_G(t)\right]^2\} \\
& - 2\{\left[\int_0^T \cos(\omega t)dN_G(t)\right]\left[\int_0^T t^2\cos(\omega t)dN_G(t)\right] \\
& + \left[\int_0^T \sin(\omega t)dN_G(t)\right]\left[\int_0^T t^2\sin(\omega t)dN_G(t)\right]\} \\
= & 2\{\left[\int_0^T t\sin(\omega t)E\left[dN_G(t)\right] + \int_0^T t\sin(\omega t)dZ_G(t)\right]^2 \\
& + \left[\int_0^T t\cos(\omega t)E\left[dN_G(t)\right] + \int_0^T t\cos(\omega t)dZ_G(t)\right]^2\} \\
& - 2\{\left[\int_0^T \cos(\omega t)E\left[dN_G(t)\right] + \int_0^T \cos(\omega t)dZ_G(t)\right] \\
& \times \left[\int_0^T t^2\cos(\omega t)E\left[dN_G(t)\right] + \int_0^T t^2\cos(\omega t)dZ_G(t)\right]\} \\
& - 2\{\left[\int_0^T \sin(\omega t)E\left[dN_G(t)\right] + \int_0^T \sin(\omega t)dZ_G(t)\right] \\
& \times \left[\int_0^T t^2\sin(\omega t)E\left[dN_G(t)\right] + \int_0^T t^2\sin(\omega t)dZ_G(t)\right]\}
\end{aligned}
$$

$$
\begin{aligned}
= & 2\{\left[\int_0^T t\sin(\omega t)E\left[dN_G(t)\right]\right]^2 \\
& + 2\int_0^T t\sin(\omega t)E\left[dN_G(t)\right]\int_0^T t\sin(\omega t)dZ_G(t) + \left[\int_0^T t\sin(\omega t)dZ_G(t)\right]^2\}
\end{aligned}
$$

$$
\begin{aligned}
&+ 2\{\left[\int_0^T t\cos(\omega t)E\left[dN_G(t)\right]\right]^2 \\
&+ 2\int_0^T t\cos(\omega t)E\left[dN_G(t)\right]\int_0^T t\cos(\omega t)dZ_G(t) \\
&+ \left[\int_0^T t\cos(\omega t)dZ_G(t)\right]^2\} \\
&- 2\{\int_0^T \cos(\omega t)E\left[dN_G(t)\right]\int_0^T t^2\cos(\omega t)E\left[dN_G(t)\right] \\
&+ \int_0^T \cos(\omega t)dZ_G(t)\int_0^T t^2\cos(\omega t)E\left[dN_G(t)\right]\} \\
&- 2\{\int_0^T \cos(\omega t)E\left[dN_G(t)\right]\int_0^T t^2\cos(\omega t)dZ_G(t) \\
&+ \int_0^T \cos(\omega t)dZ_G(t)\int_0^T t^2\cos(\omega t)dZ_G(t)\}
\end{aligned}
$$

$$
\begin{aligned}
&-2\{\int_0^T \sin(\omega t)E\left[dN_G(t)\right]\int_0^T t^2\sin(\omega t)E\left[dN_G(t)\right] \\
&+ \int_0^T \sin(\omega t)dZ_G(t)\int_0^T t^2\sin(\omega t)E\left[dN_G(t)\right]\} \\
&-2\{\int_0^T \sin(\omega t)E\left[dN_G(t)\right]\int_0^T t^2\sin(\omega t)dZ_G(t) \\
&+ \int_0^T \sin(\omega t)dZ_G(t)\int_0^T t^2\sin(\omega t)dZ_G(t)\}. \qquad \text{(B.99)}
\end{aligned}
$$

Hence, from equations (1.36) and (2.7), and the Chapter 2 Lemma 8, we conclude that

$$2\pi T I_T''(\omega_k) = 2\{\left[\int_0^T t\sin(\omega_k t)E\left[dN_G(t)\right]\right]^2 + 2\int_0^T t\sin(\omega_k t)E\left[dN_G(t)\right]\left(T^{\frac{3}{2}}Y_k\right) + \left[T^{\frac{3}{2}}Y_k\right]^2\}$$

$$+ 2\left\{\left[\int_0^T t\cos(\omega_k t)E\left[dN_G(t)\right]\right]^2 + 2\int_0^T t\cos(\omega_k t)E\left[dN_G(t)\right]\left(T^{\frac{3}{2}}X_k\right) + \left[T^{\frac{3}{2}}X_k\right]^2\right\}$$
$$- 2\left\{\int_0^T \cos(\omega_k t)E\left[dN_G(t)\right]\int_0^T t^2\cos(\omega_k t)E\left[dN_G(t)\right] + \left(T^{\frac{1}{2}}V_k\right)\int_0^T t^2\cos(\omega_k t)E\left[dN_G(t)\right]\right\}$$
$$- 2\left\{\int_0^T \cos(\omega_k t)E\left[dN_G(t)\right]\int_0^T t^2\cos(\omega_k t)dZ_G(t) + \left(T^{\frac{1}{2}}V_k\right)\int_0^T t^2\cos(\omega_k t)dZ_G(t)\right\}$$
$$- 2\left\{\int_0^T \sin(\omega_k t)E\left[dN_G(t)\right]\int_0^T t^2\sin(\omega_k t)E\left[dN_G(t)\right] + \left(T^{\frac{1}{2}}W_k\right)\int_0^T t^2\sin(\omega_k t)E\left[dN_G(t)\right]\right\}$$
$$- 2\left\{\int_0^T \sin(\omega_k t)E\left[dN_G(t)\right]\int_0^T t^2\sin(\omega_k t)dZ_G(t) + \left(T^{\frac{1}{2}}W_k\right)\int_0^T t^2\sin(\omega_k t)dZ_G(t)\right\}$$

$$= 2\{\left[-T^2\frac{A_k}{4\kappa}\sin(\phi_k) + T^2 o(1)\right]^2$$
$$+ 2\left[-T^2\frac{A_k}{4\kappa}\sin(\phi_k) + T^2 o(1)\right]\left(T^{\frac{3}{2}}Y_k\right) + \left[T^{\frac{3}{2}}Y_k\right]^2\}$$
$$+ 2\{\left[T^2\frac{A_k}{4\kappa}\cos(\phi_k) + T^2 o(1)\right]^2$$
$$+ 2\left[T^2\frac{A_k}{4\kappa}\cos(\phi_k) + T^2 o(1)\right]\left(T^{\frac{3}{2}}X_k\right) + \left[T^{\frac{3}{2}}X_k\right]^2\}$$
$$- 2\{\left[T\frac{A_k}{2\kappa}\cos(\phi_k) + T o(1)\right]\left[T^3\frac{A_k}{6\kappa}\cos(\phi_k) + T^3 o(1)\right]$$

$$
\begin{aligned}
&+\left(T^{\frac{1}{2}}V_k\right)\left[T^3\frac{A_k}{6\kappa}\cos(\phi_k)+T^3o(1)\right]\}\\
&-2\{\left[T\frac{A_k}{2\kappa}\cos(\phi_k)+To(1)\right]\int_0^T t^2\cos(\omega_k t)dZ_G(t)\\
&+\left(T^{\frac{1}{2}}V_k\right)\int_0^T t^2\cos(\omega_k t)dZ_G(t)\}\\
&-2\{\left[-T\frac{A_k}{2\kappa}\sin(\phi_k)+To(1)\right]\left[-T^3\frac{A_k}{6\kappa}\sin(\phi_k)+T^3o(1)\right]\}\\
&+\left(T^{\frac{1}{2}}W_k\right)\left[-T^3\frac{A_k}{6\kappa}\sin(\phi_k)+T^3o(1)\right]\\
&-2\{\left[-T\frac{A_k}{2\kappa}\sin(\phi_k)+To(1)\right]\int_0^T t^2\sin(\omega_k t)dZ_G(t)\\
&+\left(T^{\frac{1}{2}}W_k\right)\int_0^T t^2\sin(\omega_k t)dZ_G(t)\}. \qquad \text{(B.100)}
\end{aligned}
$$

Therefore, we have

$$
2\pi T^{-3}I_T''(\omega_k)=2\{\left[-\frac{A_k}{4\kappa}\sin(\phi_k)+o(1)\right]^2+2T^{-\frac{1}{2}}\left[-\frac{A_k}{4\kappa}\sin(\phi_k)+o(1)\right]Y_k+T^{-1}\left[Y_k\right]^2\}
$$

$$
\begin{aligned}
&+2\{\left[\frac{A_k}{4\kappa}\cos(\phi_k)+o(1)\right]^2\\
&+2T^{-\frac{1}{2}}\left[\frac{A_k}{4\kappa}\cos(\phi_k)+o(1)\right]X_k+T^{-1}\left[X_k\right]^2\}\\
&-2\{\left[\frac{A_k}{2\kappa}\cos(\phi_k)+o(1)\right]\left[\frac{A_k}{6\kappa}\cos(\phi_k)+o(1)\right]\\
&+T^{-\frac{1}{2}}V_k\left[\frac{A_k}{6\kappa}\cos(\phi_k)+o(1)\right]\}
\end{aligned}
$$

$$
\begin{aligned}
& -2\{T^{-3}\left[\frac{A_k}{2\kappa}\cos(\phi_k)+o(1)\right]\int_0^T t^2\cos(\omega_k t)dZ_G(t) \\
& +T^{-\frac{7}{2}}V_k\int_0^T t^2\cos(\omega_k t)dZ_G(t)\} \\
& -2\{\left[-\frac{A_k}{2\kappa}\sin(\phi_k)+o(1)\right]\left[-\frac{A_k}{6\kappa}\sin(\phi_k)+o(1)\right] \\
& +T^{-\frac{1}{2}}W_k\left[-\frac{A_k}{6\kappa}\sin(\phi_k)+o(1)\right]\} \\
& -2\{T^{-3}\left[-\frac{A_k}{2\kappa}\sin(\phi_k)+o(1)\right]\int_0^T t^2\sin(\omega_k t)dZ_G(t) \\
& +T^{-\frac{7}{2}}W_k\int_0^T t^2\sin(\omega_k t)dZ_G(t)\} \\
= \;& 2\left\{\left[-\frac{A_k}{4\kappa}\sin(\phi_k)+o(1)\right]^2\right\} \\
& +2\left\{\left[\frac{A_k}{4\kappa}\cos(\phi_k)+o(1)\right]^2\right\} \\
& -2\left\{\left[\frac{A_k}{2\kappa}\cos(\phi_k)+o(1)\right]\left[\frac{A_k}{6\kappa}\cos(\phi_k)+o(1)\right]\right\} \\
& -2\left\{\left[-\frac{A_k}{2\kappa}\sin(\phi_k)+o(1)\right]\left[-\frac{A_k}{6\kappa}\sin(\phi_k)+o(1)\right]\right\}+o(1), \qquad \text{(B.101)}
\end{aligned}
$$

and after expanding, we have

$$
\begin{aligned}
2\pi T^{-3}I_T''(\omega_k) &= 2\left\{\left[\frac{A_k}{4\kappa}\right]^2-\frac{A_k^2}{12\kappa^2}\right\}+o(1) \\
&= -\frac{A_k^2}{24\kappa^2}+o(1). \qquad \text{(B.102)}
\end{aligned}
$$

If we let $\bar{\omega}_{k,T}$ be a frequency such that $0 < |\bar{\omega}_{k,T} - \omega_k| \leq |\hat{\omega}_{k,T} - \omega_k|$, then

$$2\pi T^{-3} I_T^{''}(\bar{\omega}_{k,T}) = -\frac{A_k^2}{24\kappa^2} + o(1), \tag{B.103}$$

which establishes equation (2.11). □

B.1.1.5 Proof of Proposition 11

Proof. We begin by finding the $\lim_{T\to\infty} E\left[T^{\frac{3}{2}}\left(\hat{\omega}_{k,T} - \omega_k\right)\right]$. Since for $t > 0$, we have $E\left[dN_G(t)\right] = \lambda_2(t)dt + o(dt)$, and since equation (1.36) implies that $\lambda_2(t) = \frac{1}{\kappa}\lambda_1(t)$ $+ O(\lambda_1(t)\exp\{-a\Lambda_1(t)\})$, it then follows from equations (2.7) and (2.12) that

$$\begin{aligned}\lim_{T\to\infty} E\left[T^{\frac{3}{2}}\left(\hat{\omega}_{k,T} - \omega_k\right)\right] &= \lim_{T\to\infty}[\frac{24\kappa}{A_k}\{E\left[V_k\right]\frac{1}{2}\sin(\phi_k) + E\left[W_k\right]\frac{1}{2}\cos(\phi_k) \\ &\quad - E\left[X_k\right]\sin(\phi_k) - E\left[Y_k\right]\cos(\phi_k)\} + o(1)] \\ &= 0. \end{aligned} \tag{B.104}$$

Next, we find the $\lim_{T\to\infty} \mathrm{var}\left\{T^{\frac{3}{2}}\left(\hat{\omega}_{k,T} - \omega_k\right)\right\}$. From equation (2.12), we have $\mathrm{var}\left\{T^{\frac{3}{2}}\left(\hat{\omega}_{k,T} - \omega_k\right)\right\}$

$$= \left[\frac{24\kappa}{A_k}\right]^2 \mathrm{var}\left\{V_k\frac{1}{2}\sin(\phi_k) + W_k\frac{1}{2}\cos(\phi_k) - X_k\sin(\phi_k) - Y_k\cos(\phi_k)\right\} + o(1)$$

$$\begin{aligned}
= \quad & \left[\frac{24\kappa}{2A_k}\sin(\phi_k)\right]^2 \operatorname{var}\{V_k\} + \left[\frac{24\kappa}{2A_k}\cos(\phi_k)\right]^2 \operatorname{var}\{W_k\} + \left[\frac{24\kappa}{A_k}\sin(\phi_k)\right]^2 \operatorname{var}\{X_k\} \\
& + \left[\frac{24\kappa}{A_k}\cos(\phi_k)\right]^2 \operatorname{var}\{Y_k\} + 2\left[\frac{24\kappa}{A_k}\right]^2 \frac{1}{4}\sin(\phi_k)\cos(\phi_k)\operatorname{cov}\{V_k,\ W_k\} \\
& -2\left[\frac{24\kappa}{A_k}\right]^2 \frac{1}{2}\sin^2(\phi_k)\operatorname{cov}\{V_k,\ X_k\} - 2\left[\frac{24\kappa}{A_k}\right]^2 \frac{1}{2}\sin(\phi_k)\cos(\phi_k)\operatorname{cov}\{V_k,\ Y_k\} \\
& -2\left[\frac{24\kappa}{A_k}\right]^2 \frac{1}{2}\sin(\phi_k)\cos(\phi_k)\operatorname{cov}\{W_k,\ X_k\} - 2\left[\frac{24\kappa}{A_k}\right]^2 \frac{1}{2}\cos^2(\phi_k)\operatorname{cov}\{W_k,\ Y_k\} \\
& +2\left[\frac{24\kappa}{A_k}\right]^2 \sin(\phi_k)\cos(\phi_k)\operatorname{cov}\{X_k,\ Y_k\} + o(1). \qquad \text{(B.105)}
\end{aligned}$$

Therefore, from the variance-covariance properties of Proposition 10, we have

$\lim_{T\to\infty} \operatorname{var}\left\{T^{\frac{3}{2}}\left(\hat{\omega}_{k,T} - \omega_k\right)\right\}$

$$= \left[\frac{24\kappa}{A_k}\right]^2 \{\frac{1}{4}\sin^2(\phi_k)\left[\frac{1}{4\kappa^2}\sum_{j=1}^{K} A_j\cos(\phi_j)\left\{\delta_{j,\ k+k'} + \delta_{j,\ k-k'} + \delta_{j,\ k'-k}\right\} + \frac{B}{2\kappa^2}\delta_{k,\ k'}\right]$$

$$+\frac{1}{4}\cos^2(\phi_k)\left[\frac{1}{4\kappa^2}\sum_{j=1}^{K} A_j\cos(\phi_j)\left\{-\delta_{j,k'+k} + \delta_{j,k-k'} + \delta_{j,k'-k}\right\} + \frac{B}{2\kappa^2}\delta_{k,k'}\right]$$

$$+\sin^2(\phi_k)\left[\frac{1}{12\kappa^2}\sum_{j=1}^{K} A_j\cos(\phi_j)\left\{\delta_{j,\ k+k'} + \delta_{j,\ k-k'} + \delta_{j,\ k'-k}\right\} + \frac{B}{6\kappa^2}\delta_{k,k'}\right]$$

$$+\cos^2(\phi_k)\left[\frac{1}{12\kappa^2}\sum_{j=1}^{K}A_j\cos(\phi_j)\left\{-\delta_{j,\,k+k'}+\delta_{j,\,k-k'}+\delta_{j,\,k'-k}\right\}+\frac{B}{6\kappa^2}\delta_{k,k'}\right]$$

$$+\frac{1}{2}\sin(\phi_k)\cos(\phi_k)\left[\frac{1}{4\kappa^2}\sum_{j=1}^{K}A_j\sin(\phi_j)\left\{-\delta_{j,k+k'}+\delta_{j,k-k'}-\delta_{j,k'-k}\right\}\right]$$

$$-\sin^2(\phi_k)\left[\frac{1}{8\kappa^2}\sum_{j=1}^{K}A_j\cos(\phi_j)\left\{\delta_{j,\,k+k'}+\delta_{j,\,k-k'}+\delta_{j,\,k'-k}\right\}+\frac{B}{4\kappa^2}\delta_{k,\,k'}\right]$$

$$-\sin(\phi_k)\cos(\phi_k)\left[\frac{1}{8\kappa^2}\sum_{j=1}^{K}A_j\sin(\phi_j)\left\{-\delta_{j,\,k+k'}+\delta_{j,\,k-k'}-\delta_{j,\,k'-k}\right\}\right]$$

$$-\sin(\phi_k)\cos(\phi_k)\left[\frac{1}{8\kappa^2}\sum_{j=1}^{K}A_j\sin(\phi_j)\left\{-\delta_{j,\,k+k'}+\delta_{j,\,k-k'}-\delta_{j,\,k'-k}\right\}\right]$$

$$-\cos^2(\phi_k)\left[\frac{1}{8\kappa^2}\sum_{j=1}^{K}A_j\cos(\phi_j)\left\{-\delta_{j,\,k+k'}+\delta_{j,\,k-k'}+\delta_{j,\,k'-k}\right\}+\frac{B}{4\kappa^2}\delta_{k,\,k'}\right]$$

$$+2\sin(\phi_k)\cos(\phi_k)\left[\frac{1}{12\kappa^2}\sum_{j=1}^{K}A_j\sin(\phi_j)\left\{-\delta_{j,\,k+k'}+\delta_{j,\,k-k'}-\delta_{j,\,k'-k}\right\}\right]\Bigg\}. \quad \text{(B.106)}$$

Since $k = k'$ and $\omega_k > 0$, we can cancel out the coefficients of $\delta_{j,\, k-k'}$ and $\delta_{j,\, k'-k}$.

Therefore,

$\lim_{T\to\infty} \mathrm{var}\left\{T^{\frac{3}{2}}\left(\hat{\omega}_{k,T} - \omega_k\right)\right\}$

$$= \left[\frac{24\kappa}{A_k}\right]^2 \{\frac{1}{4}\sin^2(\phi_k)\left[\frac{1}{4\kappa^2}\sum_{j=1}^{K} A_j \cos(\phi_j)\left\{\delta_{j,\, k+k'}\right\} + \frac{B}{2\kappa^2}\delta_{k,\, k'}\right]$$

$$+\frac{1}{4}\cos^2(\phi_k)\left[\frac{1}{4\kappa^2}\sum_{j=1}^{K} A_j \cos(\phi_j)\left\{-\delta_{j,k'+k}\right\} + \frac{B}{2\kappa^2}\delta_{k,k'}\right]$$

$$+\sin^2(\phi_k)\left[\frac{1}{12\kappa^2}\sum_{j=1}^{K} A_j \cos(\phi_j)\left\{\delta_{j,\, k+k'}\right\} + \frac{B}{6\kappa^2}\delta_{k,k'}\right]$$

$$+\cos^2(\phi_k)\left[\frac{1}{12\kappa^2}\sum_{j=1}^{K} A_j \cos(\phi_j)\left\{-\delta_{j,\, k+k'}\right\} + \frac{B}{6\kappa^2}\delta_{k,k'}\right]$$

$$+\frac{1}{2}\sin(\phi_k)\cos(\phi_k)\frac{1}{4\kappa^2}\sum_{j=1}^{K} A_j \sin(\phi_j)\left\{-\delta_{j,k+k'}\right\}$$

$$-\sin^2(\phi_k)\left[\frac{1}{8\kappa^2}\sum_{j=1}^{K} A_j \cos(\phi_j)\left\{\delta_{j,\, k+k'}\right\} + \frac{B}{4\kappa^2}\delta_{k,\, k'}\right]$$

$$-\sin(\phi_k)\cos(\phi_k)\frac{1}{8\kappa^2}\sum_{j=1}^{K} A_j \sin(\phi_j)\left\{-\delta_{j,\, k+k'}\right\}$$

$$-\sin(\phi_k)\cos(\phi_k)\frac{1}{8\kappa^2}\sum_{j=1}^{K} A_j \sin(\phi_j)\left\{-\delta_{j,\, k+k'}\right\}$$

$$-\cos^2(\phi_k)\left[\frac{1}{8\kappa^2}\sum_{j=1}^{K}A_j\cos(\phi_j)\left\{-\delta_{j,\,k+k'}\right\}+\frac{B}{4\kappa^2}\delta_{k,\,k'}\right]$$

$$+\,2\sin(\phi_k)\cos(\phi_k)\frac{1}{12\kappa^2}\sum_{j=1}^{K}A_j\sin(\phi_j)\left\{-\delta_{j,\,k+k'}\right\}\}. \qquad \text{(B.107)}$$

After grouping like terms together, we have

$\lim_{T\to\infty}\operatorname{var}\left\{T^{\frac{3}{2}}\left(\hat{\omega}_{k,T}-\omega_k\right)\right\}$

$$= \quad \left[\frac{24\kappa}{A_k}\right]^2\sum_{j=1}^{K}A_j\delta_{j,\,k+k'}[\frac{1}{48\kappa^2}\sin^2(\phi_k)\cos(\phi_j)-\frac{1}{48\kappa^2}\cos^2(\phi_k)\cos(\phi_j)$$
$$-\frac{1}{24\kappa^2}\sin(\phi_k)\cos(\phi_k)\sin(\phi_j)]+\frac{24B}{A_k^2}, \qquad \text{(B.108)}$$

which can be expressed as

$\lim_{T\to\infty}\operatorname{var}\left\{T^{\frac{3}{2}}\left(\hat{\omega}_{k,T}-\omega_k\right)\right\}$

$$=\left[\frac{24\kappa}{A_k}\right]^2\sum_{j=1}^{K}A_j\delta_{j,\,k+k'}\{$$
$$\frac{1}{48\kappa^2}\frac{1}{4}\left[2\cos(\phi_j)-\cos(2\phi_k+\phi_j)-\cos(2\phi_k-\phi_j)\right]$$
$$-\frac{1}{48\kappa^2}\frac{1}{4}\left[2\cos(\phi_j)+\cos(2\phi_k+\phi_j)+\cos(2\phi_k-\phi_j)\right]$$
$$-\frac{1}{24\kappa^2}\frac{1}{4}\left[-\cos(2\phi_k+\phi_j)+\cos(2\phi_k-\phi_j)\right]\}+\frac{24B}{A_k^2}$$

$$
\begin{aligned}
&= \left[\frac{24\kappa}{A_k}\right]^2 \sum_{j=1}^{K} A_j \delta_{j,\,k+k'} \{-2\frac{1}{48\kappa^2}\frac{1}{4}\cos(2\phi_k+\phi_j) - 2\frac{1}{48\kappa^2}\frac{1}{4}\cos(2\phi_k-\phi_j) \\
&\quad + \frac{1}{24\kappa^2}\frac{1}{4}\left[\cos(2\phi_k+\phi_j) - \cos(2\phi_k-\phi_j)\right]\} + \frac{24B}{A_k^2} \\
&= \left[\frac{24\kappa}{A_k}\right]^2 \sum_{j=1}^{K} A_j \delta_{j,\,k+k'} \frac{-1}{48\kappa^2}\left\{\cos(2\phi_k-\phi_j)\right\} + \frac{24B}{A_k^2} \\
&= -\frac{12}{A_k^2}\sum_{j=1}^{K} A_j \delta_{j,\,k+k'}\left\{\cos(2\phi_k-\phi_j)\right\} + \frac{24B}{A_k^2} \\
&= \frac{12}{A_k^2}\left\{2B - \sum_{j=1}^{K} A_j \delta_{j,\,k+k'}\left\{\cos(2\phi_k-\phi_j)\right\}\right\}. \qquad \text{(B.109)}
\end{aligned}
$$

Next, we find the $\lim_{T\to\infty} \operatorname{cov}\left\{T^{\frac{3}{2}}\left(\hat{\omega}_{k,T}-\omega_k\right),\ T^{\frac{3}{2}}\left(\hat{\omega}_{k',T}-\omega_{k'}\right)\right\}$. We notice from equation (2.12) that for $k \neq k'$, we have

$\lim_{T\to\infty} \operatorname{cov}\left\{T^{\frac{3}{2}}\left(\hat{\omega}_{k,T}-\omega_k\right),\ T^{\frac{3}{2}}\left(\hat{\omega}_{k',T}-\omega_{k'}\right)\right\}$

$$
\begin{aligned}
=&\frac{24^2\kappa^2}{A_kA_{k'}}\operatorname{cov}\{V_k\frac{1}{2}\sin(\phi_k) + W_k\frac{1}{2}\cos(\phi_k) - X_k\sin(\phi_k) - Y_k\cos(\phi_k), \\
&V_{k'}\frac{1}{2}\sin(\phi_{k'}) + W_{k'}\frac{1}{2}\cos(\phi_{k'}) - X_{k'}\sin(\phi_{k'}) - Y_{k'}\cos(\phi_{k'})\} \\
=&\frac{24^2\kappa^2}{A_kA_{k'}}\{\frac{1}{4}\sin(\phi_{\mathrm{k}})\sin(\phi_{\mathrm{k}'})\operatorname{cov}\{V_k,\ V_{k'}\} + \frac{1}{4}\sin(\phi_k)\cos(\phi_{k'})\operatorname{cov}\{V_k,\ W_{k'}\} \\
&-\frac{1}{2}\sin(\phi_k)\sin(\phi_{k'})\operatorname{cov}\{V_k,\ X_{k'}\} - \frac{1}{2}\sin(\phi_k)\cos(\phi_{k'})\operatorname{cov}\{V_k,\ Y_{k'}\} \\
&+\frac{1}{4}\cos(\phi_{\mathrm{k}})\sin(\phi_{\mathrm{k}'})\operatorname{cov}\{W_k,\ V_{k'}\} + \frac{1}{4}\cos(\phi_{\mathrm{k}})\cos(\phi_{\mathrm{k}'})\operatorname{cov}\{W_k,\ W_{k'}\} \\
&-\frac{1}{2}\cos(\phi_{\mathrm{k}})\sin(\phi_{\mathrm{k}'})\operatorname{cov}\{W_k,\ X_{k'}\} - \frac{1}{2}\cos(\phi_{\mathrm{k}})\cos(\phi_{\mathrm{k}'})\operatorname{cov}\{W_k,\ Y_{k'}\}
\end{aligned}
$$

$$-\frac{1}{2}\sin(\phi_k)\sin(\phi_{k'})\mathrm{cov}\left\{X_k,\ V_{k'}\right\}-\frac{1}{2}\sin(\phi_k)\cos(\phi_{k'})\mathrm{cov}\left\{X_k,\ W_{k'}\right\}$$

$$+\sin(\phi_{\mathrm{k}})\sin(\phi_{\mathrm{k'}})\mathrm{cov}\left\{X_k,\ X_{k'}\right\}+\sin(\phi_{\mathrm{k}})\cos(\phi_{\mathrm{k'}})\mathrm{cov}\left\{X_k,\ Y_{k'}\right\}$$

$$-\frac{1}{2}\cos(\phi_{\mathrm{k}})\sin(\phi_{\mathrm{k'}})\mathrm{cov}\left\{Y_k,\ V_{k'}\right\}-\frac{1}{2}\cos(\phi_{\mathrm{k}})\cos(\phi_{\mathrm{k'}})\mathrm{cov}\left\{Y_k,\ W_{k'}\right\}$$

$$+\cos(\phi_{\mathrm{k}})\sin(\phi_{\mathrm{k'}})\mathrm{cov}\left\{Y_k,\ X_{k'}\right\}+\cos(\phi_{\mathrm{k}})\cos(\phi_{\mathrm{k'}})\mathrm{cov}\left\{Y_k,\ Y_{k'}\right\}\}$$

$$=\frac{24^2\kappa^2}{A_kA_{k'}}\{\frac{1}{4}\sin(\phi_{\mathrm{k}})\sin(\phi_{\mathrm{k'}})\left\{\frac{1}{4\kappa^2}\sum_{\mathrm{j=1}}^{\mathrm{K}}\mathrm{A_j}\cos(\phi_{\mathrm{j}})\left\{\delta_{\mathrm{j,\ k+k'}}+\delta_{\mathrm{j,\ k-k'}}+\delta_{\mathrm{j,\ k'-k}}\right\}+\frac{\mathrm{B}}{2\kappa^2}\delta_{\mathrm{k,\ k'}}\right\} \tag{B.110}$$

$$+\frac{1}{4}\sin(\phi_k)\cos(\phi_{k'})\left\{\frac{1}{4\kappa^2}\sum_{j=1}^{K}A_j\sin(\phi_j)\left\{-\delta_{j,k+k'}+\delta_{j,k-k'}-\delta_{j,k'-k}\right\}\right\} \tag{B.111}$$

$$-\frac{1}{2}\sin(\phi_k)\sin(\phi_{k'})\left\{\frac{1}{8\kappa^2}\sum_{j=1}^{K}A_j\cos(\phi_j)\left\{\delta_{j,k+k'}+\delta_{j,k-k'}+\delta_{j,k'-k}\right\}+\frac{B}{4\kappa^2}\delta_{k,k'}\right\} \tag{B.112}$$

$$-\frac{1}{2}\sin(\phi_k)\cos(\phi_{k'})\left\{\frac{1}{8\kappa^2}\sum_{j=1}^{K}A_j\sin(\phi_j)\left\{-\delta_{j,\ k+k'}+\delta_{j,\ k-k'}-\delta_{j,\ k'-k}\right\}\right\} \tag{B.113}$$

$$+\frac{1}{4}\cos(\phi_{\mathrm{k}})\sin(\phi_{\mathrm{k'}})\left\{\frac{1}{4\kappa^2}\sum_{j=1}^{K}A_j\sin(\phi_j)\left\{-\delta_{j,k'+k}+\delta_{j,k'-k}-\delta_{j,k-k'}\right\}\right\} \tag{B.114}$$

$$+\frac{1}{4}\cos(\phi_{\mathrm{k}})\cos(\phi_{\mathrm{k'}})\left\{\frac{1}{4\kappa^2}\sum_{\mathrm{j=1}}^{\mathrm{K}}\mathrm{A_j}\cos(\phi_{\mathrm{j}})\left\{-\delta_{\mathrm{j,k'+k}}+\delta_{\mathrm{j,k-k'}}+\delta_{\mathrm{j,k'-k}}\right\}+\frac{\mathrm{B}}{2\kappa^2}\delta_{\mathrm{k,k'}}\right\} \tag{B.115}$$

$$-\frac{1}{2}\cos(\phi_{\mathrm{k}})\sin(\phi_{\mathrm{k'}})\left\{\frac{1}{8\kappa^2}\sum_{\mathrm{j=1}}^{\mathrm{K}}\mathrm{A_j}\sin(\phi_{\mathrm{j}})\left\{-\delta_{\mathrm{j,\,k+k'}}+\delta_{\mathrm{j,\,k'-k}}-\delta_{\mathrm{j,\,k-k'}}\right\}\right\} \tag{B.116}$$

$$-\frac{1}{2}\cos(\phi_{\mathrm{k}})\cos(\phi_{\mathrm{k'}})\left\{\frac{1}{8\kappa^2}\sum_{\mathrm{j=1}}^{\mathrm{K}}\mathrm{A_j}\cos(\phi_{\mathrm{j}})\left\{-\delta_{\mathrm{j,\,k+k'}}+\delta_{\mathrm{j,\,k-k'}}+\delta_{\mathrm{j,\,k'-k}}\right\}+\frac{\mathrm{B}\delta_{\mathrm{k,\,k'}}}{4\kappa^2}\right\} \tag{B.117}$$

$$-\frac{1}{2}\sin(\phi_k)\sin(\phi_{k'})\left\{\frac{1}{8\kappa^2}\sum_{j=1}^{K}A_j\cos(\phi_j)\left\{\delta_{j,k+k'}+\delta_{j,k'-k}+\delta_{j,k-k'}\right\}+\frac{B}{4\kappa^2}\delta_{k,k'}\right\} \tag{B.118}$$

$$-\frac{1}{2}\sin(\phi_k)\cos(\phi_{k'})\left\{\frac{1}{8\kappa^2}\sum_{j=1}^{K}A_j\sin(\phi_j)\left\{-\delta_{j,\,k'+k}+\delta_{j,\,k-k'}-\delta_{j,\,k'-k}\right\}\right\} \tag{B.119}$$

$$+\sin(\phi_{\mathrm{k}})\sin(\phi_{\mathrm{k'}})\left\{\frac{1}{12\kappa^2}\sum_{\mathrm{j=1}}^{\mathrm{K}}\mathrm{A_j}\cos(\phi_{\mathrm{j}})\left\{\delta_{\mathrm{j,\,k+k'}}+\delta_{\mathrm{j,\,k-k'}}+\delta_{\mathrm{j,\,k'-k}}\right\}+\frac{\mathrm{B}}{6\kappa^2}\delta_{\mathrm{k,k'}}\right\} \tag{B.120}$$

$$+\sin(\phi_{\mathrm{k}})\cos(\phi_{\mathrm{k'}})\left\{\frac{1}{12\kappa^2}\sum_{\mathrm{j=1}}^{\mathrm{K}}\mathrm{A_j}\sin(\phi_{\mathrm{j}})\left\{-\delta_{\mathrm{j,\,k+k'}}+\delta_{\mathrm{j,\,k-k'}}-\delta_{\mathrm{j,\,k'-k}}\right\}\right\} \tag{B.121}$$

$$-\frac{1}{2}\cos(\phi_{\mathrm{k}})\sin(\phi_{\mathrm{k'}})\left\{\frac{1}{8\kappa^2}\sum_{j=1}^{K}A_j\sin(\phi_j)\left\{-\delta_{j,\,k'+k}+\delta_{j,\,k'-k}-\delta_{j,\,k-k'}\right\}\right\} \tag{B.122}$$

$$-\frac{1}{2}\cos(\phi_{\mathrm{k}})\cos(\phi_{\mathrm{k'}})\left\{\frac{1}{8\kappa^2}\sum_{j=1}^{K}A_j\cos(\phi_j)\left\{-\delta_{j,\,k'+k}+\delta_{j,\,k'-k}+\delta_{j,\,k-k'}\right\}+\frac{B\delta_{k,\,k'}}{4\kappa^2}\right\} \tag{B.123}$$

$$+\cos(\phi_{\mathrm{k}})\sin(\phi_{\mathrm{k'}})\left\{\frac{1}{12\kappa^2}\sum_{j=1}^{K}A_j\sin(\phi_j)\left\{-\delta_{j,\,k'+k}+\delta_{j,\,k'-k}-\delta_{j,\,k-k'}\right\}\right\} \tag{B.124}$$

$$+\cos(\phi_{\mathrm{k}})\cos(\phi_{\mathrm{k'}})\left\{\frac{1}{12\kappa^2}\sum_{\mathrm{j=1}}^{\mathrm{K}}\mathrm{A_j}\cos(\phi_{\mathrm{j}})\left\{-\delta_{\mathrm{j,\,k+k'}}+\delta_{\mathrm{j,\,k-k'}}+\delta_{\mathrm{j,\,k'-k}}\right\}+\frac{\mathrm{B}\delta_{\mathrm{k,k'}}}{6\kappa^2}\right\}\Big\}. \tag{B.125}$$

Since $k \neq k'$, we notice that $\delta_{k,k'} = 0$. After setting $\delta_{k,k'} = 0$, combining equations (B.110) and (B.112), combining equations (B.111) and (B.113), combining equations

(B.114) and (B.116), and combining (B.115) and (B.117), equation (B.125) becomes

$$= \frac{24^2}{A_k A_{k'}}\{-\sin(\phi_k)\sin(\phi_{k'})\left\{\frac{1}{16}\sum_{j=1}^{K} A_j\cos(\phi_j)\left\{\delta_{j,k+k'} + \delta_{j,k'-k} + \delta_{j,k-k'}\right\}\right\} \tag{B.126}$$

$$-\sin(\phi_k)\cos(\phi_{k'})\left\{\frac{1}{16}\sum_{j=1}^{K} A_j\sin(\phi_j)\left\{-\delta_{j,\ k'+k} + \delta_{j,\ k-k'} - \delta_{j,\ k'-k}\right\}\right\} \tag{B.127}$$

$$+\sin(\phi_\mathrm{k})\sin(\phi_{\mathrm{k}'})\left\{\frac{1}{12}\sum_{\mathrm{j}=1}^{\mathrm{K}} \mathrm{A_j}\cos(\phi_\mathrm{j})\left\{\delta_{\mathrm{j,\ k+k'}} + \delta_{\mathrm{j,\ k-k'}} + \delta_{\mathrm{j,\ k'-k}}\right\}\right\} \tag{B.128}$$

$$+\sin(\phi_\mathrm{k})\cos(\phi_{\mathrm{k}'})\left\{\frac{1}{12}\sum_{\mathrm{j}=1}^{\mathrm{K}} \mathrm{A_j}\sin(\phi_\mathrm{j})\left\{-\delta_{\mathrm{j,\ k+k'}} + \delta_{\mathrm{j,\ k-k'}} - \delta_{\mathrm{j,\ k'-k}}\right\}\right\} \tag{B.129}$$

$$-\cos(\phi_\mathrm{k})\sin(\phi_{\mathrm{k}'})\left\{\frac{1}{16}\sum_{j=1}^{K} A_j\sin(\phi_j)\left\{-\delta_{j,\ k'+k} + \delta_{j,\ k'-k} - \delta_{j,\ k-k'}\right\}\right\} \tag{B.130}$$

$$-\cos(\phi_\mathrm{k})\cos(\phi_{\mathrm{k}'})\left\{\frac{1}{16}\sum_{j=1}^{K} A_j\cos(\phi_j)\left\{-\delta_{j,\ k'+k} + \delta_{j,\ k'-k} + \delta_{j,\ k-k'}\right\}\right\} \tag{B.131}$$

$$+\cos(\phi_\mathrm{k})\sin(\phi_{\mathrm{k}'})\left\{\frac{1}{12}\sum_{j=1}^{K} A_j\sin(\phi_j)\left\{-\delta_{j,\ k'+k} + \delta_{j,\ k'-k} - \delta_{j,\ k-k'}\right\}\right\} \tag{B.132}$$

$$+\cos(\phi_\mathrm{k})\cos(\phi_{\mathrm{k}'})\left\{\frac{1}{12}\sum_{\mathrm{j}=1}^{\mathrm{K}} \mathrm{A_j}\cos(\phi_\mathrm{j})\left\{-\delta_{\mathrm{j,\ k+k'}} + \delta_{\mathrm{j,\ k-k'}} + \delta_{\mathrm{j,\ k'-k}}\right\}\right\}\}. \tag{B.133}$$

After combining equations (B.126) and (B.128), combining equations (B.127) and (B.129), combining equations (B.130) and (B.132), and equations (B.131) and (B.133), we have

$$= \frac{24^2}{A_k A_{k'}}\{\sin(\phi_k)\sin(\phi_{k'})\left\{\sum_{j=1}^{K} A_j\cos(\phi_j)\left\{\frac{1}{48}\delta_{j,k+k'} + \frac{1}{48}\delta_{j,k'-k} + \frac{1}{48}\delta_{j,k-k'}\right\}\right\} \tag{B.134}$$

$$+\sin(\phi_k)\cos(\phi_{k'})\left\{\sum_{j=1}^{K}A_j\sin(\phi_j)\left\{-\frac{1}{48}\delta_{j,\,k'+k}+\frac{1}{48}\delta_{j,\,k-k'}-\frac{1}{48}\delta_{j,\,k'-k}\right\}\right\} \tag{B.135}$$

$$+\frac{1}{48}\cos(\phi_{\mathrm{k}})\sin(\phi_{\mathrm{k}'})\left\{\sum_{j=1}^{K}A_j\sin(\phi_j)\left\{-\delta_{j,\,k'+k}+\delta_{j,\,k'-k}-\delta_{j,\,k-k'}\right\}\right\} \tag{B.136}$$

$$+\frac{1}{48}\cos(\phi_{\mathrm{k}})\cos(\phi_{\mathrm{k}'})\left\{\sum_{j=1}^{K}A_j\cos(\phi_j)\left\{-\delta_{j,\,k'+k}+\delta_{j,\,k'-k}+\delta_{j,\,k-k'}\right\}\right\}\}. \tag{B.137}$$

After factoring out the $\frac{1}{48}$ and factoring in the cosine and sine terms, equation (B.137) becomes

$$=\frac{12}{A_kA_{k'}}\{\left\{\sum_{j=1}^{K}A_j\sin(\phi_k)\sin(\phi_{k'})\cos(\phi_j)\left\{\delta_{j,k+k'}+\delta_{j,k'-k}+\delta_{j,k-k'}\right\}\right\} \tag{B.138}$$

$$+\left\{\sum_{j=1}^{K}A_j\sin(\phi_k)\cos(\phi_{k'})\sin(\phi_j)\left\{-\delta_{j,\,k'+k}+\delta_{j,\,k-k'}-\delta_{j,\,k'-k}\right\}\right\} \tag{B.139}$$

$$+\left\{\sum_{j=1}^{K}A_j\cos(\phi_k)\sin(\phi_{k'})\sin(\phi_j)\left\{-\delta_{j,\,k'+k}+\delta_{j,\,k'-k}-\delta_{j,\,k-k'}\right\}\right\} \tag{B.140}$$

$$+\left\{\sum_{j=1}^{K}A_j\cos(\phi_{\mathrm{k}})\cos(\phi_{\mathrm{k}'})\cos(\phi_j)\left\{-\delta_{j,\,k'+k}+\delta_{j,\,k'-k}+\delta_{j,\,k-k'}\right\}\right\}\}. \tag{B.141}$$

Next, we break equation (B.141) into three parts. We will first look at the coefficients of $\delta_{j,k+k'}$, then $\delta_{j,k'-k}$, and then $\delta_{j,k-k'}$. First, let's consider the coefficient of $\delta_{j,k+k'}$.

We notice that

$$\frac{12}{A_k A_{k'}} \sum_{j=1}^{K} A_j \delta_{j,k+k'} \{\sin(\phi_k)\sin(\phi_{k'})\cos(\phi_j) - \sin(\phi_k)\cos(\phi_{k'})\sin(\phi_j)$$
$$- \cos(\phi_k)\sin(\phi_{k'})\sin(\phi_j) - \cos(\phi_\mathrm{k})\cos(\phi_{\mathrm{k}'})\cos(\phi_j)\} \tag{B.142}$$

becomes

$$\frac{12}{A_k A_{k'}} \sum_{j=1}^{K} A_j \delta_{j,k+k'} \frac{1}{4}\{$$
$$\{-\cos(\phi_k + \phi_{k'} + \phi_j) + \cos(-\phi_k + \phi_{k'} + \phi_j) + \cos(\phi_k - \phi_{k'} + \phi_j) - \cos(-\phi_k - \phi_{k'} + \phi_j)\}$$
$$+\{\cos(\phi_k + \phi_{k'} + \phi_j) - \cos(-\phi_k + \phi_{k'} + \phi_j) + \cos(\phi_k - \phi_{k'} + \phi_j) - \cos(-\phi_k - \phi_{k'} + \phi_j)\}$$
$$+\{\cos(\phi_k + \phi_{k'} + \phi_j) + \cos(-\phi_k + \phi_{k'} + \phi_j) - \cos(\phi_k - \phi_{k'} + \phi_j) - \cos(-\phi_k - \phi_{k'} + \phi_j)\}$$
$$+\{-\cos(\phi_k + \phi_{k'} + \phi_j) - \cos(-\phi_k + \phi_{k'} + \phi_j) - \cos(\phi_k - \phi_{k'} + \phi_j) - \cos(-\phi_k - \phi_{k'} + \phi_j)\}\}$$

$$= \quad \frac{12}{A_k A_{k'}} \sum_{j=1}^{K} A_j \delta_{j,k+k'} \frac{1}{4}\{-4\cos(-\phi_k - \phi_{k'} + \phi_j)\}. \tag{B.143}$$

Second, we look at the coefficients of $\delta_{j,k'-k}$. We notice that

$$\frac{12}{A_k A_{k'}} \sum_{j=1}^{K} A_j \delta_{j,k'-k} \{\sin(\phi_k)\sin(\phi_{k'})\cos(\phi_j) - \sin(\phi_k)\cos(\phi_{k'})\sin(\phi_j)$$
$$+ \cos(\phi_k)\sin(\phi_{k'})\sin(\phi_j) + \cos(\phi_\mathrm{k})\cos(\phi_{\mathrm{k}'})\cos(\phi_j)\} \tag{B.144}$$

becomes

$$\frac{12}{A_k A_{k'}} \sum_{j=1}^{K} A_j \delta_{j,k'-k} \frac{1}{4} \{$$

$$\{-\cos(\phi_k + \phi_{k'} + \phi_j) + \cos(-\phi_k + \phi_{k'} + \phi_j) + \cos(\phi_k - \phi_{k'} + \phi_j) - \cos(-\phi_k - \phi_{k'} + \phi_j)\}$$

$$+\{\cos(\phi_k + \phi_{k'} + \phi_j) - \cos(-\phi_k + \phi_{k'} + \phi_j) + \cos(\phi_k - \phi_{k'} + \phi_j) - \cos(-\phi_k - \phi_{k'} + \phi_j)\}$$

$$+\{-\cos(\phi_k + \phi_{k'} + \phi_j) - \cos(-\phi_k + \phi_{k'} + \phi_j) + \cos(\phi_k - \phi_{k'} + \phi_j) + \cos(-\phi_k - \phi_{k'} + \phi_j)\}$$

$$+\{\cos(\phi_k + \phi_{k'} + \phi_j) + \cos(-\phi_k + \phi_{k'} + \phi_j) + \cos(\phi_k - \phi_{k'} + \phi_j) + \cos(-\phi_k - \phi_{k'} + \phi_j)\}\}$$

$$= \frac{12}{A_k A_{k'}} \sum_{j=1}^{K} A_j \delta_{j,k'-k} \frac{1}{4} \{4\cos(\phi_k - \phi_{k'} + \phi_j)\}. \tag{B.145}$$

Lastly, we look at the coefficients of $\delta_{j,k-k'}$. We notice that

$$\frac{12}{A_k A_{k'}} \sum_{j=1}^{K} A_j \delta_{j,k-k'} \{\sin(\phi_k)\sin(\phi_{k'})\cos(\phi_j) + \sin(\phi_k)\cos(\phi_{k'})\sin(\phi_j)$$
$$-\cos(\phi_k)\sin(\phi_{k'})\sin(\phi_j) + \cos(\phi_\mathrm{k})\cos(\phi_{\mathrm{k}'})\cos(\phi_j)\} \tag{B.146}$$

becomes

$$\frac{12}{A_k A_{k'}} \sum_{j=1}^{K} A_j \delta_{j,k-k'} \frac{1}{4} \{$$

$$\{-\cos(\phi_k + \phi_{k'} + \phi_j) + \cos(-\phi_k + \phi_{k'} + \phi_j) + \cos(\phi_k - \phi_{k'} + \phi_j) - \cos(-\phi_k - \phi_{k'} + \phi_j)\}$$

$$+\{-\cos(\phi_k+\phi_{k'}+\phi_j)+\cos(-\phi_k+\phi_{k'}+\phi_j)-\cos(\phi_k-\phi_{k'}+\phi_j)+\cos(-\phi_k-\phi_{k'}+\phi_j)\}$$

$$+\{\cos(\phi_k+\phi_{k'}+\phi_j)+\cos(-\phi_k+\phi_{k'}+\phi_j)-\cos(\phi_k-\phi_{k'}+\phi_j)-\cos(-\phi_k-\phi_{k'}+\phi_j)\}$$

$$+\{\cos(\phi_k+\phi_{k'}+\phi_j)+\cos(-\phi_k+\phi_{k'}+\phi_j)+\cos(\phi_k-\phi_{k'}+\phi_j)+\cos(-\phi_k-\phi_{k'}+\phi_j)\}\}$$

$$= \frac{12}{A_kA_{k'}}\sum_{j=1}^{K}A_j\delta_{j,k-k'}\frac{1}{4}\{4\cos(-\phi_k+\phi_{k'}+\phi_j)\}. \tag{B.147}$$

After combining equations (B.143), (B.145), and (B.147), we have

$$\begin{aligned}
&= \frac{12}{A_kA_{k'}}\sum_{j=1}^{K}A_j\frac{1}{4}\{-4\delta_{j,k+k'}\cos(-\phi_k-\phi_{k'}+\phi_j)\\
&\quad +4\delta_{j,k'-k}\cos(\phi_k-\phi_{k'}+\phi_j)+4\delta_{j,k-k'}\cos(-\phi_k+\phi_{k'}+\phi_j)\}\\
&= \frac{12}{A_kA_{k'}}\sum_{j=1}^{K}A_j\{-\cos(-\phi_k-\phi_{k'}+\phi_j)\,\delta_{j,k+k'}\\
&\quad +\cos(\phi_k-\phi_{k'}+\phi_j)\,\delta_{j,k'-k}+\cos(-\phi_k+\phi_{k'}+\phi_j)\,\delta_{j,k-k'}\}.
\end{aligned}$$

□

B.1.1.6 Proof of Equations (2.15) and (2.18)

Proof. Here we establish equations (2.15) and (2.18). From equation (2.14), it follows that

$$
\begin{aligned}
T^{\frac{1}{2}}\left(\widehat{A}^2_{k,T} - A^2_k\right) &= T^{\frac{1}{2}}\left(\frac{8\kappa^2\pi}{T} I_T(\hat{\omega}_{k,T}) - A^2_k\right) \\
&= T^{-\frac{1}{2}} 8\kappa^2\pi I_T(\hat{\omega}_{k,T}) - T^{\frac{1}{2}} A^2_k \\
&= T^{-\frac{1}{2}} 8\kappa^2\pi I_T(\hat{\omega}_{k,T}) - T^{-\frac{1}{2}} 8\kappa^2\pi I_T(\omega_k) + T^{-\frac{1}{2}} 8\kappa^2\pi I_T(\omega_k) - T^{\frac{1}{2}} A^2_k \\
&= -T^{-\frac{1}{2}} 8\kappa^2\pi \left(I_T(\omega_k) - I_T(\hat{\omega}_{k,T})\right) + T^{\frac{1}{2}}\left(\frac{8\kappa^2\pi}{T} I_T(\omega_k) - A^2_k\right), \quad \text{(B.148)}
\end{aligned}
$$

which establishes equation (2.15). From equations (B.148) and (2.17), we have

$$
T^{\frac{1}{2}}\left(\widehat{A}^2_{k,T} - A^2_k\right) = -T^{-\frac{1}{2}} 8\kappa^2\pi \left(\frac{I''_T(\bar{\omega}_{k,T})}{2!}\left(\omega_k - \hat{\omega}_{k,T}\right)^2\right) + T^{\frac{1}{2}}\left(\frac{8\kappa^2\pi}{T} I_T(\omega_k) - A^2_k\right),
$$

which from equation (2.16), we have

$$
\begin{aligned}
&T^{\frac{1}{2}}\left(\widehat{A}^2_{k,T} - A^2_k\right) \\
&= - T^{-\frac{1}{2}} 8\kappa^2\pi \left(\frac{I''_T(\bar{\omega}_{k,T})}{2!}\left(\omega_k - \hat{\omega}_{k,T}\right)^2\right) + T^{\frac{1}{2}}\left(\frac{8\kappa^2\pi}{T} I_T(\omega_k) - A^2_k\right) \\
&= - T^{-\frac{1}{2}} 8\kappa^2\pi \left(\frac{I''_T(\bar{\omega}_{k,T})}{2!}\left(\omega_k - \hat{\omega}_{k,T}\right)^2\right) \\
&\quad + T^{\frac{1}{2}}\left(8\kappa^2\pi\left[\frac{A^2_k}{8\pi\kappa^2} + \frac{A_k}{2\pi\kappa}\cos(\phi_k)\left(T^{-\frac{1}{2}} V_k\right) - \frac{A_k}{2\pi\kappa}\sin(\phi_k)\left(T^{-\frac{1}{2}} W_k\right)\right] - A^2_k\right) \\
&\quad + o(1)
\end{aligned}
$$

$$
\begin{aligned}
&= -T^{-\frac{1}{2}} 8\kappa^2 \pi \left(\frac{I_T''(\bar{\omega}_{k,T})}{2!} \left(\omega_k - \hat{\omega}_{k,T}\right)^2 \right) \\
&\quad + T^{\frac{1}{2}} \left(A_k^2 + 4\kappa A_k \cos(\phi_k) \left(T^{-\frac{1}{2}} V_k\right) - 4\kappa A_k \sin(\phi_k) \left(T^{-\frac{1}{2}} W_k\right) - A_k^2 \right) + o(1) \\
&= -T^{-\frac{1}{2}} 8\kappa^2 \pi \left(\frac{I_T''(\bar{\omega}_{k,T})}{2!} \left(\omega_k - \hat{\omega}_{k,T}\right)^2 \right) + \\
&\quad T^{\frac{1}{2}} \left(4\kappa A_k \cos(\phi_k) \left(T^{-\frac{1}{2}} V_k\right) - 4\kappa A_k \sin(\phi_k) \left(T^{-\frac{1}{2}} W_k\right) \right) + o(1) \\
&= -T^{-\frac{1}{2}} 8\kappa^2 \pi \left(\frac{I_T''(\bar{\omega}_{k,T})}{2!} \left(\omega_k - \hat{\omega}_{k,T}\right)^2 \right) \\
&\quad + \left(4\kappa A_k \cos(\phi_k) V_k - 4\kappa A_k \sin(\phi_k) W_k\right) + o(1). \qquad \text{(B.149)}
\end{aligned}
$$

And from equations (2.11) and (2.12), we have

$$
\begin{aligned}
2\pi T^{-3} I_T^{''}(\bar{\omega}_{k,T}) T^3 \left(\hat{\omega}_{k,T} - \omega_k\right)^2 &= -\frac{A_k^2}{24\kappa^2} \left[\frac{24\kappa}{A_k}\right]^2 \{V_k \frac{1}{2} \sin(\phi_k) + W_k \frac{1}{2} \cos(\phi_k) \\
&\quad - X_k \sin(\phi_k) - Y_k \cos(\phi_k)\}^2 + o(1),
\end{aligned}
$$

which implies

$$
\begin{aligned}
2\pi I_T^{''}(\bar{\omega}_{k,T}) \left(\hat{\omega}_{k,T} - \omega_k\right)^2 &= -24\{V_k \frac{1}{2} \sin(\phi_k) + W_k \frac{1}{2} \cos(\phi_k) \\
&\quad - X_k \sin(\phi_k) - Y_k \cos(\phi_k)\}^2 + o(1),
\end{aligned}
$$

which implies

$$
\begin{aligned}
-T^{-\frac{1}{2}} 8\kappa^2 \pi \frac{I_T''(\bar{\omega}_{k,T})}{2!} \left(\hat{\omega}_{k,T} - \omega_k\right)^2 &= T^{-\frac{1}{2}} 48\kappa^2 \{V_k \frac{1}{2}\sin(\phi_k) + W_k \frac{1}{2}\cos(\phi_k) \\
&\quad -X_k \sin(\phi_k) - Y_k \cos(\phi_k)\}^2 + o(1) \\
&= 48\kappa^2 \{\frac{1}{T^4} V_k \frac{1}{2}\sin(\phi_k) + \frac{1}{T^4} W_k \frac{1}{2}\cos(\phi_k) \\
&\quad -\frac{1}{T^4} X_k \sin(\phi_k) - \frac{1}{T^4} Y_k \cos(\phi_k)\}^2 + o(1) \\
&= o(1).
\end{aligned}
$$

Therefore, equation (B.149) becomes

$$
\begin{aligned}
T^{\frac{1}{2}} \left(\widehat{A}_{k,T}^2 - A_k^2\right) &= -T^{-\frac{1}{2}} 8\kappa^2 \pi \left(\frac{I_T''(\bar{\omega}_{k,T})}{2!} \left(\omega_k - \hat{\omega}_{k,T}\right)^2\right) \\
&\quad + \left(4\kappa A_k \cos(\phi_k) V_k - 4\kappa A_k \sin(\phi_k) W_k\right) + o(1) \\
&= 4\kappa A_k \left\{\cos(\phi_k) V_k - \sin(\phi_k) W_k\right\} + o(1), \qquad \text{(B.150)}
\end{aligned}
$$

which establishes equation (2.18). □

B.1.1.7 Proof of Proposition 12

Proof. We begin by quoting Cramer's Theorem which will be used throughout this proof. Let g be a mapping $g: \mathbb{R}^d \to \mathbb{R}^k$ such that $\dot{g}(x)$ is continuous in a neighborhood of $\mu \in \mathbb{R}^d$. If X_n is a sequence of d-dimensional random vectors such that $\sqrt{n}\left(X_n - \mu\right) \xrightarrow{\mathcal{L}} X$, then $\sqrt{n}\left(g(X_n) - g(\mu)\right) \xrightarrow{\mathcal{L}} \dot{g}(\mu) X$ (Ferguson (1996, pg. 45)).

From equation (2.18), for each $k = 1,\ 2,\ \ldots,\ K$, we have $T^{\frac{1}{2}}\left(\widehat{A}^2_{k,T} - A^2_k\right) = 4\kappa A_k\{\cos(\phi_k)V_k - \sin(\phi_k)W_k\} + o(1)$, which we know from Proposition 10, converges to some distribution with mean 0 (established in equation (B.1.1.7)) and variance $\lim_{\mathrm{T}\to\infty}\mathrm{var}\{\mathrm{T}^{\frac{1}{2}}(\widehat{\mathrm{A}}^2_{\mathrm{k,T}} - \mathrm{A}^2_{\mathrm{k}})\}$ (established in equation (B.154)). For $k,\ k' = 1,\ 2,\ \ldots,\ K$, we define $\Sigma_{k,\ k'} :=$

$$\begin{bmatrix} \mathrm{var}\left\{\mathrm{T}^{\frac{1}{2}}\left(\widehat{\mathrm{A}}^2_{\mathrm{k,T}} - \mathrm{A}^2_{\mathrm{k}}\right)\right\} & \mathrm{cov}\left\{T^{\frac{1}{2}}\left(\widehat{A}^2_{k,T} - A^2_k\right),\ T^{\frac{1}{2}}\left(\widehat{A}^2_{k',T} - A^2_{k'}\right)\right\} \\ \mathrm{cov}\left\{T^{\frac{1}{2}}\left(\widehat{A}^2_{k,T} - A^2_k\right),\ T^{\frac{1}{2}}\left(\widehat{A}^2_{k',T} - A^2_{k'}\right)\right\} & \mathrm{var}\left\{\mathrm{T}^{\frac{1}{2}}\left(\widehat{\mathrm{A}}^2_{\mathrm{k',T}} - \mathrm{A}^2_{\mathrm{k'}}\right)\right\} \end{bmatrix}.$$

Then from Cramer's Theorem, we know that for $k,\ k' = 1,\ 2,\ \ldots,\ K$, the random vector $[T^{\frac{1}{2}}\left(\widehat{A}_{k,T} - A_k\right),\ T^{\frac{1}{2}}\left(\widehat{A}_{k',T} - A_{k'}\right)]'$converges to a distribution with mean 0 and variance-covariance matrix

$$\lim_{T\to\infty} \dot{g}_1(A^2_k,\ A^2_{k'})\Sigma_{k,\ k'}\dot{g}_1(A^2_k,\ A^2_{k'})',$$

where $g_1(x,\ y) = \left[\sqrt{x},\ \sqrt{y}\right]$, $\dot{g}_1(x,\ y) = \begin{bmatrix} \frac{1}{2\sqrt{x}} & 0 \\ 0 & \frac{1}{2\sqrt{y}} \end{bmatrix}$, $\dot{g}_1(x,\ y)' = \begin{bmatrix} \frac{1}{2\sqrt{x}} & 0 \\ 0 & \frac{1}{2\sqrt{y}} \end{bmatrix}$, and

$$\dot{g}_1(A^2_k,\ A^2_{k'})\Sigma_{k,\ k'}\dot{g}_1(A^2_k,\ A^2_{k'})'$$

$$\begin{aligned} = \ & \dot{g}_1(A^2_k,\ A^2_{k'}) \times \\ & \begin{bmatrix} \frac{1}{2\sqrt{\mathrm{A}^2_{\mathrm{k}}}}\mathrm{var}\{\mathrm{T}^{\frac{1}{2}}(\widehat{\mathrm{A}}^2_{\mathrm{k,T}} - \mathrm{A}^2_{\mathrm{k}})\} & \frac{1}{2\sqrt{\mathrm{A}^2_{\mathrm{k'}}}}\mathrm{cov}\{T^{\frac{1}{2}}(\widehat{A}^2_{k,T} - A^2_k),\ T^{\frac{1}{2}}(\widehat{A}^2_{k',T} - A^2_{k'}) \\ \frac{1}{2\sqrt{\mathrm{A}^2_{\mathrm{k}}}}\mathrm{cov}\{T^{\frac{1}{2}}(\widehat{A}^2_{k,T} - A^2_k),\ T^{\frac{1}{2}}(\widehat{A}^2_{k',T} - A^2_{k'})\} & \frac{1}{2\sqrt{A^2_{k'}}}\mathrm{var}\{T^{\frac{1}{2}}(\widehat{A}^2_{k',T} - A^2_{k'})\} \end{bmatrix} \end{aligned}$$

$$= \left[\begin{array}{cc} \frac{1}{4\mathrm{A}_{\mathrm{k}}^2}\mathrm{var}\{\mathrm{T}^{\frac{1}{2}}(\widehat{\mathrm{A}}_{\mathrm{k,T}}^2 - \mathrm{A}_{\mathrm{k}}^2)\} & \frac{1}{4\mathrm{A}_{\mathrm{k}}\mathrm{A}_{\mathrm{k}'}}\mathrm{cov}\{T^{\frac{1}{2}}(\widehat{A}_{k,T}^2 - A_k^2),\ T^{\frac{1}{2}}(\widehat{A}_{k',T}^2 - A_{k'}^2)\} \\ \frac{1}{4\mathrm{A}_{\mathrm{k}}\mathrm{A}_{\mathrm{k}'}}\mathrm{cov}\{T^{\frac{1}{2}}(\widehat{A}_{k,T}^2 - A_k^2),\ T^{\frac{1}{2}}(\widehat{A}_{k',T}^2 - A_{k'}^2)\} & \frac{1}{4A_{k'}^2}\mathrm{var}\left\{T^{\frac{1}{2}}(\widehat{A}_{k',T}^2 - A_{k'}^2)\right\} \end{array} \right]. \tag{B.151}$$

Next, we establish the variance-covariance of equation (B.151). The main variance result is given below in equation (B.154) and the main covariance result is given below in equitation (B.155). In the notation of equation (2.7), from equation (2.18) and Lemma 8 of Section 2.2, it follows that

$$\begin{aligned} \lim_{T\to\infty} E\left[T^{\frac{1}{2}}\left(\widehat{A}_{k,T}^2 - A_k^2\right)\right] &= \lim_{T\to\infty}\left\{E\left[4\kappa A_k\left\{\cos(\phi_k)V_k - \sin(\phi_k)W_k\right\}\right] + o(1)\right\} \\ &= 0. \end{aligned} \tag{B.152}$$

Likewise, from equation (B.150), it follows that

$$\begin{aligned} \mathrm{var}\left\{T^{\frac{1}{2}}\left(\widehat{A}_{k,T}^2 - A_k^2\right)\right\} &= \mathrm{var}\left\{4\kappa A_k\left\{\cos(\phi_k)V_k - \sin(\phi_k)W_k\right\}\right\} + o(1) \\ &= 16\kappa^2 A_k^2 \mathrm{var}\left\{\cos(\phi_k)V_k - \sin(\phi_k)W_k\right\} + o(1) \\ &= 16\kappa^2 A_k^2\{\cos^2(\phi_k)\mathrm{var}\left\{V_k\right\} + \sin^2(\phi_k)\mathrm{var}\left\{W_k\right\} \\ &\quad -2\cos(\phi_k)\sin(\phi_k)\mathrm{cov}\left\{V_k,\ W_k\right\}\} + o(1). \end{aligned} \tag{B.153}$$

From Proposition 10, it then follows that

$$\lim_{\mathrm{T}\to\infty} \mathrm{var}\left\{T^{\frac{1}{2}}\left(\widehat{A}^2_{k,T} - A^2_k\right)\right\} = 16\kappa^2 A^2_k\{$$

$$\cos^2(\phi_k)\left[\frac{1}{4\kappa^2}\sum_{j=1}^{K} A_j\cos(\phi_j)\left\{\delta_{j,\ k+k} + \delta_{j,\ k-k} + \delta_{j,\ k-k}\right\} + \frac{B}{2\kappa^2}\delta_{k,\ k}\right]$$

$$+\sin^2(\phi_k)\left[\frac{1}{4\kappa^2}\sum_{j=1}^{K} A_j\cos(\phi_j)\left\{-\delta_{j,k+k} + \delta_{j,k-k} + \delta_{j,k-k}\right\} + \frac{B}{2\kappa^2}\delta_{k,k}\right]$$

$$-2\cos(\phi_k)\sin(\phi_k)\left[\frac{1}{4\kappa^2}\sum_{j=1}^{K} A_j\sin(\phi_j)\left\{-\delta_{j,k+k} + \delta_{j,k-k} - \delta_{j,k-k}\right\}\right]\}$$

$$= 16\kappa^2 A^2_k\{$$

$$\cos^2(\phi_k)\left[\frac{1}{4\kappa^2}\sum_{j=1}^{K} A_j\cos(\phi_j)\delta_{j,\ k+k} + \frac{B}{2\kappa^2}\right]$$

$$+\sin^2(\phi_k)\left[-\frac{1}{4\kappa^2}\sum_{j=1}^{K} A_j\cos(\phi_j)\delta_{j,k+k} + \frac{B}{2\kappa^2}\right]$$

$$-2\cos(\phi_k)\sin(\phi_k)\left[-\frac{1}{4\kappa^2}\sum_{j=1}^{K} A_j\sin(\phi_j)\delta_{j,k+k}\right]\}$$

$$= 16A^2_k\{\tfrac{B}{2}$$

$$+\cos^2(\phi_k)\frac{1}{4}\sum_{j=1}^{K} A_j\cos(\phi_j)\delta_{j,\ k+k}$$

$$-\sin^2(\phi_k)\frac{1}{4}\sum_{j=1}^{K} A_j\cos(\phi_j)\delta_{j,k+k}$$

$$+2\cos(\phi_k)\sin(\phi_k)\frac{1}{4}\sum_{j=1}^{K} A_j \sin(\phi_j)\delta_{j,k+k}\}$$

$= 16A_k^2\{\frac{B}{2}$

$$+\frac{1}{4}\sum_{j=1}^{K} A_j \frac{1}{4}\left[2\cos(\phi_j) + \cos(2\phi_k + \phi_j) + \cos(2\phi_k - \phi_j)\right]\delta_{j,\ k+k}$$

$$-\frac{1}{4}\sum_{j=1}^{K} A_j \frac{1}{4}\left[2\cos(\phi_j) - \cos(2\phi_k + \phi_j) - \cos(2\phi_k - \phi_j)\right]\delta_{j,k+k}$$

$$+2\frac{1}{4}\sum_{j=1}^{K} A_j \frac{1}{4}\left[-\cos(2\phi_k + \phi_j) + \cos(2\phi_k - \phi_j)\right]\delta_{j,k+k}\}$$

$= A_k^2\{8B$

$$+2\sum_{j=1}^{K} A_j \cos(2\phi_k + \phi_j)\delta_{j,\ k+k} + 2\sum_{j=1}^{K} A_j \cos(2\phi_k - \phi_j)\delta_{j,k+k}$$

$$+2\sum_{j=1}^{K} A_j \left[-\cos(2\phi_k + \phi_j) + \cos(2\phi_k - \phi_j)\right]\delta_{j,k+k}\}$$

$$\begin{aligned} &= A_k^2\{8B + 4\sum_{j=1}^{K} A_j \cos(2\phi_k - \phi_j)\delta_{j,k+k}\} \\ &= 4A_k^2\{2B + \sum_{j=1}^{K} A_j \cos(2\phi_k - \phi_j)\delta_{j,k+k}\}. \end{aligned}$$

Using Cramer's Theorem, it then follows that

$$\lim_{T\to\infty} \operatorname{var}\left\{T^{\frac{1}{2}}\left(\widehat{A}_{k,T} - A_k\right)\right\} = \left(\frac{1}{2\sqrt{A_k^2}}\right)^2 4A_k^2\{2B + \sum_{j=1}^{K} A_j \cos(2\phi_k - \phi_j)\delta_{j,k+k}\}$$
$$= \{2B + \sum_{j=1}^{K} A_j \cos(2\phi_k - \phi_j)\delta_{j,k+k}\}. \quad \text{(B.154)}$$

Next, we compute $\operatorname{cov}\left\{T^{\frac{1}{2}}\left(\widehat{A}^2_{k,T} - A^2_k\right),\ T^{\frac{1}{2}}\left(\widehat{A}^2_{k',T} - A^2_{k'}\right)\right\}$. For each $k,\ k' = 1,\ 2, \cdots,\ K$, it follows from equation (B.150) that

$$\operatorname{cov}\left\{T^{\frac{1}{2}}\left(\widehat{A}^2_{k,T} - A^2_k\right),\ T^{\frac{1}{2}}\left(\widehat{A}^2_{k',T} - A^2_{k'}\right)\right\}$$

$$= \operatorname{cov}\left\{4\kappa A_k\left\{\cos(\phi_k)V_k - \sin(\phi_k)W_k\right\},\ 4\kappa A_{k'}\left\{\cos(\phi_{k'})V_{k'} - \sin(\phi_{k'})W_{k'}\right\}\right\} + o(1)$$

$$= 16\kappa^2 A_k A_{k'} \operatorname{cov}\left\{\cos(\phi_k)V_k - \sin(\phi_k)W_k,\ \cos(\phi_{k'})V_{k'} - \sin(\phi_{k'})W_{k'}\right\} + o(1)$$

$$= 16\kappa^2 A_k A_{k'}\{$$

$$\cos(\phi_k)\cos(\phi_{k'})\operatorname{cov}\left\{V_k\ , V_{k'}\right\} - \sin(\phi_k)\cos(\phi_{k'})\operatorname{cov}\left\{W_k,\ V_{k'}\right\}$$

$$- \cos(\phi_k)\sin(\phi_{k'})\operatorname{cov}\left\{V_k,\ W_{k'}\right\} + \sin(\phi_k)\sin(\phi_{k'})\operatorname{cov}\left\{W_k,\ W_{k'}\right\}\} + o(1).$$

Therefore, we have

$$\lim_{T\to\infty} \operatorname{cov}\left\{T^{\frac{1}{2}}\left(\widehat{A}^2_{k,T}-A^2_k\right),\ T^{\frac{1}{2}}\left(\widehat{A}^2_{k',T}-A^2_{k'}\right)\right\} = 16\kappa^2 A_k A_{k'}\{$$

$$\cos(\phi_k)\cos(\phi_{k'})\left[\frac{1}{4\kappa^2}\sum_{j=1}^{K} A_j\cos(\phi_j)\left\{\delta_{j,\,k+k'}+\delta_{j,\,k-k'}+\delta_{j,\,k'-k}\right\}+\frac{B}{2\kappa^2}\delta_{k,\,k'}\right]$$

$$-\sin(\phi_k)\cos(\phi_{k'})\left[\frac{1}{4\kappa^2}\sum_{j=1}^{K} A_j\sin(\phi_j)\left\{-\delta_{j,k'+k}+\delta_{j,k'-k}-\delta_{j,k-k'}\right\}\right]$$

$$-\cos(\phi_k)\sin(\phi_{k'})\left[\frac{1}{4\kappa^2}\sum_{j=1}^{K} A_j\sin(\phi_j)\left\{-\delta_{j,k+k'}+\delta_{j,k-k'}-\delta_{j,k'-k}\right\}\right]$$

$$+\sin(\phi_k)\sin(\phi_{k'})\left[\frac{1}{4\kappa^2}\sum_{j=1}^{K} A_j\cos(\phi_j)\left\{-\delta_{j,k'+k}+\delta_{j,k-k'}+\delta_{j,k'-k}\right\}+\frac{B}{2\kappa^2}\delta_{k,\,k'}\right]\}$$

$$= 4A_kA_{k'}\{2B\left[\cos(\phi_k)\cos(\phi_{k'})+\sin(\phi_k)\sin(\phi_{k'})\right]\delta_{k,\,k'}$$

$$+\cos(\phi_k)\cos(\phi_{k'})\sum_{j=1}^{K} A_j\cos(\phi_j)\left\{\delta_{j,\,k+k'}+\delta_{j,\,k-k'}+\delta_{j,\,k'-k}\right\}$$

$$-\sin(\phi_k)\cos(\phi_{k'})\sum_{j=1}^{K} A_j\sin(\phi_j)\left\{-\delta_{j,k'+k}+\delta_{j,k'-k}-\delta_{j,k-k'}\right\}$$

$$-\cos(\phi_k)\sin(\phi_{k'})\sum_{j=1}^{K} A_j\sin(\phi_j)\left\{-\delta_{j,k+k'}+\delta_{j,k-k'}-\delta_{j,k'-k}\right\}$$

$$+\sin(\phi_k)\sin(\phi_{k'})\sum_{j=1}^{K}A_j\cos(\phi_j)\left\{-\delta_{j,k'+k}+\delta_{j,k-k'}+\delta_{j,k'-k}\right\}\}$$

$$=4A_kA_{k'}\{2B\cos(\phi_k-\phi_{k'})\delta_{k,\,k'}$$

$$+\sum_{j=1}^{K}A_j\frac{1}{4}\{\cos\left(\phi_k+\phi_{k'}+\phi_j\right)+\cos\left(-\phi_k+\phi_{k'}+\phi_j\right)+\cos\left(\phi_k-\phi_{k'}+\phi_j\right)$$

$$+\cos\left(-\phi_k-\phi_{k'}+\phi_j\right)\}\left\{\delta_{j,\,k+k'}+\delta_{j,\,k-k'}+\delta_{j,\,k'-k}\right\}$$

$$-\sum_{j=1}^{K}A_j\frac{1}{4}\{-\cos\left(\phi_k+\phi_{k'}+\phi_j\right)+\cos\left(-\phi_k+\phi_{k'}+\phi_j\right)-\cos\left(\phi_k-\phi_{k'}+\phi_j\right)$$

$$+\cos\left(-\phi_k-\phi_{k'}+\phi_j\right)\}\left\{-\delta_{j,k'+k}+\delta_{j,k'-k}-\delta_{j,k-k'}\right\}$$

$$-\sum_{j=1}^{K}A_j\frac{1}{4}\{-\cos\left(\phi_k+\phi_{k'}+\phi_j\right)-\cos\left(-\phi_k+\phi_{k'}+\phi_j\right)+\cos\left(\phi_k-\phi_{k'}+\phi_j\right)$$

$$+\cos\left(-\phi_k-\phi_{k'}+\phi_j\right)\}\left\{-\delta_{j,k+k'}+\delta_{j,k-k'}-\delta_{j,k'-k}\right\}$$

$$+\sum_{j=1}^{K}A_j\frac{1}{4}\{-\cos\left(\phi_k+\phi_{k'}+\phi_j\right)+\cos\left(-\phi_k+\phi_{k'}+\phi_j\right)+\cos\left(\phi_k-\phi_{k'}+\phi_j\right)$$

$$-\cos\left(-\phi_k-\phi_{k'}+\phi_j\right)\}\left\{-\delta_{j,k'+k}+\delta_{j,k-k'}+\delta_{j,k'-k}\right\}\}$$

$$= A_k A_{k'} \{ 8B \cos(\phi_k - \phi_{k'}) \delta_{k,\, k'}$$

$$+ \sum_{j=1}^{K} A_j \{ \cos(\phi_k + \phi_{k'} + \phi_j) + \cos(-\phi_k + \phi_{k'} + \phi_j) + \cos(\phi_k - \phi_{k'} + \phi_j)$$
$$+ \cos(-\phi_k - \phi_{k'} + \phi_j) \} \left\{ \delta_{j,\, k+k'} + \delta_{j,\, k-k'} + \delta_{j,\, k'-k} \right\}$$

$$- \sum_{j=1}^{K} A_j \{ -\cos(\phi_k + \phi_{k'} + \phi_j) + \cos(-\phi_k + \phi_{k'} + \phi_j) - \cos(\phi_k - \phi_{k'} + \phi_j)$$
$$+ \cos(-\phi_k - \phi_{k'} + \phi_j) \} \left\{ -\delta_{j,k'+k} + \delta_{j,k'-k} - \delta_{j,k-k'} \right\}$$

$$- \sum_{j=1}^{K} A_j \{ -\cos(\phi_k + \phi_{k'} + \phi_j) - \cos(-\phi_k + \phi_{k'} + \phi_j) + \cos(\phi_k - \phi_{k'} + \phi_j)$$
$$+ \cos(-\phi_k - \phi_{k'} + \phi_j) \} \left\{ -\delta_{j,k+k'} + \delta_{j,k-k'} - \delta_{j,k'-k} \right\}$$

$$+ \sum_{j=1}^{K} A_j \{ -\cos(\phi_k + \phi_{k'} + \phi_j) + \cos(-\phi_k + \phi_{k'} + \phi_j) + \cos(\phi_k - \phi_{k'} + \phi_j)$$
$$- \cos(-\phi_k - \phi_{k'} + \phi_j) \} \left\{ -\delta_{j,k'+k} + \delta_{j,k-k'} + \delta_{j,k'-k} \right\} \}$$

$$= A_k A_{k'} \{ 8B \cos(\phi_k - \phi_{k'}) \delta_{k,\, k'}$$

$$+4 \sum_{j=1}^{K} A_j \cos(-\phi_k - \phi_{k'} + \phi_j) \, \delta_{j,\, k+k'}$$

$$+\sum_{j=1}^{K} A_j\{\cos(\phi_k+\phi_{k'}+\phi_j)+\cos(-\phi_k+\phi_{k'}+\phi_j)+\cos(\phi_k-\phi_{k'}+\phi_j)$$

$$+\cos(-\phi_k-\phi_{k'}+\phi_j)\}\left\{\delta_{j,\,k-k'}+\delta_{j,\,k'-k}\right\}$$

$$-\sum_{j=1}^{K} A_j\{-\cos(\phi_k+\phi_{k'}+\phi_j)+\cos(-\phi_k+\phi_{k'}+\phi_j)-\cos(\phi_k-\phi_{k'}+\phi_j)$$

$$+\cos(-\phi_k-\phi_{k'}+\phi_j)\}\left\{\delta_{j,k'-k}-\delta_{j,k-k'}\right\}$$

$$-\sum_{j=1}^{K} A_j\{-\cos(\phi_k+\phi_{k'}+\phi_j)-\cos(-\phi_k+\phi_{k'}+\phi_j)+\cos(\phi_k-\phi_{k'}+\phi_j)$$

$$+\cos(-\phi_k-\phi_{k'}+\phi_j)\}\left\{\delta_{j,k-k'}-\delta_{j,k'-k}\right\}$$

$$+\sum_{j=1}^{K} A_j\{-\cos(\phi_k+\phi_{k'}+\phi_j)+\cos(-\phi_k+\phi_{k'}+\phi_j)+\cos(\phi_k-\phi_{k'}+\phi_j)$$

$$-\cos(-\phi_k-\phi_{k'}+\phi_j)\}\left\{\delta_{j,k-k'}+\delta_{j,k'-k}\right\}\}$$

$$=A_kA_{k'}\{8B\cos(\phi_k-\phi_{k'})\delta_{k,\,k'}$$

$$+4\sum_{j=1}^{K} A_j\cos(-\phi_k-\phi_{k'}+\phi_j)\,\delta_{j,\,k+k'}$$

$$+4\sum_{j=1}^{K} A_j \cos\left(-\phi_k + \phi_{k'} + \phi_j\right) \delta_{j,\, k-k'}$$

$$+\sum_{j=1}^{K} A_j \{\cos\left(\phi_k + \phi_{k'} + \phi_j\right) + \cos\left(-\phi_k + \phi_{k'} + \phi_j\right) + \cos\left(\phi_k - \phi_{k'} + \phi_j\right)$$
$$+ \cos\left(-\phi_k - \phi_{k'} + \phi_j\right)\}\delta_{j,\, k'-k}$$

$$-\sum_{j=1}^{K} A_j \{-\cos\left(\phi_k + \phi_{k'} + \phi_j\right) + \cos\left(-\phi_k + \phi_{k'} + \phi_j\right) - \cos\left(\phi_k - \phi_{k'} + \phi_j\right)$$
$$+ \cos\left(-\phi_k - \phi_{k'} + \phi_j\right)\}\delta_{j,k'-k}$$

$$-\sum_{j=1}^{K} A_j \{-\cos\left(\phi_k + \phi_{k'} + \phi_j\right) - \cos\left(-\phi_k + \phi_{k'} + \phi_j\right) + \cos\left(\phi_k - \phi_{k'} + \phi_j\right)$$
$$+ \cos\left(-\phi_k - \phi_{k'} + \phi_j\right)\} \left\{-\delta_{j,k'-k}\right\}$$

$$+\sum_{j=1}^{K} A_j \{-\cos\left(\phi_k + \phi_{k'} + \phi_j\right) + \cos\left(-\phi_k + \phi_{k'} + \phi_j\right) + \cos\left(\phi_k - \phi_{k'} + \phi_j\right)$$
$$- \cos\left(-\phi_k - \phi_{k'} + \phi_j\right)\}\delta_{j,k'-k}\}$$

$$= A_k A_{k'} \{8B\cos(\phi_k - \phi_{k'})\delta_{k,\,k'}$$

$$+4\sum_{j=1}^{K} A_j \cos\left(-\phi_k - \phi_{k'} + \phi_j\right)\delta_{j,\,k+k'}$$

$$+4\sum_{j=1}^{K} A_j \cos\left(-\phi_k + \phi_{k'} + \phi_j\right)\delta_{j,\,k-k'}$$

$$+4\sum_{j=1}^{K} A_j \cos\left(\phi_k - \phi_{k'} + \phi_j\right)\delta_{j,\,k'-k}\}$$

$$= 4A_k A_{k'} \{2B\cos(\phi_k - \phi_{k'})\delta_{k,\,k'}$$

$$+\sum_{j=1}^{K} A_j \cos\left(-\phi_k - \phi_{k'} + \phi_j\right)\delta_{j,\,k+k'}$$

$$+\sum_{j=1}^{K} A_j \cos\left(-\phi_k + \phi_{k'} + \phi_j\right)\delta_{j,\,k-k'}$$

$$+\sum_{j=1}^{K} A_j \cos\left(\phi_k - \phi_{k'} + \phi_j\right)\delta_{j,\,k'-k}\}.$$

Therefore, it follows that

$$\lim_{T\to\infty} \operatorname{cov}\left\{T^{\frac{1}{2}}\left(\widehat{A}_{k,T} - A_k\right),\ T^{\frac{1}{2}}\left(\widehat{A}_{k',T} - A_{k'}\right)\right\}$$

$$= \lim_{T\to\infty} \frac{1}{4\mathrm{A_k A_{k'}}} \operatorname{cov}\left\{T^{\frac{1}{2}}\left(\widehat{A}^2_{k,T} - A^2_k\right),\ T^{\frac{1}{2}}\left(\widehat{A}^2_{k',T} - A^2_{k'}\right)\right\}$$

$$= \{2B\cos(\phi_k - \phi_{k'})\delta_{k,\,k'} + \textstyle\sum_{j=1}^{K} A_j \cos\left(-\phi_k - \phi_{k'} + \phi_j\right)\delta_{j,\,k+k'}$$

$$+\sum_{j=1}^{K} A_j \cos\left(-\phi_k + \phi_{k'} + \phi_j\right) \delta_{j,\, k-k'} + \sum_{j=1}^{K} A_j \cos\left(\phi_k - \phi_{k'} + \phi_j\right) \delta_{j,\, k'-k} \}. \tag{B.155}$$

$\square$

B.1.1.8 Proof of Proposition 13

Proof. We begin by quoting Cramer's Theorem which will be used throughout this proof. Let g be a mapping $g:\ \mathbb{R}^d \rightarrow \mathbb{R}^k$ such that $\dot{g}(x)$ is continuous in a neighborhood of $\mu \in \mathbb{R}^d$. If X_n is a sequence of d-dimensional random vectors such that $\sqrt{n}\,(X_n - \mu) \stackrel{\mathcal{L}}{\rightarrow} X$, then $\sqrt{n}\,(g(X_n) - g(\mu)) \stackrel{\mathcal{L}}{\rightarrow} \dot{g}(\mu)X$ (Ferguson (1996, pg. 45)). We begin by establishing the asymptotic form of $T^{\frac{1}{2}}\{\tan(\hat{\phi}_{k,T}) - \tan(\phi_k)\}$ for the particular case when $\phi_k \neq \pm\frac{\pi}{2}$, we then use the asymptotic form of $T^{\frac{1}{2}}\{\tan(\hat{\phi}_{k,T}) - \tan(\phi_k)\}$ in conjunction with Cramer's Theorem to establish the asymptotic form of $T^{\frac{1}{2}}\{\hat{\phi}_{k,T} - \phi_k\}$, where $\phi_k \neq \pm\frac{\pi}{2}$. From the useful asymptotic integral section of Appendix B and the Chapter 2 Lemma 8, we have

$$\begin{aligned}
T^{\frac{1}{2}}\left\{\tan(\hat{\phi}_{k,T}) - \tan(\phi_k)\right\} =& T^{\frac{1}{2}}\left\{\tan(\hat{\phi}_{k,T}) - \frac{\sin(\phi_k)}{\cos(\phi_k)}\right\} \\
=& T^{\frac{1}{2}}\{\tan(\hat{\phi}_{k,T}) - \frac{-\frac{1}{T}\int_0^T \sin(\omega_k t) dN_G(t)}{\frac{1}{T}\int_0^T \cos(\omega_k t) dN_G(t)} \\
&+ \frac{-\frac{1}{T}\int_0^T \sin(\omega_k t) dN_G(t)}{\frac{1}{T}\int_0^T \cos(\omega_k t) dN_G(t)} - \frac{\sin(\phi_k)}{\cos(\phi_k)}\}
\end{aligned}$$

$$
\begin{aligned}
&= T^{\frac{1}{2}}\left\{\tan(\hat{\phi}_{k,T}) + \frac{\frac{1}{T}\int_0^T \sin(\omega_k t)dN_G(t)}{\frac{1}{T}\int_0^T \cos(\omega_k t)dN_G(t)}\right\} \\
&\quad + T^{\frac{1}{2}}\left\{\frac{-\frac{1}{T}\int_0^T \sin(\omega_k t)dN_G(t)}{\frac{1}{T}\int_0^T \cos(\omega_k t)dN_G(t)} - \frac{\sin(\phi_k)}{\cos(\phi_k)}\right\} \\
&= T^{\frac{1}{2}}\left\{\tan(\hat{\phi}_{k,T}) + \frac{\frac{1}{T}\int_0^T \sin(\omega_k t)dN_G(t)}{\frac{1}{T}\int_0^T \cos(\omega_k t)dN_G(t)}\right\} \\
&\quad + T^{\frac{1}{2}}\left\{\frac{-\cos(\phi_k)\frac{1}{T}\int_0^T \sin(\omega_k t)dN_G(t) - \sin(\phi_k)\frac{1}{T}\int_0^T \cos(\omega_k t)dN_G(t)}{\cos(\phi_k)\frac{1}{T}\int_0^T \cos(\omega_k t)dN_G(t)}\right\} \\
&= T^{\frac{1}{2}}\left\{\tan(\hat{\phi}_{k,T}) + \frac{\frac{1}{T}\int_0^T \sin(\omega_k t)dN_G(t)}{\frac{1}{T}\int_0^T \cos(\omega_k t)dN_G(t)}\right\} \\
&\quad - \frac{2\kappa}{A_k\cos^2(\phi_k) + o(1)}\left\{\cos(\phi_k)W_k + \sin(\phi_k)V_k\right\}. \qquad \text{(B.156)}
\end{aligned}
$$

To establish the asymptotic form of equation (B.156), we first establish a derivative which we use in the first order Taylor series expansion of $T^{\frac{1}{2}}\{\tan(\hat{\phi}_{k,T}) + \frac{\frac{1}{T}\int_0^T \sin(\omega_k t)dN_G(t)}{\frac{1}{T}\int_0^T \cos(\omega_k t)dN_G(t)}\}$ about ω_k. Let $\bar{\omega}_{k,T}$ be a frequency such that $0 \leq |\bar{\omega}_{k,T} - \omega_k| \leq |\hat{\omega}_{k,T} - \omega_k|$, then

$$
T^{\frac{1}{2}}\left\{\left[\frac{d}{d\omega}\frac{-\frac{1}{T}\int_0^T \sin(\omega t)dN_G(t)}{\frac{1}{T}\int_0^T \cos(\omega t)dN_G(t)}\right]_{\omega=\bar{\omega}_{k,T}}\right\}
$$

$$
\begin{aligned}
&= -T^{\frac{1}{2}}\{\frac{\left[\frac{d}{d\omega}\frac{1}{T}\int_0^T \sin(\omega t)dN_G(t)\right]\frac{1}{T}\int_0^T \cos(\omega t)dN_G(t)}{\left[\frac{1}{T}\int_0^T \cos(\omega t)dN_G(t)\right]^2} \\
&\quad - \frac{\left[\frac{d}{d\omega}\frac{1}{T}\int_0^T \cos(\omega t)dN_G(t)\right]\frac{1}{T}\int_0^T \sin(\omega t)dN_G(t)}{\left[\frac{1}{T}\int_0^T \cos(\omega t)dN_G(t)\right]^2}|_{\omega=\bar{\omega}_{k,T}}\} \\
&= -T^{\frac{1}{2}}\{\frac{\left[\frac{1}{T}\int_0^T t\cos(\bar{\omega}_{k,T}t)dN_G(t)\right]\left[\frac{1}{T}\int_0^T \cos(\bar{\omega}_{k,T}t)dN_G(t)\right]}{\left[\frac{1}{T}\int_0^T \cos(\bar{\omega}_{k,T}t)dN_G(t)\right]^2}
\end{aligned}
$$

$$+\frac{\left[\frac{1}{T}\int_0^T t\sin(\bar{\omega}_{k,T}t)dN_G(t)\right]\left[\frac{1}{T}\int_0^T \sin(\bar{\omega}_{k,T}t)dN_G(t)\right]}{\left[\frac{1}{T}\int_0^T \cos(\bar{\omega}_{k,T}t)dN_G(t)\right]^2}\}.$$

By the Chapter 2 Lemma 8 (of Section 2.2), equation (1.36), and the useful asymptotic integral section of Appendix B, it follows that

$$T^{\frac{1}{2}}\left\{\left[\frac{d}{d\omega}\frac{-\frac{1}{T}\int_0^T \sin(\omega t)dN_G(t)}{\frac{1}{T}\int_0^T \cos(\omega t)dN_G(t)}\right]_{\omega=\bar{\omega}_{k,T}}\right\}$$

$$\begin{aligned}
= \quad & -T^{\frac{1}{2}}\{\frac{\left[\frac{1}{T}\int_0^T t\cos(\bar{\omega}_{k,T}t)\frac{1}{\kappa}\lambda_1(t)dt\right]\left[\frac{1}{T}\int_0^T \cos(\bar{\omega}_{k,T}t)\frac{1}{\kappa}\lambda_1(t)dt\right]}{\left[\frac{1}{T}\int_0^T \cos(\bar{\omega}_{k,T}t)\frac{1}{\kappa}\lambda_1(t)dt\right]^2} \\
& +\frac{\left[\frac{1}{T}\int_0^T t\sin(\bar{\omega}_{k,T}t)\frac{1}{\kappa}\lambda_1(t)dt\right]\left[\frac{1}{T}\int_0^T \sin(\bar{\omega}_{k,T}t)\frac{1}{\kappa}\lambda_1(t)dt\right]}{\left[\frac{1}{T}\int_0^T \cos(\bar{\omega}_{k,T}t)\frac{1}{\kappa}\lambda_1(t)dt\right]^2}+o(1)\}
\end{aligned}$$

$$= -T^{\frac{1}{2}}\left\{\frac{T\left[\frac{A_k}{4\kappa}\cos(\phi_k)+o(1)\right]\left[\frac{A_k}{2\kappa}\cos(\phi_k)+o(1)\right]+T\left[-\frac{A_k}{4\kappa}\sin(\phi_k)+o(1)\right]\left[-\frac{A_k}{2\kappa}\sin(\phi_k)+o(1)\right]}{\left[\frac{A_k}{2\kappa}\cos(\phi_k)+o(1)\right]^2}\right\}$$

$$= -T^{\frac{1}{2}}\left\{\frac{T}{2}\frac{\left[\cos(\phi_k)+o(1)\right]\left[\cos(\phi_k)+o(1)\right]+\left[\sin(\phi_k)+o(1)\right]\left[\sin(\phi_k)+o(1)\right]}{\left[\cos(\phi_k)+o(1)\right]^2}\right\}$$

$$= -T^{\frac{1}{2}}\left\{\frac{T}{2}\frac{1+o(1)}{\cos^2(\phi_k)+o(1)}\right\}. \tag{B.157}$$

We now use the above derivative to establish the asymptotic form of

$$T^{\frac{1}{2}}\left\{\tan(\hat{\phi}_{k,T})+\frac{\frac{1}{T}\int_0^T\sin(\omega_k t)dN_G(t)}{\frac{1}{T}\int_0^T\cos(\omega_k t)dN_G(t)}\right\}.$$

By equation (B.157), we know that for some frequency $\bar{\omega}_{k,T}$ such that $0\leq|\bar{\omega}_{k,T}-\omega_k|\leq|\hat{\omega}_{k,T}-\omega_k|$, the first order Taylor series expansion of $T^{\frac{1}{2}}\left\{\tan(\hat{\phi}_{k,T})+\frac{\frac{1}{T}\int_0^T\sin(\omega_k t)dN_G(t)}{\frac{1}{T}\int_0^T\cos(\omega_k t)dN_G(t)}\right\}$ about ω_k is

$$\begin{aligned}
&T^{\frac{1}{2}}\left\{\tan(\hat{\phi}_{k,T})+\frac{\frac{1}{T}\int_0^T\sin(\omega_k t)dN_G(t)}{\frac{1}{T}\int_0^T\cos(\omega_k t)dN_G(t)}\right\}\\
=\;& T^{\frac{1}{2}}\left\{\frac{-\frac{1}{T}\int_0^T\sin(\omega_k t)dN_G(t)}{\frac{1}{T}\int_0^T\cos(\omega_k t)dN_G(t)}+\frac{\frac{1}{T}\int_0^T\sin(\omega_k t)dN_G(t)}{\frac{1}{T}\int_0^T\cos(\omega_k t)dN_G(t)}\right\}\\
&+\left\{\frac{d}{d\omega}\left[T^{\frac{1}{2}}\frac{-\frac{1}{T}\int_0^T\sin(\omega t)dN_G(t)}{\frac{1}{T}\int_0^T\cos(\omega t)dN_G(t)}-\frac{\frac{1}{T}\int_0^T\sin(\omega_k t)dN_G(t)}{\frac{1}{T}\int_0^T\cos(\omega_k t)dN_G(t)}\right]_{\omega=\omega_k}\right\}(\hat{\omega}_{k,T}-\omega_k)\\
=\;&\left\{\frac{d}{d\omega}\left[T^{\frac{1}{2}}\frac{-\frac{1}{T}\int_0^T\sin(\omega t)dN_G(t)}{\frac{1}{T}\int_0^T\cos(\omega t)dN_G(t)}\right]_{\omega=\omega_k}\right\}(\hat{\omega}_{k,T}-\omega_k)\\
=\;& T^{\frac{1}{2}}\left\{-\frac{T}{2}\frac{1+o(1)}{\cos^2(\phi_k)+o(1)}\right\}(\hat{\omega}_{k,T}-\omega_k)+o(1)\quad by\;\;(B.157)\\
=\;& -\frac{T^{\frac{3}{2}}}{2}\frac{1+o(1)}{\cos^2(\phi_k)+o(1)}(\hat{\omega}_{k,T}-\omega_k)+o(1). \qquad (B.158)
\end{aligned}$$

Therefore, from equation (2.12), equation (B.158) becomes

$$\begin{aligned}
&T^{\frac{1}{2}}\left\{\tan(\hat{\phi}_{k,T})+\frac{\frac{1}{T}\int_0^T\sin(\omega_k t)dN_G(t)}{\frac{1}{T}\int_0^T\cos(\omega_k t)dN_G(t)}\right\}\\
=\;& -\frac{12\kappa}{A_k\cos^2(\phi_k)}\left\{V_k\frac{1}{2}\sin(\phi_k)+W_k\frac{1}{2}\cos(\phi_k)-X_k\sin(\phi_k)-Y_k\cos(\phi_k)\right\}+o(1).\;(B.159)
\end{aligned}$$

We now combine equations (B.156) and (B.159) to establish the asymptotic form of

$T^{\frac{1}{2}}\{\tan(\hat{\phi}_{k,T})-\tan(\phi_k)\}$ for the particular case when $\phi_k \neq \pm\frac{\pi}{2}$. By equations (B.156) and (B.159), it follows that

$$T^{\frac{1}{2}}\left\{\tan(\hat{\phi}_{k,T}) - \tan(\phi_k)\right\}$$

$$= T^{\frac{1}{2}}\left\{\tan(\hat{\phi}_{k,T}) + \frac{\frac{1}{T}\int_0^T \sin(\omega_k t)dN_G(t)}{\frac{1}{T}\int_0^T \cos(\omega_k t)dN_G(t)}\right\} - \frac{2\kappa}{A_k\cos^2(\phi_k)+o(1)}\{\cos(\phi_k)W_k + \sin(\phi_k)V_k\}$$

$$\begin{aligned}
&= -\frac{12\kappa}{A_k\cos^2(\phi_k)}\left\{V_k\frac{1}{2}\sin(\phi_k) + W_k\frac{1}{2}\cos(\phi_k) - X_k\sin(\phi_k) - Y_k\cos(\phi_k)\right\} \\
&\quad -\frac{2\kappa}{A_k\cos^2(\phi_k)}\{\cos(\phi_k)W_k + \sin(\phi_k)V_k\} + o(1) \\
&= \frac{\kappa}{A_k\cos^2(\phi_k)}\{-8\sin(\phi_k)V_k - 8\cos(\phi_k)W_k + 12X_k\sin(\phi_k) + 12Y_k\cos(\phi_k)\} + o(1) \\
&= -\frac{4\kappa}{A_k\cos^2(\phi_k)}\{2\sin(\phi_k)V_k + 2\cos(\phi_k)W_k - 3X_k\sin(\phi_k) - 3Y_k\cos(\phi_k)\} + o(1). \quad \text{(B.160)}
\end{aligned}$$

We now use equation (B.160), to establish the asymptotic variance-covariance structure of $T^{\frac{1}{2}}\left\{\tan(\hat{\phi}_{k,T}) - \tan(\phi_k)\right\}$ and $T^{\frac{1}{2}}\left\{\tan(\hat{\phi}_{k',T}) - \tan(\phi_{k'})\right\}$, then we use Cramer's Theorem to find the asymptotic variance-covariance of $T^{\frac{1}{2}}\left\{\hat{\phi}_{k,T} - \phi_k\right\}$ and $T^{\frac{1}{2}}\left\{\hat{\phi}_{k',T} - \phi_{k'}\right\}$. We now establish the asymptotic covariance of (B.160).

$$\text{cov}\left\{T^{\frac{1}{2}}\left\{\tan(\hat{\phi}_{k,T}) - \tan(\phi_k)\right\},\ T^{\frac{1}{2}}\left\{\tan(\hat{\phi}_{k',T}) - \tan(\phi_{k'})\right\}\right\}$$

$$= \tfrac{16\kappa^2}{A_kA_{k'}\cos^2(\phi_k)\cos^2(\phi_{k'})}\{$$

$$\text{cov}\{2\sin(\phi_k)V_k + 2\cos(\phi_k)W_k - 3X_k\sin(\phi_k) - 3Y_k\cos(\phi_k),$$

$$2\sin(\phi_{k'})V_{k'} + 2\cos(\phi_{k'})W_{k'} - 3X_{k'}\sin(\phi_{k'}) - 3Y_{k'}\cos(\phi_{k'})\}\}$$

$$= \frac{16\kappa^2}{A_k A_{k'} \cos^2(\phi_k)\cos^2(\phi_{k'})}\{$$

$$\text{cov}\left\{2\sin(\phi_k)V_k,\ 2\sin(\phi_{k'})V_{k'}\right\} + \text{cov}\left\{2\sin(\phi_k)V_k,\ 2\cos(\phi_{k'})W_{k'}\right\}$$

$$+\text{cov}\left\{2\sin(\phi_k)V_k,\ -3X_{k'}\sin(\phi_{k'})\right\} + \text{cov}\left\{2\sin(\phi_k)V_k,\ -3Y_{k'}\cos(\phi_{k'})\right\}$$

$$+\text{cov}\left\{2\cos(\phi_k)W_k,\ 2\sin(\phi_{k'})V_{k'}\right\} + \text{cov}\left\{2\cos(\phi_k)W_k,\ 2\cos(\phi_{k'})W_{k'}\right\}$$

$$+\text{cov}\left\{2\cos(\phi_k)W_k,\ -3X_{k'}\sin(\phi_{k'})\right\} + \text{cov}\left\{2\cos(\phi_k)W_k,\ -3Y_{k'}\cos(\phi_{k'})\right\}$$

$$+\text{cov}\left\{-3X_k\sin(\phi_k),\ 2\sin(\phi_{k'})V_{k'}\right\} + \text{cov}\left\{-3X_k\sin(\phi_k),\ 2\cos(\phi_{k'})W_{k'}\right\}$$

$$+\text{cov}\left\{-3X_k\sin(\phi_k),\ -3X_{k'}\sin(\phi_{k'})\right\} + \text{cov}\left\{-3X_k\sin(\phi_k),\ -3Y_{k'}\cos(\phi_{k'})\right\}$$

$$+\text{cov}\left\{-3Y_k\cos(\phi_k),\ 2\sin(\phi_{k'})V_{k'}\right\} + \text{cov}\left\{-3Y_k\cos(\phi_k),\ 2\cos(\phi_{k'})W_{k'}\right\}$$

$$+\text{cov}\left\{-3Y_k\cos(\phi_k),\ -3X_{k'}\sin(\phi_{k'})\right\} + \text{cov}\left\{-3Y_k\cos(\phi_k),\ -3Y_{k'}\cos(\phi_{k'})\right\}\}$$

$$= \frac{16\kappa^2}{A_k A_{k'} \cos^2(\phi_k)\cos^2(\phi_{k'})}\{$$

$$4\sin(\phi_k)\sin(\phi_{k'})\mathrm{cov}\{V_k,\ V_{k'}\} + 4\sin(\phi_k)\cos(\phi_{k'})\mathrm{cov}\{V_k,\ W_{k'}\}$$

$$-6\sin(\phi_k)\sin(\phi_{k'})\mathrm{cov}\{V_k,\ X_{k'}\} - 6\sin(\phi_k)\cos(\phi_{k'})\mathrm{cov}\{V_k,\ Y_{k'}\}$$

$$+4\cos(\phi_k)\sin(\phi_{k'})\mathrm{cov}\{W_k,\ V_{k'}\} + 4\cos(\phi_k)\cos(\phi_{k'})\mathrm{cov}\{W_k,\ W_{k'}\}$$

$$-6\cos(\phi_k)\sin(\phi_{k'})\mathrm{cov}\{W_k,\ X_{k'}\} - 6\cos(\phi_k)\cos(\phi_{k'})\mathrm{cov}\{W_k,\ Y_{k'}\}$$

$$-6\sin(\phi_k)\sin(\phi_{k'})\mathrm{cov}\{X_k,\ V_{k'}\} - 6\sin(\phi_k)\cos(\phi_{k'})\mathrm{cov}\{X_k,\ W_{k'}\}$$

$$+9\sin(\phi_k)\sin(\phi_{k'})\mathrm{cov}\{X_k,\ X_{k'}\} + 9\sin(\phi_k)\cos(\phi_{k'})\mathrm{cov}\{X_k,\ Y_{k'}\}$$

$$-6\cos(\phi_k)\sin(\phi_{k'})\mathrm{cov}\{Y_k,\ V_{k'}\} - 6\cos(\phi_k)\cos(\phi_{k'})\mathrm{cov}\{Y_k,\ W_{k'}\}$$

$$+9\cos(\phi_k)\sin(\phi_{k'})\mathrm{cov}\{Y_k,\ X_{k'}\} + 9\cos(\phi_k)\cos(\phi_{k'})\mathrm{cov}\{Y_k,\ Y_{k'}\}\}$$

$$= \frac{16\kappa^2}{A_k A_{k'} \cos^2(\phi_k)\cos^2(\phi_{k'})}\{$$

$$4\sin(\phi_k)\sin(\phi_{k'})\left[\frac{1}{4\kappa^2}\sum_{j=1}^{K}A_j\cos(\phi_j)\left\{\delta_{j,\ k+k'}+\delta_{j,\ k-k'}+\delta_{j,\ k'-k}\right\}+\frac{B}{2\kappa^2}\delta_{k,\ k'}\right] \tag{B.161}$$

$$+4\sin(\phi_k)\cos(\phi_{k'})\frac{1}{4\kappa^2}\sum_{j=1}^{K}A_j\sin(\phi_j)\left\{-\delta_{j,k+k'}+\delta_{j,k-k'}-\delta_{j,k'-k}\right\} \tag{B.162}$$

$$-6\sin(\phi_k)\sin(\phi_{k'})\left[\frac{1}{8\kappa^2}\sum_{j=1}^{K}A_j\cos(\phi_j)\left\{\delta_{j,k+k'}+\delta_{j,k-k'}+\delta_{j,k'-k}\right\}+\frac{B}{4\kappa^2}\delta_{k,k'}\right] \tag{B.163}$$

$$-6\sin(\phi_k)\cos(\phi_{k'})\frac{1}{8\kappa^2}\sum_{j=1}^{K}A_j\sin(\phi_j)\left\{-\delta_{j,\ k+k'}+\delta_{j,\ k-k'}-\delta_{j,\ k'-k}\right\} \tag{B.164}$$

$$+4\cos(\phi_k)\sin(\phi_{k'})\frac{1}{4\kappa^2}\sum_{j=1}^{K}A_j\sin(\phi_j)\left\{-\delta_{j,k'+k}+\delta_{j,k'-k}-\delta_{j,k-k'}\right\} \tag{B.165}$$

$$+4\cos(\phi_k)\cos(\phi_{k'})\left[\frac{1}{4\kappa^2}\sum_{j=1}^{K}A_j\cos(\phi_j)\left\{-\delta_{j,k'+k}+\delta_{j,k-k'}+\delta_{j,k'-k}\right\}+\frac{B}{2\kappa^2}\delta_{k,k'}\right] \tag{B.166}$$

$$-6\cos(\phi_k)\sin(\phi_{k'})\frac{1}{8\kappa^2}\sum_{j=1}^{K}A_j\sin(\phi_j)\left\{-\delta_{j,\ k+k'}+\delta_{j,\ k'-k}-\delta_{j,\ k-k'}\right\} \tag{B.167}$$

$$- 6\cos(\phi_k)\cos(\phi_{k'})\left[\frac{1}{8\kappa^2}\sum_{j=1}^{K} A_j\cos(\phi_j)\left\{-\delta_{j,\,k+k'}+\delta_{j,\,k-k'}+\delta_{j,\,k'-k}\right\}+\frac{B}{4\kappa^2}\delta_{k,\,k'}\right] \tag{B.168}$$

$$- 6\sin(\phi_k)\sin(\phi_{k'})\left[\frac{1}{8\kappa^2}\sum_{j=1}^{K} A_j\cos(\phi_j)\left\{\delta_{j,k'+k}+\delta_{j,k'-k}+\delta_{j,k-k'}\right\}+\frac{B}{4\kappa^2}\delta_{k,k'}\right] \tag{B.169}$$

$$- 6\sin(\phi_k)\cos(\phi_{k'})\frac{1}{8\kappa^2}\sum_{j=1}^{K} A_j\sin(\phi_j)\left\{-\delta_{j,\,k'+k}+\delta_{j,\,k-k'}-\delta_{j,\,k'-k}\right\} \tag{B.170}$$

$$+9\sin(\phi_k)\sin(\phi_{k'})\left[\frac{1}{12\kappa^2}\sum_{j=1}^{K} A_j\cos(\phi_j)\left\{\delta_{j,\,k+k'}+\delta_{j,\,k-k'}+\delta_{j,\,k'-k}\right\}+\frac{B}{6\kappa^2}\delta_{k,k'}\right] \tag{B.171}$$

$$+ 9\sin(\phi_k)\cos(\phi_{k'})\frac{1}{12\kappa^2}\sum_{j=1}^{K} A_j\sin(\phi_j)\left\{-\delta_{j,\,k+k'}+\delta_{j,\,k-k'}-\delta_{j,\,k'-k}\right\} \tag{B.172}$$

$$- 6\cos(\phi_k)\sin(\phi_{k'})\frac{1}{8\kappa^2}\sum_{j=1}^{K} A_j\sin(\phi_j)\left\{-\delta_{j,\,k'+k}+\delta_{j,\,k'-k}-\delta_{j,\,k-k'}\right\} \tag{B.173}$$

$$- 6\cos(\phi_k)\cos(\phi_{k'})\left[\frac{1}{8\kappa^2}\sum_{j=1}^{K} A_j\cos(\phi_j)\left\{-\delta_{j,\,k'+k} + \delta_{j,\,k'-k} + \delta_{j,\,k-k'}\right\} + \frac{B}{4\kappa^2}\delta_{k,\,k'}\right] \tag{B.174}$$

$$+ 9\cos(\phi_k)\sin(\phi_{k'})\frac{1}{12\kappa^2}\sum_{j=1}^{K} A_j\sin(\phi_j)\left\{-\delta_{j,\,k'+k} + \delta_{j,\,k'-k} - \delta_{j,\,k-k'}\right\} \tag{B.175}$$

$$+ 9\cos(\phi_k)\cos(\phi_{k'})\left[\frac{1}{12\kappa^2}\sum_{j=1}^{K} A_j\cos(\phi_j)\left\{-\delta_{j,\,k+k'} + \delta_{j,\,k-k'} + \delta_{j,\,k'-k}\right\} + \frac{B}{6\kappa^2}\delta_{k,k'}\right]\}. \tag{B.176}$$

Next we combine equations (B.161), (B.163), (B.169), and (B.171). Also, we combine equations (B.162), (B.164), (B.170), and (B.172). Also, we combine equations (B.165), (B.167), (B.173), and (B.175). Lastly, we combine equations (B.166), (B.168), (B.174), and (B.176).

$= \frac{16\kappa^2}{A_k A_{k'}\cos^2(\phi_k)\cos^2(\phi_{k'})}\{$

$$\sin(\phi_k)\sin(\phi_{k'})\left[\frac{1}{4\kappa^2}\sum_{j=1}^{K} A_j\cos(\phi_j)\left\{\delta_{j,\,k+k'} + \delta_{j,\,k-k'} + \delta_{j,\,k'-k}\right\} + \frac{B}{2\kappa^2}\delta_{k,\,k'}\right] \tag{B.177}$$

$$+ \sin(\phi_k)\cos(\phi_{k'})\frac{1}{4\kappa^2}\sum_{j=1}^{K} A_j\sin(\phi_j)\left\{-\delta_{j,k+k'} + \delta_{j,k-k'} - \delta_{j,k'-k}\right\} \tag{B.178}$$

$$+\cos(\phi_k)\sin(\phi_{k'})\left[\frac{1}{4\kappa^2}\sum_{j=1}^{K}A_j\sin(\phi_j)\left\{-\delta_{j,k'+k}+\delta_{j,k'-k}-\delta_{j,k-k'}\right\}\right] \tag{B.179}$$

$$+\cos(\phi_k)\cos(\phi_{k'})\left[\frac{1}{4\kappa^2}\sum_{j=1}^{K}A_j\cos(\phi_j)\left\{-\delta_{j,k'+k}+\delta_{j,k-k'}+\delta_{j,k'-k}\right\}+\frac{B}{2\kappa^2}\delta_{k,k'}\right]\Big\} \tag{B.180}$$

$$=\tfrac{16\kappa^2}{A_kA_{k'}\cos^2(\phi_k)\cos^2(\phi_{k'})}\Big\{$$

$$\sin(\phi_k)\sin(\phi_{k'})\frac{B}{2\kappa}\delta_{k,\,k'}+\cos(\phi_k)\cos(\phi_{k'})\frac{B}{2\kappa^2}\delta_{k,k'}$$

$$-\frac{1}{16\kappa^2}\sum_{j=1}^{K}A_j\cos\left(-\phi_k-\phi_{k'}+\phi_j\right)\delta_{j,\,k+k'}$$

$$+\frac{1}{4\kappa^2}\sum_{j=1}^{K}A_j\frac{1}{4}\{-\cos\left(\phi_k+\phi_{k'}+\phi_j\right)+\cos\left(-\phi_k+\phi_{k'}+\phi_j\right)+\cos\left(\phi_k-\phi_{k'}+\phi_j\right)$$
$$-\cos\left(-\phi_k-\phi_{k'}+\phi_j\right)\}\left\{\delta_{j,\,k-k'}+\delta_{j,\,k'-k}\right\} \tag{B.181}$$

$$+\frac{1}{4\kappa^2}\sum_{j=1}^{K}A_j\frac{1}{4}\{-\cos\left(\phi_k+\phi_{k'}+\phi_j\right)+\cos\left(-\phi_k+\phi_{k'}+\phi_j\right)-\cos\left(\phi_k-\phi_{k'}+\phi_j\right)$$
$$+\cos\left(-\phi_k-\phi_{k'}+\phi_j\right)\}\left\{\delta_{j,k-k'}-\delta_{j,k'-k}\right\} \tag{B.182}$$

$$+\frac{1}{4\kappa^2}\sum_{j=1}^{K} A_j \frac{1}{4}\{-\cos(\phi_k+\phi_{k'}+\phi_j)-\cos(-\phi_k+\phi_{k'}+\phi_j)+\cos(\phi_k-\phi_{k'}+\phi_j)$$

$$+\cos(-\phi_k-\phi_{k'}+\phi_j)\}\left\{\delta_{j,k'-k}-\delta_{j,k-k'}\right\} \tag{B.183}$$

$$+\frac{1}{4\kappa^2}\sum_{j=1}^{K} A_j \frac{1}{4}\{\cos(\phi_k+\phi_{k'}+\phi_j)+\cos(-\phi_k+\phi_{k'}+\phi_j)+\cos(\phi_k-\phi_{k'}+\phi_j)$$

$$+\cos(-\phi_k-\phi_{k'}+\phi_j)\}\left\{\delta_{j,k-k'}+\delta_{j,k'-k}\right\}\} \tag{B.184}$$

$= \frac{16\kappa^2}{A_k A_{k'}\cos^2(\phi_k)\cos^2(\phi_{k'})}\{$

$$\cos(\phi_k-\phi_{k'})\frac{B}{2\kappa^2}\delta_{k,k'}$$

$$-\frac{1}{4\kappa^2}\sum_{j=1}^{K} A_j\cos(-\phi_k-\phi_{k'}+\phi_j)\,\delta_{j,\,k+k'}$$

$$+\frac{1}{4\kappa^2}\sum_{j=1}^{K} A_j\cos(-\phi_k+\phi_{k'}+\phi_j)\,\delta_{j,\,k-k'}$$

$$+\frac{1}{16\kappa^2}\sum_{j=1}^{K} A_j\{-\cos(\phi_k+\phi_{k'}+\phi_j)+\cos(-\phi_k+\phi_{k'}+\phi_j)+\cos(\phi_k-\phi_{k'}+\phi_j)$$

$$-\cos(-\phi_k-\phi_{k'}+\phi_j)\}\delta_{j,\,k'-k} \tag{B.185}$$

$$+\frac{1}{16\kappa^2}\sum_{j=1}^{K} A_j\{-\cos(\phi_k+\phi_{k'}+\phi_j)+\cos(-\phi_k+\phi_{k'}+\phi_j)-\cos(\phi_k-\phi_{k'}+\phi_j)$$

$$+\cos(-\phi_k-\phi_{k'}+\phi_j)\}\left\{-\delta_{j,k'-k}\right\} \quad \text{(B.186)}$$

$$+\frac{1}{16\kappa^2}\sum_{j=1}^{K} A_j\{-\cos(\phi_k+\phi_{k'}+\phi_j)-\cos(-\phi_k+\phi_{k'}+\phi_j)+\cos(\phi_k-\phi_{k'}+\phi_j)$$

$$+\cos(-\phi_k-\phi_{k'}+\phi_j)\}\delta_{j,k'-k} \quad \text{(B.187)}$$

$$+\frac{1}{16\kappa^2}\sum_{j=1}^{K} A_j\{\cos(\phi_k+\phi_{k'}+\phi_j)+\cos(-\phi_k+\phi_{k'}+\phi_j)+\cos(\phi_k-\phi_{k'}+\phi_j)$$

$$+\cos(-\phi_k-\phi_{k'}+\phi_j)\}\delta_{j,k'-k}\} \quad \text{(B.188)}$$

$$= \tfrac{16\kappa^2}{A_k A_{k'}\cos^2(\phi_k)\cos^2(\phi_{k'})}\{$$

$$\cos(\phi_k-\phi_{k'})\frac{B}{2\kappa^2}\delta_{k,k'}-\frac{1}{4\kappa^2}\sum_{j=1}^{K} A_j\cos(-\phi_k-\phi_{k'}+\phi_j)\,\delta_{j,\,k+k'}$$

$$+\frac{1}{4\kappa^2}\sum_{j=1}^{K} A_j\cos(-\phi_k+\phi_{k'}+\phi_j)\,\delta_{j,\,k-k'}+\frac{1}{4\kappa^2}\sum_{j=1}^{K} A_j\cos(\phi_k-\phi_{k'}+\phi_j)\,\delta_{j,\,k'-k}\}.$$

Therefore, we have

$$\lim_{T\to\infty} \operatorname{cov}\left\{T^{\frac{1}{2}}\left\{\tan(\hat{\phi}_{k,T}) - \tan(\phi_k)\right\},\ T^{\frac{1}{2}}\left\{\tan(\hat{\phi}_{k',T}) - \tan(\phi_{k'})\right\}\right\}$$
$$= \tfrac{8}{A_k A_{k'} \cos^2(\phi_k)\cos^2(\phi_{k'})}\{\cos(\phi_k - \phi_{k'})B\delta_{k,k'} + \tfrac{1}{2}\textstyle\sum_{j=1}^{K} A_j[-\cos\left(-\phi_k - \phi_{k'} + \phi_j\right)\delta_{j,\ k+k'}$$

$$+\cos\left(-\phi_k + \phi_{k'} + \phi_j\right)\delta_{j,\ k-k'} + \cos\left(\phi_k - \phi_{k'} + \phi_j\right)\delta_{j,\ k'-k}]\}.$$

It then follows from Cramer's Theorem with $f(x,y) = [\tan^{-1}(x),\ \tan^{-1}(y)]$, $\mathring{f}(x,y) = \begin{bmatrix} \frac{1}{x^2+1} & 0 \\ 0 & \frac{1}{y^2+1} \end{bmatrix}$, and

$$\begin{aligned}
\mathring{f}(\tan(\phi_k),\ \tan(\phi_{k'})) &= \begin{bmatrix} \frac{1}{(\tan(\phi_k))^2+1} & 0 \\ 0 & \frac{1}{(\tan(\phi_{k'}))^2+1} \end{bmatrix} \\
&= \begin{bmatrix} \frac{1}{\left(\frac{\sin(\phi_k)}{\cos(\phi_k)}\right)^2+1} & 0 \\ 0 & \frac{1}{\left(\frac{\sin(\phi_{k'})}{\cos(\phi_{k'})}\right)^2+1} \end{bmatrix} \\
&= \begin{bmatrix} \cos^2(\phi_k) & 0 \\ 0 & \cos^2(\phi_{k'}) \end{bmatrix},
\end{aligned}$$

that $\lim_{T\to\infty} \operatorname{cov}\left\{T^{\frac{1}{2}}\left\{\hat{\phi}_{k,T} - \phi_k\right\},\ T^{\frac{1}{2}}\left\{\hat{\phi}_{k',T} - \phi_{k'}\right\}\right\}$

$$= \lim_{T\to\infty} \cos^2(\phi_k)\operatorname{cov}\left\{T^{\frac{1}{2}}\left\{\tan(\hat{\phi}_{k,T}) - \tan(\phi_k)\right\},\ T^{\frac{1}{2}}\left\{\tan(\hat{\phi}_{k',T}) - \tan(\phi_{k'})\right\}\right\}\cos^2(\phi_{k'})$$
$$= \tfrac{4}{A_k A_{k'}}\{\cos(\phi_k - \phi_{k'})2B\delta_{k,k'} + \textstyle\sum_{j=1}^{K} A_j[-\cos\left(-\phi_k - \phi_{k'} + \phi_j\right)\delta_{j,\ k+k'}$$

$$+\cos\left(-\phi_k + \phi_{k'} + \phi_j\right)\delta_{j,\ k-k'} + \cos\left(\phi_k - \phi_{k'} + \phi_j\right)\delta_{j,\ k'-k}]\}. \tag{B.189}$$

We now consider the case when $\phi_k = -\frac{\pi}{2}$ or $\phi_k = \frac{\pi}{2}$. From the useful integral section of Appendix B and the Chapter 2 Lemma 8, it is clear that $\frac{1}{T}\int_0^T \cos(\hat{\phi}_{k,T}t)dN_G(t)$ $\to 0$ as $T \to \infty$ and $-\frac{1}{T}\int_0^T \sin(\hat{\phi}_{k,T}t)dN_G(t) \to \frac{A_k}{2\kappa}\sin(\phi_k)$ as $T \to \infty$. So as $T \to \infty$ and $\phi_k \to \frac{\pi}{2}$, $\hat{\phi}_{k,T} = \tan^{-1}(\frac{-\frac{1}{T}\int_0^T \sin(\hat{\phi}_{k,T}t)dN_G(t)}{\frac{1}{T}\int_0^T \cos(\hat{\phi}_{k,T}t)dN_G(t)}) \to \frac{\pi}{2}$, and similar results apply to the case when $\phi_k \to -\frac{\pi}{2}$. So $\hat{\phi}_{k,T}$ is a consistent estimator of ϕ_k when $\phi_k = -\frac{\pi}{2}$ or $\phi_k = \frac{\pi}{2}$, and the asymptotic covariance of equation (B.189) holds when $\phi_k = -\frac{\pi}{2}$ or $\phi_k = \frac{\pi}{2}$. □

B.1.1.9 Proof of Proposition 15

Proof. We begin by quoting Cramer's Theorem which will be used throughout this proof. Let g be a mapping $g: \mathbb{R}^d \to \mathbb{R}^k$ such that $\dot{g}(x)$ is continuous in a neighborhood of $\mu \in \mathbb{R}^d$. If X_n is a sequence of d-dimensional random vectors such that $\sqrt{n}\,(X_n - \mu) \xrightarrow{\mathcal{L}} X$, then $\sqrt{n}\,(g(X_n) - g(\mu)) \xrightarrow{\mathcal{L}} \dot{g}(\mu)X$ (Ferguson (1996, pg. 45)). We now establish the variance-covariance of the parameter estimators.

We begin by establishing the asymptotic covariance of

$$\mathrm{cov}\{T^{\frac{3}{2}}\,(\hat{\omega}_{k,T} - \omega_k)\,,\ T^{\frac{1}{2}}\{\hat{\phi}_{k',T} - \phi_{k'}\}\}.$$

From equations (2.12) and (2.25), we have

$$\mathrm{cov}\left\{T^{\frac{3}{2}}\left(\hat{\omega}_{k,T}-\omega_k\right),\ T^{\frac{1}{2}}\left\{\tan(\hat{\phi}_{k',T})-\tan(\phi_{k'})\right\}\right\}$$

$$\begin{aligned}
= \quad & \mathrm{cov}\{\frac{24\kappa}{A_k}\left\{V_k\frac{1}{2}\sin(\phi_k)+W_k\frac{1}{2}\cos(\phi_k)-X_k\sin(\phi_k)-Y_k\cos(\phi_k)\right\}, \\
& -\frac{4\kappa}{A_{k'}\cos^2(\phi_{k'})}\left\{2\sin(\phi_{k'})V_{k'}+2\cos(\phi_{k'})W_{k'}-3X_{k'}\sin(\phi_{k'})-3Y_{k'}\cos(\phi_{k'})\right\}\} \\
& +o(1)
\end{aligned}$$

$= \frac{-96\kappa^2}{A_kA_{k'}\cos^2(\phi_{k'})}\{$

$$\mathrm{cov}\{V_k\frac{1}{2}\sin(\phi_k)+W_k\frac{1}{2}\cos(\phi_k)-X_k\sin(\phi_k)-Y_k\cos(\phi_k),$$

$$2\sin(\phi_{k'})V_{k'}+2\cos(\phi_{k'})W_{k'}-3X_{k'}\sin(\phi_{k'})-3Y_{k'}\cos(\phi_{k'})\}+o(1)$$

$= \frac{-96\kappa^2}{A_kA_{k'}\cos^2(\phi_{k'})}\{$

$$\sin(\phi_k)\sin(\phi_{k'})\mathrm{cov}\left\{V_k,\ V_{k'}\right\}+\sin(\phi_k)\cos(\phi_{k'})\mathrm{cov}\left\{V_k,\ W_{k'}\right\}$$

$$-\frac{3}{2}\sin(\phi_k)\sin(\phi_{k'})\mathrm{cov}\left\{V_k,\ X_{k'}\right\}-\frac{3}{2}\sin(\phi_k)\cos(\phi_{k'})\mathrm{cov}\left\{V_k,\ Y_{k'}\right\}$$

$$+\cos(\phi_k)\sin(\phi_{k'})\mathrm{cov}\left\{W_k,\ V_{k'}\right\}+\cos(\phi_k)\cos(\phi_{k'})\mathrm{cov}\left\{W_k,\ W_{k'}\right\}$$

$$-\frac{3}{2}\cos(\phi_k)\sin(\phi_{k'})\mathrm{cov}\left\{W_k,\ X_{k'}\right\}-\frac{3}{2}\cos(\phi_k)\cos(\phi_{k'})\mathrm{cov}\left\{W_k,\ Y_{k'}\right\}$$

$$-2\sin(\phi_k)\sin(\phi_{k'})\mathrm{cov}\left\{X_k,\ V_{k'}\right\}-2\sin(\phi_k)\cos(\phi_{k'})\mathrm{cov}\left\{X_k,\ W_{k'}\right\}$$

$$+3\sin(\phi_k)\sin(\phi_{k'})\mathrm{cov}\left\{X_k,\ X_{k'}\right\}+3\sin(\phi_k)\cos(\phi_{k'})\mathrm{cov}\left\{X_k,\ Y_{k'}\right\}$$

$$-2\cos(\phi_k)\sin(\phi_{k'})\mathrm{cov}\left\{Y_k,\ V_{k'}\right\}-2\cos(\phi_k)\cos(\phi_{k'})\mathrm{cov}\left\{Y_k,\ W_{k'}\right\}$$

$$+3\cos(\phi_k)\sin(\phi_{k'})\mathrm{cov}\left\{Y_k,\ X_{k'}\right\}+3\cos(\phi_k)\cos(\phi_{k'})\mathrm{cov}\left\{Y_k,\ Y_{k'}\right\}\}+o(1).$$

From Proposition 10, it then follows that

$$\lim_{T\to\infty}\mathrm{cov}\left\{T^{\frac{3}{2}}\left(\hat{\omega}_{k,T}-\omega_k\right),\ T^{\frac{1}{2}}\left\{\tan(\hat{\phi}_{k',T})-\tan(\phi_{k'})\right\}\right\}=\tfrac{-96\kappa^2}{A_kA_{k'}\cos^2(\phi_{k'})}\{$$

$$\sin(\phi_k)\sin(\phi_{k'})\left[\frac{1}{4\kappa^2}\sum_{j=1}^{K}A_j\cos(\phi_j)\left\{\delta_{j,\ k+k'}+\delta_{j,\ k-k'}+\delta_{j,\ k'-k}\right\}+\frac{B}{2\kappa^2}\delta_{k,\ k'}\right]\tag{B.190}$$

$$+\sin(\phi_k)\cos(\phi_{k'})\frac{1}{4\kappa^2}\sum_{j=1}^{K}A_j\sin(\phi_j)\left\{-\delta_{j,k+k'}+\delta_{j,k-k'}-\delta_{j,k'-k}\right\}\tag{B.191}$$

$$-\frac{3}{2}\sin(\phi_k)\sin(\phi_{k'})\left[\frac{1}{8\kappa^2}\sum_{j=1}^{K}A_j\cos(\phi_j)\left\{\delta_{j,k+k'}+\delta_{j,k-k'}+\delta_{j,k'-k}\right\}+\frac{B}{4\kappa^2}\delta_{k,k'}\right]\tag{B.192}$$

$$-\frac{3}{2}\sin(\phi_k)\cos(\phi_{k'})\frac{1}{8\kappa^2}\sum_{j=1}^{K}A_j\sin(\phi_j)\left\{-\delta_{j,\ k+k'}+\delta_{j,\ k-k'}-\delta_{j,\ k'-k}\right\}\tag{B.193}$$

$$+\cos(\phi_k)\sin(\phi_{k'})\frac{1}{4\kappa^2}\sum_{j=1}^{K}A_j\sin(\phi_j)\left\{-\delta_{j,k'+k}+\delta_{j,k'-k}-\delta_{j,k-k'}\right\} \tag{B.194}$$

$$+\cos(\phi_k)\cos(\phi_{k'})\left[\frac{1}{4\kappa^2}\sum_{j=1}^{K}A_j\cos(\phi_j)\left\{-\delta_{j,k'+k}+\delta_{j,k-k'}+\delta_{j,k'-k}\right\}+\frac{B}{2\kappa^2}\delta_{k,k'}\right] \tag{B.195}$$

$$-\frac{3}{2}\cos(\phi_k)\sin(\phi_{k'})\frac{1}{8\kappa^2}\sum_{j=1}^{K}A_j\sin(\phi_j)\left\{-\delta_{j,\,k+k'}+\delta_{j,\,k'-k}-\delta_{j,\,k-k'}\right\} \tag{B.196}$$

$$-\frac{3}{2}\cos(\phi_k)\cos(\phi_{k'})\left[\frac{1}{8\kappa^2}\sum_{j=1}^{K}A_j\cos(\phi_j)\left\{-\delta_{j,\,k+k'}+\delta_{j,\,k-k'}+\delta_{j,\,k'-k}\right\}+\frac{B}{4\kappa^2}\delta_{k,\,k'}\right] \tag{B.197}$$

$$-2\sin(\phi_k)\sin(\phi_{k'})\left[\frac{1}{8\kappa^2}\sum_{j=1}^{K}A_j\cos(\phi_j)\left\{\delta_{j,k'+k}+\delta_{j,k'-k}+\delta_{j,k-k'}\right\}+\frac{B}{4\kappa^2}\delta_{k,k'}\right] \tag{B.198}$$

$$-2\sin(\phi_k)\cos(\phi_{k'})\frac{1}{8\kappa^2}\sum_{j=1}^{K}A_j\sin(\phi_j)\left\{-\delta_{j,\,k'+k}+\delta_{j,\,k-k'}-\delta_{j,\,k'-k}\right\} \tag{B.199}$$

$$+3\sin(\phi_k)\sin(\phi_{k'})\left[\frac{1}{12\kappa^2}\sum_{j=1}^{K}A_j\cos(\phi_j)\left\{\delta_{j,\,k+k'}+\delta_{j,\,k-k'}+\delta_{j,\,k'-k}\right\}+\frac{B}{6\kappa^2}\delta_{k,k'}\right] \tag{B.200}$$

$$+3\sin(\phi_k)\cos(\phi_{k'})\frac{1}{12\kappa^2}\sum_{j=1}^{K}A_j\sin(\phi_j)\left\{-\delta_{j,\,k+k'}+\delta_{j,\,k-k'}-\delta_{j,\,k'-k}\right\} \tag{B.201}$$

$$-2\cos(\phi_k)\sin(\phi_{k'})\frac{1}{8\kappa^2}\sum_{j=1}^{K}A_j\sin(\phi_j)\left\{-\delta_{j,\,k'+k}+\delta_{j,\,k'-k}-\delta_{j,\,k-k'}\right\} \tag{B.202}$$

$$-2\cos(\phi_k)\cos(\phi_{k'})\left[\frac{1}{8\kappa^2}\sum_{j=1}^{K}A_j\cos(\phi_j)\left\{-\delta_{j,\,k'+k}+\delta_{j,\,k'-k}+\delta_{j,\,k-k'}\right\}+\frac{B}{4\kappa^2}\delta_{k,\,k'}\right] \tag{B.203}$$

$$+3\cos(\phi_k)\sin(\phi_{k'})\frac{1}{12\kappa^2}\sum_{j=1}^{K}A_j\sin(\phi_j)\left\{-\delta_{j,\,k'+k}+\delta_{j,\,k'-k}-\delta_{j,\,k-k'}\right\} \tag{B.204}$$

$$+3\cos(\phi_k)\cos(\phi_{k'})\left[\frac{1}{12\kappa^2}\sum_{j=1}^{K}A_j\cos(\phi_j)\left\{-\delta_{j,\,k+k'}+\delta_{j,\,k-k'}+\delta_{j,\,k'-k}\right\}+\frac{B}{6\kappa^2}\delta_{k,k'}\right]\}. \tag{B.205}$$

After combining equations (B.190) and (B.198), equations (B.191) and (B.199), equations (B.192) and (B.200), equations (B.193) and (B.201), equations (B.194) (B.196) (B.202) (B.204), and equations (B.195) (B.197) (B.203) (B.205), from the useful trigonometric identity section of Appendix B we have

$\lim_{T\to\infty}\operatorname{cov}\left\{T^{\frac{3}{2}}\left(\hat{\omega}_{k,T}-\omega_k\right),\ T^{\frac{1}{2}}\left\{\tan(\hat{\phi}_{k',T})-\tan(\phi_{k'})\right\}\right\}=\frac{-96\kappa^2}{A_kA_{k'}\cos^2(\phi_{k'})}\{$

$$\sin(\phi_k)\sin(\phi_{k'})\left[\frac{1}{16\kappa^2}\sum_{j=1}^{K}A_j\cos(\phi_j)\left\{\delta_{j,k+k'}+\delta_{j,k-k'}+\delta_{j,k'-k}\right\}+\frac{B}{8\kappa^2}\delta_{k,k'}\right] \tag{B.206}$$

$$+\sin(\phi_k)\cos(\phi_{k'})\frac{1}{16\kappa^2}\sum_{j=1}^{K}A_j\sin(\phi_j)\left\{-\delta_{j,\,k+k'}+\delta_{j,\,k-k'}-\delta_{j,\,k'-k}\right\} \tag{B.207}$$

$$+\cos(\phi_k)\sin(\phi_{k'})\frac{1}{16\kappa^2}\sum_{j=1}^{K}A_j\sin(\phi_j)\left\{-\delta_{j,k'+k}+\delta_{j,k'-k}-\delta_{j,k-k'}\right\} \tag{B.208}$$

$$+\cos(\phi_k)\cos(\phi_{k'})\left[\frac{1}{16\kappa^2}\sum_{j=1}^{K}A_j\cos(\phi_j)\left\{-\delta_{j,k'+k}+\delta_{j,k-k'}+\delta_{j,k'-k}\right\}+\frac{B}{8\kappa^2}\delta_{k,k'}\right] \tag{B.209}$$

$$=\tfrac{-6}{A_kA_{k'}\cos^2(\phi_{k'})}\{2B\cos(\phi_k-\phi_{k'})\delta_{k,k'}$$

$$+\sum_{j=1}^{K}A_j\frac{1}{4}\{-\cos(\phi_k+\phi_{k'}+\phi_j)+\cos(-\phi_k+\phi_{k'}+\phi_j)+\cos(\phi_k-\phi_{k'}+\phi_j)$$
$$-\cos(-\phi_k-\phi_{k'}+\phi_j)\}\left\{\delta_{j,k+k'}+\delta_{j,k-k'}+\delta_{j,k'-k}\right\} \tag{B.210}$$

$$+\sum_{j=1}^{K}A_j\frac{1}{4}\{-\cos(\phi_k+\phi_{k'}+\phi_j)+\cos(-\phi_k+\phi_{k'}+\phi_j)-\cos(\phi_k-\phi_{k'}+\phi_j)$$
$$+\cos(-\phi_k-\phi_{k'}+\phi_j)\}\left\{-\delta_{j,\,k+k'}+\delta_{j,\,k-k'}-\delta_{j,\,k'-k}\right\} \tag{B.211}$$

$$+\sum_{j=1}^{K}A_j\frac{1}{4}\{-\cos(\phi_k+\phi_{k'}+\phi_j)-\cos(-\phi_k+\phi_{k'}+\phi_j)+\cos(\phi_k-\phi_{k'}+\phi_j)$$
$$+\cos(-\phi_k-\phi_{k'}+\phi_j)\}\left\{-\delta_{j,k'+k}+\delta_{j,k'-k}-\delta_{j,k-k'}\right\} \tag{B.212}$$

$$+\sum_{j=1}^{K} A_j \frac{1}{4}\{\cos(\phi_k + \phi_{k'} + \phi_j) + \cos(-\phi_k + \phi_{k'} + \phi_j) + \cos(\phi_k - \phi_{k'} + \phi_j)$$
$$+\cos(-\phi_k - \phi_{k'} + \phi_j)\}\left\{-\delta_{j,k'+k} + \delta_{j,k-k'} + \delta_{j,k'-k}\right\} \tag{B.213}$$

$$= \frac{-6}{A_k A_{k'} \cos^2(\phi_{k'})}\{2B\cos(\phi_k - \phi_{k'})\delta_{k,k'} - \textstyle\sum_{j=1}^{K} A_j \cos(-\phi_k - \phi_{k'} + \phi_j)\,\delta_{j,k+k'}$$

$$+\sum_{j=1}^{K} A_j \cos(-\phi_k + \phi_{k'} + \phi_j)\,\delta_{j,k-k'} + \sum_{j=1}^{K} A_j \cos(\phi_k - \phi_{k'} + \phi_j)\,\delta_{j,k'-k}\}.$$

It then follows from Cramer's Theorem with $f(x,y) = [x,\ \tan^{-1}(y)]$, $\mathring{f}(x,y) = \begin{bmatrix} 1 & 0 \\ 0 & \frac{1}{y^2+1} \end{bmatrix}$, and

$$\begin{aligned}
\mathring{f}(\omega_k,\ \tan^{-1}(\phi_{k'})) &= \begin{bmatrix} 1 & 0 \\ 0 & \frac{1}{(\tan(\phi_{k'}))^2+1} \end{bmatrix} \\
&= \begin{bmatrix} 1 & 0 \\ 0 & \frac{1}{\left(\frac{\sin(\phi_{k'})}{\cos(\phi_{k'})}\right)^2+1} \end{bmatrix} \\
&= \begin{bmatrix} 1 & 0 \\ 0 & \cos^2(\phi_{k'}) \end{bmatrix},
\end{aligned}$$

that $\lim_{T\to\infty} \operatorname{cov}\left\{T^{\frac{3}{2}}(\hat{\omega}_{k,T} - \omega_k),\ T^{\frac{1}{2}}\left\{\hat{\phi}_{k',T} - \phi_{k'}\right\}\right\}$

$$= \lim_{T\to\infty} \cos^2(\phi_{k'})\operatorname{cov}\left\{T^{\frac{3}{2}}(\hat{\omega}_{k,T} - \omega_k),\ T^{\frac{1}{2}}\left\{\tan(\hat{\phi}_{k',T}) - \tan(\phi_{k'})\right\}\right\}$$

$$= \frac{-6}{A_k A_{k'}}\{2B\cos(\phi_k - \phi_{k'})\delta_{k,k'} - \sum_{j=1}^{K} A_j \cos\left(-\phi_k - \phi_{k'} + \phi_j\right)\delta_{j,k+k'}$$

$$+ \sum_{j=1}^{K} A_j \cos\left(-\phi_k + \phi_{k'} + \phi_j\right)\delta_{j,k-k'} + \sum_{j=1}^{K} A_j \cos\left(\phi_k - \phi_{k'} + \phi_j\right)\delta_{j,k'-k}\}$$

$$\begin{aligned} = \quad & \frac{6}{A_k A_{k'}}\{-2B\cos(\phi_k - \phi_{k'})\delta_{k,k'} + \sum_{j=1}^{K} A_j[\cos\left(-\phi_k - \phi_{k'} + \phi_j\right)\delta_{j,k+k'} \\ & - \cos\left(-\phi_k + \phi_{k'} + \phi_j\right)\delta_{j,k-k'} - \cos\left(\phi_k - \phi_{k'} + \phi_j\right)\delta_{j,k'-k}]\}. \end{aligned}$$

Next, we establish the asymptotic covariance of

$$\operatorname{cov}\left\{T^{\frac{1}{2}}\left(\widehat{A}_{k,T} - A_k\right),\ T^{\frac{1}{2}}\left\{\hat{\phi}_{k',T} - \phi_{k'}\right\}\right\}.$$

From equations (2.18) and (2.25), we have

$$\operatorname{cov}\left\{T^{\frac{1}{2}}\left(\widehat{A}^2_{k,T} - A^2_k\right),\ T^{\frac{1}{2}}\left\{\tan(\hat{\phi}_{k',T}) - \tan(\phi_{k'})\right\}\right\}$$

$$\begin{aligned} = \quad & \operatorname{cov}\{4\kappa A_k\left\{\cos(\phi_k)V_k - \sin(\phi_k)W_k\right\}, \\ & -\frac{4\kappa}{A_{k'}\cos^2(\phi_{k'})}\left\{2\sin(\phi_{k'})V_{k'} + 2\cos(\phi_{k'})W_{k'} - 3X_{k'}\sin(\phi_{k'}) - 3Y_{k'}\cos(\phi_{k'})\right\}\} \\ & +o(1) \end{aligned}$$

$$= \quad -\frac{16\kappa^2 A_k}{A_{k'}\cos^2(\phi_{k'})}\mathrm{cov}\{\{\cos(\phi_k)V_k - \sin(\phi_k)W_k\}\,,$$

$$\{2\sin(\phi_{k'})V_{k'} + 2\cos(\phi_{k'})W_{k'} - 3X_{k'}\sin(\phi_{k'}) - 3Y_{k'}\cos(\phi_{k'})\}\} + o(1)$$

$$= -\tfrac{16\kappa^2 A_k}{A_{k'}\cos^2(\phi_{k'})}\{$$

$$\mathrm{cov}\left\{\cos(\phi_k)V_k,\ 2\sin(\phi_{k'})V_{k'}\right\} + \mathrm{cov}\left\{\cos(\phi_k)V_k,\ 2\cos(\phi_{k'})W_{k'}\right\}$$

$$+\mathrm{cov}\left\{\cos(\phi_k)V_k,\ -3X_{k'}\sin(\phi_{k'})\right\} + \mathrm{cov}\left\{\cos(\phi_k)V_k,\ -3Y_{k'}\cos(\phi_{k'})\right\}$$

$$+\mathrm{cov}\left\{-\sin(\phi_k)W_k,\ 2\sin(\phi_{k'})V_{k'}\right\} + \mathrm{cov}\left\{-\sin(\phi_k)W_k,\ 2\cos(\phi_{k'})W_{k'}\right\}$$

$$+\mathrm{cov}\left\{-\sin(\phi_k)W_k,\ -3X_{k'}\sin(\phi_{k'})\right\} + \mathrm{cov}\left\{-\sin(\phi_k)W_k,\ -3Y_{k'}\cos(\phi_{k'})\right\}\} + o(1)$$

$$= -\tfrac{16\kappa^2 A_k}{A_{k'}\cos^2(\phi_{k'})}\{$$

$$2\cos(\phi_k)\sin(\phi_{k'})\mathrm{cov}\left\{V_k,\ V_{k'}\right\} + 2\cos(\phi_k)\cos(\phi_{k'})\mathrm{cov}\left\{V_k,\ W_{k'}\right\}$$

$$-3\cos(\phi_k)\sin(\phi_{k'})\mathrm{cov}\left\{V_k,\ X_{k'}\right\} - 3\cos(\phi_k)\cos(\phi_{k'})\mathrm{cov}\left\{V_k,\ Y_{k'}\right\}$$

$$-2\sin(\phi_k)\sin(\phi_{k'})\text{cov}\left\{W_k,\ V_{k'}\right\} - 2\sin(\phi_k)\cos(\phi_{k'})\text{cov}\left\{W_k,\ W_{k'}\right\}$$

$$+3\sin(\phi_k)\sin(\phi_{k'})\text{cov}\left\{W_k,\ X_{k'}\right\} + 3\sin(\phi_k)\cos(\phi_{k'})\text{cov}\left\{W_k,\ Y_{k'}\right\}\} + o(1).$$

From Proposition 10, it then follows that

$\lim_{T\to\infty} \text{cov}\left\{T^{\frac{1}{2}}\left(\widehat{A}^2_{k,T} - A^2_k\right),\ T^{\frac{1}{2}}\left\{\tan(\hat{\phi}_{k',T}) - \tan(\phi_{k'})\right\}\right\}$
$= -\frac{16\kappa^2 A_k}{A_{k'}\cos^2(\phi_{k'})}\{$

$$2\cos(\phi_k)\sin(\phi_{k'})\left[\frac{1}{4\kappa^2}\sum_{j=1}^{K} A_j\cos(\phi_j)\left\{\delta_{j,\ k+k'} + \delta_{j,\ k-k'} + \delta_{j,\ k'-k}\right\} + \frac{B}{2\kappa^2}\delta_{k,\ k'}\right] \tag{B.214}$$

$$+ 2\cos(\phi_k)\cos(\phi_{k'})\frac{1}{4\kappa^2}\sum_{j=1}^{K} A_j\sin(\phi_j)\left\{-\delta_{j,k+k'} + \delta_{j,k-k'} - \delta_{j,k'-k}\right\} \tag{B.215}$$

$$- 3\cos(\phi_k)\sin(\phi_{k'})\left[\frac{1}{8\kappa^2}\sum_{j=1}^{K} A_j\cos(\phi_j)\left\{\delta_{j,k+k'} + \delta_{j,k-k'} + \delta_{j,k'-k}\right\} + \frac{B}{4\kappa^2}\delta_{k,k'}\right] \tag{B.216}$$

$$- 3\cos(\phi_k)\cos(\phi_{k'})\frac{1}{8\kappa^2}\sum_{j=1}^{K} A_j\sin(\phi_j)\left\{-\delta_{j,\ k+k'} + \delta_{j,\ k-k'} - \delta_{j,\ k'-k}\right\} \tag{B.217}$$

$$- 2\sin(\phi_k)\sin(\phi_{k'})\frac{1}{4\kappa^2}\sum_{j=1}^{K} A_j\sin(\phi_j)\left\{-\delta_{j,k'+k} + \delta_{j,k'-k} - \delta_{j,k-k'}\right\} \tag{B.218}$$

$$-2\sin(\phi_k)\cos(\phi_{k'})\left[\frac{1}{4\kappa^2}\sum_{j=1}^{K}A_j\cos(\phi_j)\left\{-\delta_{j,k'+k}+\delta_{j,k-k'}+\delta_{j,k'-k}\right\}+\frac{B}{2\kappa^2}\delta_{k,k'}\right] \quad \text{(B.219)}$$

$$+3\sin(\phi_k)\sin(\phi_{k'})\frac{1}{8\kappa^2}\sum_{j=1}^{K}A_j\sin(\phi_j)\left\{-\delta_{j,\,k+k'}+\delta_{j,\,k'-k}-\delta_{j,\,k-k'}\right\} \quad \text{(B.220)}$$

$$+3\sin(\phi_k)\cos(\phi_{k'})\left[\frac{1}{8\kappa^2}\sum_{j=1}^{K}A_j\cos(\phi_j)\left\{-\delta_{j,\,k+k'}+\delta_{j,\,k-k'}+\delta_{j,\,k'-k}\right\}+\frac{B}{4\kappa^2}\delta_{k,\,k'}\right]\}. \quad \text{(B.221)}$$

After combining equations (B.214) and (B.216), combining equations (B.215) and (B.217), combining equations (B.218) and (B.220), we have

$\lim_{T\to\infty}\operatorname{cov}\left\{T^{\frac{1}{2}}\left(\widehat{A}^2_{k,T}-A^2_k\right),\ T^{\frac{1}{2}}\left\{\tan(\hat{\phi}_{k',T})-\tan(\phi_{k'})\right\}\right\}$

$=-\frac{16\kappa^2 A_k}{A_{k'}\cos^2(\phi_{k'})}\{$

$$\cos(\phi_k)\sin(\phi_{k'})\left[\frac{1}{8\kappa^2}\sum_{j=1}^{K}A_j\cos(\phi_j)\left\{\delta_{j,\,k+k'}+\delta_{j,\,k-k'}+\delta_{j,\,k'-k}\right\}+\frac{B}{4\kappa^2}\delta_{k,\,k'}\right] \quad \text{(B.222)}$$

$$+\cos(\phi_k)\cos(\phi_{k'})\frac{1}{8\kappa^2}\sum_{j=1}^{K}A_j\sin(\phi_j)\left\{-\delta_{j,k+k'}+\delta_{j,k-k'}-\delta_{j,k'-k}\right\} \quad \text{(B.223)}$$

$$-\sin(\phi_k)\sin(\phi_{k'})\frac{1}{8\kappa^2}\sum_{j=1}^{K}A_j\sin(\phi_j)\left\{-\delta_{j,k'+k}+\delta_{j,k'-k}-\delta_{j,k-k'}\right\} \quad \text{(B.224)}$$

$$
- \sin(\phi_k)\cos(\phi_{k'})\left[\frac{1}{8\kappa^2}\sum_{j=1}^{K} A_j \cos(\phi_j)\left\{-\delta_{j,k'+k}+\delta_{j,k-k'}+\delta_{j,k'-k}\right\}+\frac{B}{4\kappa^2}\delta_{k,k'}\right]. \quad \text{(B.225)}
$$

$= -\frac{16\kappa^2 A_k}{A_{k'}\cos^2(\phi_{k'})}\{\frac{B}{4}\sin(\phi_{k'}-\phi_k)\delta_{k,\,k'}$

$$
+\frac{1}{8\kappa^2}\sum_{j=1}^{K} A_j \frac{1}{4}\{\sin(\phi_k+\phi_{k'}+\phi_j)+\sin(-\phi_k+\phi_{k'}+\phi_j)-\sin(\phi_k-\phi_{k'}+\phi_j)
$$
$$
-\sin(-\phi_k-\phi_{k'}+\phi_j)\}\left\{\delta_{j,\,k+k'}+\delta_{j,\,k-k'}+\delta_{j,\,k'-k}\right\} \quad \text{(B.226)}
$$

$$
+\frac{1}{8\kappa^2}\sum_{j=1}^{K} A_j \frac{1}{4}\{\sin(\phi_k+\phi_{k'}+\phi_j)+\sin(-\phi_k+\phi_{k'}+\phi_j)+\sin(\phi_k-\phi_{k'}+\phi_j)
$$
$$
+\sin(-\phi_k-\phi_{k'}+\phi_j)\}\left\{-\delta_{j,k+k'}+\delta_{j,k-k'}-\delta_{j,k'-k}\right\} \quad \text{(B.227)}
$$

$$
-\frac{1}{8\kappa^2}\sum_{j=1}^{K}[-\frac{1}{4}]A_j\{\sin(\phi_k+\phi_{k'}+\phi_j)-\sin(-\phi_k+\phi_{k'}+\phi_j)-\sin(\phi_k-\phi_{k'}+\phi_j)
$$
$$
+\sin(-\phi_k-\phi_{k'}+\phi_j)\}\left\{-\delta_{j,k'+k}+\delta_{j,k'-k}-\delta_{j,k-k'}\right\} \quad \text{(B.228)}
$$

$$
-\frac{1}{8\kappa^2}\sum_{j=1}^{K} A_j \frac{1}{4}\{\sin(\phi_k+\phi_{k'}+\phi_j)-\sin(-\phi_k+\phi_{k'}+\phi_j)+\sin(\phi_k-\phi_{k'}+\phi_j)
$$
$$
-\sin(-\phi_k-\phi_{k'}+\phi_j)\}\left\{-\delta_{j,k'+k}+\delta_{j,k-k'}+\delta_{j,k'-k}\right\} \quad \text{(B.229)}
$$

$= -\frac{16\kappa^2 A_k}{A_{k'}\cos^2(\phi_{k'})}\{\frac{B}{4}\sin(\phi_{k'}-\phi_k)\delta_{k,\,k'} - \frac{1}{8\kappa^2}\sum_{j=1}^{K} A_j \sin(-\phi_k - \phi_{k'} + \phi_j)\,\delta_{j,\,k+k'}$

$$+\frac{1}{8\kappa^2}\sum_{j=1}^{K} A_j \sin(-\phi_k + \phi_{k'} + \phi_j)\,\delta_{j,\,k-k'} - \frac{1}{8\kappa^2}\sum_{j=1}^{K} A_j \sin(\phi_k - \phi_{k'} + \phi_j)\,\delta_{j,\,k'-k}\}.$$

It then follows from Cramer's Theorem with $f(x,y) = [\sqrt{x},\ \tan^{-1}(y)]$, $\mathring{f}(x,y) = \begin{bmatrix} \frac{1}{2\sqrt{x}} & 0 \\ 0 & \frac{1}{y^2+1} \end{bmatrix}$, and $\mathring{f}(A_k^2,\ \tan(\phi_{k'})) = \begin{bmatrix} \frac{1}{2A_k} & 0 \\ 0 & \frac{1}{(\tan(\phi_{k'}))^2+1} \end{bmatrix} = \begin{bmatrix} \frac{1}{2A_k} & 0 \\ 0 & \cos^2(\phi_{k'}) \end{bmatrix}$, that

$\lim_{T\to\infty} \operatorname{cov}\left\{T^{\frac{1}{2}}\left(\widehat{A}_{k,T} - A_k\right),\ T^{\frac{1}{2}}\left\{\hat{\phi}_{k',T} - \phi_{k'}\right\}\right\}$

$= \lim_{T\to\infty} \frac{1}{2A_k}\operatorname{cov}\left\{T^{\frac{1}{2}}\left(\widehat{A}^2_{k,T} - A_k^2\right),\ T^{\frac{1}{2}}\left\{\tan(\hat{\phi}_{k',T}) - \tan(\phi_{k'})\right\}\right\}\cos^2(\phi_{k'})$

$= -\frac{8\kappa^2}{A_{k'}}\{\frac{B}{4}\sin(\phi_{k'}-\phi_k)\delta_{k,\,k'} - \frac{1}{8\kappa^2}\sum_{j=1}^{K} A_j \sin(-\phi_k - \phi_{k'} + \phi_j)\,\delta_{j,\,k+k'}$

$$+\frac{1}{8\kappa^2}\sum_{j=1}^{K} A_j \sin(-\phi_k + \phi_{k'} + \phi_j)\,\delta_{j,\,k-k'} - \frac{1}{8\kappa^2}\sum_{j=1}^{K} A_j \sin(\phi_k - \phi_{k'} + \phi_j)\,\delta_{j,\,k'-k}\}$$

$= -\frac{1}{A_{k'}}\{2B\sin(\phi_{k'}-\phi_k)\delta_{k,\,k'} - \sum_{j=1}^{K} A_j \sin(-\phi_k - \phi_{k'} + \phi_j)\,\delta_{j,\,k+k'}$

$$+\sum_{j=1}^{K} A_j \sin(-\phi_k + \phi_{k'} + \phi_j)\,\delta_{j,\,k-k'} - \sum_{j=1}^{K} A_j \sin(\phi_k - \phi_{k'} + \phi_j)\,\delta_{j,\,k'-k}\}$$

$$\begin{aligned} =\quad & \frac{1}{A_{k'}}\{-2B\sin(\phi_{k'}-\phi_k)\delta_{k,\,k'} + \sum_{j=1}^{K} A_j[\sin(-\phi_k - \phi_{k'} + \phi_j)\,\delta_{j,\,k+k'} \\ & -\sin(-\phi_k + \phi_{k'} + \phi_j)\,\delta_{j,\,k-k'} + \sin(\phi_k - \phi_{k'} + \phi_j)\,\delta_{j,\,k'-k}]\}. \end{aligned}$$

Next, we establish the asymptotic covariance of

$$\lim_{T\to\infty} \mathrm{cov}\left\{T^{\frac{1}{2}}\left(\widehat{A}_{k,T}-A_k\right),\ T^{\frac{1}{2}}\left(\hat{B}_T-B\right)\right\}.$$

From equations (2.18) and (2.27), we have

$$\mathrm{cov}\left\{T^{\frac{1}{2}}\left(\widehat{A}^2_{k,T}-A^2_k\right),\ T^{\frac{1}{2}}\left(\hat{B}_T-B\right)\right\} = \mathrm{cov}\{4\kappa A_k\left\{\cos(\phi_k)V_k-\sin(\phi_k)W_k\right\},$$
$$T^{\frac{1}{2}}(\frac{N_G(T)}{T}\kappa-B)\}+o(1)$$

$$= \mathrm{cov}\left\{4\kappa A_k\left\{\cos(\phi_k)V_k-\sin(\phi_k)W_k\right\},\ T^{\frac{1}{2}}\frac{N_G(T)}{T}\kappa\right\}+o(1)$$
$$= 4A_k\kappa^2\mathrm{cov}\left\{\cos(\phi_k)V_k-\sin(\phi_k)W_k,\ T^{-\frac{1}{2}}N_G(T)\right\}+o(1)$$

$$\begin{aligned}
&= 4A_k\kappa^2\left[\cos(\phi_k)\mathrm{cov}\left\{V_k,\ T^{-\frac{1}{2}}N_G(T)\right\}-\sin(\phi_k)\mathrm{cov}\left\{W_k,\ T^{-\frac{1}{2}}N_G(T)\right\}\right]\\
&\quad +o(1)\\
&= 4A_k\kappa^2\left[\cos(\phi_k)\mathrm{cov}\left\{V_k,\ T^{-\frac{1}{2}}\int_0^T dN_G(t)\right\}-\sin(\phi_k)\mathrm{cov}\left\{W_k,\ T^{-\frac{1}{2}}\int_0^T dN_G(t)\right\}\right]\\
&\quad +o(1)\\
&= 4A_k\kappa^2\left[\cos(\phi_k)\mathrm{cov}\left\{V_k,\ T^{-\frac{1}{2}}\int_0^T dZ_G(t)\right\}-\sin(\phi_k)\mathrm{cov}\left\{W_k,\ T^{-\frac{1}{2}}\int_0^T dZ_G(t)\right\}\right]\\
&\quad +o(1)\\
&= 4A_k\kappa^2\left[\cos(\phi_k)\mathrm{cov}\left\{V_k,\ U\right\}-\sin(\phi_k)\mathrm{cov}\left\{W_k,\ U\right\}\right]+o(1).
\end{aligned}$$

From Proposition 10, it then follows that

$\lim_{T\to\infty} \operatorname{cov}\left\{T^{\frac{1}{2}}\left(\widehat{A}^2_{k,T} - A^2_k\right),\ T^{\frac{1}{2}}\left(\hat{B}_T - B\right)\right\}$

$$\begin{aligned} &= 4A_k\kappa^2\left[\cos(\phi_k)\frac{A_k}{2\kappa^2}\cos(\phi_k) - \sin(\phi_k)\left\{-\frac{A_k}{2\kappa^2}\sin(\phi_k)\right\}\right] \\ &= 2A_k^2. \end{aligned}$$

It then follows from Cramer's Theorem with $f(x,y) = [\sqrt{x},\ y]$, $\mathring{f}(x,y) = \begin{bmatrix} \frac{1}{2\sqrt{x}} & 0 \\ 0 & 1 \end{bmatrix}$,

and $\mathring{f}(A_k^2,\ B) = \begin{bmatrix} \frac{1}{2A_k} & 0 \\ 0 & 1 \end{bmatrix}$ that

$\lim_{T\to\infty} \operatorname{cov}\left\{T^{\frac{1}{2}}\left(\widehat{A}_{k,T} - A_k\right),\ T^{\frac{1}{2}}\left(\hat{B}_T - B\right)\right\}$

$$\begin{aligned} &= \lim_{T\to\infty}\frac{1}{2A_k}\operatorname{cov}\left\{T^{\frac{1}{2}}\left(\widehat{A}^2_{k,T} - A^2_k\right),\ T^{\frac{1}{2}}\left(\hat{B}_T - B\right)\right\} \\ &= \frac{1}{2A_k}2A_k^2 \\ &= A_k. \end{aligned} \tag{B.230}$$

Next, we establish the asymptotic covariance of

$$\operatorname{cov}\left\{T^{\frac{3}{2}}\left(\hat{\omega}_{k,T} - \omega_k\right),\ T^{\frac{1}{2}}\left(\widehat{A}_{k',T} - A_{k'}\right)\right\}.$$

We notice from equations (2.12) and (2.18), that

$$\operatorname{cov}\left\{T^{\frac{3}{2}}\left(\hat{\omega}_{k,T}-\omega_k\right),\ T^{\frac{1}{2}}\left(\widehat{A}^2_{k',T}-A^2_{k'}\right)\right\}$$

$$\begin{aligned}
&= \operatorname{cov}\{\frac{24\kappa}{A_k}\left\{V_k\frac{1}{2}\sin(\phi_k)+W_k\frac{1}{2}\cos(\phi_k)-X_k\sin(\phi_k)-Y_k\cos(\phi_k)\right\}, \\
&\qquad 4\kappa A_{k'}\left\{\cos(\phi_{k'})V_{k'}-\sin(\phi_{k'})W_{k'}\right\}\}+o(1) \\
&= \frac{96\kappa^2 A_{k'}}{A_k}\operatorname{cov}\{V_k\frac{1}{2}\sin(\phi_k)+W_k\frac{1}{2}\cos(\phi_k)-X_k\sin(\phi_k)-Y_k\cos(\phi_k), \\
&\quad \cos(\phi_{k'})V_{k'}-\sin(\phi_{k'})W_{k'}\}+o(1)
\end{aligned}$$

$= \frac{96\kappa^2 A_{k'}}{A_k}\{$

$$\frac{1}{2}\sin(\phi_k)\cos(\phi_{k'})\operatorname{cov}\left\{V_k,\ V_{k'}\right\}+\frac{1}{2}\cos(\phi_k)\cos(\phi_{k'})\operatorname{cov}\left\{W_k,\ V_{k'}\right\}$$

$$-\sin(\phi_k)\cos(\phi_{k'})\operatorname{cov}\left\{X_k,\ V_{k'}\right\}-\cos(\phi_k)\cos(\phi_{k'})\operatorname{cov}\left\{Y_k,\ V_{k'}\right\}$$

$$-\frac{1}{2}\sin(\phi_k)\sin(\phi_{k'})\operatorname{cov}\left\{V_k,\ W_{k'}\right\}-\frac{1}{2}\cos(\phi_k)\sin(\phi_{k'})\operatorname{cov}\left\{W_k,\ W_{k'}\right\}$$

$$+\sin(\phi_k)\sin(\phi_{k'})\operatorname{cov}\left\{X_k,\ W_{k'}\right\}+\cos(\phi_k)\sin(\phi_{k'})\operatorname{cov}\left\{Y_k,\ W_{k'}\right\}\}+o(1).$$

From Proposition 10, it then follows that

$\lim_{T\to\infty}\operatorname{cov}\left\{T^{\frac{3}{2}}\left(\hat{\omega}_{k,T}-\omega_k\right),\ T^{\frac{1}{2}}\left(\widehat{A}^2_{k',T}-A^2_{k'}\right)\right\}$
$= \frac{96\kappa^2 A_{k'}}{A_k}\{$

$$\frac{1}{2}\sin(\phi_k)\cos(\phi_{k'})\left[\frac{1}{4\kappa^2}\sum_{j=1}^{K}A_j\cos(\phi_j)\left\{\delta_{j,\,k+k'}+\delta_{j,\,k-k'}+\delta_{j,\,k'-k}\right\}+\frac{B}{2\kappa^2}\delta_{k,\,k'}\right]$$

$$+\frac{1}{2}\cos(\phi_k)\cos(\phi_{k'})\frac{1}{4\kappa^2}\sum_{j=1}^{K}A_j\sin(\phi_j)\left\{-\delta_{j,k'+k}+\delta_{j,k'-k}-\delta_{j,k-k'}\right\}$$

$$-\sin(\phi_k)\cos(\phi_{k'})\left[\frac{1}{8\kappa^2}\sum_{j=1}^{K}A_j\cos(\phi_j)\left\{\delta_{j,k'+k}+\delta_{j,k'-k}+\delta_{j,k-k'}\right\}+\frac{B}{4\kappa^2}\delta_{k,k'}\right]$$

$$-\cos(\phi_k)\cos(\phi_{k'})\frac{1}{8\kappa^2}\sum_{j=1}^{K}A_j\sin(\phi_j)\left\{-\delta_{j,\,k'+k}+\delta_{j,\,k'-k}-\delta_{j,\,k-k'}\right\}$$

$$-\frac{1}{2}\sin(\phi_k)\sin(\phi_{k'})\frac{1}{4\kappa^2}\sum_{j=1}^{K}A_j\sin(\phi_j)\left\{-\delta_{j,k+k'}+\delta_{j,k-k'}-\delta_{j,k'-k}\right\}$$

$$-\frac{1}{2}\cos(\phi_k)\sin(\phi_{k'})\left[\frac{1}{4\kappa^2}\sum_{j=1}^{K}A_j\cos(\phi_j)\left\{-\delta_{j,k'+k}+\delta_{j,k-k'}+\delta_{j,k'-k}\right\}+\frac{B}{2\kappa^2}\delta_{k,k'}\right]$$

$$+\sin(\phi_k)\sin(\phi_{k'})\frac{1}{8\kappa^2}\sum_{j=1}^{K}A_j\sin(\phi_j)\left\{-\delta_{j,\,k'+k}+\delta_{j,\,k-k'}-\delta_{j,\,k'-k}\right\}$$

$$+\cos(\phi_k)\sin(\phi_{k'})\left[\frac{1}{8\kappa^2}\sum_{j=1}^{K}A_j\cos(\phi_j)\left\{-\delta_{j,\,k'+k}+\delta_{j,\,k'-k}+\delta_{j,\,k-k'}\right\}+\frac{B}{4\kappa^2}\delta_{k,\,k'}\right]$$

$= \frac{96\kappa^2 A_{k'}}{A_k}\{$

$$\frac{1}{2}\sin(\phi_k)\cos(\phi_{k'})\frac{1}{4\kappa^2}\sum_{j=1}^{K}A_j\cos(\phi_j)\left\{\delta_{j,\,k+k'}+\delta_{j,\,k-k'}+\delta_{j,\,k'-k}\right\}$$

$$+\frac{1}{2}\cos(\phi_k)\cos(\phi_{k'})\frac{1}{4\kappa^2}\sum_{j=1}^{K}A_j\sin(\phi_j)\left\{-\delta_{j,k'+k}+\delta_{j,k'-k}-\delta_{j,k-k'}\right\}$$

$$-\sin(\phi_k)\cos(\phi_{k'})\frac{1}{8\kappa^2}\sum_{j=1}^{K}A_j\cos(\phi_j)\left\{\delta_{j,k'+k}+\delta_{j,k'-k}+\delta_{j,k-k'}\right\}$$

$$-\cos(\phi_k)\cos(\phi_{k'})\frac{1}{8\kappa^2}\sum_{j=1}^{K}A_j\sin(\phi_j)\left\{-\delta_{j,\,k'+k}+\delta_{j,\,k'-k}-\delta_{j,\,k-k'}\right\}$$

$$-\frac{1}{2}\sin(\phi_k)\sin(\phi_{k'})\frac{1}{4\kappa^2}\sum_{j=1}^{K}A_j\sin(\phi_j)\left\{-\delta_{j,k+k'}+\delta_{j,k-k'}-\delta_{j,k'-k}\right\}$$

$$-\frac{1}{2}\cos(\phi_k)\sin(\phi_{k'})\frac{1}{4\kappa^2}\sum_{j=1}^{K}A_j\cos(\phi_j)\left\{-\delta_{j,k'+k}+\delta_{j,k-k'}+\delta_{j,k'-k}\right\}$$

$$+\sin(\phi_k)\sin(\phi_{k'})\frac{1}{8\kappa^2}\sum_{j=1}^{K}A_j\sin(\phi_j)\left\{-\delta_{j,\,k'+k}+\delta_{j,\,k-k'}-\delta_{j,\,k'-k}\right\}$$

$$+\cos(\phi_k)\sin(\phi_{k'})\frac{1}{8\kappa^2}\sum_{j=1}^{K}A_j\cos(\phi_j)\left\{-\delta_{j,\,k'+k}+\delta_{j,\,k'-k}+\delta_{j,\,k-k'}\right\}\}$$

$$=0.$$

It then follows from Cramer's Theorem with $f(x,y)=\left[x,\ \sqrt{y}\right]$, $\mathring{f}(x,y)=\begin{bmatrix}1 & 0\\ 0 & \frac{1}{2\sqrt{x}}\end{bmatrix}$,

and $\mathring{f}(\omega_k,\ A_k^2)=\begin{bmatrix}1 & 0\\ 0 & \frac{1}{2A_k}\end{bmatrix}$ that

$\lim_{T\to\infty}\operatorname{cov}\{T^{\frac{3}{2}}(\hat{\omega}_{k,T}-\omega_k),\ T^{\frac{1}{2}}(\widehat{A}_{k',T}-A_{k'})\}$

$$=\lim_{T\to\infty}\operatorname{cov}\{T^{\frac{3}{2}}(\hat{\omega}_{k,T}-\omega_k),\ T^{\frac{1}{2}}(\widehat{A}^2_{k',T}-A^2_{k'})\}\frac{1}{2A_k}$$

$$=0.$$

Next, we establish the asymptotic covariance of

$$\operatorname{cov}\left\{T^{\frac{3}{2}}\left(\hat{\omega}_{k,T}-\omega_k\right),\ T^{\frac{1}{2}}\left(\hat{B}_T-B\right)\right\}.$$

From equations (2.12) and (2.27), we have

$$\operatorname{cov}\left\{T^{\frac{3}{2}}\left(\hat{\omega}_{k,T}-\omega_k\right),\ T^{\frac{1}{2}}\left(\hat{B}_T-B\right)\right\}$$

$$=\operatorname{cov}\{\frac{24\kappa}{A_k}\{V_k\frac{1}{2}\sin(\phi_k)+W_k\frac{1}{2}\cos(\phi_k)-X_k\sin(\phi_k)-Y_k\cos(\phi_k)\},\ T^{\frac{1}{2}}(\frac{N_G(T)}{T}\kappa-B)\}$$
$$+o(1)$$

$$=\frac{24\kappa^2}{A_k}\operatorname{cov}\{V_k\frac{1}{2}\sin(\phi_k)+W_k\frac{1}{2}\cos(\phi_k)-X_k\sin(\phi_k)-Y_k\cos(\phi_k),\ T^{-\frac{1}{2}}\int_0^T dN_G(t)\}$$
$$+o(1)$$

$$=\frac{24\kappa^2}{A_k}\operatorname{cov}\left\{V_k\frac{1}{2}\sin(\phi_k)+W_k\frac{1}{2}\cos(\phi_k)-X_k\sin(\phi_k)-Y_k\cos(\phi_k),\ T^{-\frac{1}{2}}\int_0^T dZ_G(t)\right\}$$
$$+o(1)$$

$$=\quad\frac{24\kappa^2}{A_k}\operatorname{cov}\left\{V_k\frac{1}{2}\sin(\phi_k)+W_k\frac{1}{2}\cos(\phi_k)-X_k\sin(\phi_k)-Y_k\cos(\phi_k),\ U\right\}+o(1)$$

$$
\begin{aligned}
= \quad & \frac{24\kappa^2}{A_k}[\frac{1}{2}\sin(\phi_k)\text{cov}\left\{V_k,\ U\right\} + \frac{1}{2}\cos(\phi_k)\text{cov}\left\{W_k,\ U\right\} \\
& - \sin(\phi_k)\text{cov}\left\{X_k,\ U\right\} - \cos(\phi_k)\text{cov}\left\{Y_k,\ U\right\}] + o(1).
\end{aligned}
$$

From Proposition 10, it then follows that

$\lim_{T\to\infty} \text{cov}\left\{T^{\frac{3}{2}}\left(\hat{\omega}_{k,T} - \omega_k\right),\ T^{\frac{1}{2}}\left(\hat{B}_T - B\right)\right\}$

$$
\begin{aligned}
=& \frac{24\kappa^2}{A_k}\{\frac{1}{2}\sin(\phi_k)\frac{A_k}{2\kappa^2}\cos(\phi_k) + \frac{1}{2}\cos(\phi_k)(-\frac{A_k}{2\kappa^2}\sin(\phi_k)) \\
& - \sin(\phi_k)\frac{A_k}{4\kappa^2}\cos(\phi_k) - \cos(\phi_k)(-\frac{A_k}{4\kappa^2}\sin(\phi_k))\}
\end{aligned}
$$

$$
\begin{aligned}
= \quad & \frac{24A_k}{4A_k}\{\sin(\phi_k)\cos(\phi_k) - \cos(\phi_k)\sin(\phi_k) \\
& - \sin(\phi_k)\cos(\phi_k) + \cos(\phi_k)\sin(\phi_k)\} \\
= \quad & 0.
\end{aligned}
$$

Next, we establish the asymptotic covariance of

$$
\text{cov}\left\{T^{\frac{1}{2}}\left\{\hat{\phi}_{k,T} - \phi_k\right\},\ T^{\frac{1}{2}}\left(\hat{B}_T - B\right)\right\}.
$$

From equations (2.25) and (2.27), we have

$\text{cov}\left\{T^{\frac{1}{2}}\left\{\tan(\hat{\phi}_{k,T}) - \tan(\phi_k)\right\},\ T^{\frac{1}{2}}\left(\hat{B}_T - B\right)\right\}$

$$= \mathrm{cov}\{-\frac{4\kappa}{A_k \cos^2(\phi_k)}\{2\sin(\phi_k)V_k + 2\cos(\phi_k)W_k - 3X_k\sin(\phi_k) - 3Y_k\cos(\phi_k)\},$$
$$T^{\frac{1}{2}}(\frac{N_G(T)}{T}\kappa - B)\} + o(1)$$

$$= -\frac{4\kappa^2}{A_k \cos^2(\phi_k)}\mathrm{cov}\{2\sin(\phi_k)V_k + 2\cos(\phi_k)W_k - 3X_k\sin(\phi_k) - 3Y_k\cos(\phi_k),$$
$$T^{-\frac{1}{2}}\int_0^T dN_G(t)\} + o(1)$$

$$= -\frac{4\kappa^2}{A_k \cos^2(\phi_k)}\mathrm{cov}\{2\sin(\phi_k)V_k + 2\cos(\phi_k)W_k - 3X_k\sin(\phi_k) - 3Y_k\cos(\phi_k),$$
$$T^{-\frac{1}{2}}\int_0^T dZ(t)\} + o(1)$$

$$= -\frac{4\kappa^2}{A_k \cos^2(\phi_k)}\mathrm{cov}\{2\sin(\phi_k)V_k + 2\cos(\phi_k)W_k - 3X_k\sin(\phi_k) - 3Y_k\cos(\phi_k),\ U\} + o(1)$$

$$\begin{aligned}
= \quad & -\frac{4\kappa^2}{A_k \cos^2(\phi_k)}\{\mathrm{cov}\left\{2\sin(\phi_k)V_k,\ U\right\} + \mathrm{cov}\left\{2\cos(\phi_k)W_k,\ U\right\} \\
& +\mathrm{cov}\left\{-3X_k\sin(\phi_k),\ U\right\} + \mathrm{cov}\left\{-3Y_k\cos(\phi_k),\ U\right\}\} + o(1) \\
= \quad & -\frac{4\kappa^2}{A_k \cos^2(\phi_k)}\{2\sin(\phi_k)\mathrm{cov}\left\{V_k,\ U\right\} + 2\cos(\phi_k)\mathrm{cov}\left\{W_k,\ U\right\} \\
& -3\sin(\phi_k)\mathrm{cov}\left\{X_k,\ U\right\} - 3\cos(\phi_k)\mathrm{cov}\left\{Y_k,\ U\right\}\} + o(1).
\end{aligned}$$

From Proposition 10, we have

$$\lim_{T\to\infty} \mathrm{cov}\left\{T^{\frac{1}{2}}\left\{\tan(\hat{\phi}_{k,T}) - \tan(\phi_k)\right\},\ T^{\frac{1}{2}}\left(\hat{B}_T - B\right)\right\}$$

$$= -\frac{4\kappa^2}{A_k \cos^2(\phi_k)}\{2\sin(\phi_k)\frac{A_k}{2\kappa^2}\cos(\phi_k) + 2\cos(\phi_k)\left(-\frac{A_k}{2\kappa^2}\sin(\phi_k)\right)$$

$$- 3\sin(\phi_k)\frac{A_k}{4\kappa^2}\cos(\phi_k) - 3\cos(\phi_k)\left(-\frac{A_k}{4\kappa^2}\sin(\phi_k)\right)\}$$

$$= -\frac{4}{\cos(\phi_k)}\{\sin(\phi_k) - \sin(\phi_k) - 3\sin(\phi_k)\frac{1}{4} + 3\frac{1}{4}\sin(\phi_k)\}$$

$$= 0$$

Therefore, by Cramer's Theorem

$$\lim_{T\to\infty} \operatorname{cov}\left\{T^{\frac{1}{2}}\left\{\hat{\phi}_{k,T} - \phi_k\right\},\, T^{\frac{1}{2}}\left(\hat{B}_T - B\right)\right\} = 0.$$

□

B.1.1.10 The proof of the claim that the estimator of the baseline intensity function, $\lambda_1(\cdot)$, of an inhomogeneous Gamma process which satisfies Assumptions $1-3$ of Section 2.2 is $\hat{\lambda}_{1,T}(T) = \lambda_1(T) + O(T^{-\frac{1}{2}})$, where $T > 0$. This claim is stated after Proposition 14.

Proof. We show that $\hat{\lambda}_{1,T}(T) = \lambda_1(T) + O(T^{-\frac{1}{2}})$. We notice that

$$\begin{aligned}
\hat{\lambda}_{1,T}(T) - \lambda_1(T) &= \sum_{k=1}^{K}\hat{A}_k\cos(\hat{\omega}_k T + \hat{\phi}_k) + \hat{B} - \left[\sum_{k=1}^{K}A_k\cos(\omega_k T + \phi_k) + B\right] \\
&= \sum_{k=1}^{K}(\hat{A}_k - A_k)\cos(\hat{\omega}_k T + \hat{\phi}_k) + \sum_{k=1}^{K}A_k\left\{\cos(\hat{\omega}_k T + \hat{\phi}_k) - \cos(\omega_k T + \phi_k)\right\} \\
&\quad + \left[\frac{1}{T}N_G(T)\kappa - B\right]. \qquad \text{(B.231)}
\end{aligned}$$

By Proposition 14 of Section 2.2, it follows that

$$\frac{1}{T} N_G(T)\kappa - B = O(T^{-\frac{1}{2}}), \tag{B.232}$$

and by Proposition 12 of Section 2.2, we have

$$\sum_{k=1}^{K} (\hat{A}_k - A_k)\cos(\hat{\omega}_k T + \hat{\phi}_k) = O(T^{-\frac{1}{2}}). \tag{B.233}$$

From the Taylor series expansion of the cosine function, we know that for some number c between $\hat{\omega}_k T + \hat{\phi}_k$ and $\omega_k T + \phi_k$, we have

$\cos(\hat{\omega}_k T + \hat{\phi}_k) =$

$$\cos(\omega_k T + \phi_k) - \sin(\omega_k T + \phi_k)((\hat{\omega}_k - \omega_k)T + (\hat{\phi}_k - \phi_k)) - \frac{\cos(c)}{2!}\Big((\hat{\omega}_k - \omega_k)T + (\hat{\phi}_k - \phi_k)\Big)^2.$$

It then follows from Propositions 11 and 13 of Section 2.2 that

$$\sum_{k=1}^{K} A_k \Big\{\cos(\hat{\omega}_k T + \hat{\phi}_k) - \cos(\omega_k T + \phi_k)\Big\} = O(T^{-\frac{1}{2}}). \tag{B.234}$$

Therefore, from equations (B.232)-(B.234), it follows that equation (B.231) becomes

$$\hat{\lambda}_{1,T}(T) - \lambda_1(T) = O(T^{-\frac{1}{2}}),$$

where $T > 0$. $\square$

B.1.2 Proofs for Chapter 2 Section 3

B.1.2.1 Proof of Proposition 16

Proof. From equation (2.29), it follows that the conditional density function of w_T is given by

$$f_{w_T}(w) = \lambda_2(T + w \mid H_{T+w}) \exp\left\{-\int_T^{T+w} \lambda_2(u \mid H_u)du\right\} I_{\{w \geq 0\}}, \tag{B.235}$$

where $T > 0$. Therefore, we have

$$\begin{aligned}
\hat{T}_{n+1} &:= T + E\left[w_T \mid H_T\right] \\
&= T + \int_0^\infty w\lambda_2(T + w \mid H_{T+w}) \exp\left\{-\int_T^{T+w} \lambda_2(u \mid H_u)du\right\} dw \\
&= T + \int_0^\infty w\lambda_2(T + w \mid H_{T+w}) \exp\left\{-\int_0^{w} \lambda_2(T + y \mid H_{T+y})dy\right\} dw \\
&= T + \left[-w \exp\left\{-\int_0^{w} \lambda_2(T + y \mid H_{T+y})dy\right\}\right]_0^\infty \\
&\quad + \int_0^\infty \exp\left\{-\int_0^{w} \lambda_2(T + y \mid H_{T+y})dy\right\} dw \\
&= T + \int_0^\infty \exp\left\{-\int_0^{w} \lambda_2(T + y \mid H_{T+y})dy\right\} dw.
\end{aligned} \tag{B.236}$$

Next, we establish $\nu_{n(T)} := E\left[\left(T_{n(T)+1} - \hat{T}_{n(T)+1}\right)^2\right]$. We begin by computing $E\left[w_T^2 \middle| H_T\right]$. From equation (B.235), it follows that

$$\begin{aligned}
E\left[w_T^2 \middle| H_T\right] &= \int_0^\infty w^2 \lambda_2(T+w \mid H_{T+w}) \exp\left\{-\int_T^{T+w} \lambda_2(u \mid H_u) du\right\} dw \\
&= \int_0^\infty w^2 \lambda_2(T+w \mid H_{T+w}) \exp\left\{-\int_0^{w} \lambda_2(T+y \mid H_{T+y}) dy\right\} dw \\
&= \left[-w^2 \exp\left\{-\int_0^{w} \lambda_2(T+y \mid H_{T+y}) dy\right\}\right]_0^\infty \\
&\quad +2\int_0^\infty w \exp\left\{-\int_0^{w} \lambda_2(T+y \mid H_{T+y}) dy\right\} dw \\
&= 2\int_0^\infty w \exp\left\{-\int_0^{w} \lambda_2(T+y \mid H_{T+y}) dy\right\} dw. \qquad \text{(B.237)}
\end{aligned}$$

Therefore, it follows that

$$\begin{aligned}
\nu_{n(T)} &\coloneqq E\left[\left(T_{n(T)+1} - \hat{T}_{n(T)+1}\right)^2\right] \\
&= E_{H_T}\left[E\left[\left(w_T - E\left[w_T \middle| H_T\right]\right)^2 \mid H_T\right]\right] \\
&= E_{H_T}\left[E\left[w_T^2 \middle| H_T\right] - \left[E\left[w_T \middle| H_T\right]\right]^2 \mid H_T\right] \\
&= E_{H_T}[2\int_0^\infty w \exp\left\{-\int_0^{w} \lambda_2(T+y \mid H_{T+y}) dy\right\} dw \\
&\quad -\left[\int_0^\infty \exp\left\{-\int_0^{w} \lambda_2(T+y \mid H_{T+y}) dy\right\} dw\right]^2]. \qquad \text{(B.238)}
\end{aligned}$$

□

B.1.2.2 Proof of Chapter 2 Equations (2.32) and (2.33)

Proof. We begin by proving equation (2.32). From Chapter 2 Proposition 16, it follows that

$$
\begin{aligned}
\mu_{n(T)}^{HPP} &= E\left[\left(T_{n(T)+1}-\widetilde{T}_{n(T)+1}^{HPP}\right)^2\right]-E\left[\left(T_{n(T)+1}-\hat{T}_{n(T)+1}\right)^2\right] \\
&= E_{H_T}\left[E\left[\left(w_T-\frac{\kappa}{B}\right)^2 \mid H_T\right]\right]-E_{H_T}\left[E\left[\left(T_{n(T)+1}-\hat{T}_{n(T)+1}\right)^2 \mid \ H_T\right]\right] \\
&= E_{H_T}\left[E\left[w_T^2 \mid H_T\right]-2\frac{\kappa}{B}E\left[w_T \mid H_T\right]+\frac{\kappa^2}{B^2}-\left(E\left[w_T^2 \mid H_T\right]-\left[E\left[w_T \mid H_T\right]\right]^2\right)\right] \\
&= E_{H_T}\left[-\frac{2}{B}\kappa E\left[w_T \mid H_T\right]+\frac{\kappa^2}{B^2}+\left[E\left[w_T \mid H_T\right]\right]^2\right] \\
&= E_{H_T}\left[\left(E\left[w_T \mid H_T\right]-\frac{\kappa}{B}\right)^2\right] \\
&= E_{H_T}\left[\left(\int_0^\infty \exp\left\{-\int_0^w \lambda_2(T+y \mid H_{T+y})dy\right\}dw-\frac{\kappa}{B}\right)^2\right], \qquad \text{(B.239)}
\end{aligned}
$$

which establishes equation (2.32). Next, we prove equation (2.33). From Chapter 2 Proposition 16, it follows that

$$
\begin{aligned}
\mu_{n(T)}^{NHPP} &= E\left[\left(T_{n(T)+1}-\widetilde{T}_{n(T)+1}^{NHPP}\right)^2\right]-E\left[\left(T_{n(T)+1}-\hat{T}_{n(T)+1}\right)^2\right] \\
&= E\left[\left(T_{n(T)+1}-\widetilde{T}_{n(T)+1}^{NHPP}\right)^2\right]-E_{H_T}\left[\left(E\left[w_T^2 \mid H_T\right]-\left[E\left[w_T \mid H_T\right]\right]^2\right)\right] \\
&= E_{H_T}\left[E\left[\left(w_T-\int_0^\infty \exp\left\{-\frac{1}{\kappa}\int_0^w \lambda_1(T+y)dy\right\}dw\right)^2 \mid H_T\right]\right] \\
&\quad -E_{H_T}\left[E\left[w_T^2 \mid H_T\right]-\left[E\left[w_T \mid H_T\right]\right]^2\right] \\
&= E_{H_T}[E\left[w_T^2 \mid H_T\right]-2\int_0^\infty \exp\left\{-\frac{1}{\kappa}\int_0^w \lambda_1(T+y)dy\right\}dw E\left[w_T \mid H_T\right] \\
&\quad +\left[\int_0^\infty \exp\left\{-\frac{1}{\kappa}\int_0^w \lambda_1(T+y)dy\right\}dw\right]^2-\left(E\left[w_T^2 \mid H_T\right]-\left[E\left[w_T \mid H_T\right]\right]^2\right)]
\end{aligned}
$$

$$
\begin{aligned}
&= E_{H_T}[-2\int_0^\infty \exp\left\{-\frac{1}{\kappa}\int_0^w \lambda_1(T+y)dy\right\} dwE\left[w_T \middle| H_T\right] \\
&\quad + \left[\int_0^\infty \exp\left\{-\frac{1}{\kappa}\int_0^w \lambda_1(T+y)dy\right\} dw\right]^2 + \left[E\left[w_T \middle| H_T\right]\right]^2] \\
&= E_{H_T}[\left(E\left[w_T \middle| H_T\right] - \int_0^\infty \exp\left\{-\frac{1}{\kappa}\int_0^w \lambda_1(T+y)dy\right\} dw\right)^2] \\
&= E_{H_T}[(\int_0^\infty \exp\left\{-\int_0^w \lambda_2(T+y \mid H_T)dy\right\} dw \\
&\quad - \int_0^\infty \exp\left\{-\frac{1}{\kappa}\int_0^w \lambda_1(T+y)dy\right\} dw)^2], \qquad \text{(B.240)}
\end{aligned}
$$

which establishes equation (2.33). □

B.1.2.3 Proof of Chapter 2 Proposition 17

Proof. To compute $\hat{T}_{n+1} \coloneqq E\left[T_{n+1} \mid T_1 = t_1, \ldots,\ T_n = t_n\right]$, we need to first establish the integral

$$
\begin{aligned}
I_\kappa(t) &\coloneqq \int_t^\infty \frac{\lambda_1(s)}{\Gamma(\kappa)}\left[\int_{t_n}^s \lambda_1(x)dx\right]^{\kappa-1} \exp\left\{-\int_{t_n}^s \lambda_1(x)dx\right\} ds \\
&= \exp\left\{-\int_{t_n}^t \lambda_1(x)dx\right\} \sum_{i=0}^{\kappa-1} \frac{\left[\int_{t_n}^t \lambda_1(x)dx\right]^i}{i!}, \qquad \text{(B.241)}
\end{aligned}
$$

where $t \geq t_n$ and $\kappa \in \mathbb{N}$.

We begin by letting, $F(s) = \int_{t_n}^s \lambda_1(x)dx$, $f(s) = \frac{d}{ds}\left[F(s)\right] = \lambda_1(s)$, and

$$
I_\kappa(t) = \int_t^\infty \frac{f(s)}{\Gamma(\kappa)}\left\{F(s)\right\}^{\kappa-1} \exp\left\{-F(s)\right\} ds,
$$

where $s \geq t \geq 0$. Then using u substitution with $u = F(s)$ and $du = f(s)ds$, we have

$I_1(t) = \int_t^\infty \frac{f(s)}{\Gamma(1)} \exp\{-F(s)\}\, ds = \int_{F(t)}^\infty \exp\{-u\}\, du = -\exp\{-u\}\,|_{F(t)}^\infty = \exp\{-F(t)\}$.

Therefore,

$$I_1(t) = \exp\{-F(t)\}.$$

Likewise, we have

$I_2(t) = \int_t^\infty \frac{f(s)}{\Gamma(2)} \{F(s)\} \exp\{-F(s)\}\, ds = \int_{F(t)}^\infty u \exp\{-u\}\, du = -(u+1)\exp\{-u\}\,|_{F(t)}^\infty$ $= (F(t)+1)\exp\{-F(t)\}$. Therefore,

$$I_2(t) = I_1(t) + I_1(t)F(t).$$

Similarly, we have

$I_3(t) = \int_t^\infty \frac{f(s)}{\Gamma(3)} \{F(s)\}^2 \exp\{-F(s)\}\, ds = \int_{F(t)}^\infty \frac{1}{\Gamma(3)} u^2 \exp\{-u\}\, du = -\frac{1}{\Gamma(3)}(u^2 + 2u + 2)\exp\{-u\}\,|_{F(t)}^\infty = \frac{1}{\Gamma(3)}(F(t)^2 + 2F(t) + 2)\exp\{-F(t)\}$. Therefore,

$$I_3(t) = I_1(t) + I_1(t)F(t) + I_1(t)\frac{F(t)^2}{2!}.$$

Continuing in a similar fashion, we see that

$$\begin{aligned} I_\kappa(t) &= I_1(t) \sum_{i=0}^{\kappa-1} \frac{[F(t)]^i}{i!} \\ &= \exp\left\{-\int_{t_n}^t \lambda_1(s) ds\right\} \sum_{i=0}^{\kappa-1} \frac{\left[\int_{t_n}^t \lambda_1(s) ds\right]^i}{i!}. \end{aligned} \tag{B.242}$$

Now, from equation (1.27), we have

$$\begin{aligned}\hat{T}_{n+1} &\coloneqq E\left[T_{n+1} \mid T_1 = t_1, \ldots, T_n = t_n\right] \\ &= \int_{t_n}^{\infty} s \frac{\lambda_1(s)}{\Gamma(\kappa)} \left[\int_{t_n}^{s} \lambda_1(x)dx\right]^{\kappa-1} \exp\left\{-\int_{t_n}^{s} \lambda_1(x)dx\right\} ds. \end{aligned} \tag{B.243}$$

To evaluate (B.243), we use integration by parts by setting

$$u = s \text{ and } dv = \frac{\lambda_1(s)}{\Gamma(\kappa)} \left[\int_{t_n}^{s} \lambda_1(x)dx\right]^{\kappa-1} \exp\left\{-\int_{t_n}^{s} \lambda_1(x)dx\right\} ds.$$

From which, it follows that

$$du = ds \text{ and } v = -\exp\left\{-\int_{t_n}^{s} \lambda_1(x)dx\right\} \sum_{i=0}^{\kappa-1} \frac{\left[\int_{t_n}^{s} \lambda_1(x)dx\right]^{i}}{i!}.$$

Upon using integration by parts, it then follows from equation (B.241) and equation (B.243) that for $\kappa \in \mathbb{N}$, we have

$$\begin{aligned}\hat{T}_{n+1} &= \int_{t_n}^{\infty} s \frac{\lambda_1(s)}{\Gamma(\kappa)} \left[\int_{t_n}^{s} \lambda_1(x)dx\right]^{\kappa-1} \exp\left\{-\int_{t_n}^{s} \lambda_1(x)dx\right\} ds. \\ &= \left[-s \exp\left\{-\int_{t_n}^{s} \lambda_1(x)dx\right\} \sum_{i=0}^{\kappa-1} \frac{\left[\int_{t_n}^{s} \lambda_1(x)dx\right]^{i}}{i!}\right]_{t_n}^{\infty} + \int_{t_n}^{\infty} I_\kappa(s)ds \\ &= t_n + \int_{t_n}^{\infty} I_\kappa(s)ds \\ &= t_n + \int_{t_n}^{\infty} \exp\left\{-\int_{t_n}^{s} \lambda_1(x)dx\right\} \sum_{i=0}^{\kappa-1} \frac{\left[\int_{t_n}^{s} \lambda_1(x)dx\right]^{i}}{i!} ds,\end{aligned}$$

where $0 < t_1 < t_2 < \cdots < t_n$. $\square$

Bibliography

[1] Anderson, David R., and Kenneth P. Burnham. "Avoiding pitfalls when using information-theoretic methods." The Journal of Wildlife Management (2002): 912-918.

[2] Akaike, Hirotogu. "Information theory and an extension of the maximum likelihood principle." Breakthroughs in statistics. Springer New York, 1992. 610-624.

[3] Bandyopadhyay, Nibedita, and Ananda Sen. "Non-standard asymptotics in an inhomogeneous gamma process." Annals of the Institute of Statistical Mathematics 57.4 (2005): 703.

[4] Barbieri, Riccardo, et al. "Construction and analysis of non-Poisson stimulus-response models of neural spiking activity." Journal of neuroscience methods 105.1 (2001): 25-37.

[5] Barbieri, Riccardo, et al. "Diagnostic methods for statistical models of place cell spiking activity." Neurocomputing 38 (2001): 1087-1093.

[6] Bartlett, Maurice S. "Statistical estimation of density functions." Sankhyā: The Indian Journal of Statistics, Series A (1963): 245-254.

[7] Bartlett, M. S. "The spectral analysis of point processes." Journal of the Royal Statistical Society. Series B (Methodological) (1963): 264-296.

[8] Berman, M. "Comment on “Likelihood analysis of point processes and its applications to seismological data” by Ogata." Bulletin Internatl. Stat. Instit 50 (1983): 412-418.

[9] Berman, Mark. "Inhomogeneous and modulated gamma processes." Biometrika 68.1 (1981): 143-152.

[10] Berman, Mark, and T. Rolf Turner. "Approximating point process likelihoods with GLIM." Applied Statistics (1992): 31-38.

[11] Bohr, Harald. "Almost periodic functions." (1947).

[12] Brillinger, David R. "Maximum likelihood analysis of spike trains of interacting nerve cells." Biological cybernetics 59.3 (1988): 189-200.

[13] Brillinger, David R. "The spectral analysis of stationary interval functions." Proceedings of the Sixth Berkeley Symposium on Mathematical Statistics and Probability, Volume 1: Theory of Statistics. The Regents of the University of California, 1972.

[14] Brillinger, David R. "The finite Fourier transform of a stationary process." Handbook of statistics 3 (1983): 21-37.

[15] Brown, Timothy C., and M. Gopalan Nair. "A simple proof of the multivariate random time change theorem for point processes." Journal of Applied Probability (1988): 210-214.

[16] Brown, Emery N., et al. "A statistical paradigm for neural spike train decoding applied to position prediction from ensemble firing patterns of rat hippocampal place cells." The Journal of Neuroscience 18.18 (1998): 7411-7425.

[17] Brown, Emery N., et al. "The time-rescaling theorem and its application to neural spike train data analysis." Neural computation 14.2 (2002): 325-346.

[18] Brown, Emery N., et al. "Likelihood methods for neural spike train data analysis." Computational neuroscience: A comprehensive approach (2003): 253-286.

[19] Brown, Emery N. "Course 14 Theory of point processes for neural systems." Les Houches 80 (2005): 691-727.

[20] Carling, P. A., and M. A. Hurley. "Time-varying stochastic model of the frequency and magnitude of bed load transport events in two small trout streams." Sediment Transfer in Gravel-Bed Rivers. John Wiley & Sons New York. 1987. p 897-917, 4 tab, 7 fig, 26 ref. (1987).

[21] Carling, Paul A., and Nigel A. Reader. "Structure, composition and bulk properties of upland stream gravels." Earth Surface Processes and Landforms 7.4 (1982): 349-365.

[22] Casella, George, and Roger L. Berger. Statistical inference. Vol. 2. Pacific Grove, CA: Duxbury, 2002.

[23] Chen, Shaojie. Statistical Analysis of Point Processes and Associated Marks. University of California, Riverside, 2006.

[24] Chung, Kai Lai. "Crudely stationary counting processes." The American Mathematical Monthly 79.8 (1972): 867-877.

[25] Corduneanu, Constantin. Almost periodic functions. Chelsea Pub Co, 1989.

[26] Cox, David Roxbee, et al. Renewal theory. Vol. 1. London: Methuen, 1962.

[27] Cox, David Roxbee, and Valerie Isham. Point processes. Vol. 12. CRC Press, 1980.

[28] Daley, Daryl J., and David Vere-Jones. An introduction to the theory of point processes: volume II: general theory and structure. Springer Science & Business Media, 2003.

[29] Feller, Willliam. An introduction to probability theory and its applications. Vol. 2. John Wiley & Sons, 2008.

[30] Ferguson, Thomas Shelburne. A course in large sample theory. Vol. 49. London: Chapman & Hall, 1996.

[31] Gakis, K. G., and B. D. Sivazlian. "Distribution of order statistics of waiting times in an ordinary renewal process and the covariance of the renewal increments." Stochastic Analysis and Applications 11.4 (1993): 441-458.

[32] Hurley, M. A. "Modelling bedload transport events using an inhomogeneous gamma process." Journal of Hydrology 138.3-4 (1992): 529-541.

[33] Jacobsen, Martin. Statistical analysis of counting processes. Vol. 12. Springer Science & Business Media, 1982.

[34] Lee, Sanghoon, James R. Wilson, and Melba M. Crawford. "Modeling and simulation of a nonhomogeneous Poisson process having cyclic behavior." Communications in Statistics-Simulation and Computation 20.2-3 (1991): 777-809.

[35] Lewis, P. A. W. "Remarks on the theory, computation and application of the spectral analysis of series of events." Journal of Sound and Vibration 12.3 (1970): 353-375.

[36] Lewis, Peter AW. Recent results in the statistical analysis of univariate point processes. Monterey, California. Naval Postgraduate School, 1971.

[37] Ogata, Yosihiko. "On Lewis' simulation method for point processes." IEEE Transactions on Information Theory 27.1 (1981): 23-31.

[38] Ogata, Yosihiko. "Statistical models for earthquake occurrences and residual analysis for point processes." Journal of the American Statistical association 83.401 (1988): 9-27.

[39] Ogata, Yosihiko. "Space-time point-process models for earthquake occurrences." Annals of the Institute of Statistical Mathematics 50.2 (1998): 379-402.

[40] Lewis, Peter A., and Gerald S. Shedler. "Simulation of nonhomogeneous Poisson processes by thinning." Naval Research Logistics Quarterly 26.3 (1979): 403-413.

[41] Papangelou, F. "Integrability of expected increments of point processes and a related random change of scale." Transactions of the American Mathematical Society 165 (1972): 483-506.

[42] Pulcini, Gianpaolo. "Mechanical reliability and maintenance models." Handbook of Reliability Engineering. Springer London, 2003. 317-348.

[43] Rohatgi, Vijay K., and A. K. Md. Ehsanes Saleh. An Introduction to Probability and Statistics. 2nd ed. New York, NY: John Wiley & Sons, 2001.

[44] Ross, Sheldon M. Applied probability models with optimization applications. Courier Corporation, 2013.

[45] Ross, Sheldon M. Introduction to probability models. Academic press, 2014.

[46] Shao, Nan. Modeling Almost Periodicity in Point Processes. University of California, Riverside, 2010.

[47] Shao, Nan, and Keh-Shin Lii. "Modelling non-homogeneous Poisson processes with almost periodic intensity functions." Journal of the Royal Statistical Society: Series B (Statistical Methodology) 73.1 (2011): 99-122.

[48] Sigman, K. "Stationary Marked Point Processes: An Intuitive Approach. 1995."

[49] Schwarz, Gideon. "Estimating the dimension of a model." The annals of statistics 6.2 (1978): 461-464.

[50] Vere-Jones, D. "On the estimation of frequency in point-process data." Journal of Applied Probability (1982): 383-394.

[51] Vere-Jones, D., and T. Ozaki. "Some examples of statistical estimation applied to earthquake data." Annals of the Institute of Statistical Mathematics 34.1 (1982): 189-207.

[52] Walker, A. M. "On the estimation of a harmonic component in a time series with stationary independent residuals." Biometrika 58.1 (1971): 21-36.